ULB UNIVERSITÉ LIBRE DE BRUXELLES, UNIVERSITÉ D'EUROPE

FACULTE DES SCIENCES

Département des Sciences de la Terre et de l'Environnement
Laboratoire d'Océanographie Chimique et Géochimie des Eaux

Silica dynamics and retention in the Scheldt tidal river and estuary (Belgium/The Netherlands)

The Scheldt estuary – Google Maps

Thèse de doctorat présentée par

Vincent Carbonnel

En vue de l'obtention du grade de

Docteur en Sciences

Promoteur

Prof. Lei Chou

Juin 2009

ULB UNIVERSITÉ LIBRE DE BRUXELLES, UNIVERSITÉ D'EUROPE

FACULTE DES SCIENCES

Département des Sciences de la Terre et de l'Environnement
Laboratoire d'Océanographie Chimique et Géochimie des Eaux

Silica dynamics and retention in the Scheldt tidal river and estuary (Belgium/The Netherlands)

The Scheldt estuary – Google Maps

Thèse de doctorat présentée par

Vincent Carbonnel

En vue de l'obtention du grade de

Docteur en Sciences

Promoteur

Prof. Lei Chou

Juin 2009

Remerciements

Je remercie chaleureusement le professeur Lei Chou de m'avoir accueilli dans son laboratoire, de m'avoir fait confiance et de m'avoir guidé, conseillé, aidé et soutenu pendant ces années.

Je tiens à remercier particulièrement Jean-Pierre Vanderborght, pour tous les échanges, suggestions et commentaires qui m'ont été d'une aide primordiale pour finaliser ce travail.

Merci aussi à tous mes collègues et amis du LOCGE, Traitement des eaux et Pollution et autres laboratoires, avec qui j'ai eu le plaisir de travailler, mais aussi d'échanger et discuter.

Merci ensuite à tous mes amis, qui font de ces années une belle aventure humaine, ceux avec qui j'ai dansé ou joué de la musique, ceux avec qui j'ai randonné, ou simplement fait la fête.

Enfin, un immense merci va bien sûr à ma famille, pour son soutien et son encouragement.

Merci à vous tous.

Résumé

Les concentrations en silice dissoute (DSi) et silice particulaire biogène (BSi) ont été mesurées pendant une année complète (en 2003) dans la zone tidale de la rivière Escaut et dans ses tributaires aux limites tidales. Alors que la DSi est restée, dans les tributaires, à des concentrations élevées toute au long de l'année, et que la BSi s'est maintenue à des concentrations faibles, la DSi a été entièrement consommée pendant l'été dans la rivière tidale et les concentrations en BSi ont augmenté. En comparant ces concentrations avec celles de la biomasse des diatomées et de la matière en suspension, il a pu être estimé que la majeure partie de la BSi en été était associée aux diatomées vivantes. Des bilans de masse de la DSi et de ces deux fractions de BSi ont été effectués sur différentes zones de la rivière tidale pendant la période durant laquelle les diatomées se développent (période productive, Mai à Octobre). Ceci a permis l'estimation de la croissance et de la mortalité des diatomées, ainsi que de la sédimentation nette de la BSi durant cette période : la moitié de la DSi apportée par les rivières a été transformée en BSi dans la rivière tidale, et la rétention de la silice y a atteint un tiers des apports fluviaux en silice "totale" (TSi = DSi + BSi). Les flux annuels de silice ont aussi été calculés pour replacer à une échelle annuelle les résultats obtenus pendant la période productive : les rétentions annuelles de DSi et la de TSi ne s élevèrent respectivement qu'à 14 et 6 %.

L'échantillonnage de l'estuaire a été effectué sur l'ensemble du gradient de salinité au cours de 11 campagnes réparties sur trois ans (de 2003 à 2005). Du fait du mélange des eaux douces et marines, les concentrations en DSi diminuèrent toujours de l'amont vers l'aval, mais les profils étaient généralement convexes ou concaves. Ils ont été interprétés en les comparant avec ceux obtenus à l'aide de la modélisation du transport conservatif. Les flux à l'embouchure ont aussi pu être recalculés, ce qui a permis de quantifier la consommation ou le relargage de DSi au sein de l'estuaire : un maximum de consommation a été observé au printemps, mais l'estuaire a été une source nette de DSi d'août à décembre. A l'échelle annuelle, 28 % des apports de DSi à l'estuaire ont été consommés.

La comparaison des profils de BSi avec ceux de la biomasse des diatomées et ceux de la matière en suspension indiqua que la plupart de la BSi dans l'estuaire était détritique (c'est-à-dire non associée aux diatomées vivantes). Ces résultats ont été confirmés par des expériences d'incorporation de silice radioactive qui, bien que la méthodologie soit

complètement différente, apportèrent des résultats comparables. La dynamique complexe de la BSi a donc pu être interprétée à l'aide de celle déjà bien étudiée de la matière en suspension dans l'estuaire de l'Escaut, et un bilan de masse de la BSi dans l'estuaire a pu être établi à partir d'un bilan pour la matière en suspension obtenu de la littérature. En plus de la production de diatomées, l'estuaire a reçu presque autant de BSi de la rivière tidale que de la zone côtière. Ceci induisit que la rétention de TSi dans l'estuaire (59 %) a été plus importante que celle de la DSi.

Au final, le système tidal de l'Escaut apparaît comme un filtre important pour la silice : les rétentions globales de DSi et TSi dans ce système s'élevèrent respectivement à 39 et 61 %. La comparaison des dynamiques de la silice dans la rivière tidale et dans l'estuaire mit en évidence l'importance du rôle de l'estuaire. La consommation de DSi et la déposition de BSi par unité de surface étaient certes plus intenses dans la rivière tidale mais, à l'échelle de l'écosystème, les effets y furent limités du fait de sa faible surface comparée à celle de l'estuaire. L'une des observations les plus importantes de cette étude est celle de l'apport net de BSi à l'estuaire depuis la zone côtière, ce qui induisit une importante rétention estuarienne de la silice. Les différences importantes entre les rétentions de DSi et de TSi mettent ainsi en évidence la nécessité de prendre en compte la dynamique de la BSi dans l'étude de celle de la silice. De plus, l'importance de la BSi détritique implique que la dynamique de la BSi ne peut être étudiée de part l'observation seule de celle des diatomées. Enfin, l'apport net de BSi vers l'estuaire à l'embouchure, ainsi que l'origine en grande partie marine des diatomées se développant dans l'estuaire, soulignent l'importance de prendre en compte l'importance des échanges à l'embouchure pour le fonctionnement biogéochimique de la silice dans l'estuaire ; l'estuaire ne doit pas être vu comme un simple filtre à sens unique des espèces dissoutes et particulaires provenant uniquement des rivières en amont.

Table of contents

1 Introduction

1.1 Natural forms of silicon

Silicon, which contributes to 27 % of the Earth's crust, is the second most abundant element on Earth after oxygen. In the natural environment, it is mainly found in the forms of silicon dioxide (silica, i.e. bound to two atoms of oxygen) (Canfield et al. 2005); this includes:

- hundreds of different types of ubiquitous ordered silicate minerals (lithogenic silica) such as quartz, feldspars and clays,
- the dissolved silicic acid (H_4SiO_4 and its dissociated anions, called hereafter dissolved silica, DSi), found in surface- and ground-water at concentrations ranging from nanomolars to generally 1-2 millimolars (which corresponds to the concentration at equilibrium with amorphous silica at pH below 9: DSi may polymerise at higher concentrations),
- the particulate amorphous siliceous material, mostly biogenic (called hereafter biogenic silica, BSi), such as skeletons of diatoms, radiolarians and silicoflagellates, sponge spicules, as well as phytoliths of higher plants, but also possibly authigenic.

In the framework of the present study, we will focus on silica in the aquatic environment and, in particular, in estuaries.

1.2 Diatoms and silica

DSi is a key nutrient for the aquatic ecosystem as it is an essential element for diatoms (Bacillariophycae), ubiquitous unicellular phytosynthetic algae. The size of the diatoms generally ranges between 5 and 200 μm, but there also exists cells of more than 1 mm (Sabater 2009). Diatoms require DSi (mostly as H_4SiO_4) to build up their ornamented frustules: rigid outer transparent perforated cell walls made of hydrated BSi, which may account for 15-75 % of the mass of the cell (Conley and Kilham 1989; Martin-Jézéquel et al. 2000; Sabater 2009). The frustules present various shapes and ornaments which are species-specific; there exists more than ten thousands known species but the total number may be much higher (Martin-Jézéquel et al. 2000; Sabater 2009). It has been hypothesized that the formation of such BSi cell walls may provide low-energy pathways for organic matter

synthesis, protection against grazing or viral attacks and/or the possibility of sinking as a survival strategy (Martin-Jézéquel et al. 2000; Raven and Waite 2004; Ragueneau et al. 2006a). Although BSi may be produced by other aquatic organisms (such as sponges or radiolarians), about 90 % of the aquatic BSi production is attributed to diatoms (Canfield et al. 2005 and reference therein).

Diatoms are an important constituent of the aquatic biota. They can be found in almost all illuminated environments where water is at least occasionally present; this includes freshwater, brackish, marine habitats, with diatoms being in the water column (planktonic), at the bottom or on inter-tidal areas (benthic), attached to mud (epipelic), sand (episammic), rocks (epilithic) or even to plants (epiphytic) (Sabater 2009). Diatoms may also attach to each other to form chain or aggregates. Some benthic diatoms may be found in the water column (tychoplanktonic), while some planktonic ones may have a benthic survival phase (meroplanktonic) (Reynolds et al. 1994). As diatoms have low light requirements, they often dominate the primary production in turbid aquatic environments such as lakes, rivers, estuaries and coastal zones (Ragueneau et al. 2000) and account for respectively 35 % and 75 % of the primary production in the open ocean and in the world's coastal areas (43 % in total in the marine environment, Nelson et al. 1995). In addition, they may play a significant role in the sequestration of the atmospheric CO_2 (Tréguer and Pondaven 2000). Due to their relatively large size, they can support a short and efficient aquatic food chain (Turner et al. 1998; Ragueneau et al. 2006a). BSi is not assimilated by grazers but egested in the faecal pellets (Tande and Slagstad 1985), which sink rapidly out of the surface waters due to the density and the ballast effect of the BSi (Ragueneau et al. 2000; Ploug et al. 2008). As for fast sinking diatom aggregates, these faecal pellets may contribute significantly to the export of carbon from surface waters (Ragueneau et al. 2000).

The diatom frustule is composed of two distinct parts (thecae), which fit into each other like a Petri dish. The outer theca is called the epitheca and the inner one the hypotheca. In general, diatoms reproduce asexually by cellular division, at doubling rates ranging from 0.3 to 5 five times per day (Sabater 2009). Prior to the effective division, two new thecae are synthesised inside the mother cell; they will be the hypothecae of the two daughter cells, while the epithecae will be made of the thecae of the mother cell. As a result, the average cell size of a diatom population gradually decreases with time. Nevertheless, once a too small size is reached, diatoms can sexually reproduce to recover their initial dimension (Sabater et al. 2009). Although natural waters are generally under-saturated with respect to amorphous

silica, the dissolution of the frustules is prevented by the presence of an outer organic coating. But the frustules may nevertheless dissolve after the death of the diatoms and the bacteria-mediated remineralisation of this organic coating (Bidle and Azam 1999; Roubeix et al. 2008).

The cellular silica content in diatoms varies from one species to another (Conley and Kilham 1989; Rousseau et al. 2002). In particular, freshwater diatoms are on the average almost one order of magnitude more silicified than marine ones (Conley and Kilham 1989). This may be explained by the adaption of freshwater diatoms to generally higher DSi concentrations in rivers than in the ocean (Claquin et al. 2006). Also, in contrast to the marine environment where diatom cells should remain in the photic zone, higher BSi contents and sinking rates may correspond to a survival strategy in rivers where resuspension is generally possible. Sinking may prevent the diatom from being flushed too rapidly out of the system (Reynolds et al. 1994) and, when for instance DSi becomes limiting, some species may switch to dormant phases in the sediment and wait for better growth conditions (Claquin et al. 2006; Sabater 2009).

The silica uptake and deposition mechanisms in diatoms are not yet fully understood and they seem to be species-specific (Martin-Jézéquel et al. 2000). It has nevertheless been shown that they are linked to the cell cycle (which may not be synchronised with the day/night cycle, Ragueneau et al. 2000), taking place mostly during some arrest points of the cell cycle: G_2 and M phases (Martin-Jézéquel et al. 2000; Claquin and Martin-Jézéquel 2005). As a result, silicification can also vary within a single species: if the growth rates decrease (or increase), more (or less) time is spent in the G_2 + M phase, and silicification increase (or decrease) (Claquin et al. 2002). In contrast, when ambient DSi concentrations drop below species-specific thresholds, diatoms may adapt by reducing their silica content albeit decreasing growth rates. As a result, they may maintain high division rates even when their DSi uptake rates are limited by the availability of DSi (Ragueneau et al. 2000).

1.3 The silica cycle and its importance for the marine ecosystem

The terrestrial source of DSi

Most of the DSi is originally produced during weathering of silicate minerals on land, which is a slow process at biological time-scales. In addition to the release of DSi, different secondary minerals are formed depending on the ambient conditions, such as the presence of

ions or the importance of the rainfall (Appelo and Postma 1996). For example, albite may be weathered into montmorillonite, kaolinite or gibbsite (which can also transform into each other) while kaolinite may also be the secondary mineral of the weathering of K-feldspar, anorthite, pyroxene or biotite. As protons are generally consumed in the weathering process, the latter acts as an important buffer mechanism against acidification of soil and groundwater (Appelo and Postma 1996), which participates in the long-term regulation of the atmospheric CO_2 (Conley 2002 and references therein). Dissolution rates are not only dependent on the rainfall, temperature and pH (Appelo and Postma 1996), but they can also be enhanced by the terrestrial plants and microbiota (Alexandre et al. 1997; Conley 2002). Nonetheless, reverse weathering processes and the formation of authigenic clay material can also occur (Wollast 1974; Alexandre et al. 1997; Michalopoulos and Aller 2004).

The terrestrial silica cycle

Before reaching the aquatic ecosystem, DSi may participate in the terrestrial cycle: higher plants can take up DSi through their roots to deposit it in their leaves, stems and/or roots as BSi particles of a few to several tens of micrometers, called phytoliths (Conley 2002). The lack of DSi may affect the development of the plants and their resistance to external stresses. The BSi content in plant varies widely, from 0.1 % to more than 10 % dry weight (in average 1-3 %; Conley 2002). Phytoliths are taxonomically species-specific and ubiquitous. Although some phytoliths or a fraction of them can be easily dissolved in soils or in water after the decay of the plants, a significant pool seems to be refractory, even to hot alkaline solutions (Alexandre et al. 1997; Struyf et al. 2007a; Triplett et al. 2008). This pool is preserved in soils, rendering paleo-environment reconstructions possible (Conley 2002). Although the size of lithogenic silica pool exceeds by far that of the phytoliths in soils, which is itself several orders of magnitude higher than that contained in aboveground biomass, phytoliths undergo a significantly higher turnover than minerals. As a result, in most of the ecosystems investigated so far (except for the coniferous forests), the major part of the DSi exported to groundwater originated from phytolith dissolution rather than directly from mineral weathering (Alexandre et al. 1997; Conley 2002; Derry et al. 2005).

Transport of silica in rivers and estuaries, and importance of the BSi fluxes

During its journey to the coastal zone, DSi participates in aquatic biogeochemical cycles in rivers and estuaries (Conley et al. 1993), involving a number of biological, chemical

and physical processes (Chou and Wollast 2006). Diatom blooms occurring in spring/summer in rivers and estuaries result in significant decreases in DSi and concomitant increases in BSi concentrations, which can account for 50-70 % of the total riverine silica load (Admiraal et al. 1990; Conley 1997). As particulate material, BSi can settle and accumulate in the sediments, inducing retention of silica in the ecosystem. It can also be transported downstream as suspended material (Admiraal et al. 1990) and/or, in contrast to lithogenic silica (Conley and Kilham 1989; Ragueneau et al. 2006a), be dissolved at biological timescales (Roubeix et al. 2008; Loucaides et al. 2008). BSi dissolution is however not expected to occur at the same rate along the salinity gradient: BSi dissolution rate increases with salinity (Loucaides et al. 2008) and the bacterial community can significantly enhance the remineralisation (Bidle and Azam 1999; Roubeix et al. 2008). In addition, phytoliths can add a significant, if not major, contribution to the BSi pool carried by rivers (Cary et al. 2005). They can originate from top soil erosion (Cary et al. 2005) as well as directly from the vegetation of the river banks or tidal marshes (Struyf et al. 2006). Marshes can retain significant amounts of silica in the aboveground biomass and in sediments, and DSi and BSi exchange between the river channel and the marshes can affect the estuarine silica cycle (Struyf et al. 2005, 2006). Thus, because of the potentially important riverine and estuarine BSi concentrations, its specific biogeochemical behaviour and its interaction with DSi, the study of BSi dynamics should not be omitted when silica fluxes and mass-balances in rivers and estuaries are assessed.

Anthropogenic perturbations

Riverine DSi fluxes have also been altered by human activities during the last decades. Land-use activities, such as deforestation, may affect the DSi inputs to rivers (Conley et al. 2008) and the use of silica in washing powders (Verbanck et al. 1994) and fertilizers (Datnoff et al. 2001) may also constitute an additional DSi source to rivers. In contrast, eutrophication results in enhanced silica retention in lakes, rivers and estuaries (Conley et al. 1993). Decreased silica concentrations are also induced by river damming and river regulation, which cause particle trapping and reduce contact between the water and the riparian vegetated zone containing DSi-rich interstitial waters (Humborg et al. 2006).

The marine silica cycle

Diatoms are important constituent of the marine phytoplankton, contributing to 43 % of the global oceanic primary production (Nelson et al. 1995). The marine silica cycle has

thus received much attention since the 60s. Global silica mass-balances have been performed already since the 70s (Wollast 1974; DeMaster 1981; Wollast and Mackenzie 1983) and they agree remarkably well with the more recent oceanic budget proposed by Tréguer et al. (1995) and Nelson et al. (1995). In the oceans, the diatom growth can often be limited by low DSi concentrations (Tréguer et al. 1995; Nelson et al. 1995). The diatom production (200-400 Tmol yr^{-1}; Wollast 1974; Nelson et al. 1995) is mainly fuelled by BSi dissolution in the water column; 12 % of the BSi produced in the ocean reaches the seafloor, and only 2.5 % gets preserved (Tréguer et al. 1995). This preservation compensates the DSi inputs to the ocean, which are mainly attributed to the riverine discharge of silica (5-7 Tmol yr^{-1}; Wollast 1974; Tréguer et al. 1995). Compared to this source, the others including eolian inputs, hydrothermal vents and submarine weathering were lower by at least one order of magnitude (Wollast 1974; Tréguer et al. 1995).

Due to the proximity of the riverine DSi sources, the diatom production rates are generally higher in the coastal zones compared to the ocean (Ragueneau et al. 2000). Due to shallower depths, the coastal silica cycle in the water column may be influenced by benthic processes. Submarine groundwater discharge and BSi dissolution, occurring principally in the sediments or at the water-sediment interface, may constitute significant sources of DSi (Ragueneau et al. 2006a). In contrast, the preservation of BSi may also be enhanced due to reverse weathering processes enabled by the presence of lithogenic material (Michalopoulos and Aller 2004). In addition, the coastal silica cycle can be affected (and even driven) by benthic diatoms and/or suspension feeders (Ragueneau et al. 2005; Ragueneau et al. 2006a).

Eutrophication and importance of the riverine silica fluxes

Due to the specific need for silica by diatoms, the availability of DSi and its relative abundance compared to the other nutrients can influence the composition of the phytoplankton community. While the spring diatom bloom may terminate due to a complete consumption of the DSi, the left-over nitrogen and phosphorous can allow the development of flagellate or cyanobacteria blooms. Higher trophic levels and the whole ecological functioning of the ecosystem may subsequently be altered (Officer and Ryther 1980; Conley et al. 1993; Lancelot 1995; Turner et al. 1998).

Although this modification of the phytoplankton speciation has also been observed in lakes, rivers and estuaries, this phenomenon affects particularly the coastal zones. The number of ecosystems concerned as well as the frequency and the magnitude of these alterations have

increased in the past decades as a result of anthropogenic pressure (Ragueneau et al. 2006b). Nitrogen and phosphorus riverine loads indeed increased due to the use of fertilizers and washing powders and due to the direct discharge of untreated wastewater in rivers (Billen et al. 2005). In contrast, DSi concentrations may have remained unchanged, or have even been reduced due to eutrophication or hydrological alterations (see above). In addition, the recycling of nitrogen and phosphorus, which is biologically mediated, is faster than that of silica whose regeneration involves the much slower dissolution process. Furthermore, flagellate species, such as those responsible for the undesirable coastal blooms in summer, may have the ability to acquire nitrogen and phosphorous in the organic form, while the diatom growth may be hampered by phosphorous or nitrogen limitation (Ragueneau et al. 2006b and reference therein). Nevertheless, diatoms may survive at low ambient DSi concentrations due to a growth sustained by BSi dissolution or due to their capacity to adapt their Si content.

The knowledge of the DSi fluxes to eutrophicated coastal zones is thus of primary importance to understand the biogeochemical and biological functioning of the ecosystem. In the context of global climate change, riverine DSi sources and estuarine DSi retention deserve to be more accurately estimated as well, due to their importance in the global oceanic silica cycle and to the potentially important role played by diatoms in the fixation and export of carbon dioxide to the deep-sea sediments.

1.4 Characteristics of estuaries

In the land to ocean continuum, estuaries are key ecosystems as they represent the meeting point between the freshwater and marine waters; they are nevertheless specific habitats that differ from the adjacent rivers and coastal zones (Elliot and McLusky 2002). Estuaries are also highly valuable environments, from an ecological point of view due to the wildlife they host, as well as for socio-economical concerns (Meire et al. 2005).

Estuaries are diverse ecosystems, which are characterised by continuous and coupled geophysical, hydrodynamic, geochemical and biological gradients (McLusky 1993; Elliot and McLusky 2002). The hydrodynamics are obviously influenced by the geomorphology, but the water movement, mostly due to tidal oscillations in macrotidal systems, may also shape the estuary by driving the sediment transport, deposition and redistribution (Fettweis et al. 1998; Elliot and McLusky 2002; Chen et al. 2005). In turn, this physical forcing may affect the

concentrations of the dissolved compounds, either directly by sorption/desorption processes (e.g. trace metals), or via their link to the phytoplankton dynamics that are influenced by light availability and water residence times (Arndt et al. 2007).

In contrast to rivers, an important feature in estuaries is that the net transport of suspended particulate material may be strongly uncoupled to that of the water. In the lower reaches, particles may be transported landwards (Van Maldegem et al. 1993) resulting in an accumulation of suspended particulate material in the regions of low salinities (particularly in macrotidal estuaries with long residence times, Uncles et al. 2002). The residence time of the particles in estuaries may thus be much higher than that of the water. Also, the accumulated material may eventually deposit and form mudflats and sandbars. As a result, estuaries may also be characterised by the presence of substantial intertidal areas, providing habitats for an important benthic fauna and flora (Elliot and McLusky 2002; Meire et al. 2005). Nonetheless, possibly due to the high turbidity, the strong hydrodynamic forcing, the salinity gradient and/or the low oxygen concentrations in the upstream reaches, the species diversity in estuaries has been observed to be lower than in the adjacent areas, and in particular was found to be at a minimum around salinity 5-8 (McLusky 1993; Muylaert et al. 1999; Elliot and McLusky 2002). Conversely, species abundance and productivity in estuaries may remain high: for instance, a high phytoplankton biomass may be sustained by a continuous nutrient supply by rivers and lateral sources, and by higher water residence times than in the upstream reaches (see below). As a result, nutrient concentrations (as well as those of trace metals and dissolved gases) may undergo significant alterations along the salinity gradient, being transformed, consumed or released (see above for DSi; Billen et al. 1991; Soetaert et al. 2006).

Despite these common characteristics, estuaries are protean and may display contrasting dynamics. Several classifications have been established: they may be for instance coastal plain, fjord, bar-built or tectonic estuaries, homogenous, partially mixed or weakly or highly stratified, micro-, meso- or macrotidal, of funnel, mixed or prismatic shapes. There is still much debate about the definition of estuaries, principally as they may as well be based on geographical, chemical, hydrodynamic and biological considerations. The classical chemical definition proposed by Pritchard (1967, quoted in McLusky 1993 and in Elliot and McLusky 2002) limits the estuary to the extent of the salinity gradient, although the upstream boundary may drift with the tidal oscillations and with the variation of the freshwater discharge. Also, in some estuaries, the tidal influence propagates further inland than salt intrusion, leading to

the existence of tidal freshwater reaches, which should not be neglected as they generally host important chemical and biological processes (McLusky 1993; Schuchardt et al. 1993; Elliot and McLusky 2002; Muylaert et al. 2005). In particular, tidal freshwater reaches exhibit specific features which can influence the phytoplankton dynamics (Schuchardt et al. 1993; Lionard 2006) and thus the biogeochemical cycle of nutrients. They differ from the adjacent rivers by longer water residence times and the presence of tides, which induces higher turbulence and turbidity (Schuchardt et al. 1993; McLusky 1993). The resulting low light conditions may limit phytoplankton growth but may also favour diatoms due to their lower light requirements compared to other algae (Reynolds 1988; Cushing 1989; Lionard 2006). In contrast to the downstream areas where freshwater and seawater mix, there is no phytoplankton mortality due to salinity stress in tidal freshwater reaches (Schuchardt et al. 1993; Muylaert et al. 2000). Thus, if the residence time is sufficiently long, a maximum in the diatom production and the associated DSi consumption may occur in the tidal freshwater reaches (Anderson 1986; Schuchardt and Schirmer 1991; De Sève 1993; Schuchardt et al. 1993; Muylaert et al. 2005; Arndt et al. 2007).

1.5 The Scheldt estuary and the Belgian coastal zone

In the present study, we focus on the Scheldt estuary which comprises an extensive tidal freshwater area. The biogeochemistry of silica and the fluxes of this nutrient in the continuum of the Scheldt are of primary importance as they can affect the ecosystem in the adjacent coastal zone. Earlier works have shown that DSi drives the extent of the early spring diatom bloom in this zone, while the excess of dissolved inorganic nitrogen stimulates a subsequent massive development of flagellates (*Phaeocystis* sp.) which alters both the food web and the environment (Lancelot 1995).

The highest (diatom-dominated) phytoplankton biomass and production of the Scheldt estuary were observed in the tidal freshwater reaches, resulting in strong seasonal patterns in DSi concentrations, possibly consumed down to limiting levels in summer (Muylaert et al. 2001; Struyf et al. 2004; Muylaert et al. 2005; Van Damme et al. 2005; Soetaert et al. 2006). Low chlorophyll *a* concentrations were observed in the brackish reaches (Van Damme et al. 2005), but Soetaert (et al. 2006) estimated that a significant amount of DSi was nevertheless consumed in this area. DSi dynamics in the Scheldt estuary have been studied in the late 60s and early 70s (Wollast and De Broeu 1971; Beckers and Wollast 1976; Wollast 1978). The

long-term evolution of DSi concentrations as well as the variation of DSi concentrations with increasing discharge have recently been investigated (Muylaert et al. 2001; Struyf et al. 2004; Soetaert et al. 2006).

Silica dynamics were also investigated by Arndt et al. (2007, 2009), Arndt and Regnier (2007) and Arndt (2008) using model simulations of diatom dynamics calibrated with DSi concentrations. These studies suggested that, BSi dissolution was of minor importance but that the diatom dynamics along the Scheldt were driven by the physical forcing in the tidal freshwater reaches, and in the brackish reaches by the import of diatoms from the coastal bloom. The retention of DSi was also estimated for the tidal freshwater and brackish reaches of the Scheldt. However, apart from the fate of BSi in sediments in the tidal river (Arndt and Regnier 2007), these studies focused principally on DSi dynamics; in particular, BSi fluxes and their contribution to the transport of silica along the Scheldt were not investigated.

Marshes along the Scheldt tidal system may act as DSi recyclers or sinks for estuarine BSi, and may play a role in the estuarine silica cycle (Struyf et al. 2006; Struyf et al. 2007b). In summer, the DSi released by marshes to the DSi-depleted estuarine waters may support the estuarine diatom growth (Struyf et al. 2006), but modelling studies suggested that, on an annual basis, recycling is of minor importance compared to riverine inputs of DSi (Arndt and Regnier 2007). As this particular ecosystem may contain significant amounts of phytolith in the aboveground biomass (Struyf et al. 2005), BSi as phytoliths may be delivered to the estuarine waters by tidal exchange of this biogenic material between the river channel and marshes.

BSi dynamics in the water column of the Scheldt have not been studied until now and little is known about the present silica biogeochemical cycle in the Scheldt tidal system. Low summer DSi concentrations and high diatom-dominated phytoplankton biomass in the tidal freshwater reaches (Muylaert et al. 2000; Van Damme et al. 2005; Lionard 2006) suggest that BSi can be a major constituent of the silica pool. In addition, a significant fraction of the BSi in the water column may not be associated with living diatoms, due to diatom mortality, resuspension of dead diatom frustules and the possible presence of phytoliths. The dynamics of this latter fraction may differ from that of living diatoms; instead it may be linked to the complex spatial and temporal variability of the SPM (Chen et al. 2005). The relative importance of the BSi pool compared to the DSi pool on the one hand, and, on the other hand the extent of the link between the dynamics of BSi and that of the living diatoms or that of detrital material, have yet to be explored.

1.6 Objectives of the study and outline of the thesis

Framework

The present study was performed within the framework of the SISCO project (Silica Retention in the Scheldt Continuum and Its Impact on Coastal Eutrophication) financed by the Belgian Federal Science Policy Office. SISCO aimed at investigating the silica dynamics in the water column as well as in the sediments in the Scheldt river-estuary-coastal zone continuum, in relation to the phytoplankton dynamics and to the development of a fully-transient coupled benthic-pelagic model. This project gathered expertises of the Laboratoire d'Oceanographie Chimique et Géochimie des Eaux (Université Libre de Bruxellles), Protistology and Aquatic Ecology of the Biology Department (Gent Universiteit) and the Department of Earth Sciences (University of Utrecht).

Objectives

The principal objective of this thesis was to investigate pelagic DSi and BSi dynamics and retention in the Scheldt tidal system. Particularly, we aimed at identifying and quantifying the sources, sinks and process affecting the behaviour of silica in this ecosystem and, in turn, at assessing the impact of this system on the transport of silica to the coastal zone.

The contributions of the BSi to the total silica pool and retention were assessed, and the influence of the dynamics of the phytoplankton and of the detrital material on those of BSi was investigated. The seasonality of the silica fluxes and their link to the physical and biological functioning of the Scheldt tidal system were also explored. Also, mass-balances were performed to estimate the retention of silica in this ecosystem.

Outline

The morphology, the hydrodynamics and the geochemical and biological functioning of Scheldt tidal system are described in **Chapter 2**. The sampling strategy and the methodologies for the chemical analyses (of DSi, BSi, phytoplankton biomass and speciation, and other parameters), for the calculation of the fraction of the BSi associated with living diatoms, and for the ^{32}Si incorporation experiments are also presented in this chapter.

The Scheldt tidal system forms a continuum but the transport of dissolved and particulate material is expected to present different characteristics in the tidal freshwater reaches and along the salinity gradient. The study of the silica dynamics was thus firstly

conducted in the tidal freshwater reaches only, i.e. independently from that in the brackish reaches. The results are presented in **Chapter 3**. DSi and BSi concentrations were measured during one complete year at the tidal limits and at stations along the tidal freshwater reaches. The fraction of the BSi associated with living diatoms was estimated by comparing BSi concentrations with the diatom biomass and the concentration of suspended particulate material. DSi and BSi fluxes were calculated, and a budget for the productive period was established in order to quantify the DSi uptake by diatoms, the diatom mortality and the retention of BSi in the different sections of the tidal freshwater reaches. Silica fluxes and retention at an annual time-scale were also estimated. In addition, to provide further insights about the link between silica and diatom dynamics, the Si/C ratios were measured in cultures of two strains of diatoms isolated from the tidal freshwater reaches, and the dependence of the specific uptake rate on the ambient DSi concentrations was investigated using ^{32}Si. These latter results are presented in one of the annexes to Chapter 3.

One characteristic of the transport of the suspended particulate material along the salinity gradient is that it may be strongly uncoupled to that of the water, and even possibly directed landwards (see above). Although the DSi and BSi dynamics may be linked by uptake and dissolution processes, their assessments would require different methodologies and were carried out in two separate studies. The DSi versus salinity profiles that were measured at different seasons along the entire salinity gradient are shown in **Chapter 4**. Such estuarine profiles may have been interpreted using the classical "Apparent Zero End-member" method, but it has been shown that such procedure is irrelevant in the case of the Scheldt (Regnier et al. 1998). Instead, seasonal pattern of the uptake and/or release of DSi within the estuary, as well as the net annual amounts were investigated by comparing these measured results (or, for the fluxes, with those recalculated using model outputs) with those obtained by model simulations of the conservative transport.

The BSi dynamics in the brackish reaches of the Scheldt are presented in **Chapter 5**. Similarly to Chapter 3, BSi concentrations were compared with the diatom biomass and the suspended particulate matter concentrations to estimate the fraction of the BSi that was associated with living diatoms. Also, ^{32}Si incorporation experiments were performed to assess the physiological status of the diatoms. Due to the complex dynamics of the suspended matter, a BSi mass-balance was not established directly but using a SPM budget taken from the literature; this budget provided an estimate of the annual accumulation of BSi in these reaches.

Using the results obtained in the previous chapters, the overall impact of the Scheldt tidal system on the annual transport of silica from its tributaries to the adjacent coastal zone could finally be evaluated and presented in **Chapter 6**. Perspectives for further studies, such as possible improvements of the mass-balance calculations were also proposed. Future studies of the silica cycle in the Scheldt may provide as well the opportunity to investigate response of the silica dynamics to the restoration of the ecological status in the Scheldt.

1.7 References

Admiraal W, Breugem P, Jacobs DMLHA, de Ruyter van Steveninck ED (1990) Fixation of dissolved silicate and sedimentation of biogenic silicate in the lower river Rhine during diatom blooms. Biogeochemistry 9:175-185

Alexandre A, Meunier J-D, Colin F, Koud J-M (1997) Plant impact on the biogeochemical cycle of silicon and related weathering processes. Geochim Cosmochim Acta 61(3):677-682

Anderson GF (1986) Silica, diatoms and a freshwater productivity maximum in Atlantic coastal plain estuaries, Chesapeake Bay. Estuar Coast Shelf Sci 22:183-197

Appelo CAJ, Postma D (eds) (1996) Geochemistry, groundwater and pollution. A.A.Balkema, Rotterdam.

Arndt S, Regnier P (2007) A model for the benthic-pelagic coupling of silica in estuarine ecosystems: sensitivity analysis and system scale simulation. Biogeosciences 4:331-352

Arndt S, Vanderborght J-P, Regnier P (2007) Diatom growth response to physical forcing in a macrotidal estuary: Coupling hydrodynamics, sediment transport, and biogeochemistry. J Geophys Res 112:C05045

Arndt S (2008) Physical controls on the biogeochemical structure and functioning of a land-ocean transition system (Chapter 6). In: Arndt S. Biogeochemical transformations and fluxes in redox-stratified environments: from the shallow coastal ocean to the deep subsurface. Ph. D. thesis. Univ. of Utrecht, The Netherlands. pp 147-179.

Arndt S, Regnier P, Vanderborght J-P (2009) Seasonally-resolved nutrient export fluxes and filtering capacities in a macrotidal estuary. J Mar Syst (in press). DOI 10.1016/j.jmarsys.2009.02.008

Beckers O, Wollast R (1976) Comportement de la silice dissoute dans l'estuaire de l'Escaut. In: Nihoul JCJ, Wollast R (eds) Projet Mer, Rapport Final. Volume 10: L'Estuaire de l'Escaut. Services du Premier Ministre, programmation de la Politique Scientifique, Bruxelles. pp 153-170 (In French).

Bidle KD, Azam F (1999) Accelerated dissolution of diatom silica by marine bacterial assemblages. Nature 397:508-512

Billen G, Lancelot C, Meybeck M (1991) N, P, and Si retention along the aquatic continuum from land to ocean. In: Mantoura RFC, Martin J-M, Wollast R (eds) Ocean Margin Processes in Global Change, Dahlem Workshop Report. Wiley-Interscience pp 19-44.

Billen G, Garnier J, Rousseau V (2005) Nutrient fluxes and water quality in the drainage network of the Scheldt basin over the last 50 years. Hydrobiologia 540(1-3):47-67

Canfield DE, Kristensen E, Thamdrup B (2005) The Silicon Cycle. In: Canfield DE, Kristensen E, Thamdrup B (eds) Aquatic Geomicrobiology. Advances in Marine Biology 48. Academic Press, Elsevier pp 441-463.

Cary L, Alexandre A, Meunier J-D, Boeglin J-L, Braun J-J (2005) Contribution of phytoliths to the suspended load of biogenic silica in the Nyong basin rivers (Cameroon). Biogeochemistry 74:101-104

Chen MS, Wartel S, Van Eck B, Van Maldegem D (2005) Suspended matter in the Scheldt estuary. Hydrobiologia 540(1-3):79-104

Chou L, Wollast R (2006) Estuarine silicon dynamics. In: Ittekot V, Unger D, Humborg C, TacAn N (eds) The silicon cycle. Human perturbations and impacts on aquatic systems. SCOPE 66. Island Press, Washington, Covelo, London. pp 93-120.

Claquin P, Martin-Jézéquel V, Kromkamp JC, Veldhuis MJW, Kraay GW (2002) Uncoupling of silicon compared with carbon and nitrogen metabolisms and the role of the cell cycle in continuous cultures of *Thalassiosira pseudonana* (Bacillariophyceae) under light, nitrogen, and phosphorus control. J Phycol 38:922-930

Claquin P, Martin-Jézéquel V (2005) Regulation of the Si and C uptake and of the soluble free-silicon pool in a synchronised culture of *Cylindrotheca fusiformis* (Bacillariophyceae): effects on the Si/C ratio. Mar Biol 146:877-886

Claquin P, Leynaert A, Sferratore A, Garnier J, Ragueneau O (2006) Physiological ecology of diatoms along the river-sea continuum. In: Ittekot V, Unger D, Humborg C, TacAn N (eds) The silicon cycle. Human perturbations and impacts on aquatic systems. SCOPE 66. Island Press, Washington, Covelo, London. pp 121-137.

Conley DJ, Kilham SS (1989) Differences in silica content between marine and freshwater diatoms. Limnol Oceanogr 34(1):205-213

Conley DJ, Schelske CL, Stoermer EF (1993) Modification of the biogeochemical cycle of silica with eutrophication. Mar Ecol Prog Ser 101:179-192

Conley DJ (1997) Riverine contribution of biogenic silica to the oceanic silica budget. Limnol Oceanogr 42(4):774-777

Conley DJ (2002) Terrestrial ecosystems and the global biogeochemical silica cycle. Global Biogeochemical Cycles 16(4):68-1-68-7

Conley DJ, Likens GE, Buso DC, Saccone L, Bailey SW, Johnson CE (2008) Deforestation causes increased dissolved silicate losses in the Hubbard Brook Experimental Forest. Glob Change Biol 14(11):2548-2554

Cushing DH (1989) A difference in structure between ecosystems in strongly stratified waters and in those that are only weakly stratified. J Plankton Res 11(1):1-13

Datnoff LE, Snyder GH, Korndorfer GH (eds) (2001) Silicon in agriculture. Studies in Plant Science 8. Elsevier B.V.

De Sève MA (1993) Diatom bloom in the tidal freshwater zone of a turbid and shallow estuary, Rupert Bay (James Bay, Canada). Hydrobiologia 269/270:225-233

DeMaster DJ (1981) The supply and accumulation of silica in the marine environment. Geochimica et Cosmochimica Acta 45:1715-1732

Derry LA, Kurtz AC, Ziegler K, Chadwick OA (2005) Biological control of terrestrial silica cycling and export fluxes to watersheds. Nature 433:728-731

Elliot M, McLusky DS (2002) The need for definitions in understanding estuaries. Estuar Coast Shelf Sci 55:815-827

Fettweis M, Sas M, Monbaliu J (1998) Seasonal, neap-spring and tidal variation of cohesive sediment concentration in the Scheldt estuary, Belgium. Estuar Coast Shelf Sci 47:21-36

Humborg C, Pastuszak M, Aigars J, Siegmund H, Mörth C-M, Ittekot V (2006) Decreased silica land-sea fluxes through damming in the Baltic Sea catchment - significance of particle trapping and hydrological alterations. Biogeochemistry 77:265-281

Lancelot C (1995) The mucilage phenomenon in the continental coastal waters of the North Sea. Sci Total Environ 165(1-3):83-102

Lionard M (2006) Spatio-temporal phytoplankton dynamics along the Scheldt-North Sea continuum based on HPLC/CHEMTAX pigment analysis. Ph. D. thesis. Univ. of Ghent, Belgium.

Loucaides S, Van Cappellen P, Behrends T (2008) Dissolution of biogenic silica from land to ocean: Role of salinity and pH. Limnol Oceanogr 53(4):1614-1621

Martin-Jézéquel V, Hildebrand M, Brzezinski MA (2000) Silicon metabolism in diatoms: implications for growth. J Phycol 36:821-840

McLusky DS (1993) Marine and estuarine gradients - an overview. Neth J Aquat Ecol 27(2-4):489-493

Meire P, Ysebaert T, Van Damme S, Van den Bergh E, Maris T, Struyf E (2005) The Scheldt estuary: a description of a changing ecosystem. Hydrobiologia 540(1-3):1-11

Michalopoulos P, Aller RC (2004) Early diagenesis of biogenic silica in the Amazon delta: alteration, authigenic clay formation, and storage. Geochim Cosmochim Acta 68(5):1061-1085

Muylaert K, Sabbe K (1999) Spring phytoplankton assemblages in and around the maximum turbidity zone of the estuaries of the Elbe (Germany), the Schelde (Belgium/The Netherlands) and the Gironde (France). Journal of Marine Systems 22(2-3):133-149

Muylaert K, Sabbe K, Vyverman W (2000) Spatial and temporal dynamics of phytoplankton communities in a freshwater tidal estuary (Schelde, Belgium). Estuar Coast Shelf Sci 50(5):673-687

Muylaert K, Van Wichelen J, Sabbe K, Vyverman W (2001) Effects of freshets on phytoplankton dynamics in a freshwater tidal estuary (Schelde, Belgium). Arch Hydrobiol 150(2):269-288

Muylaert K, Tackx M, Vyverman W (2005) Phytoplankton growth rates in the freshwater tidal reaches of the Schelde estuary (Belgium) estimated using a simple light-limited primary production model. Hydrobiologia 540(1-3):127-140

Nelson DM, Tréguer P, Brzezinski MA, Leynaert A, Quéguiner B (1995) Production and dissolution of biogenic silica in the ocean: revised global estimates, comparison with regional data and relationship to biogenic sedimentation. Glob Biogeochem Cycle 9(3):359-372

Officer CB, Ryther JH (1980) The possible importance of silicon in marine eutrophication. Mar Ecol Prog Ser 3:83-91

Ploug H, Iversen MH, Koski M, Buitenhuis ET (2008) Production, oxygen respiration rates, and sinking velocity of copepod fecal pellets: Direct measurements of ballasting by opal and calcite. Limnol Oceanogr 53(2):469-476

Ragueneau O, Tréguer P, Leynaert A, Anderson RF, Brzezinski MA, DeMaster DJ, Dugdale RC, Dymond J, Fischer G, Francois R, Heinze C, Maier-Reimer E, Martin-Jézéquel V, Nelson DM, Quéguiner B (2000) A review of the Si cycle in the modern ocean: recent progress and missing gaps in the application of biogenic opal as a paleoproductivity proxy. Glob Planet Change 26(4):317-365

Ragueneau O, Chauvaud L, Moriceau B, Leynaert A, Thouzeau G, Donval A, Le Loc'h F, Jean F (2005) Biodeposition by an invasive suspension feeder impacts the biogeochemical cycle of Si in a coastal ecosystem (Bay of Brest, France). Biogeochemistry 75:19-41

Ragueneau O, Conley DJ, Leynaert A, Ni Longphuirt S, Slomp CP (2006a) Role of diatoms in silicon cycling and coastal marine food webs. In: Ittekot V, Unger D, Humborg C, TacAn N (eds) The silicon cycle. Human perturbations and impacts on aquatic systems. SCOPE 66. Island Press, Washington, Covelo, London. pp 163-195.

Ragueneau O, Conley DJ, Leynaert A, Ni Longphuirt S, Slomp CP (2006b) Responses of coastal ecosystems to anthropogenic perturbations of silicon cycling. In: Ittekot V, Unger D, Humborg C, TacAn N (eds) The silicon cycle. Human perturbations and impacts on aquatic systems. SCOPE 66. Island Press, Washington, Covelo, London. pp 197-213.

Raven JA, Waite AM (2004) The evolution of silicification in diatoms: inescapable sinking and sinking as escape? New Phytol 162:45-61

Regnier P, Mouchet A, Wollast R, Ronday R (1998) A discussion of methods for estimating residual fluxes in strong tidal estuaries. Cont Shelf Res 18:1543-1571

Reynolds CS (1988) Potamoplankton: paradigms, paradoxes and prognoses. In: Round FE (ed) Algae and the aquatic environment. Biopress, Bristom. pp 285-311.

Reynolds CS, Descy J-P, Padisák J (1994) Are phytoplankton dynamics in rivers so different from those in shallow lakes? Hydrobiologia 289:1-7

Roubeix V, Becquevort S, Lancelot C (2008) Influence of bacteria and salinity on diatom biogenic silica dissolution in estuarine systems. Biogeochemistry 88(1):47-62

Rousseau V, Leynaert A, Daoud N, Lancelot C (2002) Diatom succesion, silification and silicic acid availability in Belgian coastal waters (Southern North Sea). Marine Ecology Progress Series 236:61-73

Sabater S (2009) Diatoms. In: Likens GE (eds) Encyclopedia of Inland Waters. Volume 1. Elsevier, Oxford. pp 149-156.

Schuchardt B, Schirmer M (1991) Phytoplankton maxima in the tidal freshwater reaches of two coastal plain estuaries. Estuar Coast Shelf Sci 32:187-206

Schuchardt B, Haesloop U, Schirmer M (1993) The tidal freshwater reach of the Weser Estuary: riverine or estuarine? Neth J Aquat Ecol 27(2-4):215-226

Soetaert K, Middelburg JJ, Heip C, Meire P, Van Damme S, Maris T (2006) Long-term change in dissolved inorganic nutrients in the heterotrophic Scheldt estuary (Belgium, The Netherlands). Limnol Oceanogr 51(1, part 2):409-423

Struyf E, Van Damme S, Meire P (2004) Possible effects of climate change on estuarine nutrient fluxes: a case study in the highly nutrified Schelde estuary (Belgium, The Netherlands). Estuar Coast Shelf Sci 60(4):649-661

Struyf E, Van Damme S, Gribsholt B, Middelburg JJ, Meire P (2005) Biogenic silica in tidal freshwater marsh sediments and vegetation (Schelde estuary, Belgium). Mar Ecol Prog Ser 303:51-60

Struyf E, Dausse A, Van Damme S, Bal K, Gribsholt B, Boschker HTS, Middelburg JJ, Meire P (2006) Tidal marshes and biogenic silica recycling at the land-sea interface. Limnol Oceanogr 51(2):836-846

Struyf E, Van Damme S, Gribsholt B, Bal K, Beauchard O, Middelburg JJ, Meire P (2007a) *Phragmites australis* and silica cycling in tidal wetlands. Aquat Bot 87:134-140

Struyf E, Temmerman S, Meire P (2007b) Dynamics of biogenic Si in freshwater tidal marshes: Si regeneration and retention in marsh sediments (Scheldt estuary). Biogeochemistry 82:41-53

Tande KS, Slagstad D (1985) Assimilation efficiency in herbivorous aquatic organisms - The potential of the ratio method using ^{14}C and biogenic silica as markers. Limnol Oceanogr 30(5):1093-1099

Tréguer P, Nelson DM, Van Bennekom AJ, DeMaster DJ, Leynaert A, Quéguiner B (1995) The silica balance in the world ocean: a reestimate. Science 268:375-379

Tréguer P, Pondaven P (2000) Silica control of carbon dioxide. Nature 406:358-359

Triplett LD, Engstrom DR, Conley DJ, Schellhaass SM (2008) Silica fluxes and trapping in two contrasting natural impoundments of the upper Mississippi River. Biogeochemistry 87:217-230

Turner RE, Qureshi N, Rabalais NN, Dortch Q, Justic' D, Shaw RF, Cope J (1998) Fluctuating silicate:nitrate ratios and coastal plankton food webs. Proc Natl Acad Sci USA 95:13048-13051

Uncles RJ, Stephens JA, Smith RE (2002) The dependence of estuarine turbidity on tidal intrusion length, tidal range and residence time. Continental Shelf Research 22(11-13):1835-1856

Van Damme S, Struyf E, Maris T, Ysebaert T, Dehairs F, Tackx M, Heip C, Meire P (2005) Spatial and temporal patterns of water quality along the estuarine salinity gradient of the Scheldt estuary (Belgium and The Netherlands): results of an integrated monitoring approach. Hydrobiologia 540(1-3):29-45

Van Maldegem DC, Mulder HPJ, Langerak A (1993) A cohesive sediment balance for the Scheldt Estuary. Neth J Aquat Ecol 27(2-4):247-256

Verbanck M, Vanderborght J-P, Wollast R (1994) Major ion content of urban wastewater: assessment of per capita loading. Research Journal Water Pollution Control Federation 61(11/12):1722-1728

Wollast R, De Broeu F (1971) Study of the behavior of dissolved silica in the estuary of the Scheldt. Geochim Cosmochim Acta 35:613-620

Wollast R (1974) The silica problem. In: Goldberg ED (ed) The Sea, Vol. 5. Wiley, New York. pp 359-392.

Wollast R (1978) Modelling of biological and chemical processes in the Scheldt estuary. In: Nihoul JCJ (eds) Hydrodynamics of Estuaries and Fjords. Elsevier Oceanography Series, 23, Amsterdam, Oxford, New-York. pp 63-77.

Wollast R, Mackenzie FT (1983) The global cycle of silica. In: Aston SR (ed) Silicon Geochemistry and Biogeochemistry. Academic Press, London. pp 39-76.

2 Study area & material and methods

2.1 Study area: description of the Scheldt tidal system

The 355 km long Scheldt river and estuary takes its source in Northern France. It flows through Belgium where it receives waters mainly from the Leie (confluence at Ghent), the Dender and the Rupel, and discharges into the North Sea via the Netherlands (Fig. 2.1). The catchment area amounts to approximately 21863 km^2 and about 10 million people live in the river basin (477 inhabitants km^{-2}, Meire et al. 2005) .The shallow, well-mixed and turbid macrotidal estuary of the Scheldt has been extensively described (e.g. Chen et al. 2005a; Meire et al. 2005; Van Damme et al. 2005; Soetaert et al. 2006).

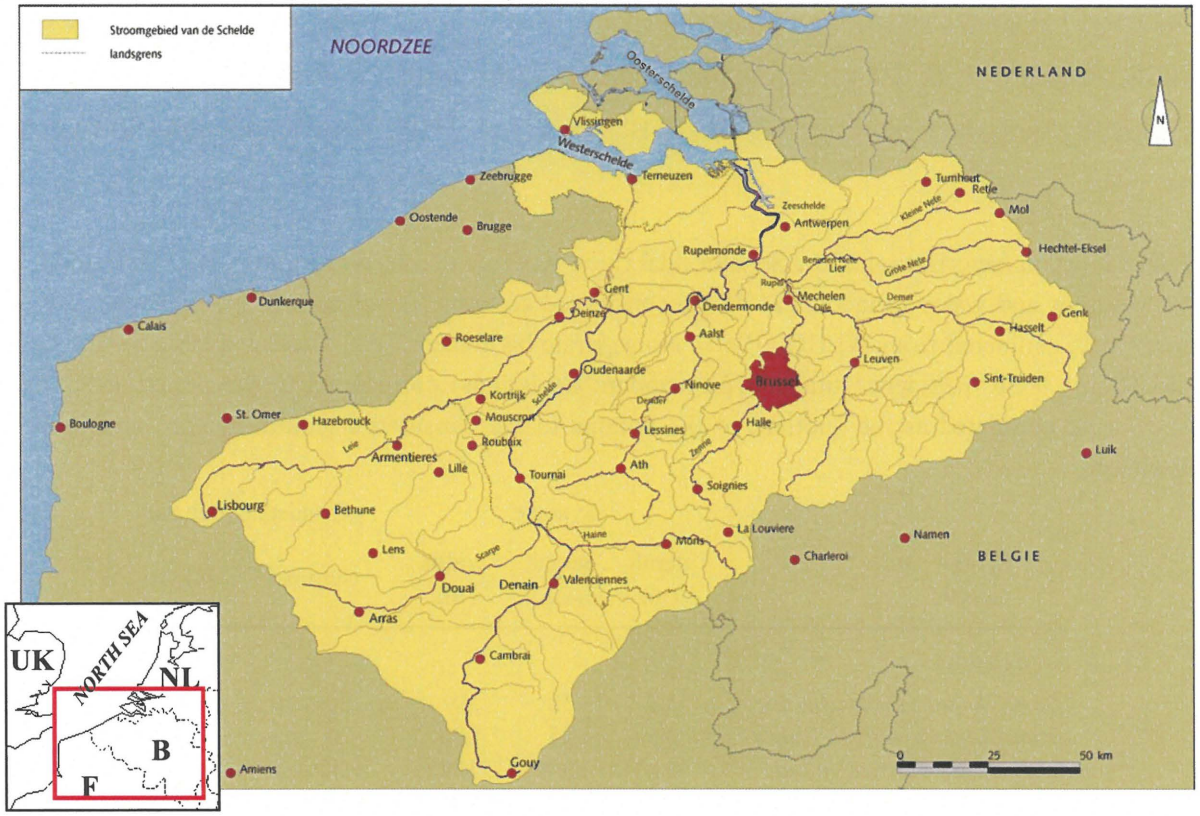

Fig. 2.1: Catchment area and major tributaries of the Scheldt.
Source: Schelde Informatie Centrum (www.scheldenet.nl).

Morphology

The Scheldt estuary will hereafter only comprise the Western Scheldt ("Westerschelde" in Dutch, Fig. 2.1); the Eastern Scheldt ("Oosterschelde") was a second branch of the Scheldt estuary but it is not linked anymore to the Scheldt (except by canals). The Western Scheldt refers in fact only to the Dutch part of the Scheldt estuary; the Belgian part may be called Sea Scheldt (or "Zeeschelde" in Dutch). The latter comprises a tidal freshwater part, which stretches from roughly the confluence with the Rupel (at Rupelmonde, km 94, i.e. 94 km from the mouth of the estuary at Vlissingen) to Ghent (km 157). The tidal wave is blocked by sluices at Ghent and at the mouth of the river Dender. The tidal freshwater system (called hereafter the "tidal river") also includes the river Rupel and the downstream parts of its four tributaries where the tidal influence decreases naturally (Fig. 2.1). The tidal river consists of a single ebb/flood shallow channel (Table 2.1) bordered by mudflats and marshes, but however almost completely canalised upstream of Dendermonde (Meire et al. 2005). Downstream, the section between Rupelmonde and Vlissingen (called hereafter the "estuary") is characterised by a gradual increase in salinity up to about 30 (Van Damme et al. 2005; Soetaert et al. 2006); the salinity pattern varies with the tidal oscillations and also seasonally with the freshwater discharge (Baeyens et al. 1998; Van Damme et al. 2005). The

Table 2.1: Characterization of the Scheldt tidal river. Average depths and widths were calculated from the volumes and water surface areas of the considered sections. Lengths, volumes and water surface areas were estimated from WLHO (1966). No separate bathymetric data were available for the Grote and Kleine Nete. Residence times (with standard deviations) correspond to the period 1996-2005. They were computed as the quotient of the volume of the considered section by the average water discharge.

	Average			Residence time (d)	
River *section*	depth (m)	length (km)	width (m)	Summer	Winter
Scheldt					
from Ghent to Dendermonde	3.2	38	68	4.0 ±1.7	1.3 ±0.9
from Dendermonde to Temse	4.5	25	190	7.4 ±2.8	2.3 ±1.5
from Temse to Rupel mouth	4.8	6	394	3.8 ±1.4	1.2 ±0.8
from Rupel mouth to Hemiksem	6.9	3	363	1.2 ±0.3	0.5 ±0.2
Rupel *(entire)*	4.2	11	180	2.3 ±0.5	1.1 ±0.4
Nete *(entire)*	2.8	16	49	1.9 ±0.6	0.8 ±0.3
Zenne *(last 10 km)*	1.6	(10)	32	0.6 ±0.1	0.4 ±0.1
Dijle *(last 8 km)*	2.5	(8)	35	0.4 ±0.1	0.2 ±0.1

Belgian part of the estuary still consists of a single well-defined ebb/flood channel, but the morphology of the funnel shaped Dutch part is a complex network of ebb/flood channels delimiting large sandflats and bordered by extensive intertidal mudflats and marshes (Fig. 2.2; Van Maldegem et al. 1993). The intertidal zone accounts for 28 % of the total surface in the tidal river and the Belgian part of the estuary, and for 35 % in the Dutch part of the estuary (Meire et al. 2005).

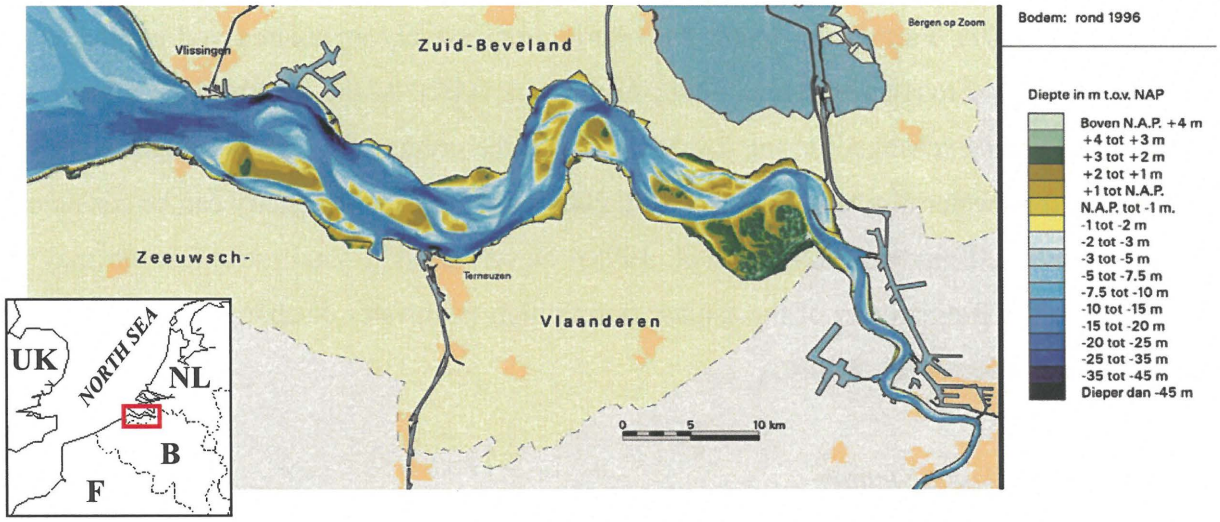

Fig. 2.2: Bathymetry of the Scheldt estuary (around 1996, depth in meters below NAP).
Source: A. Schouwenaar, Ministerie van Verkeer en Waterstaat, Directoraat-Generaal Rijkswaterstaat, Rijksinstituut voor Kust en Zee, RIKZ Middelburg.

Hydrology

The Scheldt is a rain-fed river: the freshwater water discharge exhibits strong seasonal and inter-annual variations related to the precipitation pattern (Soetaert et al. 2006). The long-term annual average amounts to 104 $m^3 s^{-1}$ after the confluence with the Rupel, and maximum and minimum annual discharges of respectively 207 $m^3 s^{-1}$ and 43 $m^3 s^{-1}$ have been recorded (Meire et al. 2005). The average winter discharge (180 $m^3 s^{-1}$ with peak values of 600 $m^3 s^{-1}$) is also higher than the summer one (60 $m^3 s^{-1}$, with values as low as 20 $m^3 s^{-1}$) (Baeyens et al. 1998). Annually, 56 % of the freshwater discharge in the tidal river originates from the Rupel (Baeyens et al. 1998). But, before it enters the Scheldt estuary, the water from the river Scheldt may be partially or even completely deviated towards the Ghent – Terneuzen canal to sustain industrial and navigation needs. The contribution of the Rupel to the total freshwater input can therefore increase from about 46 % in winter to more than 70 % during dry

summers. The increase in freshwater residence time during the summer period is thus more pronounced in the Scheldt between Ghent, Dendermonde and Temse than in the Rupel and in the Nete (Table 2.1). For the estuary, residence times of 50 days in winter and 70 days in summer have been estimated by Soetaert and Herman (1995) using model simulations.

The Scheldt is a macrotidal estuary. At the mouth of the estuary, the mean tidal range is 3.8 m, but due to the funnel shape of the estuary, it increases up to about 5 m in the zone between Antwerp and the confluence with the Rupel (Baeyens et al. 1998; Meire et al. 2005; Arndt et al. 2007). Further upstream, the tide is progressively attenuated and at Ghent, the average range is 2 m (Baeyens et al. 1998; Arndt et al. 2007). At the mouth of the estuary, the amount of water exchanged during a tide cycle is three orders of magnitude higher than the amount of freshwater discharged (Arndt et al. 2007) and the Scheldt estuary can be considered as vertically well-mixed (Baeyens et al. 1998). Nevertheless a small stratification may be observed in the Belgian part of the estuary during high freshwater discharge events (Baeyens et al. 1998; Soetaert et al. 2006).

Suspended particulate matter

The suspended particulate material (SPM) contains about 10-20 % of organic matter (Chen et al. 2005a) mainly of anthropogenic origin, but with significant contributions of the organic matter from soil and vegetation and from phytoplankton (Abril et al. 2002; Van Damme et al. 2005). The inorganic fraction is generally composed of silty clays; the contribution of the sandy grain-size fraction remains generally low but can possibly increase in the turbidity maximum area (Chen et al. 2005a, 2005b). The SPM from the Scheldt has thus the tendency to form flocs (Chen et al. 2005a, 2005b). Both the mud and sand fractions are composed predominantly of quartz, but also of feldspars, clay minerals (illite, kaolinite, montmorillonite), carbonates and iron hydroxides (Wollast and De Broeu 1971; Wartel 1977; Bouezmarni and Wollast 2005). Except for the muddy deposits on the banks, the grain-size distribution is generally coarser in bottom sediments of the channel, with generally sandy deposits in the tidal river and in the Dutch part of the estuary, and coarse sediments or even hard bottom in the Belgian part of the estuary upstream Antwerp (Wartel 1977). Downstream Antwerp however, the bottom sediments are composed of sand, sandy mud and mud in the channel, and even purely muddy sediments are encountered in the access channels to harbours (Wartel 1977; Wartel et al. 1999).

The distribution of the SPM is strongly related to the water energy pattern, which is principally driven by two components: the energy originating from tides and that from the riverine, freshwater discharge (Fig. 2.3; Chen et al. 2005a; Arndt et al. 2007). As a result, two local SPM maxima of several hundreds of milligrams per litre can be observed: one in the upper part of the tidal river induced by the riverine energy, and a more important one, between Antwerp and the confluence with the Rupel, corresponding to the maximum of the tidal energy (Fig. 2.3; Chen et al. 2005a; Arndt et al. 2007). As the latter one is located at the freshwater-brackish water interface, it has also been attributed to flocculation processes and to the convergence of bottom currents directed landwards in the estuary and seawards in the tidal river (Fig. 2.4; Baeyens et al. 1998; Chen et al. 2005a). This turbidity maximum is characterised by alternating settling and resuspension processes during the tidal cycle, leading high short-term variations in the SPM concentrations (Chen et al. 2005a). The SPM transport is also strongly influenced by the local morphology (Chen et al. 2005a).

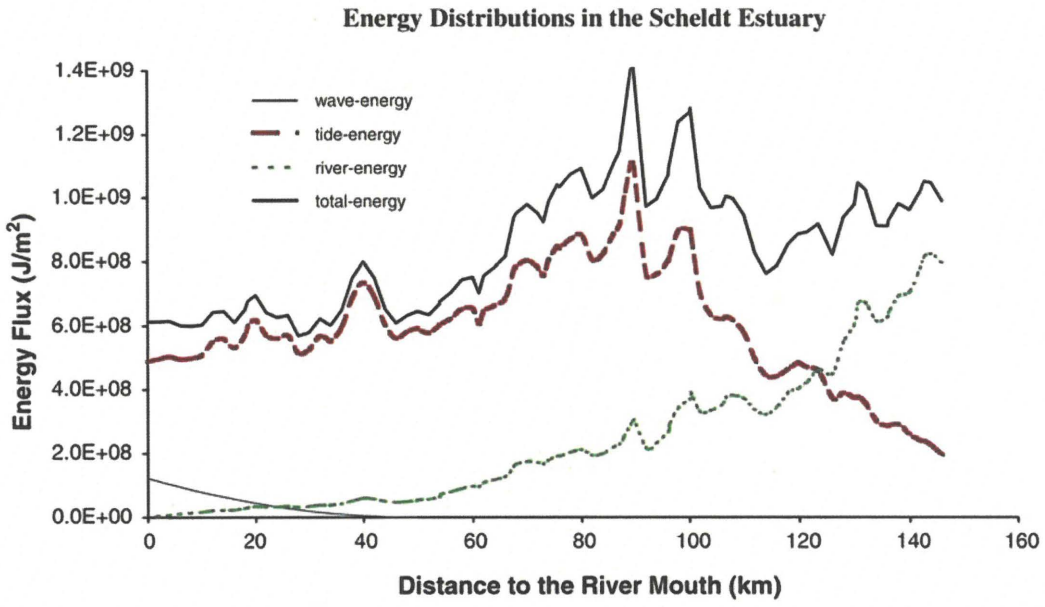

Fig. 2.3: The water energy distribution along the Scheldt tidal system. The figure is redrawn from Chen at al. (2005a). Wave energy ranges from 2.5 to 107 J/m^2 at the river mouth to zero near 50 km; it has been multiplied by a factor 5 to allow its representation on the graph.

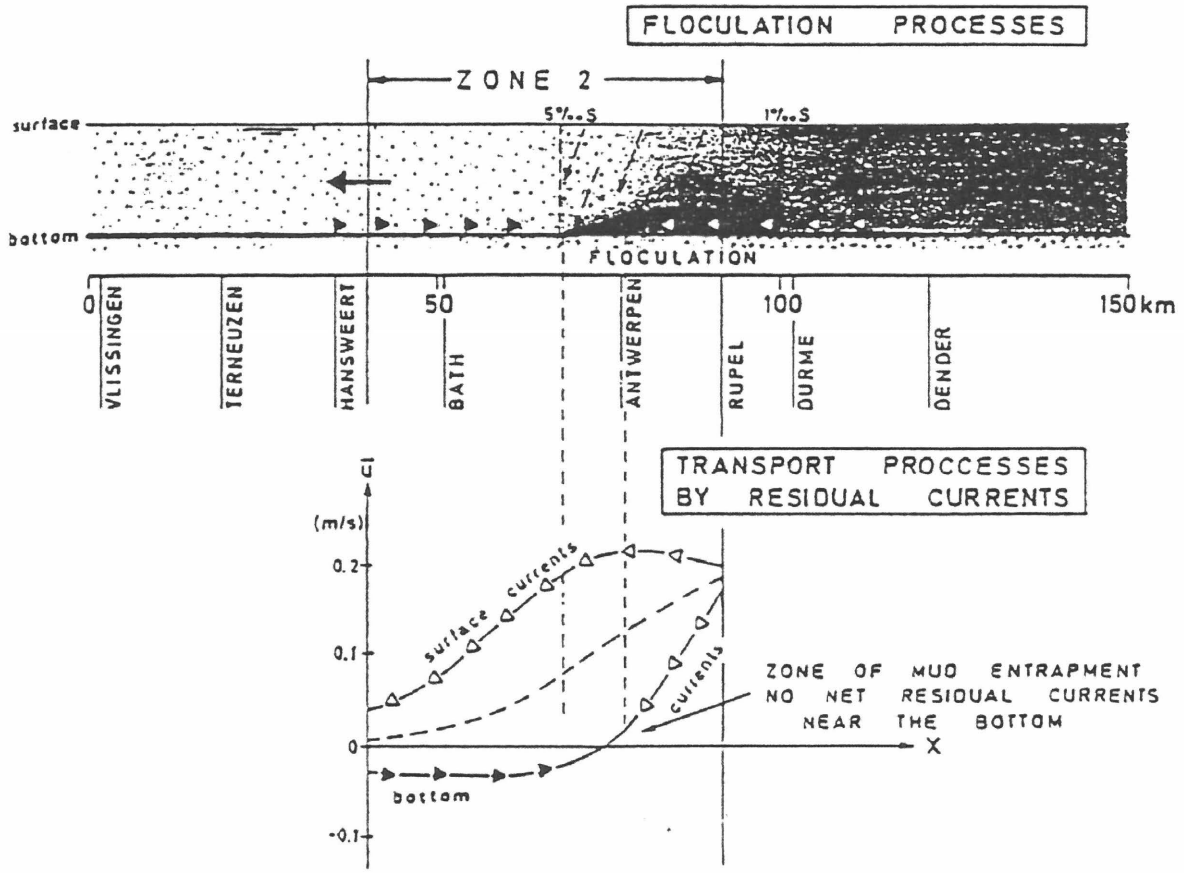

Fig. 2.4: Influence of flocculation processes and of the residual surface and bottom currents on the accumulation of mud between Antwerp and the confluence with the Rupel. The figure is redrawn from Wollast (1988).

While the net transport of SPM is in the same direction of that of the water in the tidal river, the estuarine SPM consists of a gradual mixture of SPM of freshwater source and that of marine origin (Verlaan et al. 1998). There is indeed a net import of SPM from the coastal zone at the mouth of the estuary (Van Maldegem et al. 1993), implying that an intense dredging activity is required in the estuary to ensure the shipping access to harbours of Antwerp (Chen et al. 2005a; Meire et al. 2005).

Nutrients and oxygen

After decades of heavy pollution history, the Scheldt estuary is still strongly affected by human activities, and nitrogen and phosphorous are never limiting factors for phytoplankton growth (Van Damme et al. 2005; Soetaert et al. 2006; Van der Zee et al. 2007). In 2003, maximum dissolved inorganic nitrogen and phosphorous concentrations reached

1300 µmol L^{-1} and 50 µmol L^{-1} respectively (Van der Zee et al. 2007). In contrast, silica can be depleted in summer in case of low water discharge (Muylaert et al. 2001).

Most of the anthropogenic pressure to the Scheldt is concentrated on the tidal river (Meire et al. 2005). Due to the high amount of organic matter and ammonium in communal and industrial wastes (particularly in the wastewater from Brussels, which was only partially treated at the time of this study), the oxygen level is severely under-saturated in most of the tidal river and the Belgian part of the estuary (Van Damme et al. 2005). However, the oxygen content rises quickly in the Dutch part of the estuary, leading to oxygen saturation or even super-saturation in spring due to the phytoplankton production.

Phytoplankton

The phytoplankton speciation in the Scheldt is representative of that generally observed in temperate estuaries of the Northern hemisphere (Muylaert and Sabbe 1999 and references therein).

Tidal river

The phytoplankton community in the tidal river is dominated by diatoms throughout the year (Muylaert et al. 2000; Lionard 2006; Lionard et al. 2008a). Two blooms have been identified: one in spring, originating from the upper Scheldt river and dominated by *Stephanodiscus hanszchii*; another one in summer, which develops *in situ* near Dendermonde and is dominated by *Cyclotella scaldensis*, a genus closely related to *C. meneghiniana* (Muylaert et al. 2000). The summer bloom in the tidal river can lead to a high biomass: chlorophyll *a* concentrations of several hundreds of micrograms per litre are frequently observed in summer (Van Damme et al. 2005; Lionard et al. 2008b).

Estuary

In the estuary, highest chlorophyll *a* levels are generally observed in spring but they never reach the high values measured in the tidal river in summer (Van Damme et al. 2005). Also, chlorophyll *a* concentrations display a local minimum between Antwerp and the Belgian/Dutch boundary (Van Damme et al. 2005).

Diatoms were reported as being the dominant species along the estuary, but green algae and euglenid species (such as *Scenedesmus* sp., *Nannochloris* sp. and *Euglena* sp.) could nevertheless be important constituents of the phytoplankton community, especially in the zone corresponding to the maximum of turbidity (Rijstenbil et al. 1993; Muylaert and Sabbe 1999; Lemaire et al. 2002; Boschker et al. 2005; Brochard et al. 2005; Dijkman and

Kromkamp 2006a, 2006b). *Phaeocystis* may also be encountered in the Scheldt estuary. These species bloom in the adjacent coastal zone in April and May (Lancelot 1995); as for diatoms (Arndt 2008; Muylaert et al. 2009), they may be transported into the Scheldt estuary as far as salinity 10 (Brochard et al. 2005; Dijkman and Kromkamp 2006a). *Phaeocystis* can contribute to about half of the phytoplankton biomass in the lower part of the estuary but this should nevertheless only concern the months of April and May, as almost no *Phaeocystis* cells are generally observed outside this two-month period in the Belgian coastal zone (Rousseau et al. 2002; Brochard et al. 2005; Muylaert et al. 2006).

In the most freshwater part of the estuary, the diatom community was clearly dominated by *Cyclotella meneghiniana* and/or *Actinocyclus normanii*, which were very likely originating from the tidal river. In the rest of the estuary, the diatom community was composed of marine species of different sizes, such as *Thalassiosira* sp., *Asterionella* sp., *Ditylum brightwellii*, *Odontella* sp., *Raphoneis amphiceros*, *Coscinodiscus* sp., *Rhizosolenia* sp., *Skeletonema costatum*, *Chaetoceros* sp. and *Thalassionema nitzschioides* (Rijstenbil et al. 1993; Muylaert and Sabbe 1999; Koeman et al. 2004; Boschker et al. 2005; Brochard et al. 2005, 2006; Dijkman and Kromkamp 2006b; Muylaert et al. 2009). Some of these species were probably originating from the coastal zone (such as *Rhizosolenia* sp., *S. costatum* and *Chaetoceros* sp.) as they are typical components of the diatom communities of this area (Rousseau et al. 2002; Muylaert et al. 2006; Muylaert et al. 2009), but some others were specific to the estuary (such as *Odontella* sp. and *R. amphiceros*) as they were not encountered at the highest salinities (Dijkman and Kromkamp 2006b; Muylaert et al. 2009).

Inter-tidal areas and shallow waters account for a large fraction of the surface area of the Scheldt estuary: they represent respectively 19 % and 10 % of the total surface area of the Dutch part of the Scheldt estuary (Meire et al. 2005). The microphytobenthos, mainly composed of benthic diatoms (de Jong and de Jonge 1995; Lucas et al. 2001), contributes to 17 % of the total gross primary production in the Scheldt (de Jong and de Jonge 1995; Gazeau et al. 2005) and it can be resuspended by tidal oscillations (Lucas et al. 2001) and wind-induced waves (de Jonge and van Beusekom 1995). So, even if most of the diatoms observed by Muylaert and Sabbe (1999) in May 1993 from salinity 0.5 to 20 were planktonic species, benthic and tycoplanktonic species (such as *Odontella sp.*, *R. amphiceros*, *Thalassiosira proschkinae*, *Navicula sp. and Nitzschia sp.*) were frequently observed in surface water samples (Muylaert and Sabbe 1999; Boschker et al. 2002; Koeman et al. 2004; Brochard et al. 2005, 2006; Dijkman and Kromkamp 2006a).

Zooplankton

In the tidal river, the zooplankton community is dominated by rotifers (Tackx et al. 2004), which are not expected to exert a strong pressure on the diatom community responsible for the summer bloom (Muylaert et al. 2005). This is also supported by the fact that diatoms can reach a high biomass in summer (Muylaert et al. 2000; Lionard et al. 2008b). In the Dutch part of the estuary however, better oxygen conditions and longer water residence times allow the domination of the zooplankton community by endemic or neritic calanoid copepods (Soetaert and Van Rijswijk 1993). Even, the increase of the oxygen concentrations in the Belgian part of the estuary during the last decade resulted in an upstream shift in the presence of the calanoid copepod *Eurytemora affinis* (Appeltans et al. 2003).

2.2 Sampling

The Scheldt tidal river and its tributaries were sampled once a week from February 2003 to February 2004, except in winter (once a month). The sampling was performed from a bridge or a landing stage. The upper Scheldt river and the five main tributaries (the Dender, Zenne, Dijle, Kleine and Grote Nete) were sampled at the tidal limits and the tidal river was sampled at three stations: Dendermonde (km 124), Temse (km 101) and Hemiksem (km 91) (Fig. 2.5). Hemiksem was considered as the downstream limit of the tidal river, as the salinity at this station was on average 1 and never exceed 2.9.

The Scheldt estuary and the coastal zone were sampled during 11 campaigns on board of the *RV Belgica* from 2003 to 2005 (2003: 17-21 March, 30 June - 3 July; 2004: 3 February, 13-19 May, 19-20 July, 6-10 September, 29 November - 2 December; 2005: 11-14 April, 2-3 May, 11-15 July, 11-14 October). Surface water samples were taken using Niskin bottles. In the estuary, the sampling was performed along the navigation channel over the entire salinity gradient (from Rupelmonde, km 94, to Vlissingen, km 0, Fig. 2.5). From 10 to 20 water samples were taken per campaign; some sampling stations were fixed and the other ones were chosen depending on the salinity. The coastal zone was sampled at 5 fixed locations (Fig. 2.6).

The sampling was performed irrespective to the tide phase in both the tidal river and the estuary. Our study period (2003-2005) could be considered as representative for years with low water discharges, especially for the period between May and October (Table 2.2).

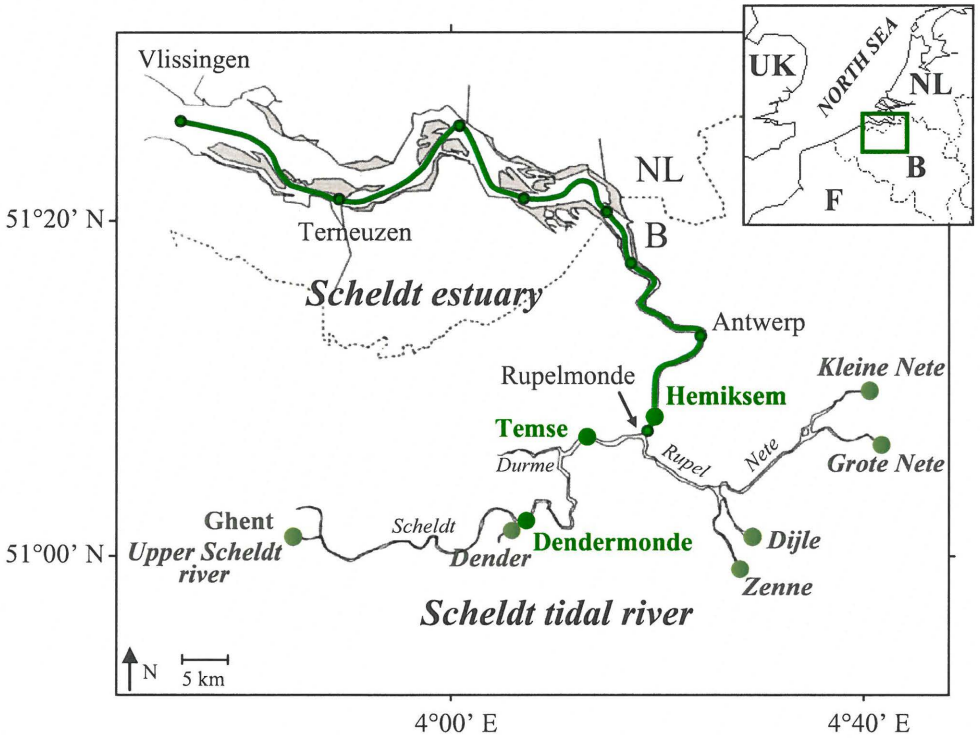

Fig. 2.5: Map of the sampling in the Scheldt tidal river and estuary. City and river names are in regular and italic fonts, respectively. The Durme is nowadays a dead arm with negligible discharge. The sampling stations in the tidal river (in bold) are indicated by green dots for the tidal limits (Ghent, Dender, Zenne, Dijle, Grote Nete, Kleine Nete) and by red dots for stations along the tidal river. In the estuary, the sampling was performed along the navigation channel, which is indicated in blue. Blue dots indicate fixed sampling stations. The dashed line follows the border between Belgium and the Netherlands.

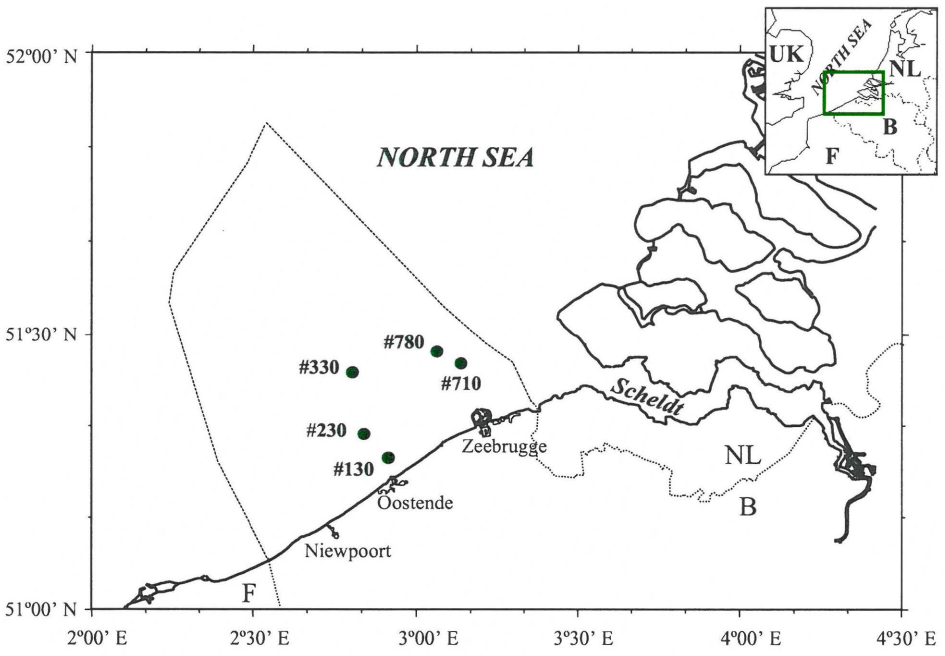

Fig. 2.6: Map of the sampling locations in the Belgian coastal zone. Sampling stations are indicated by dots. The dash line in the North Sea represents the Belgian Exclusive Economic Zone.

Table 2.2: Average freshwater discharge (in $m^3 s^{-1}$). The standard deviation of the annual or seasonal average discharges during 1980-2005 is also indicated (± SD).

	1980-2005	2003	2004	2005
Full year	124 ± 31	113	95	94
May-October	80 ± 21	67	64	68
Jan.-Apr. and Nov.-Dec.	167 ± 46	159	126	120

2.3 Chemical analyses

SPM, DSi and BSi

Sampling and SPM

Water samples (from 20 to 150 mL) were vacuum filtered on a pre-weighed polycarbonate filter (Whatman Nuclepore, Ø 47 mm, 0.4 µm pore size). The SPM collected on the filter was rinsed with Milli-Q water and dried overnight at 50°C. The filter was weighed again for the SPM determination by weight difference and the filter was kept for BSi analysis. The filtrate was acidified (with 200 µL of 2 mol L^{-1} HCl per 50 mL of sample) and kept in the dark at 4°C until DSi analysis.

DSi analyses

Samples from the tidal river were measured colorimetrically for DSi on a Skalar Auto-analyser following a method adapted from Koroleff (1983).

In the estuary, samples were measured manually following the colorimetric method of Koroleff (1983). The salinity effect was taken into account by performing calibrations in artificial solutions of different salinities (the solution of salinity 35 was obtained with 32 g L^{-1} of NaCl and 14 g L^{-1} of $MgSO_4$). Slopes at intermediate salinities were retrieved by linear interpolation. When needed, samples were diluted with Milli-Q water and the induced shift in salinity was taken into account.

The slopes displayed important variations from one measurement to another, especially at the lower salinities (Fig. 2.7). It was verified by replicate analyses on samples that, as expected, this variability did not have any incidence on the measurement of the DSi concentration. The causes of the variability of the standard slopes were not investigated, but observations suggested that the freshness of the molybdate solution could play a role (the ascorbic acid solution was renewed each time) (Koroleff, 1983), as well as, possibly, the ambient temperature.

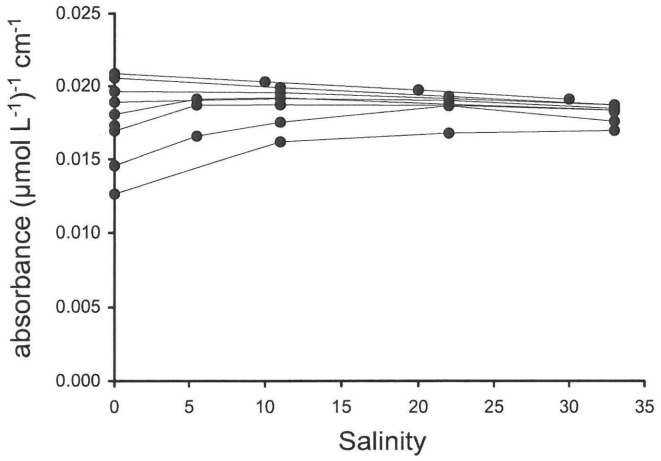

Fig. 2.7: Slopes of the DSi analysis calibrations performed during the measurement of the DSi versus salinity profiles in the estuary.

BSi analyses

BSi was determined by a wet-alkaline method. Because high amounts of lithogenic silica are present in the SPM of the tidal river (Bouezmarni and Wollast 2005), the aluminium released during the digestions was used to correct for the concomitant dissolution of Si from lithogenic material following the methods from Kamatani and Oku (2000) and Ragueneau et al. (2005), which were combined and modified. The digestion was performed on a single SPM filter and, compared to Ragueneau et al. (2005), four digestion steps were performed (instead of two) to improve the correction (Fig. 2.8). Furthermore, the SPM was not rinsed between the steps to reduce the time necessary for the digestion.

The filter with the SPM was placed at the bottom of a 15 mL polypropylene centrifugation tube and covered with 10 mL (V_D) of 0.2 mol L^{-1} NaOH (Fig. 3). The tube was incubated in a shaking water bath at 95°C for one hour (step 1), and centrifuged at 5000 rpm, 5°C during 10 minutes. A 5 mL (V_A) aliquot of the supernatant was taken and acidified with 1.25 mL of 1 mol L^{-1} HCl. This digestion step was then repeated three times (steps 2 to 4): 5 mL of 0.2 mol L^{-1} NaOH was added to the remaining solution in the centrifugation tube, and the tube was placed again in the shaking water bath but for 30 minutes.

The four aliquots of the supernatant solutions were analysed for DSi and Al concentrations (Si_n and Al_n, with n = 1 to 4), either by ICP-OES (Inductively Coupled Plasma – Optic Emission Spectroscopy) or by colorimetry: using a Skalar Auto-analyser for DSi (as described previously) and manually for dissolved Al following Dougan and Wilson (1974).

There were no significant differences between the results obtained by the two methods for DSi analyses.

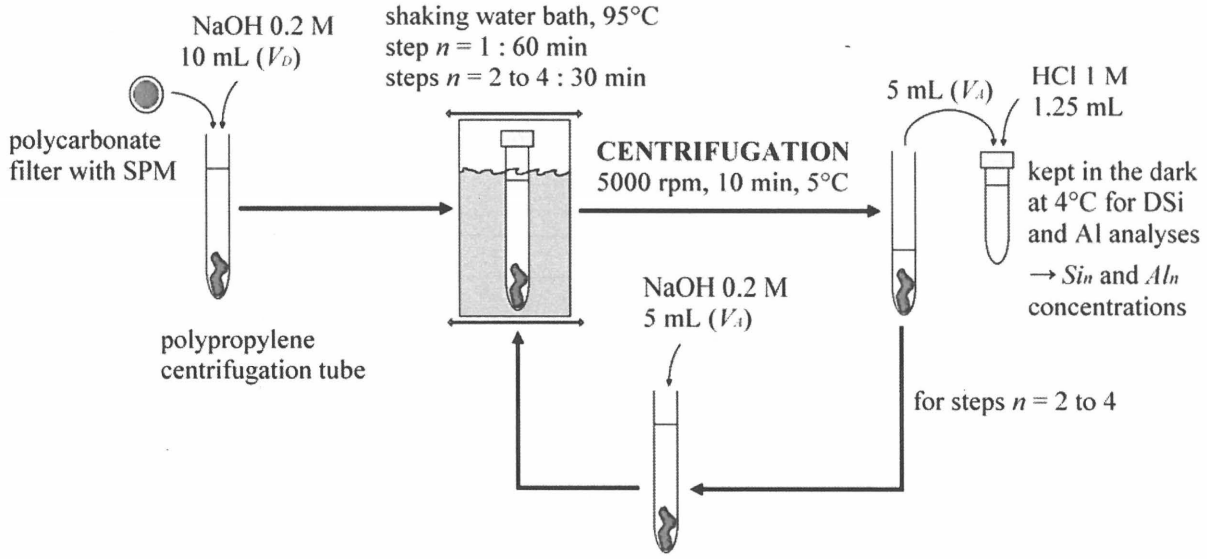

Fig. 2.8: Scheme of the BSi digestion protocol.

Following Kamatani and Oku (2000) and Ragueneau et al. (2005), we assumed that: 1) all the BSi is dissolved during the first digestion step, 2) all the Al measured originates from the digestion of lithogenic material and 3) this lithogenic material dissolves with a constant Si/Al ratio (designated here k). Under these assumptions, the DSi and Al concentrations measured in the aliquots follow the equation:

$$Si_n = c_n \cdot \frac{BSi}{V_D \cdot d} + k \cdot Al_n \qquad \text{(Eq. 2.1)}$$

with:

$$c_n = \left(\frac{V_D - V_A}{V_D} \right)^{n-1} \qquad \text{(Eq. 2.2)}$$

where BSi is the amount of BSi on the filter, V_D and V_A the volumes of 0.2 mol L^{-1} NaOH additions (respectively 10 and 5 mL, Fig. 3) and d the dilution factor of 1.25 due to the addition of HCl in the aliquots of the supernatant solutions. BSi (as well as k, not shown) is then calculated by a least-squares multiple regression on Si_n:

$$BSi = V_D \cdot d \cdot \frac{\left(\sum_{n=1}^{4} Al_n^{\,2} \right) \cdot \left(\sum_{n=1}^{4} c_n \cdot Si_n \right) - \left(\sum_{n=1}^{4} c_n \cdot Al_n \right) \cdot \left(\sum_{n=1}^{4} Si_n \cdot Al_n \right)}{\left(\sum_{n=1}^{4} c_n^{\,2} \right) \cdot \left(\sum_{n=1}^{4} Al_n^{\,2} \right) - \left(\sum_{n=1}^{4} c_n \cdot Al_n \right)^2} \qquad \text{(Eq. 2.3)}$$

Among the 455 correlation coefficients (r^2) obtained from the multiple regressions performed for each BSi measurement presented in this study, most values were higher than 0.999 (Fig. 2.9). In addition, the method was tested on pure lithogenic and biogenic silica suspensions, and known mixtures of the two (Carbonnel 2003). This supports the three assumptions indicated above and validates the use of Eq. 2.1.

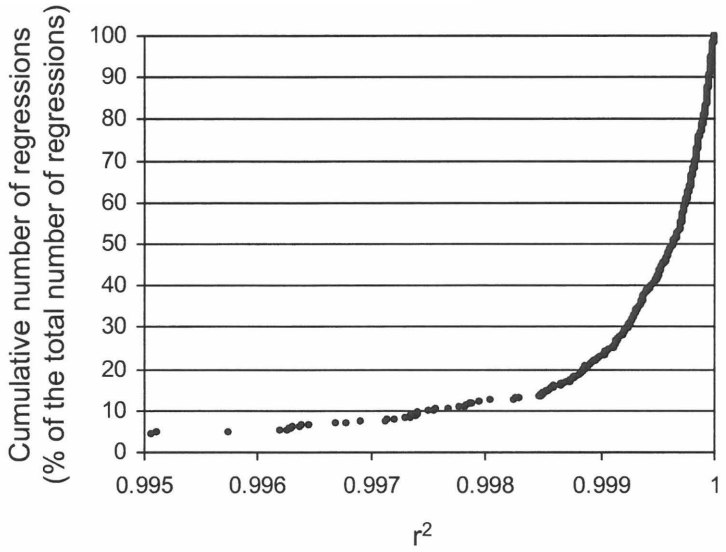

Fig. 2.9: Cumulative number of correlation coefficients (r^2) expressed as a percentage of the total number (455) of BSi analyses presented in this study.

Ragueneau et al. (2005) considered that BSi can be correctly measured using their method only if the amount of BSi on the filter does not exceed 10 µmol. Nonetheless, with our method, quantities up to 20-25 µmol (in the tidal river in summer) were successively measured, as shown by high correlation coefficients (r^2 higher than 0.9995). This may be due to the fact that the duration of our first digestion (60 min) was longer than that set by Ragueneau et al. (2005) (40 min).

As in the method proposed by Kamatani and Oku (2000), an estimation of *BSi* could have also been provided by the y-axis intercept which would have been obtained when plotting the total amounts of DSi released after each digestion step against those of Al. As this methodology and Eq. 2.3 were based on the same assumptions (see above), they provided similar results (not shown). The advantage of Eq. 2.3 is that the DSi and Al concentrations of each digestion step are processed independently from those of the other steps: Eq. 2.3 permits the direct calculation of *BSi* even if a digestion step needs to be discarded (for instance due to

incomplete dissolution of the BSi during step 1, or to doubtful DSi or Al concentrations at steps 1 to 4).

In the following, BSi concentrations are expressed in μmol L^{-1} but the BSi content of SPM is expressed as the mass content of hydrated silica $SiO_2.mH_2O$, with $m \leq 2$ (Martin-Jézéquel et al. 2000); we assumed $m = 1/3$, a value close to the measurement of Kamatani and Oku (2000).

Particulate organic carbon and contribution of diatoms to the chlorophyll a concentrations

Sampling

SPM was collected on a precombusted (4h, 500°C) GF/F filter (Ø 47 mm, 0.7 μm pore size) for the determination of particulate organic carbon (POC), and on a GF/F filter (Ø 25 mm, 0.7 μm porosity) for the measurement of chlorophyll *a* and marker pigments. Both filters were kept frozen at -20°C until analysis.

POC

POC was measured using a Fisons NA-1500 elemental analyser after carbonate removal from the filters by overnight exposure to strong acid fumes. The measurements of the POC concentrations at Hemiksem and in the estuary were performed by N. Roevros (LOCGE-ULB).

Pigments and diatom chlorophyll *a* concentrations

Pigments concentrations were measured by HPLC (High Pressure Liquid Chromatography) following Wright and Jeffrey (1997). The CHEMTAX software (Mackey et al. 1996) was used to calculate the contribution of different algal groups to the total chlorophyll *a* using ratios of marker pigments (specific for algal groups) to chlorophyll *a* (Lionard 2006, 2008a). The chlorophyll *a* concentrations ascribed to diatoms (DiatChl*a*) were estimated using fucoxanthin, diatoxanthin and diadinoxanthin as marker pigments for diatoms. The contribution of the diatoms to the phytoplankton biomass was assessed as the ratio between DiatChl*a* and chlorophyll *a* concentrations. The measurements of the pigment concentrations and the CHEMTAX calculations were performed by M. Lionard (UG).

CHEMTAX matrixes

The CHEMTAX matrix that was used in the tidal river was identical to that of Lionard et al. (2008a); the initial and final matrixes are reported in Lionard (2006). Comparisons with microscopic observations revealed that this method can indeed provide a good estimate of the

phytoplankton speciation and of the phytoplankton and diatom biomasses in the Scheldt tidal river (Lionard et al. 2008a).

In the coastal zone and in the most seaward part of the estuary, the contribution of *Phaeocystis* to total chlorophyll *a* could not be disentangled from that of the diatoms. Indeed, *Phaeocystis* contain fucoxanthin, diatoxanthin and diadinoxanthin, which are the marker pigments used for diatoms (Llewellyn and Gibb 2000). Usually, *Phaeocystis* can be distinguished by their specific marker pigment 19′–hexanoyloxyfucoxanthin (Llewellyn and Gibb 2000), but the strains of the Belgian coastal zone do not contain this pigment (Antajan et al. 2004). Muylaert et al. (2006) successfully used the chlorophyll c_3 as a specific marker pigment for *Phaeocystis* but the elution method we employed could not allow the separation of this pigment, and thus nor the accurate measurement of its concentration. As a result, the contribution of the *Phaeocystis* to the total chlorophyll *a* in our samples was lumped with that of the diatoms. The CHEMTAX matrix was adapted from that of Muylaert et al. (2006) and Lionard et al. (2008a): it includes neoxanthin and violaxanthin as marker pigments for chlorophytes (Lionard et al. 2008a), and diatoms and *Phaeocystis* constitute a single group with fucoxanthin, diatoxanthin and diadinoxanthin ratios corresponding to the average ones of those for diatoms and *Phaeocystis* used by Muylaert et al. (2006). The initial and final CHEMTAX matrixes applied on our pigment data at salinities higher than 24 are reported in Table 2.3 ("Salinity 24-35").

The estuarine phytoplankton is of freshwater origin in the upper part of the estuary (salinities lower than 10) but predominantly composed of marine species in the rest of the estuary (see above). So the estuarine pigment dataset was divided in two groups, one corresponding to salinities 0-13 and another one to salinities 7-24 (these groups also included the pigment datasets obtained for pre-filtered water samples for ^{32}Si incorporation, see below), on which independent CHEMTAX analyses were performed using slightly different matrixes for both groups (Table 2.3). The pigment data at salinities 7-13 and 24-30 were included in two groups, but the corresponding phytoplankton compositions calculated using the two matrixes led to similar results. Still, the transitions of the contribution of the different algal groups to the total chlorophyll *a* between salinities 7-13 and 24-30 were ensured by linear interpolation versus the salinity. The initial and final CHEMTAX matrixes are also reported in Table 2.3.

Table 2.3: Initial/final pigment ratios in the CHEMTAX analyses for the three estuarine groups.

	Peridin	Fucoxanthin	Neoxanthin	Violaxanthin	Diadinoxanthin Diatoxanthin	Alloxanthin	Lutein	Zeaxanthin	Chlorophyll *b*
Salinity 0-13									
chlorophytes	0	0	0.018 / 0.024	0.024 / 0.034	0	0	0.232 / 0.313	0.025 / 0.034	0.096 / 0.130
cryptophytes	0	0	0	0	0	0.275 / 0.408	0	0	0
cyanobacteria	0	0	0	0	0	0	0	0.202 / 0.200	0
diatoms	0	0.378 / 0.508	0	0	0.043 / 0.057	0	0	0	0
dinophytes	0.366 / 0.513	0	0	0	0.152 / 0.161	0	0	0	0
euglenophytes	0	0	0	0	0.137 / 0.151	0	0	0	0.277 / 0.277
Salinity 7-30									
chlorophytes	0	0	0.018 / 0.021	0.024 / 0.028	0	0	0.058 / 0.081	0.034 / 0.040	0.240 / 0.157
cryptophytes	0	0	0	0	0	0.275 / 0.280	0	0	0
cyanobacteria	0	0	0	0	0	0	0	0.232 / 0.230	0
diatoms (+ *Phaeocystis*)	0	0.383 / 0.380	0	0	0.028 / 0.028	0	0	0	0
dinophytes	0.366 / 0.432	0	0	0	0.152 / 0.177	0	0	0	0
euglenophytes	0	0	0	0	0.137 / 0.137	0	0	0	0.277 / 0.277
Salinity 24-35									
chlorophytes	0	0	0.018 / 0.025	0.024 / 0.033	0	0	0.058 / 0.079	0.034 / 0.046	0.240 / 0.328
cryptophytes	0	0	0	0	0	0.275 / 0.284	0	0	0
cyanobacteria	0	0	0	0	0	0	0	0.232 / 0.230	0
diatoms + *Phaeocystis*	0	0.383 / 0.511	0	0	0.028 / 0.038	0	0	0	0
dinophytes	0.366 / 0.505	0	0	0	0.152 / 0.169	0	0	0	0
euglenophytes	0	0	0	0	0.137 / 0.184	0	0	0	0.277 / 0.371

2.4 Distinction between fractions of BSi associated or not with living diatoms

BSi may not only be associated with living diatom (BSi_{liv}) as a significant fraction may consist of detrital biogenic silica (BSi_{det}) such as frustules of dead diatoms or phytoliths. It was assumed that the dynamics of BSi_{liv} and BSi_{det} followed respectively those of DiatChl*a* and of the fraction of the SPM which is not linked to BSi nor to living diatoms (SPM_{nbld}), estimated as:

$$SPM_{nbld} = SPM - BSi \cdot M_{BSiO2} - DiatChla \cdot \beta_{POC/Chla} \cdot \beta_{OM/POC} \quad \text{(Eq. 2.4)}$$

with:

- DiatChl*a* and SPM expressed in mg L^{-1}, and BSi in mmol L^{-1},
- the molar mass of BSi (as hydrated SiO_2): $M_{BSiO2} = 66$ g mol^{-1},
- the chlorophyll *a* to POC mass ratio in the (diatom-dominated) phytoplankton of the Scheldt tidal river: $\beta_{POC/Chla} = 30$ (Muylaert et al. 2001),
- the conversion factor from POC to organic matter: $\beta_{OM/POC} = 2.5$. This value corresponds to the ratio of the molar masses of CH_2O and C, and was also observed in an eutrophic estuary by Suzumura et al. (2004).

The distinction between BSi_{liv} and BSi_{det} was made by performing a multiple regression between BSi and the two explicative variables DiatChl*a* and SPM_{nBld}: the partial coefficients associated with DiatChl*a* and SPM_{nBld} (respectively k_1 and k_2) were fitted to obtain the best correlation between measured BSi concentrations and those estimated by the multiple regression ($\hat{BSi}$) calculated as:

$$\hat{BSi} = k_1 \cdot DiatChla + k_2 \cdot SPM_{nbld} \quad \text{(Eq. 2.5)}$$

BSi_{liv} was estimated as the product of k_1 (called hereafter BSi_{liv}/DiatChl*a*) and DiatChl*a*, and BSi_{det} was calculated as the difference between BSi and BSi_{liv}. The multiple regressions (as well as correlations and statistical Student's t-tests) were performed following Dagnelie (1973, 2006) but without any independent constant terms, as the latter would not have been significantly different from zero (at 95 % confidence) if they were appended. In the tidal river, the multiple regression was kept linear, but in the estuary, the residuals displayed a significant pattern (see Chapter 5), indicating that a better regression could be obtained by a non-linear multiple regression; the procedure and the non-linear multiple regression model are described in Chapter 5.

2.5 ^{32}Si incorporation experiments

In 2005, kinetic experiments of ^{32}Si incorporation were performed at 8 selected stations in the estuary (mainly the fixed ones) and at #330 in the coastal zone. ^{32}Si incorporation experiments were also performed on diatom cultures: the incubation procedure is described in Annex 3B, but the radioactivity counting and the calculations were nevertheless performed as described below.

Methodology for ^{32}Si incorporation experiments (Scheldt water samples)

Water from the same Niskin bottle as that used for the determination of the other parameters was pre-filtered on a 400 µm mesh to remove the zooplankton, and kept in the dark for 1-3 hours. Chlorophyll *a* and DiatChl*a* concentrations in the pre-filtered water were also measured as described above.

In April and May 2005, the water was dispatched in polycarbonate 50 mL bottles. To evaluate the abiotic sorption of DSi on particles, one bottle was added with 300 µL of 10 % azide to inhibit the phytoplankton growth. The samples were spiked with 50 µL of the ^{32}Si source (101.9 nCi mL^{-1}, 23570 Bq µg^{-1}), corresponding to a (neglected) increase of the ambient DSi concentration by 5.7 nmol L^{-1}. Five or seven aliquots of 1 or 2 mL were taken in each bottle and kept frozen for the measurement of the initial ^{32}Si activity.

In July 2005, the water was spiked with the radiotracer and 1 mL aliquots were taken before it was dispatched in 50 mL incubation bottles. One bottle also contained azide. At station #330, the ambient DSi concentration was low (1.2 µmol L^{-1}, Chapter 4) and the variation of the DSi uptake rate with ambient DSi concentration was also investigated by adding cold DSi in 6 extra spiked Scheldt water samples so that final DSi concentrations ranged from 1.7 to 13.1 µmol L^{-1}. The samples were incubated for about 24 hours together with those for the time-course experiment.

The sample bottles were incubated under a continuous light of an intensity of about 120-150 µE m^{-2} s^{-1}, from 2 hours to 24-30 hours for the time-course experiments, and for 24 hours for the DSi addition experiment. The bottles containing azide were placed in the dark at the same temperature for 24 hours. The incubators could not be circulated with the water from the Scheldt because of the high SPM content, which would have attenuated the light and accumulated in the incubators. Instead, they were filled up with the tap water on board the

ship and only little amounts of water could be kept flowing. Nevertheless, the temperature in the incubators did not differ by more than a few degrees compared to the in-situ temperature.

At the end of the incubation period, the samples were filtered on a Whatman Nuclepore, 0.4 µm pore size, Ø 47 mm polycarbonate filter, which was rinsed with filtered water from the station. The filter was folded and placed at the bottom of a scintillation vial and was kept frozen until the counting of the radioactivity following the procedure described below.

Counting of the radioactivity

Choice of a method

^{32}Si is a weak β^- emitter with a half-life of 134 years, but its daughter product ^{32}P is a strong β^- emitter with a half-life of 14.3 days (Leynaert et al. 1996; Brzezinski and Phillips 1997). The radioactivity of the ^{32}Si can be assessed by scintillation liquid counting with a high efficiency (about 90 %) but the interference of the activity of the ^{32}P has to be taken into account, requiring quench curves and complex calibrations using ^{32}P and ^{32}Si (Brzezinski and Phillips 1997). However, due to the different half-lives of ^{32}Si and ^{32}P, the number of disintegrations of ^{32}P per second equilibrates to that of ^{32}Si after about 4 months while the radioactivity of the ^{32}Si is practically unchanged (Leynaert et al. 1996; Brzezinski and Phillips 1997). In addition, the radioactivity of ^{32}P is strong enough to generate Cerenkov radiations, in contrast to that of ^{32}Si (Tréguer et al. 1991; Leynaert et al. 1996). Thus the radioactivity of ^{32}Si can be simply and directly measured in water by Cerenkov counting when the samples have reached the secular equilibrium, i.e. at least four months after the end of the incorporation experiment (Tréguer et al. 1991; Leynaert et al. 1996). Although the efficiency of the Cerenkov counting is about 50 % (Tréguer et al. 1991; Brzezinksi and Pillips 1997), this method was preferred due to its simplicity: the low efficiency is compensated by the fact this method did not require any correction for interferences, calibrations or quench curves, which could be a source of imprecision. In addition, the sample could be recovered for further analyses as, for instance, liquid scintillation counting if necessary.

Methodology

Five millilitres of 2.5 mol L^{-1} HF were added to vials containing the folded filters. Care was taken to ensure that the filters were completely covered by the solution. The standards were added with diluted HF so that the volume of the final solution was 5 mL and the HF concentration 2.5 mol L^{-1}: 4 mL of 3.13 mol L^{-1} HF to the 1 mL standards, and 3 mL

of 4.17 mol L^{-1} HF to the 2 mL standards. After at least 2 hours, the radioactivity of the samples was counted three times during 30 min in the range of 2-18.6 keV. This corresponds to that of tritium but without the 0-2 keV range: observations suggested that the 0-2 keV range may contain high levels of noise. The measurement of the radioactivity was provided in counts per minutes (cpm, which is the number of disintegrations per minutes multiplied by the efficiency). The triplicate values were generally all taken into account and averaged, as the standard variation was generally less than 5 %. Blanks were also processed and the radioactivity value (about 10 cpm) was subtracted from that of the samples.

Additional tests

The same final volume of solution on filters and in standards was required, as the volume affects the radioactivity assessed by Cerenkov counting: in test filter samples of about 400-450 cpm, the counts increased linearly from 2 mL to 10 mL of added water, at a rate of about 10 cpm per mL. It was chosen to add 5 mL as this was the minimal volume necessary to cover entirely the filter and as a higher volume would have hampered the possibility of a later recount using scintillation liquid.

The use of standards was supported by the fact that the radioactivity assessed by Cerenkov counting varied perfectly linearly with the amount of ^{32}Si in 5 mL solutions, with an intercept being the blank radioactivity value ($r^2 = 1.0000$, n = 22, from 10 to 6000 cpm). This linearity was still observed when a blank filter, similar to that used for filtering the incubated water, was added to the vials ($r^2 = 1.0000$, n = 17, from 10 to 6000 cpm), but the counts were lower by 5 %. This factor was taken into account in the calculations (δ_{filter}, see further).

The addition of 2.5 mol L^{-1} HF instead of pure water was recommended by Brzezinski and Phillips et al. (1997) to dissolve the BSi and to prevent ^{32}P from adsorbing to the walls of the vials. Although the same final concentration was ensured in vials for standard or for filters, the necessity and the effects of such an addition were not investigated. Brzezinski and Phillips (1997) also recommended waiting for 2 hours after the HF addition, but the radioactivity in a test sample was monitored from 0.5 to 15 hours after the HF addition and it did not display significant variations.

Calculation of the DSi uptake

The concentration of BSi formed during the incubation was estimated from the radioactivity measured on the filter and in standards, and from the ambient initial DSi concentration, assuming that there was no silica fractionation by diatoms:

$$Si_{incorp} = DSi_{init} \cdot \frac{CPM_{filter} \cdot \frac{1}{\delta_{filter}}}{CPM_{stand} \cdot \frac{V_{incub}}{V_{stand}}} \qquad \text{(Eq. 2.6)}$$

with:

- Si_{incorp}, the concentration of silica incorporated during the incubation,
- DSi_{init}, the ambient DSi concentration at the start of the incubation,
- δ_{filter}, the correction factor (here 0.95) for the decrease of the counting efficiency due to the presence of the filter,
- CPM_{filter} and CPM_{stand}, respectively the radioactivity on the filter and in the standards (in cpm),
- V_{incub} and V_{stand}, respectively the volumes of incubated water (here about 50 or 250 mL) and of the standard (here 1 or 2 mL).

Si_{incorp} values in samples containing azide ($Si_{incorp\text{-}azide}$) were always very small compared to that in azide-free samples, but the incorporated concentrations were nevertheless corrected for the abiotic sorption that was assumed to vary linearly with the duration of the incubation of the sample:

$$BSi_{new} = Si_{incorp} - Si_{incorp\text{-}azide} \cdot \frac{t_{sampl}}{t_{azide}} \qquad \text{(Eq. 2.7)}$$

with t_{sampl} and t_{azide}, respectively the duration of the incubation of the azide-free sample and of that with azide, and BSi_{new}, the concentration of incorporated silica during the incubation.

2.6 DSi and silica retentions

The percentages of DSi and total silica (DSi+BSi) retentions in the different sections of the Scheldt tidal system were calculated on the basis of DSi and BSi fluxes. As the procedures for the estimation of the fluxes in the tidal river and of the DSi and BSi fluxes in the estuary were different, they are not reported here but detailed in Chapters 3, 4 and 5.

Nevertheless the same definitions were used for DSi and silica retentions along the entire Scheldt tidal system.

DSi retention was defined as the ratio between the amount of DSi consumed within a considered ecosystem and the amount of DSi inputs at its upstream boundary for the same period:

$$\text{DSi retention (\%)} = \frac{F_{DSi}^{upstream} - F_{DSi}^{downstream}}{F_{DSi}^{upstream}} \times 100 \qquad \text{(Eq. 2.8a)}$$

where $F_{DSi}^{upstream}$ and $F_{DSi}^{downstream}$ are respectively the DSi fluxes at the upstream and downstream boundaries of the considered ecosystem (with positive signs when directed seawards).

Similarly, silica retention was defined as the ratio between the flux of BSi deposited within the ecosystem and the flux of DSi and BSi inputs at its upstream boundary for the same period:

$$\text{silica retention (\%)} = \frac{\left(F_{DSi}^{upstream} + F_{BSi}^{upstream}\right) - \left(F_{DSi}^{downstream} + F_{BSi}^{downstream}\right)}{\left(F_{DSi}^{upstream} + F_{BSi}^{upstream}\right)} \times 100 \qquad \text{(Eq. 2.8b)}$$

where $F_{BSi}^{upstream}$ and $F_{BSi}^{downstream}$ are respectively the BSi fluxes at the upstream and downstream boundaries of the considered ecosystem (with positive signs when directed seawards).

Unless specified otherwise, these correspond always to net DSi and net silica retentions.

2.7 References

Abril G, Nogueira M, Etcheber H, Cabeçadas G, Lemaire E, Brogueira MJ (2002) Behaviour of organic carbon in nine contrasting European estuaries. Estuar Coast Shelf Sci 54:241-262

Antajan E, Chrétiennot-Dinet M-J, Leblanc C, Daro M-H, Lancelot C (2004) 19'-hexanoyloxyfucoxanthin may not be the appropriate pigment to trace occurrence and fate of *Phaeocystis*: the case of *P. globosa* in Belgian coastal waters. J Sea Res 52:165-177

Appeltans W, Hannouti A, Van Damme S, Soetaert K, Vanthomme D, Tackx M (2003) Zooplankton in the Schelde estuary (Belgium/The Netherlands). The distribution of *Eurytemora affinis*: effect of oxygen? J Plankton Res 25(11):1441-1445

Arndt S, Vanderborght J-P, Regnier P (2007) Diatom growth response to physical forcing in a macrotidal estuary: Coupling hydrodynamics, sediment transport, and biogeochemistry. J Geophys Res 112:C05045

Arndt S (2008) Physical controls on the biogeochemical structure and functioning of a land-ocean transition system (Chapter 6). In: Arndt S. Biogeochemical transformations and fluxes in redox-stratified environments: from the shallow coastal ocean to the deep subsurface. Ph. D. thesis. Univ. of Utrecht, The Netherlands. pp 147-179.

Baeyens W, Van Eck B, Lambert C, Wollast R, Goeyens L (1998) General description of the Scheldt estuary. Hydrobiologia 366:1-14

Boschker HTS, Kromkamp JC, Middelburg JJ (2005) Biomarker and carbon isotopic constraints on bacterial and algal community structure and functioning in a turbid, tidal estuary. Limnol Oceanogr 50(1):70-80

Bouezmarni M, Wollast R (2005) Geochemical composition of sediments in the Scheldt estuary with emphasis on trace metals. Hydrobiologia 540(1-3):155-168

Brochard CJE, Koeman RPT, de Keijzer-de Haan AL, Verweij GL, Fockens K, Esselink P (2005) Biomonitoring van fytoplankton in de Nederlandse zoute wateren 2004, kite-diagrammen. Koeman en bijkerk bv, ecologisch onderzoek en advies, Haren, The Netherlands. (In Dutch)

Brochard CJE, Koeman RPT, de Keijzer-de Haan AL, Verweij GL, van Wezel R, Fockens K, Esselink P (2006) Biomonitoring van fytoplankton in de Nederlandse zoute wateren 2005, kite-diagrammen. Koeman en bijkerk bv, ecologisch onderzoek en advies, Haren, The Netherlands. (In Dutch)

Brzezinski MA, Phillips DR (1997) Evaluation of ^{32}Si as a tracer for measuring silica production rates in marine waters. Limnol Oceanogr 42(5):856-865

Carbonnel V (2003) Mise au point d'une méthodologie pour la détermination de la silice biogène dans le milieu estuarien. Mémoire présenté en vue de l'obtention d'un DEA en Sciences de la Terre et Géographie. Univ. Libre de Bruxelles, Belgium. (In French)

Chen MS, Wartel S, Van Eck B, Van Maldegem D (2005a) Suspended matter in the Scheldt estuary. Hydrobiologia 540(1-3):79-104

Chen MS, Wartel S, Temmerman S (2005b) Seasonal variation of floc characteristics on tidal flats, the Scheldt estuary. Hydrobiologia 540(1-3):181-195

De Jong DJ, de Jonge VN (1995) Dynamics and distribution of microphytobenthic chlorophyll-*a* in the Western Scheldt estuary (SW Netherlands). Hydrobiologia 311:21-31

De Jonge VN, Van Beusekom JEE (1995) Wind- and tide-induced resuspension of sediment and microphytobenthos from tidal flats in the Ems estuary. Limnol Oceanogr 40(4):766-778

Dijkman NA, Kromkamp JC (2006a) Phospholipid-derived fatty acids as chemotaxonomic markers for phytoplankton: application for inferring phytoplankton composition. Mar Ecol Prog Ser 324:113-125

Dijkman NA, Kromkamp JC (2006b) Photosynthetic characteristics of the phytoplankton in the Scheldt estuary: community and single-cell fluorescence measurements. Eur J Phycol 41(4):425-434

Dougan WK, Wilson AL (1974) The absorptiometric determination of aluminium in water. A comparison of some chromogenic reagents and the development of an improved method. Analyst 99:413-430

Gazeau F, Gattuso J-P, Middelburg JJ, Brion N, Schiettecatte L-S, Frankignoulle M, Borges AV (2005) Planktonic and whole system metabolism in a nutrient-rich estuary (the Scheldt estuary). Estuaries 28(6):868-883

Kamatani A, Oku O (2000) Measuring biogenic silica in marine sediments. Mar Chem 68(3):219-229

Koeman RPT, Brochard CJE, Fockens K, Verweij GL, Esselink P (2004) Biomonitoring van fytoplankton in de Nederlandse zoute wateren 2003, kite-diagrammen. Koeman en bijkerk bv, ecologisch onderzoek en advies, Haren, The Netherlands. (In Dutch)

Koroleff F (1983) Determination of silicon. In: Grasshoff K, Ehrhardt M, Kremling K (eds) Methods of seawater analysis. Second, revised and extended edition. Verlag Chemie, Weinheim, Deerfield Beach, Florida, Basel. pp 174-187.

Lancelot C (1995) The mucilage phenomenon in the continental coastal waters of the North Sea. Sci Total Environ 165(1-3):83-102

Lemaire E, Abril G, de Wit R, Etcheber H (2002) Distribution of phytoplankton pigments in nine European estuaries and implications for an estuarine typology. Biogeochemistry 59:5-23

Leynaert A, Tréguer P, Nelson DM, Del Amo Y (1996) ^{32}Si as a tracer of biogenic silica production: methodological improvements. In: Baeyens J, Dehairs F, Goeyens L (eds) Integrated marine system analysis. Minute of the first workshop meeting. VUB, Brussels, Belgium. pp 29-35.

Lionard M (2006) Spatio-temporal phytoplankton dynamics along the Scheldt-North Sea continuum based on HPLC/CHEMTAX pigment analysis. Ph. D. thesis. Univ. of Ghent, Belgium.

Lionard M, Muylaert K, Tackx M, Vyverman W (2008a) Evaluation of the performance of HPLC-CHEMTAX analysis for determining phytoplankton biomass and composition in a turbid estuary (Schelde, Belgium). Estuar Coast Shelf Sci 76(4):809-817

Lionard M, Muylaert K, Hanouti A, Maris T, Tackx M, Vyverman W (2008b) Inter-annual variability in phytoplankton summer blooms in the freshwater tidal reaches of the Schelde estuary (Belgium). Estuar Coast Shelf Sci 79(4):694-700

Llewellyn CA, Gibb SW (2000) Intra-class variability in the carbon, pigment and biomineral content of prymnesiophytes and diatoms. Mar Ecol Prog Ser 193:33-44

Lucas CH, Banham C, Holligan PM (2001) Benthic-pelagic exchange of microalgae at a tidal flat. 2. Taxonomic analysis. Mar Ecol Prog Ser 212:39-52

Mackey MD, Mackey DJ, Higgins HW, Wright SW (1996) CHEMTAX - a program for estimating class abundances from chemical markers: application to HPLC measurements of phytoplankton. Mar Ecol Prog Ser 144:265-283

Martin-Jézéquel V, Hildebrand M, Brzezinski MA (2000) Silicon metabolism in diatoms: implications for growth. J Phycol 36:821-840

Meire P, Ysebaert T, Van Damme S, Van den Bergh E, Maris T, Struyf E (2005) The Scheldt estuary: a description of a changing ecosystem. Hydrobiologia 540(1-3):1-11

Muylaert K, Sabbe K (1999) Spring phytoplankton assemblages in and around the maximum turbidity zone of the estuaries of the Elbe (Germany), the Schelde (Belgium/The Netherlands) and the Gironde (France). Journal of Marine Systems 22(2-3):133-149

Muylaert K, Sabbe K, Vyverman W (2000) Spatial and temporal dynamics of phytoplankton communities in a freshwater tidal estuary (Schelde, Belgium). Estuar Coast Shelf Sci 50(5):673-687

Muylaert K, Van Wichelen J, Sabbe K, Vyverman W (2001) Effects of freshets on phytoplankton dynamics in a freshwater tidal estuary (Schelde, Belgium). Arch Hydrobiol 150(2):269-288

Muylaert K, Tackx M, Vyverman W (2005) Phytoplankton growth rates in the freshwater tidal reaches of the Schelde estuary (Belgium) estimated using a simple light-limited primary production model. Hydrobiologia 540(1-3):127-140

Muylaert K, Gonzales R, Franck M, Lionard M, van der Zee C, Cattrijsse A, Sabbe K, Chou L, Vyverman W (2006) Spatial variation in phytoplankton dynamics in the Belgian coastal zone of the North Sea studied by microscopy, HPLC-CHEMTAX and underway fluorescence recordings. J Sea Res 55:253-265

Muylaert K, Sabbe K, Vyverman W (2009) Changes in phytoplankton diversity and community composition along the salinity gradient of the Schelde estuary (Belgium/The Netherlands). Estuar Coast Shelf Sci 82:335-340

Ragueneau O, Savoye N, Del Amo Y, Cotten J, Tardiveau B, Leynaert A (2005) A new method for the measurement of biogenic silica in suspended matter of coastal waters: using Si:Al ratios to correct for the mineral interference. Cont Shelf Res 25(5-6):697-710

Rijstenbil JW, Bakker C, Jackson RH, Merks AGA, de Visscher PRM (1993) Spatial and temporal variation in community composition and photosynthetic characteristics of phytoplankton in the upper Westerschelde estuary (Belgium, SW Netherlands). Hydrobiologia 269/270:263-273

Rousseau V, Leynaert A, Daoud N, Lancelot C (2002) Diatom succesion, silification and silicic acid availability in Belgian coastal waters (Southern North Sea). Marine Ecology Progress Series 236:61-73

Soetaert K, Herman PMJ (1995) Estimating estuarine residence times in the Westerschelde (The Netherlands) using a box model with fixed dispersion coefficients. Hydrobiologia 311:215-224

Soetaert K, Middelburg JJ, Heip C, Meire P, Van Damme S, Maris T (2006) Long-term change in dissolved inorganic nutrients in the heterotrophic Scheldt estuary (Belgium, The Netherlands). Limnol Oceanogr 51(1, part 2):409-423

Tackx M, De Pauw N, Van Mieghem R, Azémar F, Hannouti A, Van Damme S, Fiers F, Daro N, Meire P (2004) Zooplankton in the Schelde estuary, Belgium and The Netherlands. Spatial and temporal patterns. J Plankton Res 26(2):133-141

Treguer P, Van Bennekom AJ, Leynaert A, Panouse M, Jacques G (1991) Production of biogenic silica in the Weddell-Scotia Seas measured with 32Si. Limnology and Oceanography 36(6):1217-1227

Van Damme S, Struyf E, Maris T, Ysebaert T, Dehairs F, Tackx M, Heip C, Meire P (2005) Spatial and temporal patterns of water quality along the estuarine salinity gradient of the Scheldt estuary (Belgium and The Netherlands): results of an integrated monitoring approach. Hydrobiologia 540(1-3):29-45

Van der Zee C, Roevros N, Chou L (2007) Phosphorus speciation, transformation and retention in the Scheldt estuary (Belgium/The Netherlands) from the freshwater tidal limits to the North Sea. Mar Chem 106(1-2):76-91

Van Maldegem DC, Mulder HPJ, Langerak A (1993) A cohesive sediment balance for the Scheldt Estuary. Neth J Aquat Ecol 27(2-4):247-256

Wartel S (1977) Composition, transport and origin of sediments in the Scheldt estuary. Geologie en mijnbouw 56(3):219-233

Wartel S, Parker R, Francken F, Shelton P (1999) Schelde lithology (1 map). KBIN, Brussels, Belgium.

WLHO (Waterbouwkundig Laboratorium en Hydrologisch Onderzoek) (1966) Stormvloeden op de Schelde, parts 3 and 4. Borgerhout, Antwerp. (In Dutch)

Wollast R, De Broeu F (1971) Study of the behavior of dissolved silica in the estuary of the Scheldt. Geochim Cosmochim Acta 35:613-620

Wollast R (1988) The Scheldt estuary. In: Salomons W, Bayne BL, Duursma EK, Förstner U (eds) Pollution of the North Sea. An Assessment. Springer-Verlag, Berlin, Heidelberg, New-York, London, Paris, Tokyo. pp 183-193.

Wright SW, Jeffrey SW (1997) High-resolution HPLC system for chlorophylls and carotenoids of marine phytoplankton. In: Jeffrey SW, Mantoura RFC, Wright SW (eds) Phytoplankton pigments in oceanography: guidelines to modern methods. UNESCO Publishing, Paris. pp 327-341.

3 Dynamics of DSi and BSi in the tidal river

In this study, we present high resolution DSi and BSi temporal profiles during one full annual cycle along the tidal freshwater reaches of the Scheldt and its tributaries. BSi concentrations are compared with those of chlorophyll *a* and SPM to estimate the fraction of BSi associated with living diatoms. A budget is performed for DSi and the different BSi fractions (associated or not with living diatoms) for the period from May to October 2003 and annual fluxes to the brackish reaches of the Scheldt estuary are estimated. The possible contribution of phytoliths to the estuarine BSi pool as well as the influence of the silica cycling in marshes on the estimated silica fluxes are discussed.

3.1 DSi, BSi and DiatChl*a* concentration profiles

At the tidal limits of the Scheldt and its tributaries

In general, diatoms accounted for less than half of the phytoplankton biomass in the six rivers (Table 3.1) and the DiatChl*a* concentrations were below 50 µg L^{-1} (Fig. 3.1a-f). DSi concentrations remained high throughout the year with mean annual concentrations ranging from 154 µmol L^{-1} in the Kleine Nete to 288 µmol L^{-1} in the Dijle (see Annex 3A for a discussion about the DSi profiles in the tributaries). BSi concentrations were lower with mean annual concentrations varying from 2.9 µmol L^{-1} in the Dijle to 18.2 µmol L^{-1} in the upper Scheldt river. Both the DiatChl*a* and the BSi concentrations were higher in the river Scheldt (at Ghent) and in the Dender (Fig. 3.1a-b) than in the tributaries of the Rupel (Fig. 3.1c-f). Few BSi data were available for the Zenne, as mostly negative values were retrieved from Eq. 2.3 (data not shown, see discussion). At the end of March and the beginning of April in the upper Scheldt river, higher DiatChl*a* concentrations indicated a spring diatom bloom (Fig. 3.1a). However only a small increase in BSi concentrations could be observed. Other smaller concomitant increases in BSi and DiatChl*a* patterns were observed in spring in all rivers and in summer in the upper Scheldt, the Dender and the Dijle (Fig. 3.1a-f). DSi concentrations also decreased during both seasons in the upper Scheldt and the Dender.

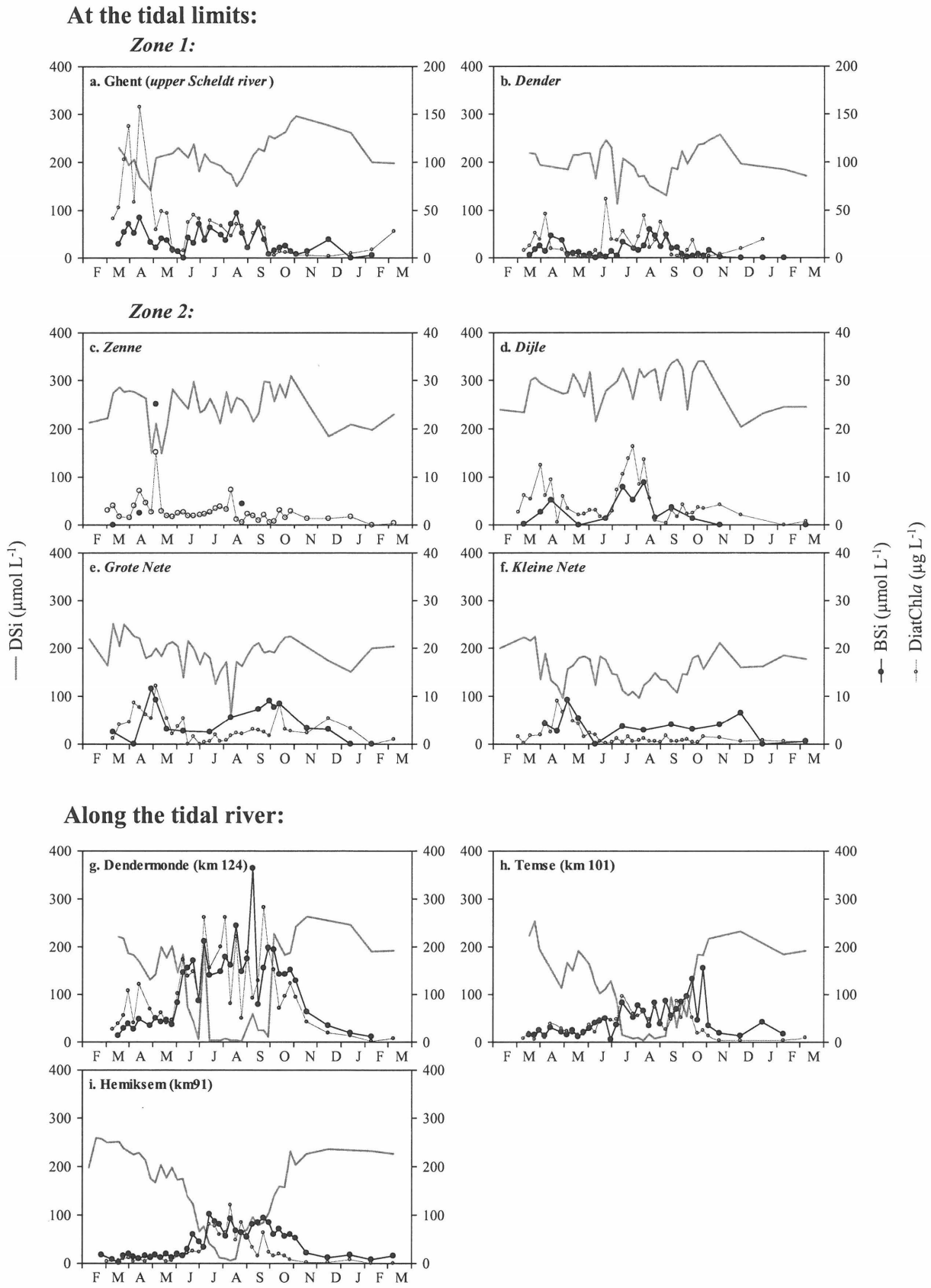

Fig. 3.1: DSi (left axis), BSi and DiatChl*a* (right axis) concentrations at the nine sampling stations from February 2003 to March 2004. Note the different scales for the BSi and DiatChl*a* concentrations for the tidal limits at Ghent, Dender, Zenne, Dijle, Grote and Kleine Nete (a. to f.).

Table 3.1: Average contributions of the diatoms to the phytoplankton biomass at the nine sampling stations (in percentages, ± standard deviations). Contributions over 50 % are indicated in bold.

Station	Spring (Mar - May)	Summer (Jun - Sep)	Fall - Winter (Oct - Feb)
Ghent	**60** ± 9	40 ± 11	39 ± 12
Dender	30 ± 17	23 ± 19	30 ± 22
Zenne	29 ± 9	16 ± 4	20 ± 15
Dijle	36 ± 11	24 ± 11	23 ± 12
Grote Nete	33 ± 10	17 ± 10	32 ± 18
Kleine Nete	26 ± 12	15 ± 8	17 ± 7
Dendermonde	**78** ± 10	**85** ± 8	**71** ± 14
Temse	**72** ± 13	**69** ± 7	**60** ± 9
Hemiksem	46 ± 9	**56** ± 11	31 ± 15

Along the tidal river

Diatoms accounted for more than 60 to 70% of the phytoplankton biomass throughout the year 2003 at Dendermonde and Temse (Table 3.1). Although the fraction of the phytoplankton biomass attributed to diatoms was significantly lower at Hemiksem (Table 3.1), diatoms were still the dominant phytoplankton species (Lionard 2006).

A spring bloom could be observed at Dendermonde at the end of March and the beginning of April (Fig. 3.1g) but was not noticeable at Temse and Hemiksem (Fig. 3.1h-i). Until the end of May, DSi concentrations remained high ranging from 150 µmol L^{-1} to 250 µmol L^{-1} at the three stations and BSi stayed low at around 36 µmol L^{-1}, 20 µmol L^{-1} and 13 µmol L^{-1} respectively at Dendermonde, Temse and Hemiksem.

In summer, DiatChl*a* and BSi concentrations increased concomitantly while DSi decreased (Fig. 3.1g-i), indicating the development of a summer diatom bloom (June to September) in the tidal river. At Dendermonde (Fig. 3.1g), DSi was consumed by diatoms down to 2 µmol L^{-1} and was entirely transformed into BSi from the beginning of July to the end of September. The BSi concentrations fluctuated at around 200 µmol L^{-1} and correlated well with the DiatChl*a* concentrations (except on 11 and 25 August 2003 when DiatChl*a* declined while BSi remained high). Increases in DSi observed at the beginning of July and September occurred a few days after sharp increases in the freshwater discharge, but the discharge peaks at the end of July induced only a small DSi increase at the beginning of August (Figs. 3.2 and 3.1g). The discharge peaks at the beginning and at the end of July led to an increase in both BSi and DiatChl*a* concentrations. However, the high discharge peak at the

end of August resulted in an increase in BSi concentration (364 µmol L^{-1}) but a decrease in DiatChl*a* concentration (92 µg L^{-1}) on 8 Sept. 2003. At Temse and at Hemiksem (Fig. 3.1h-i), DSi was also consumed down to 5 µmol L^{-1} in summer. However, the uptake started later and lasted for a shorter period at Hemiksem compared to Dendermonde and Temse. From June to August, BSi and DiatChl*a* concentrations increased and correlated well at Temse and Hemiksem, but never reached the high levels observed at Dendermonde.

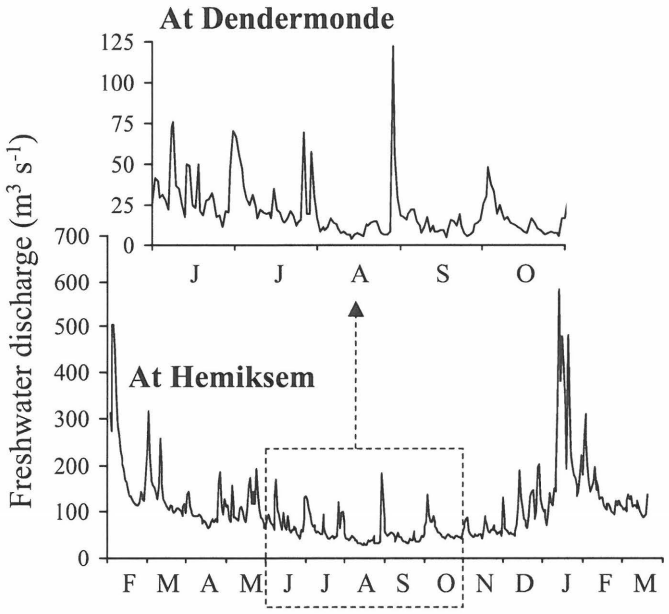

Fig. 3.2: Daily average of the residual freshwater discharge at Hemiksem (from February 2003 to March 2004) and at Dendermonde (from June to October 2003).

While the weather was summer-like in September 2003, the irradiance and the temperature dropped suddenly in October and the rainfall increased (IRMB 2003-2004). In October at Dendermonde, the DSi concentration increased rapidly following the discharge peak (Figs. 3.2 and 3.1g). DSi was no longer consumed and remained high at about 200 µmol L^{-1}, while BSi and DiatChl*a* started to decrease. In parallel to what was observed at Dendermonde, DiatChl*a* concentrations at Temse were still high in September but declined from October onwards. At Hemiksem, DiatChl*a* started to decline already in September. However, DSi concentrations reached winter levels only at the end of October at Temse and Hemiksem. Background levels of DiatChl*a* lower than 10 µg L^{-1} were recorded only in February and March 2004 at Dendermonde, whereas such low concentrations were already reached in November at Temse and Hemiksem (Fig. 3.1g-i). At these two locations, BSi did not decrease in parallel with DiatChl*a,* high BSi concentrations being even recorded on 13

and 27 October 2003 at Temse when the SPM concentration reached its highest values of respectively 249 mg L^{-1} and 409 mg L^{-1}. At Hemiksem, BSi remained high in September, but declined from October onwards (Fig. 3.1i).

3.2 Fraction of the BSi associated with living diatoms

To determine to which extent BSi was associated with living diatoms and to estimate the BSi content in living diatoms, correlations between BSi and DiatChl*a* were performed on datasets characterizing the productive period (May to October) at Dendermonde, Temse and Hemiksem. Concentrations profiles (Fig. 3.1a and g) indeed suggested a different BSi to DiatChl*a* ratio in the spring diatom community. However, the correlations were weak (r^2 = 0.22, 0.14 and 0.40 at Dendermonde, Temse and Hemiksem respectively, n = 25) due to the interfering presence of BSi_{det}. As SPM_{nbld} was not correlated to DiatChl*a* at any of the three estuarine stations ($r^2 \leq 0.01$), multiple regressions between BSi and the two explicative variables DiatChl*a* and SPM_{nbld} (see the Material and methods section) were thus performed to distinguish BSi_{liv} from BSi_{det}. SPM_{nbld} may have been further divided in organic and inorganic fractions to investigate the origin of BSi_{det} using POC and DiatChl*a* data and the β ratios defined above, but the correlation between organic and inorganic fractions ($0.54 \leq r^2 \leq 0.88$, $23 \leq n \leq 25$) ruled out the possibility to use both of them in the same multiple regression.

The BSi_{liv}/DiatChl*a* ratio at Dendermonde, Temse and Hemiksem was respectively 0.58 ± 0.23 mol g^{-1} (± 95 % confidence interval), 0.68 ± 0.15 mol g^{-1} and 0.71 ± 0.15 mol g^{-1}. Although BSi_{liv}/DiatChl*a* seemed to increase from Dendermonde to Hemiksem, it was not significantly different from one station to another (*t*-test for equality: $0.56 \leq p \leq 0.76$). The average BSi_{liv}/DiatChl*a* ratio of 0.67 ± 0.11 mol g^{-1} estimated when lumping together the data from May to October at the three stations was not significantly different from those found at each station either (*t*-test for equality: $0.34 \leq p \leq 0.99$). There was a good correlation between the BSi measured and that estimated by the regression (r^2 = 0.71, n = 75). Even, if the high-BSi data from 8 Sept. 2003 at Dendermonde (Fig. 3.1g) was excluded from the regressions, BSi_{liv}/DiatChl*a* increased to 0.66 ± 0.16 mol g^{-1} at Dendermonde (*t*-test for equality with BSi_{liv}/DiatChl*a* at Temse and Hemiksem: p = 0.90 and 0.75 respectively). A better correlation between the measured and estimated BSi was then obtained when data from the three stations were lumped together (r^2 = 0.83, n = 74) but the BSi_{liv}/DiatChl*a* ratio did not change

significantly (0.68 ± 0.07 mol g^{-1}, *t*-test for equality with BSi_{liv}/DiatChl*a* at Dendermonde: p = 0.73).

BSi_{liv} concentrations at the three estuarine stations during the productive period were therefore determined using a single BSi_{liv}/DiatChl*a* ratio of 0.67 mol g^{-1}. The BSi_{liv} fraction showed a high variability when calculated on a weekly basis, but was higher at Dendermonde and Temse than at Hemiksem as a general pattern (except in August) (Fig. 3.3). About 75 % of the measured BSi at Dendermonde and Temse from May to July could be attributed to living diatoms, while only 50 % at Hemiksem. From August onwards, the BSi_{liv} fraction decreased at Dendermonde and Temse (but not lower than 50 % at Dendermonde), while it reached its maximum in August at Hemiksem and decreased later to a value as low as 16 % in October.

A similar multiple regression applied on lumped data from mid-March to end-May at Ghent and from mid-March to end-April at Dendermonde yielded a BSi_{liv}/DiatChl*a* ratio of 0.20 ± 0.06 mol g^{-1} for the spring diatom community (r^2 = 0.88, n = 15). At Ghent, most of the BSi was associated with living diatoms, whereas most of the BSi was present as BSi_{det} in the tidal river (Fig. 3.3).

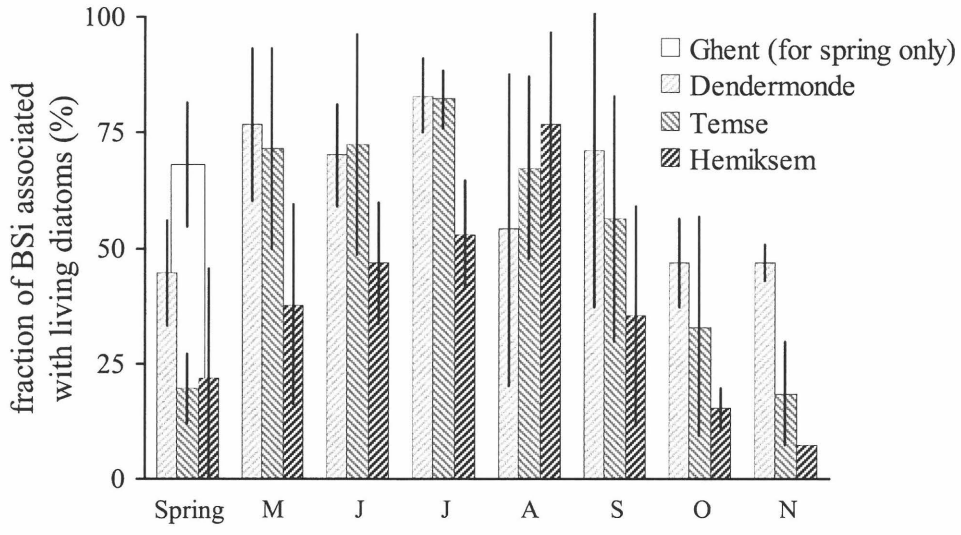

Fig. 3.3: BSi associated with living diatoms (BSi_{liv}) as a fraction of the total BSi concentration (error bars: ± standard deviation, four measurements per month in general). The BSi_{liv}/DiatChl*a* ratios used for "Spring" and for the period from May to November 2003 were respectively 0.20 mol g^{-1} and 0.67 mol g^{-1} (see text for details).

3.3 Silica fluxes and mass-balance

Methodology for discharge data, silica fluxes and mass-balances calculations

Two zones, delimited by the sampling stations, were defined for the budget calculations (Fig. 3.4). The two zones have approximately the same volume (about 3×10^7 m^3 at mid tide) and water surface area (about 7×10^6 m^2) but differ in total length (Table 2.1 in Chapter 2).

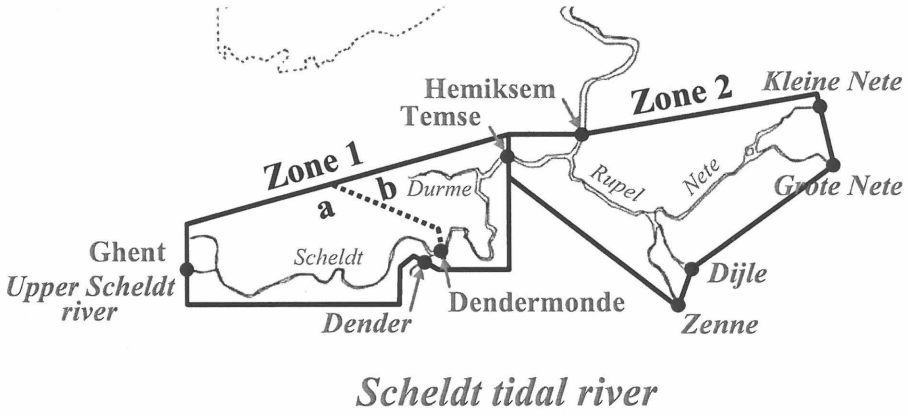

Fig. 3.4: Map of the Scheldt estuary. The sampling stations (in bold) are indicated by black dots. As for Fig. 2.5 in Chapter 2, city and river names are in regular and italic fonts, respectively. The areas (Zones 1a and 1b, and Zone 2) considered for silica budget calculations are delimited by grey lines.

Daily discharge data for the upper Scheldt river and the five main tributaries as well as an estimation of the overall lateral inputs for Zone 1 and Zone 2 were provided by the Flemish Administration (Afdeling Maritieme Toegang). The lateral inputs (non-monitored lateral sources of water discharging directly into the tidal river, such as run-off or small lateral streams) accounted for less than 10 % of the annual discharge in 2003; they were redistributed among the tributaries of the zone, according to their contribution to the total riverine water input. Discharges at Dendermonde, Temse and Hemiksem were calculated as the sum of the discharges of the upstream tributaries. However, as Dendermonde is situated roughly half-way between Ghent and Temse, half of the contribution of the lateral inputs in Zone 1 was transferred from Zone 1a to Zone 1b in the water (and the silica) mass-balance (Fig. 3.4).

Silica fluxes (kmol d^{-1}) were calculated at a weekly resolution: daily discharge data were weekly averaged and multiplied by the weekly measured silica concentration. If no sampling was carried out during a week, the concentration was estimated by linear interpolation between the two closest measurements. In the tributaries of the Rupel, BSi was

not measured every week, but weekly BSi fluxes were calculated with BSi concentrations derived from the weekly DiatChl*a* concentrations and the slopes and intercepts of the linear regressions performed between measured BSi and corresponding DiatChl*a* concentrations in each river. The intercepts of the linear regressions were assumed to provide estimations for the detrital BSi fractions. For the Zenne, as the dataset did not allow such linear regression, the slope and the intercept used were the averages of those found for the Dijle, Grote and Kleine Nete.

Silica budget during the productive period

Mass-balances were performed for DSi, BSi_{liv} and BSi_{det} in Zones 1a, 1b and 2 during the productive period (May to October 2003, 184 days, Fig. 3.5). In each zone, the loss of DSi was ascribed to DSi uptake by diatom and thus to a production of BSi_{liv}. The mass-balance between this production and the fluxes of BSi_{liv} was assumed to provide an estimate of the diatom mortality. The mass-balance between diatom mortality and fluxes of BSi_{det} was considered as representative of the BSi deposition (or resuspension) in each zone.

The Scheldt tidal river received 260 Mmol of silica (DSi + BSi) during the productive period in 2003, predominantly in the dissolved form: total BSi inputs to the tidal river accounted for only 3 % of this amount, mostly originating from the upper Scheldt river (Fig. 3.5). The contribution of the Rupel tributaries to the total DSi input was 63 %.

In Zone 1a, there was a DSi uptake (40 Mmol) corresponding to nearly half of the DSi input flux (Fig. 3.5). Most of it remained in the BSi_{liv} pool and only one fourth was transferred to the BSi_{det} pool. No settling but rather a resuspension of a small amount of BSi occurred in this zone. In Zone 1b, the opposite was observed: there was little DSi uptake but most of the BSi produced in Zone 1a settled in Zone 1b (37 Mmol). Our data did not allow us to distinguish between BSi deposited as BSi_{liv} or BSi_{det}. Indeed, settling of living diatoms could not be excluded. This is indicated by the dotted line between the "diatom mortality" and the "BSi deposition" arrows in Fig. 3.5. Despite the settling of BSi in Zone 1b, the proportion between BSi_{liv} and BSi_{det} was similar at Dendermonde and at Temse. Overall, during the productive period in Zone 1, there was a BSi loss corresponding to 71 % of the DSi uptake and a retention of 33 % of the total amount of silica inputs to the zone.

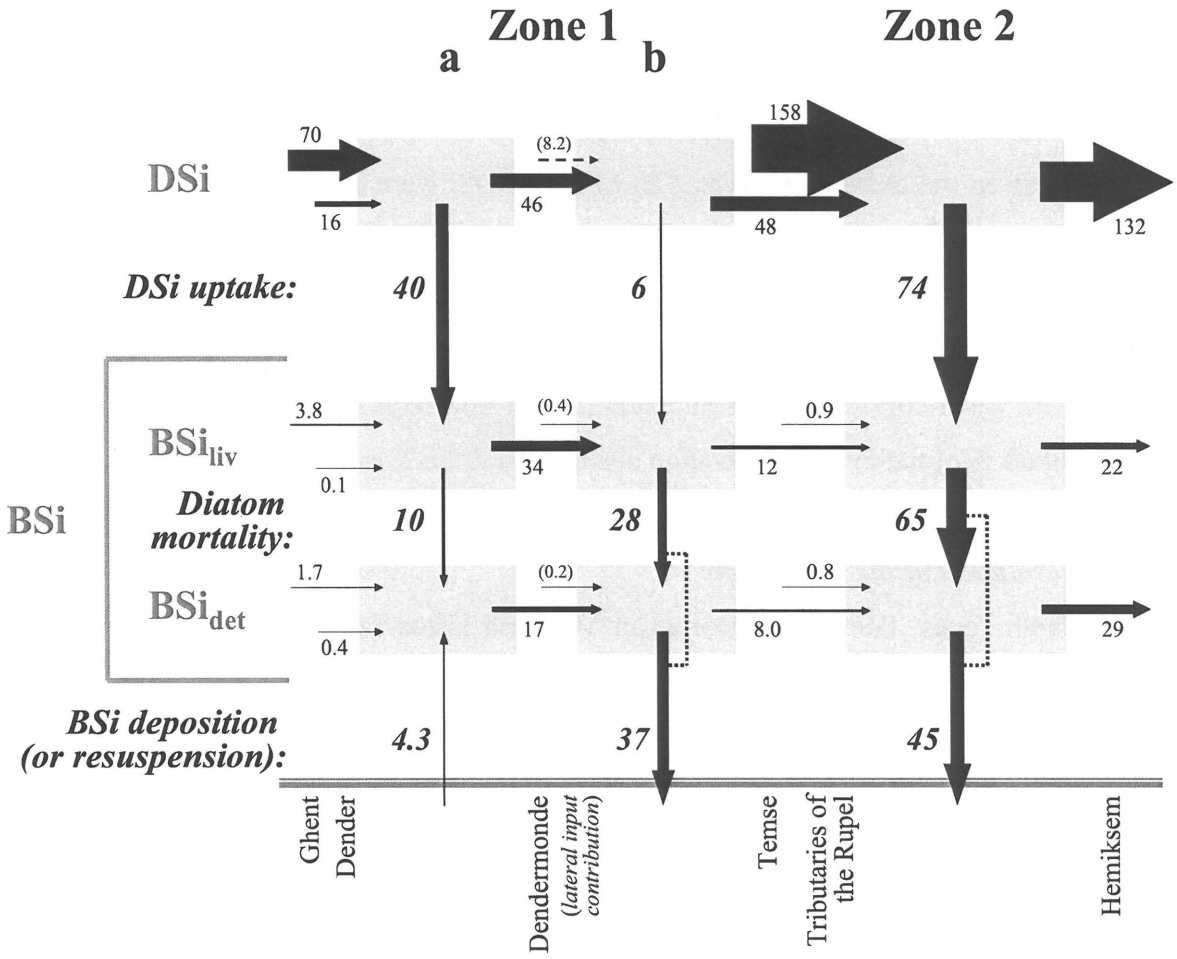

Fig. 3.5: Silica mass-balance (in Mmol) for the Scheldt tidal river over one productive period (May to October 2003, 184 days). Arrow thickness is proportional to the flux intensity. Horizontal arrows indicate DSi or BSi fluxes at each station. Lateral inputs for Zone 1a and 2 are not explicitly represented but redistributed among the tributaries (see text). For Zone 1b, the contribution of the lateral inputs is indicated in parentheses. Vertical arrows indicate productions or losses calculated as the difference, for each species, between the inputs and outputs in each zone. BSi_{liv} fluxes at Ghent and in the Dender were derived from BSi_{liv} concentrations estimated by multiple linear regressions (see text). One should bear in mind that no discrimination was possible between BSi deposited as BSi_{liv} or as BSi_{det}, as indicated by the broken dashed line between "diatom mortality" and "BSi deposition" (see text).

Zone 2 received an important amount of DSi (206 Mmol at Temse) but ten times less BSi despite the important BSi production in Zone 1. Although the water surface area is similar in both zones (about 7×10^6 m^2, Table 2.1 in Chapter 2), the DSi uptake, diatom mortality and BSi deposition in Zone 2 were all higher than in Zone 1. DSi uptake in Zone 2 amounted to 74 Mmol. Most of it was transferred to the BSi_{det} pool or deposited in this zone; the amount of BSi deposited amounted to 61 % of the BSi produced (estimated from DSi

uptake). Despite a higher amount of BSi deposited, the retention of silica in Zone 2 (20 %) was lower than in Zone 1 (33 %) due to higher DSi inputs in Zone 2. At the outlet of the tidal river, BSi accounted for 28 % of the total silica pool (DSi + BSi).

Overall in the entire tidal river, 120 Mmol of DSi were consumed, from which 65 % were deposited as BSi, leading to a 30 % retention of the total amount of silica that entered the tidal Scheldt river during the productive period. If compared to silica inputs, the relative DSi uptake and silica retention were higher in Zone 1 than in Zone 2. However the opposite was observed when considering absolute amounts of both DSi uptake and BSi loss. For the latter, about 60 % of the overall deposition occurred in Zone 2.

Temporal evolution of the DSi uptake

In both zones, DSi uptake started in May and lasted until October/November (Fig. 3.6). In May and beginning of June, DSi uptake increased identically in both zones reaching 500 kmol d^{-1} in mid-June. At that point, DSi uptake started to decrease in Zone 1a while it continued to increase in Zone 2 reaching a value of about 800 kmol d^{-1} at the end of June. DSi uptake decreased in both zones from July until the end of the productive period, more or less at the same rate, but it always stayed higher in Zone 2 than in Zone 1a by about 250 kmol d^{-1}.

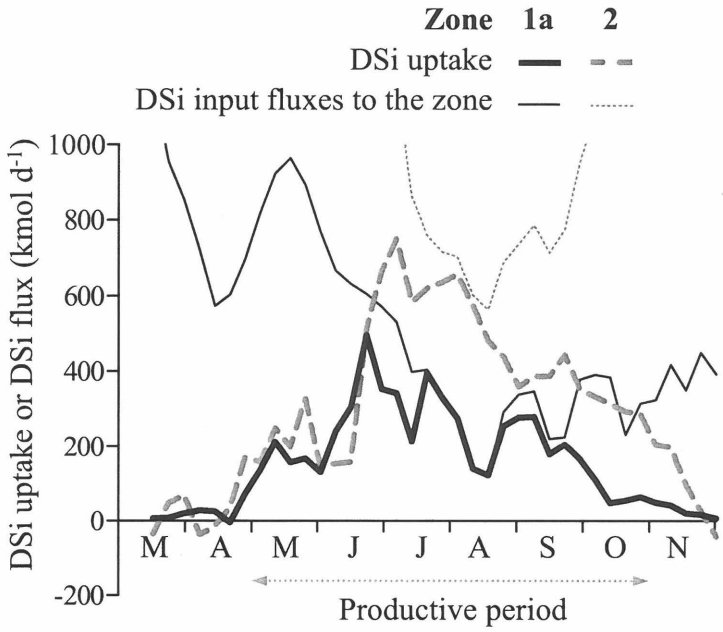

Fig. 3.6: Three-week moving average of weekly DSi uptake fluxes (in kmol d^{-1}) in Zone 1a and Zone 2 from March to November 2003. Uptake fluxes are indicated by positive values to allow the comparison with the DSi input fluxes to the zone (dotted and dashed lines). The latter correspond to the potential maximum for DSi uptake in the zone. The three-week moving averages were performed to smooth the possible aliasing induced by the water residence time out from the curves.

If DSi is completely consumed, DSi uptake equals DSi input fluxes. Thus, the DSi input flux can be seen as a potential maximum for DSi uptake. This potential maximum was higher in Zone 2 than in Zone 1 and the observed DSi uptake was complete from mid July until the end of September in Zone 1a, but only at the end of July and beginning of August in Zone 2.

Annual fluxes discharged to the brackish estuary

During our one-year study period (7 Feb. 2003 - 6 Feb. 2004), the amount of water discharged during the productive period (6 months) was two times smaller than that discharged during the rest of the year. DSi concentrations in the tributaries did not exhibit important temporal variations (Fig. 3.1a-f), but fluxes of riverine DSi delivered to the tidal river showed a minimum in summer because of the lower discharge (Fig. 3.7). At the outlet of the tidal river near Hemiksem, the annual variations in the DSi flux were further enhanced by the effect of diatom uptake superimposed to that of the decreasing river discharge. Conversely, seasonal variations in discharge flattened the BSi fluxes pattern, which ranged from 100 kmol d^{-1} in spring/autumn/winter to 400 kmol d^{-1} in summer. The annual DSi uptake and silica retention corresponded to 14 % and 6 % of total inputs, respectively. This is 3 to 5 times smaller than the estimates characterizing the productive period (Table 3.2).

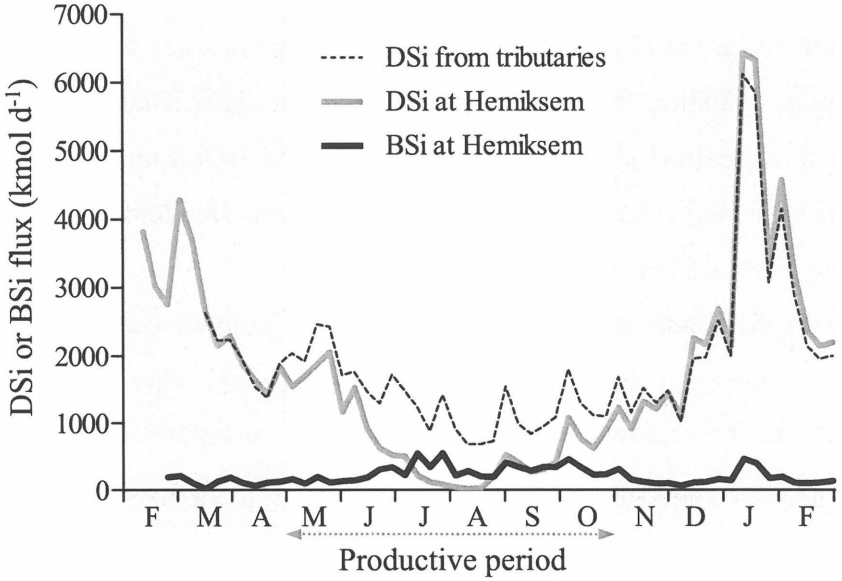

Fig. 3.7: Weekly DSi or BSi fluxes at Hemiksem from February 2003 to February 2004. DSi input in the tidal river is also indicated.

Table 3.2: DSi and BSi fluxes (in Mmol) from the tributaries and at Hemiksem, for the productive period and at an annual timescale. DSi uptake (%) consumed and total silica (DSi + BSi) retention for both periods are also given.

	Tributaries	Hemiksem	DSi consumed	Silica retention
Productive period (1 May 2003 - 30 Oct. 2003, 184 days)				
DSi	252	132	**48 %**	**30 %**
BSi	8.4	51		
Annual fluxes (7 Feb. 2003 - 6 Feb. 2004)				
DSi	713	612	**14 %**	**6 %**
BSi	21	80		

3.4 Discussion

Distinction between BSi_{liv} and BSi_{det}

In order to better investigate the dynamics of BSi, a multiple linear regression was performed with the explicative variables DiatChl*a* and SPM_{nbld} (defined in Eq. 2.4) to distinguish between BSi associated or not with living diatoms. As the two explicative variables were very poorly correlated ($r^2 = 0.02$, n = 75), the discrimination could be regarded as robust. Admittedly, it could not be excluded that empty frustules followed the distribution of living diatoms, yielding an overestimation of the BSi_{liv}/DiatChl*a* ratio. However, BSi_{liv}/DiatChl*a* was identical at Dendermonde, Temse and Hemiksem (see Results section), despite the facts that large amounts of BSi settled between Dendermonde and Temse (Fig. 3.5) and mortality increased at Hemiksem (Fig. 3.3).

The use of the linear multiple regression model implied that BSi_{liv} was calculated using an average, constant BSi_{liv}/DiatChl*a* ratio. However, silica and/or chlorophyll *a* contents in diatoms are known to exhibit important variations depending on nutrient availability, temperature and light conditions (Geider 1987; Ragueneau et al. 2000; Martin-Jézéquel et al. 2000; Hildebrand 2002). Due to the variations in DSi concentrations (Fig. 3.1g-i), light and temperature during the productive period, diatom cells in the Scheldt may thus not have had a constant content of silica and of chlorophyll *a*. But in our study, the BSi_{liv}/DiatChl*a* ratio was not intended to be estimated at the cellular scale (which would not have been possible from our dataset), but at the system and seasonal scales, where the

variations of the measured BSi concentrations were expected to depend more on the presence of detrital BSi than on the variation of the chlorophyll *a* and BSi contents of the diatoms. The multiple regression model, although very simple, reproduced indeed well the variations in BSi concentrations even if the data from the three estuarine stations were lumped together: the correlation between estimated and measured BSi was good ($r^2 = 0.71$ if $n = 75$, or $r^2 = 0.83$ if $n = 74$, see Results section) and the 95 % confidence interval associated with the BSi_{liv}/DiatChl*a* ratio was rather narrow (± 16 % if $n = 75$, or ± 11 % if $n = 74$).

The $\beta_{POC/Chla}$ and $\beta_{OM/POC}$ conversion factors were used to subtract the SPM concentration from the contribution of diatom biomass which was already represented in the multiple regression by the other explicative variable, DiatChl*a* (Eqs. 2.4 and 2.5 in Chapter 2). Due to the important fraction of non-phytoplankton organic matter in the SPM of the Scheldt tidal river (Hellings et al. 1999), these two factors could not be estimated from our dataset and average constant ratios were taken from the literature. In particular, $\beta_{POC/Chla}$ may display important variations (Geider et al. 1987). However, although a variation in these ratios can affect the estimation of the BSi_{liv}/DiatChl*a* ratio (k_1 in Eq. 2.5), their influence was not expected to be important. Using Eq. 2.4, Eq. 2.5 can indeed be rewritten as:

$$\hat{BSi} = (k_1 - k_2 \cdot \beta) \cdot \text{DiatChl}a + k_2 \cdot (SPM - BSi \cdot M_{BSiO2}) \qquad \text{(Eq. 3.1)}$$

with $\beta = \beta_{POC/Chla} \cdot \beta_{OM/POC}$

In this study, β was equal to 75. The use of another β value would indeed induce a different k_1, but k_2 and the correlation between the measured BSi concentrations and those estimated by the regression would not be altered. Furthermore, as k_2 was 0.48 mmol g^{-1} when $n = 75$ (k_2 = 0.42 when $n = 74$, cf. above), the relative variation would be 19 times smaller for k_1 than for β.

In addition, using $\beta_{POC/Chla}$, our BSi_{liv}/DiatChl*a* ratio would correspond to a Si/C molar ratio in living diatoms of 0.27 (± 0.04), which would fall in the range observed in *Cyclotella meneghiniana* cultures (0.38, Sicko-Goad et al. 1984; 0.12-0.30 for several cultures of two *Cyclotella* sp. strains isolated from the Scheldt, Annex 3B).

Phytolith contribution to the BSi pool

BSi is not produced by diatoms only. Higher plants can also take up DSi and form BSi particles called phytoliths (Conley 2002), which can contribute significantly to the BSi pool in rivers (Cary et al. 2005). The Scheldt tidal river is connected to 4.5 km^2 of marshes, where

vegetation and sediments represent large reservoirs of BSi as phytoliths (Struyf et al. 2005). At each tide, significant amounts of DSi and BSi are exchanged between the river main channel and these adjacent marshes (Struyf et al. 2006). Phytoliths may therefore be present in water samples taken in the main river. Most of the measured BSi was attributed to living diatoms (Fig. 3.3) and phytoliths would be included in the BSi_{det} pool, as higher plants do not contain the pigments that were used as markers for diatoms (Lionard et al. 2008a). Unfortunately, no microscopic investigation was performed to partition BSi_{det} (diatom frustules versus phytoliths), but several indications suggest that the contribution of phytoliths is not significant.

Among the vegetation bordering the tidal river, reeds have by far the highest silica content (Struyf et al. 2005): 7 % of Si per dry weight in dead shoots, but, due to the fact that phytoliths dissolve faster than plant tissues, the maximum silica content found in reed litter is 4 % (Struyf et al. 2005; Struyf et al. 2007a). Considering a marsh surface area of 4.5 km^2 (Struyf et al. 2005) occupied at 55 % by reeds (Soetaert et al. 2004), it would produce annually detritus amounting to 134 Mmol of carbon (Soetaert et al. 2004). With a 4 % Si content per dry weight, this would correspond to 6.1 Mmol of BSi as phytoliths. Given a 100 % annual turnover of the aboveground vegetation (Soetaert et al. 2004), this is in agreement with the maximum estimate of BSi stock in aboveground biomass (Struyf et al. 2005). This amount is small compared to the BSi fluxes during the productive period (Fig. 3.5) and cannot account for the increase of BSi_{det} (26 Mmol for the entire tidal river, Fig. 3.5). Furthermore, for all tidal cycles investigated by Struyf et al. (2006), the net transport of BSi was always from the river channel to the marsh, and there were six times more diatom frustules than phytoliths in marsh sediments (Struyf et al. 2005). Marshes thus appear to be, at first sight, rather a sink for estuarine BSi than a source of phytoliths to the main channel.

Reed detritus are nevertheless common in the SPM of the tidal Scheldt river (Lionard et al. 2008a) and phytoliths could be brought by soil erosion. Phytoliths distribution in soils is closely related to that of soil organic matter (Alexandre et al. 1997; Blecker et al. 2006) and organic matter decomposes faster than the phytoliths in immerged reed detritus (Struyf et al. 2007a). The organic matter from soil and vegetation was thus considered as an indicator of the possible presence of phytoliths. Abril et al. (2002) estimated this organic matter fraction to amount to 23 % of the non-phytoplankton POC in the tributaries; in the tidal river, a similar content was supposed for the POC not corresponding to living diatoms (POC_{nld}, estimated by difference using POC and DiatChl*a* data and $\beta_{POC/Chla} = 30$). However, the amount of

phytoliths estimated from such a POC fraction would only contribute to about 14 ± 10 % of the BSi_{det} or 5 ± 3 % of the total BSi pool during the productive period, even with a Si content of 4 % per dry weight as found in reed litter (Fig. 3.8). This content is indeed in the high range of the average values generally observed (1-3 %; Conley 2002; Blecker et al. 2006). It is however acknowledged that phytoliths may become an important, if not the major, constituent of the BSi pool in the winter season due to lower diatom production but higher litter fall and precipitations (which enhance the soil erosion).

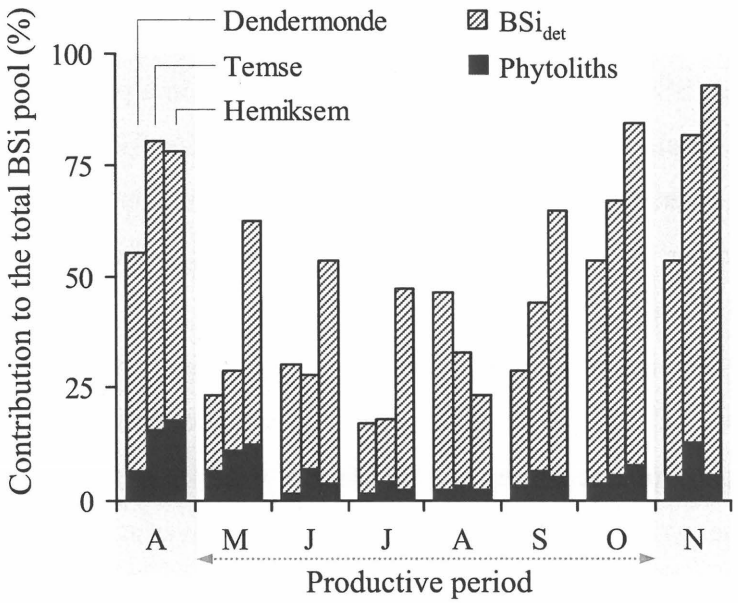

Fig. 3.8: Average monthly contributions of BSi_{det} and phytoliths to the BSi pool at the three estuarine stations from April to November 2003. The contribution of phytoliths was calculated assuming a Si content of 4 % dry weight and a POC from vegetation and soil corresponding to 23 % of POC_{nld} (see text).

Accuracy and precision of the DSi and BSi fluxes and mass-balance calculation

A source of imprecision in our mass-balance calculation may arise from the fact that integrated seasonal fluxes were estimated from discrete weekly DSi and BSi measurements. Selecting a method for evaluating annual riverine fluxes from such concentration datasets is a controversial subject (Kronvang and Bruhn 1996; Moatar and Meybeck 2005, 2007). Kronvang and Bruhn (1996) and Moatar and Meybeck (2005) tested several methods with different sampling strategies on high frequency datasets. They found that inaccuracy and imprecision could respectively reach 20 and 100 %. Unfortunately, no high frequency dataset was available in the Scheldt to test the accuracy of our integration method. Nevertheless, the values reported in Fig. 3.5 differ by less than 2 % compared to the fluxes estimated when the

often recommended "linear integration" method (Kronvang and Bruhn 1996; Moatar and Meybeck 2005) was applied to our data. Additionally, following Moatar et al. (2006) and Moatar and Meybeck (2007), all DSi and BSi fluxes provided by this latter method would be accurate (less than 0.3 % deviation) but with a precision of about 10 to 20 % (flux weighted average: 12 and 8 % for DSi and BSi respectively) (Note 3.1). As both methods led to similar results, it could thus be assumed that the values for DSi and BSi fluxes shown in Fig. 3.5 were calculated with similar precisions. However, a lower precision can be expected for BSi due to analytical errors (10 %, Ragueneau et al. 2005), and above all to the complex SPM dynamics at the tidal scale (Chen et al. 2005a), which cannot be resolved by weekly sampling. Note that the partition between BSi_{liv} and BSi_{det}, which was discussed in a previous section, influences the precision of the "diatom mortality" fluxes only, but not the "BSi deposition" fluxes. As a result, with such an overall precision, the BSi resuspension in Zone 1a and the DSi uptake in Zone 1b do not appear to be significant as they could result from the imprecision in the determination of the fluxes.

Despite low BSi concentrations and low BSi contents in the SPM (annual averages ranging from 1.3 to 3.2 %), the method used for BSi determination was considered as applicable in the case of the Dijle and the Grote and Kleine Nete. BSi and DiatChl*a* concentrations in these rivers displayed indeed concomitant variations (Fig. 3.1d-f) although correlation coefficients were low ($0.11 \leq r^2 \leq 0.56$, $13 \leq n \leq 15$). On the contrary, Eq. 2.3 gave negative correlation for the Zenne (data not shown) probably due to the presence of particulate material brought by the (at that time still) untreated wastewater from the city of Brussels. The Zenne however contributes to less than 10 % of the total water discharge. Also, BSi concentrations in the tributaries of the Rupel were not measured weekly, but weekly fluxes were calculated from linear regressions with DiatChl*a* despite weak correlations. Thus a higher level of uncertainty can be expected for the BSi input flux to the Rupel. However, the importance of this flux is limited when compared to the other fluxes in Fig. 3.5.

Note 3.1: The monographs provided by Moatar et al. (2006) were valid for annual fluxes (Moatar and Meybeck 2007), so it was assumed that they could also be used for a six-month period. The M_2 indicator for DSi and BSi at each station could not be directly determined from our dataset but it was estimated as the product of the Vw_2 and the C^*/C_{50} indicators. This estimation was observed to be valid in the data presented by Moatar and Meybeck (2007) as long as C^*/C_{50} remained lower than 2. This was the case in our dataset for DSi and BSi at all stations as C^*/C_{50} averaged to 1.1 (± 0.3 SD). The data and the definition of the different indicators can be found in Moatar and Meybeck (2007).

Another source of imprecision in the budget shown in Fig. 3.5 is linked to the estimation of DSi and BSi concentrations in lateral inputs, which were assumed identical to those found in the adjacent rivers. Lateral inputs were negligible for BSi but significant for DSi (Fig. 3.5). This is in line with the observation that 80 % of the lateral DSi input fluxes are through precipitation and run-off in the brackish estuary (Soetaert et al. 2006) and that a similar origin may be assumed for the tidal river. The rest of the lateral input fluxes comes from industrial and domestic wastes, in which the DSi concentration is twice higher than that measured in the tributaries (Soetaert et al. 2006). Therefore, with lateral inputs contributing 10 % of the total freshwater discharge and assuming that DSi concentrations in runoff waters are similar to those measured in the tributaries, taking into account the higher DSi concentrations in wastes would lead to an extra DSi input which would amount to only 1 % of the total DSi inputs to the tidal river. However, one could consider that the origin of the lateral inputs to the tributaries was similar to those of the tidal river, so that DSi concentrations measured in the tributaries already reflect the contribution of industrial and domestic wastes.

With respect to the nature of the soils in the Scheldt basin, groundwater inputs are not expected to play a significant role either (Jacobs et al. 2008). Delstanche (2004) gathered 206 values of DSi concentrations in groundwater and first order streams in the Belgian watershed of the Scheldt. Although the values ranged from 10 μmol L^{-1} to 920 μmol L^{-1}, 80 % of the measurements were between 100 and 400 μmol L^{-1}, with an average value of 270 μmol L^{-1}, similar to the level observed in the main tributaries of the Scheldt.

Importance of BSi dissolution and DSi recycling

The mass-balance estimations shown in Fig. 3.5 give only an overall picture of the processes occurring between the sampling stations. An internal cycle of silica comprising dissolution, uptake and settling cannot be excluded and would lead to a higher gross DSi uptake and BSi settling. Dissolution could potentially take place in the sediments but also in the water column as it contains a significant amount of BSi_{det} (Figs. 3.3 and 3.5).

Roubeix et al. (2008) measured a BSi specific dissolution rate of 0.084 d^{-1} in cultures of *C. meneghiniana* and bacteria originating both from the Scheldt tidal river. However, BSi dissolution rates can be lowered by the incorporation of aluminium in the BSi matrix (Van Cappelen et al. 2002). Roubeix et al. (2008) did not investigate aluminium, but concentrations of 1-2 μmol L^{-1} were measured in February 2003 in the tidal river (V. Carbonnel, unpub. results). At aluminium concentrations higher than 200 nmol L^{-1}, diatoms may build frustules

with an Al/Si atomic ratio of 0.01 (Van Beusekom 1991, cited in Van Cappellen et al. 2002). Such a ratio would result in a BSi dissolution rate as low as 0.001 d^{-1}, about 70 times lower than the rate observed for frustules of diatoms grown in aluminium-poor medium when normalised to specific surface area (Van Cappellen et al. 2002). Even higher Al/Si ratios may be reached by Al incorporation in the BSi matrix after diatom death (Van Cappellen et al. 2002). As a result, the specific dissolution rate can be expected to be, at least, as low as 0.0012 d^{-1} in the Scheldt tidal river. Less than 1-2 % of the BSi would then be dissolved considering the average residence times of water presented in Table 2.1 (in Chapter 2).

Struyf et al. (2006) found that marshes act as silica recyclers and that the flux of DSi exported from the 4.5 km^2 of marshes bordering the Scheldt tidal river may exceed the flux entering the river system when DSi concentration and freshwater discharge are low. Indeed, the average DSi flux at Dendermonde was as low as 6 kmol d^{-1} at the end July and beginning of August 2003 (this study). However, this recycling is of minor importance compared to the riverine DSi inputs during the productive period (Fig. 3.5): by extrapolation, recycling would amount to 8 ± 3 Mmol of DSi according to the rates measured by Struyf et al. (2006) during the productive period in 2002 and 2003 in a marsh located close to the mouth of the Durme (Fig. 3.4). Using model simulations, Arndt and Regnier (2007) estimated that, during the productive period in 2003, the highest recycling rates occurred indeed in Zone 1b. They found that riverine inputs and silica recycling could be of the same order of magnitude, but only in mid-August 2003. Taking spatial heterogeneity into account, they however estimated that only 2 Mmol of DSi would be recycled between Ghent and the mouth of the Rupel between June and November. As a result, less than 1 % of the overall diatom production over the productive period could be sustained by recycled DSi (Arndt and Regnier 2007). Considering that this amount was calculated with a BSi dissolution rate 25 times higher than what would be expected for BSi containing 1 % aluminium, it can be concluded that BSi dissolution is not expected to play a significant role in the silica dynamics within the tidal river during the selected study period.

DSi uptake in Zones 1 and 2 and influence of the freshwater discharge

The high DSi uptake in Zone 2 (Fig. 3.5) revealed an important diatom growth, although this was not expected because of short water residence times in the Rupel and its tributaries (Table 2.1 in Chapter 2) and of possible light limitation near and downstream of the confluence with the Rupel. Indeed, the section of the Scheldt comprised between Temse

and Hemiksem contributes to roughly half of the water surface area and of the volume of Zone 2 (Fig. 3.4; Table 2.1). But near the mouth of the Rupel, the presence of a water energy maximum results in high SPM concentrations and a longer residence time of riverborne material (Chen et al. 2005a), and water column deepens downstream of the confluence (Table 2.1; Muylaert et al. 2005). However, diatom growth might have occurred between Temse and the mouth of the Rupel, where the water depth is still shallow and where the diatom-rich but DSi-depleted Scheldt water receives DSi from the Rupel due to tidal mixing. A diatom bloom might have additionally occurred in the shallow Nete (Table 2.1) because of exceptionally low water discharges during summer 2003 (< 30 m^3 s^{-1}). A local maximum in diatom production in the lower part of the Nete was indeed predicted by the model simulation of Arndt et al. (2007) during summer 2003 (S. Arndt, pers. comm.). In August 1995, when discharge in the Scheldt tidal river was similar to that in 2003, the diatom biomass in the Nete was also among the highest of the tidal river (Muylaert et al. 1997).

The comparison of the DSi consumption in Zone 1 and 2 illustrated the influence of the discharge on the diatom production: a higher discharge in Zone 2 than in Zone 1 resulted in higher DSi inputs and also a higher diatom production in Zone 2 (Fig. 3.5). This can be explained by the fact that DSi was entirely consumed from June to September in Zone 1a (except however for periods following the discharge peaks, Fig. 3.1g), whereas this was the case only at the end July and beginning of August in Zone 2 (Fig. 3.1i). In both zones, DSi concentrations could drop below 5 µmol L^{-1}. Such low levels could limit the diatom production, as they were in the range of the half-saturation constants for the growth of strains of *Cyclotella* sp. isolated from the Scheldt (Annex 3B). During these periods, DSi uptake corresponded thus to the DSi inputs to the zones and, in particular, a minimum of DSi uptake in Zone 1a in August was induced by a low water discharge (Fig. 3.6). The higher DSi inputs in Zone 2 as compared with Zone 1a resulted in a shorter period of potential DSi limitation in Zone 2. Also, during the periods of potential DSi limitation, the DSi uptake rate in Zone 2 was limited at a higher rate than in Zone 1a (Figs. 3.5 and 3.6). A low water discharge can thus induce a low rate of diatom production due to DSi limitation. In contrast, it has already been shown that a high discharge may hamper diatom growth by flushing the diatoms out of the zone (Muylaert et al. 2001, 2005; Arndt et al. 2007). If all factors influencing diatom growth other than silica availability and discharge are kept constant, an optimal discharge can be found at which the highest diatom production is reached, as shown by model simulations

carried out on Zone 1 during summer 2003 by Arndt et al. (2007). This phenomenon was also observed on an inter-annual timescale by Peterson et al. (1985) in the San Francisco estuary.

The summer of 2003 was exceptionally dry, warm and sunny (IRMB 2003-2004) and during this period the Scheldt discharge was the lowest for the decade 1996-2005 (56 $m^3 s^{-1}$, average 1996-2005: 77 $m^3 s^{-1}$). DSi uptake and silica retention reached high values: 48 % and 30 % respectively during the productive period (Table 3.2). This is comparable to the DSi retention estimated by Garnier et al. (2002) for the Seine tidal river during the summer of a dry year (47 % in 1993). Summer diatom production and silica uptake are however expected to vary from one year to another: the percentage of DSi consumed should indeed decrease with increasing discharge and decreasing water residence times, as observed by Garnier et al. (2002) in the Seine at an inter-annual timescale. For the period 1996-2000, Struyf et al. (2004) also observed increasing summer DSi concentrations with increasing discharge in the Scheldt at Dendermonde, whereas winter DSi concentrations stayed constant at about 230 µmol L^{-1}. At highest summer discharges, the DSi concentrations could even reach winter DSi concentrations. Accordingly, Van Damme et al. (2005) reported that almost no DSi was consumed in the tidal river during the wet and mostly overcast summer 2000. Lionard et al. (2008b) found a negative correlation between the summer phytoplankton biomass and the summer discharge for the period 1996-2004. The summer DSi concentrations also decreased with increasing summer phytoplankton biomass, except however for the years 1996 and 1999 (Lionard et al. 2008b). This highlights the fact that parameters other than discharge may play a role in regulating inter-annual variations of the summer DSi concentrations.

At a seasonal timescale and for the entire tidal river, a decreasing trend could be observed between DSi uptake and discharge, but the relationship did not appear strongly linear and above all highlighted the fact that DSi uptake dropped from 100 % to 30 % from August to October even though the three-week moving average discharge stayed between 40 and 60 $m^3 s^{-1}$ (Fig. 3.9). This suggests that discharge was not the only controlling parameter for DSi uptake in the tidal river at this timescale. As in many estuarine systems, light availability is a major factor influencing phytoplankton productivity in the Scheldt (Muylaert et al. 2005; Arndt et al. 2007). The seasonal variation of light during the productive period in 2003 was uncorrelated to discharge (three-week moving average data: $r^2 = 0.06$, $n = 26$) and the drop in DSi uptake from August to October could actually be attributed to the decrease of the incident light (IRMB 2003-2004). When the multiple regression was performed between DSi uptake and the explicative variables discharge and light, the correlation coefficient (r^2 =

0.80, n = 26) was significantly improved compared to the regression shown in Fig. 3.9 and the residuals of the regression did not exhibit any significant pattern.

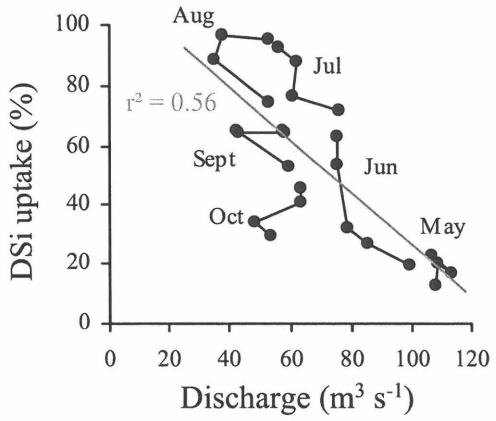

Fig. 3.9: DSi uptake (%) in the entire tidal river in 2003, estimated from DSi fluxes in the tributaries and at Hemiksem, versus discharge (m^3 s^{-1}). All values are three-week moving average.

Parameters other than discharge, light and DSi availability might have influenced diatom growth and thus DSi uptake. Limitation by nutrients other than DSi could be ruled out in the tidal river as dissolved nitrogen and phosphorus were in high concentrations during the study period (Van der Zee et al. 2007). The diatom productivity should not have been controlled by the zooplankton community, which is dominated by rotifers in the Scheldt tidal river (Muylaert et al. 2005 and reference therein). The phytoplankton biomass can have however a strong influence on phytoplankton productivity (Muylaert et al. 2005). The three weeks moving average of the biomass at Dendermonde, Temse and Hemiksem correlated well with the percentage of DSi consumed ($r^2 = 0.81$, n = 26). But, biomass also depends on light and discharge in the Scheldt tidal river (multiple linear regression: $r^2 = 0.74$, n = 26) and its effects should therefore already be implicitly included when the influence of light is taken into account.

Spatial distribution of the BSi deposition: influence of the SPM dynamics

The absence of correlation between DiatChl*a* and SPM_{nbld} ($r^2 = 0.02$, n = 75) tends to prove that living diatoms do not follow the SPM dynamics. However, the multiple regression between BSi and the two aforementioned independent variables provided a stronger correlation ($r^2 = 0.71$, n = 75) than that between BSi and DiatChl*a* only ($r^2 = 0.51$, n = 75). It indicates that BSi and SPM dynamics are nevertheless linked to some extent. As a consequence, BSi concentrations in the estuary may exhibit vertical gradients, tidal

deposition/resuspension cycles and tidal variations as it is the case for estuarine SPM, even if this SPM heterogeneity is less pronounced upstream of the confluence with the Rupel than downstream, in the zone of maximum of turbidity (Chen et al. 2005a). These processes could not be considered in our study due to the sampling frequency and to the fact that only surface water samples were taken.

The longitudinal distribution of the BSi deposition over Zone 2 could not be assessed due to the absence of an intermediate sampling station. In Zone 1, DSi uptake and BSi deposition occurred in different sub-zones (Fig. 3.5). Arndt and Regnier (2007) indeed predicted that BSi deposition should occur in Zone 1b throughout the productive period, which is in agreement with our budget. These authors also found that a smaller amount of BSi would be deposited in Zone 1a, but only in August when diatom production was shifted upstream of Dendermonde due to silica limitation. Furthermore, Arndt et al. (2007) predicted that the maximum diatom production should be located in Zone 1b in June because of lower SPM concentrations. In contrast, our findings rather suggest that the diatoms bloomed at Dendermonde or further upstream (Zone 1a) during the whole productive period and were subsequently transported downstream. DiatChl*a* was always higher at Dendermonde than at Temse. Except maybe during the first week of July because of a discharge peak, DSi was already completely consumed in June at Dendermonde (Fig. 3.1g-h). In October, the DSi uptake nevertheless occurred in Zone 1b (Fig. 3.1g-h).

Deposition in Zone 1a cannot however be excluded. SPM dynamics are driven by a complex hydrodynamic energy pattern determined by the convergence of the decreasing energies of riverine and marine origins, and by the channel morphology (Chen et al. 2005a; Arndt et al. 2007). Although there is a net downstream transport of SPM in the upstream part of the tidal river, a high fluvial hydrodynamic energy induces a turbidity maximum in Zone 1a, and a local energy minimum is observed in Zone 1b (Chen et al. 2005a; Arndt et al. 2007). Despite a high temporal variability, the average measured SPM concentrations was indeed significantly higher at Dendermonde (97 ± 61 mg L^{-1}, mean ± SD) than at Temse (69 ± 71 mg L^{-1}, *t*-test for equality: $p = 0.08$) or in the rivers Scheldt (32 ± 9 mg L^{-1}, $p = 3\times10^{-8}$) and Dender (15 ± 8 mg L^{-1}, $p = 10^{-11}$). The presence of a turbidity maximum at or upstream of Dendermonde indicates an increased residence time leading to the retention or accumulation of suspended particles in this area. A consequence of the BSi accumulation in Zone 1a is that both the BSi flux at Dendermonde and the deposition in Zone 1b may have been lower than

what we estimated (Fig. 3.5). Nevertheless, this would have altered only the spatial repartition of the deposition of BSi within Zone 1, but not the estimation of its overall amount.

The retention of particles in the water column at or upstream of Dendermonde could also explain the high BSi and DiatChla concentrations in October – November (Fig. 3.1g) while DSi uptake had stopped (Fig. 3.6). Additionally, the highest BSi concentration observed at Dendermonde (364 μmol L^{-1}, 8 Sept. 2003, Fig. 3.1g) might have been due to the presence of diatom frustules previously accumulated in the water column (or settled) upstream of Dendermonde, and flushed downwards (or resuspended) due to a sudden discharge increase (Fig. 3.2). An increase in diatom production or a high phytolith content could indeed be ruled out in view of the ratios between BSi, DiatChl*a* and POC_{nld}.

The important deposition estimated for Zone 1b is supported by the presence of the hydrodynamic energy minimum, which induces lower particle concentrations (Chen et al. 2005a, Arndt et al. 2007). Additionally, deposition in Zone 1b may have been enhanced by the deepening and widening of the channel and by the increase of the residual current (Table 2.1 in Chapter 2). A decoupling between BSi and the rest of the SPM could however be observed at this stage as the average BSi content during the productive period was significantly higher at Dendermonde (10.5 ± 7.0 %, mean ± SD) than at Temse (6.0 ± 2.8 %) (*t*-test for equality: $p = 0.004$). This suggests a preferential settling of BSi compared to non-BSi SPM in Zone 1b. This may be due to the fact that the SPM in the Scheldt tidal river is composed of more than half of clay material (< 4 μm; Chen et al. 2005b), which are finer than diatom frustules and thus expected to remain in suspension for a longer time (cultures of *C. meneghiniana* isolated from the Scheldt exhibited cell sizes ranging from 10 to 25 μm, V. Roubeix, pers. comm.). In addition, the presence of organic material around diatoms would enhance their aggregation into flocs and increase their sinking rate (Chen et al. 2005b).

Most of the BSi deposition should occur in shallow areas, such as tidal mudflats, tidal marshes and shallow parts of the river section, because of lower currents than in the main stream channel (Arndt and Regnier 2007). Struyf et al. (2006, 2007b) measured summer BSi deposition rates in two marshes along the Scheldt tidal river. All together, individual measurements varied within two orders of magnitude. The high variability could be explained by the fact that SPM deposition in marshes varies exponentially with the maximum tidal height, the marsh elevation and the distance to the creek or to the marsh edge (Temmerman et al. 2003). If the rates for the two marshes were averaged and extrapolated to a 4.5 km^2 marsh surface area (Struyf et al. 2005), they would give an overall BSi deposition of 1.3 ± 1.1 and

15.0 ± 14.6 Mmol for the entire tidal river during the productive period. This would suggest that most of the 77 Mmol of BSi deposition would have taken place in other areas such as shallow parts of the stream channel, mudflats or at the marsh edges. Mudflats represent about 39 % of the length of the tidal river banks, whereas marshes account for 32 % (Meire et al. 2005). However, BSi deposited on mudflats or at marsh edges might be re-suspended in winter by higher water currents and re-deposited further inland in marshes. Together with higher winter SPM deposition (Temmerman et al. 2003), winter BSi deposition rates in marshes are indeed higher than the summer ones (Struyf et al 2007b).

Silica fluxes at the annual timescale

In 2003, almost 80 % of the annual amount of DSi was delivered to the brackish estuary outside the productive period (November – April, Table 3.2). Despite high BSi concentrations in the tidal river (Fig. 3.1), almost 90 % of the silica discharged annually to the brackish estuary was in the form of DSi (Table 3.2). Diatom production occurred when silica input fluxes to the estuary were at their lowest values (Fig. 3.7). As a result, annual silica retention and DSi uptake were less than foreseen when only concentrations were examined (Fig. 3.1i) or when only the productive period was investigated (Fig. 3.5, Table 3.2).

Outside the productive period, sampling was performed at a monthly frequency. Following Moatar et al. (2006) and Moatar and Meybeck (2007), this would lead to an imprecision of about 30 % on all annual DSi and BSi fluxes. Such an imprecision would preclude the comparison of the net annual amounts of DSi consumed and BSi produced over the entire tidal river with the net seasonal values (Table 3.2). Nevertheless, DSi displayed a conservative behaviour outside the productive period, whereas some more BSi was produced (Fig. 3.7, Table 3.2). Most of this production was attributed to late diatom activity in November and/or resuspension during the very high discharge event around mid-January (Figs. 3.2, 3.1g-i and 3.7). The spring bloom had no significant effect on the silica cycle in the tidal river. A mass-balance constructed for the period from mid-March to end-April suggested that DSi was not significantly affected along the estuary, with only 2 Mmol of BSi produced in Zone 1a and settled in Zone 1b: the spring bloom is imported from the upper Scheldt river and cannot develop in the tidal river (Muylaert et al. 2000, 2005). In our data, high DiatChl*a* concentrations were measured in spring at Ghent and Dendermonde, but not further downstream (Fig. 3.1a, g-i).

The brackish estuary received an almost constant BSi flux compared to the DSi flux which could vary over more than two orders of magnitude (Fig. 3.7). This seasonal asymmetry in the DSi fluxes may be of significant importance for the silica cycle in the brackish estuary. However, considering the residence time of the water in the brackish estuary (70 days in summer, Soetaert and Herman 1995), the summer DSi uptake in the tidal river would not have affected the mouth of the estuary and the coastal zone before August of the same year. By late summer, blooms of diatoms and *Phaeocystis* sp. had terminated, DSi was no longer depleted and its concentration started to increase again in the coastal zone near the mouth of the estuary (Van der Zee and Chou 2005; Muylaert et al. 2006). As a result, the summer removal of DSi in the Scheldt tidal river is not expected to have had an important effect on the supply of DSi to the coastal zone during coastal phytoplankton blooms. Instead, the extent of the supply of DSi by the Scheldt to the coastal zone in spring seems to be principally supported by the winter riverine DSi flux, which is actually driven by the winter freshwater discharge because of constant winter riverine DSi concentrations.

3.5 Acknowledgements

This chapter has been submitted for publication in the journal "Biogeochemistry". The author list is, in this order, Vincent Carbonnel (LOCGE - ULB), Marie Lionard (Protistology and Aquatic Ecology - UG), Koenraad Muylaert (Protistology and Aquatic Biology - UG) and Lei Chou (LOCGE - ULB). The current status is "Revision being processed".

We are very grateful to Jean-Pierre Vanderborght for constructive discussions and comments on the manuscript. Claar van der Zee and Nathalie Roevros commented on previous versions of the manuscript. We would also like to thank Nathalie Roevros, Nicolas Canu, Renaat Dasseville, Christiane de Marneffe, Michaël Tsagaris and Stijn Vanneste for their assistance in field sampling and laboratory analyses. Victor Chepurnov isolated the *Cyclotella* sp. strains for the phytoplankton collection of the Ghent University. Data on water discharge were provided by the Ministry of the Flemish Community (Afdeling Maritieme Toegang). We would also like to thank the three anonymous reviewers for their constructive comments and suggestions. This study was financed by the Belgian Federal Science Policy Office (BELSPO) under contract number EV/11/17A (SISCO). Additional BELSPO funding from the TIMOTHY project (Interuniversity Attraction Pole, IAP, P6/13) is acknowledged. This is also a contribution to the EU IP CarboOcean (contract no. 511176–2). We would like to dedicate this paper to the late Roland Wollast who did the pioneering work on the silica biogeochemistry in the Scheldt estuary.

3.6 References

Abril G, Nogueira M, Etcheber H, Cabeçadas G, Lemaire E, Brogueira MJ (2002) Behaviour of organic carbon in nine contrasting European estuaries. Estuar Coast Shelf Sci 54:241-262

Alexandre A, Meunier J-D, Colin F, Koud J-M (1997) Plant impact on the biogeochemical cycle of silicon and related weathering processes. Geochim Cosmochim Acta 61(3):677-682

Arndt S, Vanderborght J-P, Regnier P (2007) Diatom growth response to physical forcing in a macrotidal estuary: Coupling hydrodynamics, sediment transport, and biogeochemistry. J Geophys Res 112:C05045

Arndt S, Regnier P (2007) A model for the benthic-pelagic coupling of silica in estuarine ecosystems: sensitivity analysis and system scale simulation. Biogeosciences 4:331-352

Blecker SW, McCulley RL, Chadwick OA, Kelly EF (2006) Biologic cycling of silica across a grassland bioclimosequence. Glob Biogeochem Cycle 20:GB3023

Cary L, Alexandre A, Meunier J-D, Boeglin J-L, Braun J-J (2005) Contribution of phytoliths to the suspended load of biogenic silica in the Nyong basin rivers (Cameroon). Biogeochemistry 74:101-104

Chen MS, Wartel S, Van Eck B, Van Maldegem D (2005a) Suspended matter in the Scheldt estuary. Hydrobiologia 540(1-3):79-104

Chen MS, Wartel S, Temmerman S (2005b) Seasonal variation of floc characteristics on tidal flats, the Scheldt estuary. Hydrobiologia 540(1-3):181-195

Conley DJ (2002) Terrestrial ecosystems and the global biogeochemical silica cycle. Glob Biogeochem Cycle 16(4):68(1)-68(7)

Delstanche S (2004) Contribution à l'étude du cycle biogéochimique de la silice dans le continuum aquatique de l'Escaut. MSc. thesis. Université Catholique de Louvain, Belgium. (In French)

Garnier J, d'Ayguesvives A, Billen G, Conley DJ, Sferratore A (2002) Silica dynamics in the hydrographic network of the Seine River. Océanis 28(3-4):487-508

Geider RJ (1987) Light and temperature dependence of the carbon to chlorophyll *a* ratio in microalgae and cyanobacteria: implications for physiology and growth of phytoplankton. New Phytol 106:1-34

Hellings L, Dehairs F, Tackx M, Keppens E, Baeyens W (1999) Origin and fate of organic carbon in the freshwater part of the Scheldt Estuary as traced by stable carbon isotope composition. Biogeochemistry 47:167-186

Hildebrand M (2002) Lack of coupling between silicon and other elemental metabolisms in diatoms. J Phycol 38:841-843

IRMB (Institut Royal Météorologique de Belgique) (2003-2004) Bulletins mensuels, Observations climatologiques, parties I et II. Institut Royal Météorologique de Belgique, Bruxelles. (In French/Dutch)

Jacobs S, Struyf E, Maris T, Meire P (2008) Spatiotemporal aspects of silica buffering in restored tidal marshes. Estuar Coast Shelf Sci 80(1):42-52

Kronvang B, Bruhn AJ (1996) Choice of sampling strategy and estimation method for calculating nitrogen and phosphorus transport in small lowland streams. Hydrol Process 10:1483-1501

Lionard M (2006) Spatio-temporal phytoplankton dynamics along the Scheldt-North Sea continuum based on HPLC/CHEMTAX pigment analysis. Ph. D. thesis. Univ. of Ghent, Belgium.

Lionard M, Muylaert K, Tackx M, Vyverman W (2008a) Evaluation of the performance of HPLC-CHEMTAX analysis for determining phytoplankton biomass and composition in a turbid estuary (Schelde, Belgium). Estuar Coast Shelf Sci 76(4):809-817

Lionard M, Muylaert K, Hanouti A, Maris T, Tackx M, Vyverman W (2008b) Inter-annual variability in phytoplankton summer blooms in the freshwater tidal reaches of the Schelde estuary (Belgium). Estuar Coast Shelf Sci 79(4):694-700

Martin-Jézéquel V, Hildebrand M, Brzezinski MA (2000) Silicon metabolism in diatoms: implications for growth. J Phycol 36:821-840

Meire P, Ysebaert T, Van Damme S, Van den Bergh E, Maris T, Struyf E (2005) The Scheldt estuary: a description of a changing ecosystem. Hydrobiologia 540(1-3):1-11

Moatar F, Meybeck M (2005) Compared performances of different algorithms for estimating annual nutrient loads discharged by the eutrophic River Loire. Hydrol Process 19:429-444

Moatar F, Person G, Meybeck M, Coynel A, Etcheber H, Crouzet P (2006) The influence of contrasting suspended particulate matter transport regimes on the bias and precision of flux estimates. Sci Total Environ 370:515-531

Moatar F, Meybeck M (2007) Riverine fluxes of pollutants: Towards predictions of uncertainties by flux duration indicators. C R Geosci 339:367-382

Muylaert K, Van Kerckvoorde A, Vyverman W, Sabbe K (1997) Structural characteristics of phytoplankton assemblages in tidal and non-tidal freshwater systems: a case study from the Schelde basin, Belgium. Freshw Biol 38:263-276

Muylaert K, Sabbe K, Vyverman W (2000) Spatial and temporal dynamics of phytoplankton communities in a freshwater tidal estuary (Schelde, Belgium). Estuar Coast Shelf Sci 50(5):673-687

Muylaert K, Van Wichelen J, Sabbe K, Vyverman W (2001) Effects of freshets on phytoplankton dynamics in a freshwater tidal estuary (Schelde, Belgium). Arch Hydrobiol 150(2):269-288

Muylaert K, Tackx M, Vyverman W (2005) Phytoplankton growth rates in the freshwater tidal reaches of the Schelde estuary (Belgium) estimated using a simple light-limited primary production model. Hydrobiologia 540(1-3):127-140

Muylaert K, Gonzales R, Franck M, Lionard M, van der Zee C, Cattrijsse A, Sabbe K, Chou L, Vyverman W (2006) Spatial variation in phytoplankton dynamics in the Belgian coastal zone of the North Sea studied by microscopy, HPLC-CHEMTAX and underway fluorescence recordings. J Sea Res 55:253-265

Peterson DH, Smith RE, Hager SW, Harmon DD, Herndon RE, Schemel LE (1985) Interannual variability in dissolved inorganic nutrients in Northern San Francisco Bay Estuary. Hydrobiologia 129:37-58

Ragueneau O, Tréguer P, Leynaert A, Anderson RF, Brzezinski MA, DeMaster DJ, Dugdale RC, Dymond J, Fischer G, Francois R, Heinze C, Maier-Reimer E, Martin-Jézéquel V, Nelson DM, Quéguiner B (2000) A review of the Si cycle in the modern ocean: recent progress and missing gaps in the application of biogenic opal as a paleoproductivity proxy. Glob Planet Change 26(4):317-365

Ragueneau O, Savoye N, Del Amo Y, Cotten J, Tardiveau B, Leynaert A (2005) A new method for the measurement of biogenic silica in suspended matter of coastal waters: using Si:Al ratios to correct for the mineral interference. Cont Shelf Res 25(5-6):697-710

Roubeix V, Becquevort S, Lancelot C (2008) Influence of bacteria and salinity on diatom biogenic silica dissolution in estuarine systems. Biogeochemistry 88(1):47-62

Sicko-Goad LM, Schelske CL, Stoermer EF (1984) Estimation of intracellular carbon and silica content of diatoms from natural assemblages using morphometric techniques. Limnol Oceanogr 29(6):1170-1178

Soetaert K, Herman PMJ (1995) Estimating estuarine residence times in the Westerschelde (The Netherlands) using a box model with fixed dispersion coefficients. Hydrobiologia 311:215-224

Soetaert K, Hoffmann M, Meire P, Starink M, van Oevelen D, Van Regenmortel S, Cox T (2004) Modeling growth and carbon allocation in two reed beds (*Phragmites australis*) in the Scheldt estuary. Aquat Bot 79:211-234

Soetaert K, Middelburg JJ, Heip C, Meire P, Van Damme S, Maris T (2006) Long-term change in dissolved inorganic nutrients in the heterotrophic Scheldt estuary (Belgium, The Netherlands). Limnol Oceanogr 51(1, part 2):409-423

Struyf E, Van Damme S, Meire P (2004) Possible effects of climate change on estuarine nutrient fluxes: a case study in the highly nutrified Schelde estuary (Belgium, The Netherlands). Estuar Coast Shelf Sci 60(4):649-661

Struyf E, Van Damme S, Gribsholt B, Middelburg JJ, Meire P (2005) Biogenic silica in tidal freshwater marsh sediments and vegetation (Schelde estuary, Belgium). Mar Ecol Prog Ser 303:51-60

Struyf E, Dausse A, Van Damme S, Bal K, Gribsholt B, Boschker HTS, Middelburg JJ, Meire P (2006) Tidal marshes and biogenic silica recycling at the land-sea interface. Limnol Oceanogr 51(2):836-846

Struyf E, Van Damme S, Gribsholt B, Bal K, Beauchard O, Middelburg JJ, Meire P (2007a) *Phragmites australis* and silica cycling in tidal wetlands. Aquat Bot 87:134-140

Struyf E, Temmerman S, Meire P (2007b) Dynamics of biogenic Si in freshwater tidal marshes: Si regeneration and retention in marsh sediments (Scheldt estuary). Biogeochemistry 82:41-53

Temmerman S, Govers G, Wartel S, Meire P (2003) Spatial and temporal factors controlling short-term sedimentation in a salt and freshwater tidal marsh, Scheldt estuary, Belgium, SW Netherlands. Earth Surf Process Landf 28:739-755

Van Cappellen P, Dixit S, van Beusekom J (2002) Biogenic silica dissolution in the oceans: Reconciling experimental and field-based dissolution rates. Glob Biogeochem Cycle 16(4):1075

Van Damme S, Struyf E, Maris T, Ysebaert T, Dehairs F, Tackx M, Heip C, Meire P (2005) Spatial and temporal patterns of water quality along the estuarine salinity gradient of the Scheldt estuary (Belgium and The Netherlands): results of an integrated monitoring approach. Hydrobiologia 540(1-3):29-45

Van der Zee C, Chou L (2005) Seasonal cycling of phosphorus in the Southern Bight of the North Sea. Biogeosciences 2:27-42

Van der Zee C, Roevros N, Chou L (2007) Phosphorus speciation, transformation and retention in the Scheldt estuary (Belgium/The Netherlands) from the freshwater tidal limits to the North Sea. Mar Chem 106(1-2):76-91

3A ANNEX: DSi profiles in the tributaries

3A.1 Influence of freshwater discharge

DSi concentrations in the tributaries are plotted together with the freshwater discharge in Fig. 3A.1. There was a clear relationship between the sharp increases in the freshwater discharge and the drops in DSi concentrations in the Dijle, even if our sampling resolution was low compared to the duration of these peaks (Fig. 3A.1d).

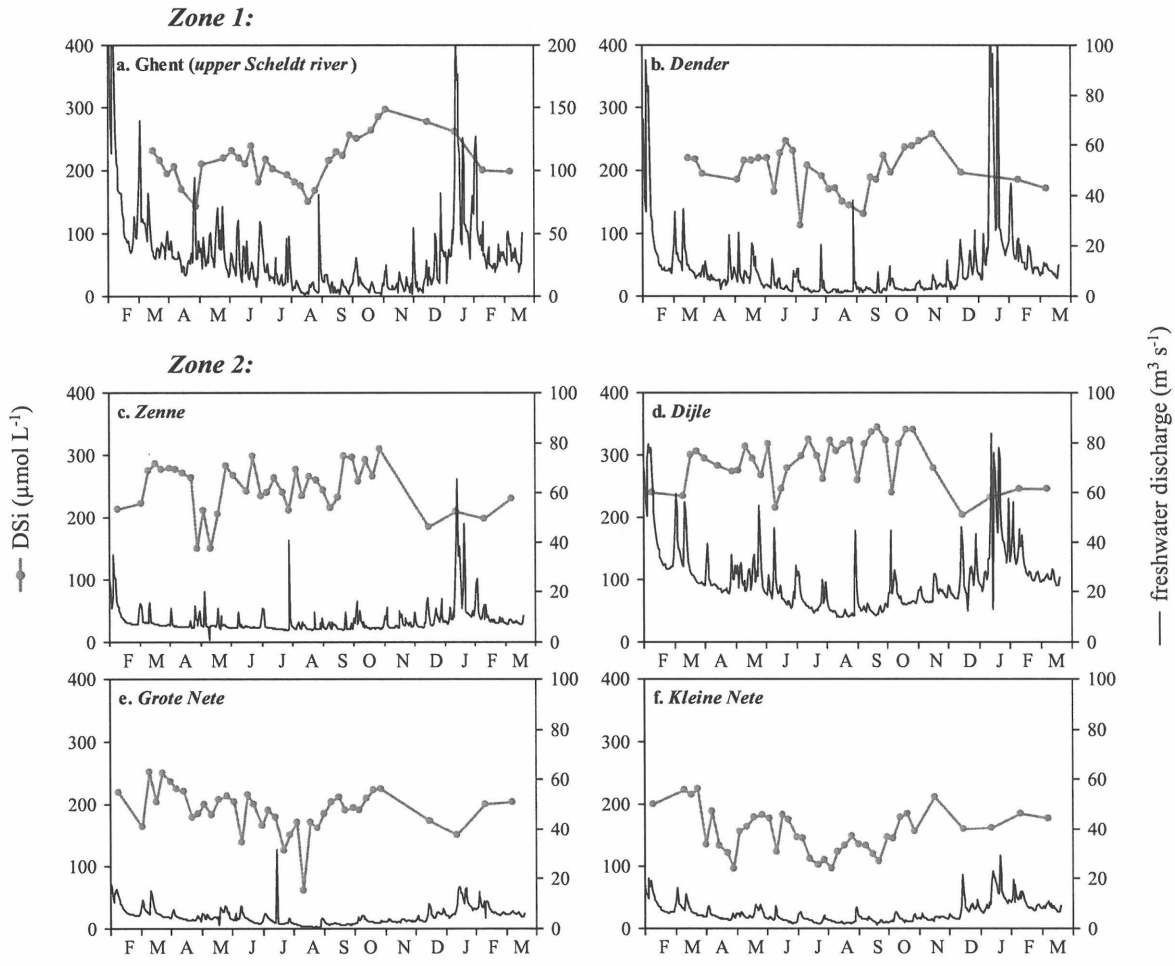

Fig. 3A.1: DSi concentrations and freshwater discharge (as measured at the sampling stations, i.e. without the added contribution of the lateral inputs, see Chapter 3) from February 2003 to March 2004. Note the different y-axis scale for freshwater discharge at Ghent.

These decreases in DSi concentration in the Dijle may be explained by dilution with run-off water not in contact with DSi-rich groundwater, as observed during winter 2002-2003 in the tidal river (see Chapter 4). No such clear correspondence could be highlighted however in any of the other tributaries (Fig. 3A.1). Nevertheless, DSi concentrations always tended to display low values from December 2003 to February-March 2004 while the freshwater discharge reached highest levels.

3A.2 Comparison between tributaries

The average DSi concentrations varied from one station to another: the highest one, measured in the Dijle, was almost twice higher than the lowest one, measured in the Kleine Nete (Chapter 3). These differences could be due to several different factors.

Biological consumption

In the upper Scheldt river and in the Dender, DSi concentrations were altered in spring and summer by diatom uptake, but the low DiatChl*a* and BSi concentrations in the tributaries of the Rupel suggested that no such consumption occurred in these rivers. In the Grote and Kleine Nete however, the fact that DSi concentrations decreased in summer suggested that there could have been some upstream biological removal of the DSi, possibly by benthic diatoms, macrophytes or some aquatic vegetation.

Lithology

The type of soils has an influence on the chemical composition of groundwater and thus of the riverine water (Appelo and Postma 1996). The Scheldt watershed is principally composed of tertiary sands, but the watersheds of the Grote and Kleine Nete may be distinguished from those of the Zenne, the Dender and the upper Scheldt river by the presence of a naturally ferric soil (A. Taillez, ULB, pers. comm.). However, as the watershed of the Dijle presents an intermediate situation, this can not explain by itself the range of the observed DSi concentrations. In addition, Delstanche (2004) did not observe any influence of different type of soils on DSi concentrations in groundwater and in first order streams of the Scheldt watershed.

Land-use activities

As DSi in soils may principally originate from phytolith dissolution (Alexandre et al. 1997; Conley 2002; Derry et al. 2005) and as plants can affect mineral weathering (Kelly et

al. 1998), land-use activities can be expected to have an influence on DSi concentrations in adjacent rivers (Conley et al. 2008). In the Scheldt basin, the most forested watersheds are those of the Dijle and of the Nete, and the watersheds with the largest surface area devoted to agriculture are those of the upper Scheldt river and of the Dender (A Taillez, pers. comm.). However, the impact of the agriculture on the water geochemistry differs strongly from one watershed to another: as for the impact of industrial activities, it is high in the Nete and in the Scheldt, but low in the Dender (Rapport Scaldit 2004). However, one should note that the influence of land-use activities on DSi concentrations is not straightforward. For instance, plants can have contrasting effects on mineral weathering (Kelly et al. 1998) and the variation of the released DSi concentration may depend on the amount of detritus left on the soil (Conley et al. 2008). As a result, riverine DSi concentrations may not be affected, or at least may not be correlated with land-use (Jordan et al. 1997; Correll et al. 2000; Holmes 2008).

Urbanisation

Urbanisation may also affect the riverine DSi concentrations: compared to tap water, the wastewater may be enriched in DSi due to the use of washing powders (Verbanck et al. 1994). DSi concentrations of 480 μmol L^{-1} have been measured in the sewage of Brussels (Verbanck et al. 1994), which is almost twice higher than that in the tap water. The impact of the urbanisation is high in the Dijle, Scheldt and Zenne, but low in the Dender and the Nete (Rapport Scaldit 2004). Nevertheless, although the watershed of the Zenne hosts a population density about 3 times higher than that in the other basins (A. Taillez, pers. comm.), the DSi concentrations in the Zenne do not exhibit especially high values (Fig. 3A.1c).

Overall, only the impact of the urbanisation seemed to be, in fact only partially, coherent with the differences in the DSi concentrations. Other factors may have also superimposed, rendering their distinctions difficult. Information on other dissolved elements may help however to track the origin of the DSi and to understand the causes of the differences in DSi concentrations observed in these tributaries.

3A.3 References

Alexandre A, Meunier J-D, Colin F, Koud J-M (1997) Plant impact on the biogeochemical cycle of silicon and related weathering processes. Geochim Cosmochim Acta 61(3):677-682

Appelo CAJ, Postma D (eds) (1996) Geochemistry, groundwater and pollution. A.A.Balkema, Rotterdam.

Conley DJ (2002) Terrestrial ecosystems and the global biogeochemical silica cycle. Global Biogeochemical Cycles 16(4):68-1-68-7

Conley DJ, Likens GE, Buso DC, Saccone L, Bailey SW, Johnson CE (2008) Deforestation causes increased dissolved silicate losses in the Hubbard Brook Experimental Forest. Glob Change Biol 14(11):2548-2554

Correll DL, Jordan TE, Weller DE (2000) Dissolved silicate dynamics of the Rhode River watershed and estuary. Estuaries 23(2):188-198

Delstanche S (2004) Contribution à l'étude du cycle biogéochimique de la silice dans le continuum aquatique de l'Escaut. MSc. thesis. Université Catholique de Louvain, Belgium. (In French)

Derry LA, Kurtz AC, Ziegler K, Chadwick OA (2005) Biological control of terrestrial silica cycling and export fluxes to watersheds. Nature 433:728-731

Holmes GT (2008) Nutrient supply, water residence time, temperature, and grazing as controls of size-fractionated phytoplankton biomass in shallow temperate estuarine ecosystems. Dissertation Abstracts International 69(1):Suppl. B, 198p

Jordan TE, Correll DL, Weller DE (1997) Relating nutrient discharges from watersheds to land use and streamflow variability. Water Resources Research 33(11):2579-2590

Kelly EF, Chadwick OA, Hilinski TE (1998) The effect of plants on mineral weathering. Biogeochemistry 42:21-53

Rapport Scaldit (2004) Analyse transnationale de l'état des lieux du District hydrographique international de l'Escaut : projet pilote pour le test des documents guides européens. Scaldit, Vlaamse Milieumaatschappij, Erembodegem. (In French)

Verbanck M, Vanderborght J-P, Wollast R (1994) Major ion content of urban wastewater: assessment of per capita loading. Research Journal Water Pollution Control Federation 61(11/12):1722-1728

3B ANNEX: Culture experiments

3B.1 Cultures

Two strains of the diatom *Cyclotella meneghiniana* isolated from the Scheldt tidal river in 2003 (by V. Chepurnov, Ghent University) were cultured in the laboratory to determine the Si/C contents and to perform experiments of kinetic incorporation of ^{32}Si at various DSi concentrations. The two strains were maintained in frequently renewed batch cultures in 50 mL incubation bottles of DSi-rich WC medium (DSi concentration of 100 µmol L^{-1}, Guillard and Lorenzen 1972), incubated under a light intensity of less than 100 µE m^{-2} s^{-1} at 13°C with a light/dark cycle of 14h/10h. For the measurements of the Si/C content and for the kinetic experiment, some of these cultures were transferred and incubated in larger volumes (1-2 litres) of WC medium. However, the light intensity to which these larger volumes were exposed is unfortunately unknown (presumably 100-150 µE m^{-2} s^{-1} for most of them).

3B.2 Si/C contents

Measurements of the Si/C contents in cultures of the two *C. meneghiniana* strains were performed repeatedly. In April and December 2004, Si/C was measured in three batch cultures of each strain, but in April 2005, Si/C was measured only in one batch culture of strain #1. The cultures were filtered on Whatman Nuclepore, 0.4 µm pore size, Ø 47 mm polycarbonate filters for BSi and on Whatman GF/F, 0.7 µm pore size, Ø 25 mm precombusted glass-fibre filters (400°C, 4h) for POC. Unlike the samples from the water of the Scheldt (Chapter 2), the analyses of the BSi content on the culture filters did not require correction for lithogenic silica: the BSi analyses were performed with only two 1-3 hours digestion steps (instead of 4 digestion steps), and without any Al correction. The second digestion was performed only to verify that all the BSi was dissolved during the first digestion: as expected, the DSi concentrations in the aliquots of the second digestion corresponded to half of the DSi concentrations in the aliquots of the first digestion (less than 1-2 % deviation after correction by the DSi concentrations measured in the aliquots during digestions of blank filters).

The measured Si/C molar ratios ranged from 0.12 to 0.30 (Table 3B.1) and supported our estimation for the Si/C ratio associated with living diatoms in the tidal river (0.27, Chapter 3). Our Si/C ratios were low compared to the average one typically observed in freshwater diatoms (0.78 ± 0.43, Conley and Kilham 1989), but within this dataset, *C. meneghiniana* was among the least silicified (0.38, Sicko-Goad et al. 1984). Furthermore, Roubeix and Lancelot (2008) observed Si/C molar ratios as low as 0.08 in cultures of *C. meneghiniana* isolated from the Scheldt. These measurements were however performed on cultures of small *C. meneghiniana* cells, which sexually reproduced shortly after (V. Roubeix, pers. com.), and cultures of regenerated cells and of intermediate sizes exhibited Si/C molar ratios of about 0.4 and 0.2 respectively (V. Roubeix, pers. com.). The range of our ratios appears then to be in close agreement with that of other studies. Even, the same variability was observed within our successive measurements: although there was little deviation within the triplicates of the batch cultures of each strain (low standard deviations), the ratios differed significantly from one strain to another and from one date to another (Table 3B.1).

Table 3B.1: Si/C molar ratios measured in cultures of the *C. meneghiniana* strains.

	April 2004	Dec. 2004	July 2005
strain #1	0.298 ± 0.051	0.187 ± 0.005	0.150
strain #2	0.118 ± 0.003	0.129 ± 0.008	-

In addition to the fact that the silica content is different from one diatom species to another (in particular freshwater species tend to be more silicified that marine ones, Conley and Kilham 1989), up to 4-fold variations in Si/C ratio within a diatom species can be observed (Martin-Jézéquel et al. 2000). They may be due to several factors.

As observed by V. Roubeix (see above, pers.com.), Si/C ratios can decrease with size-reduction (Durbin 1977). This may explain the decrease with time of the Si/C ratios in cultures of strain #1 (Table 3B.1), but Si/C ratios in cultures of strain #2 increased between April and December 2004. This hypothesis could not be experimentally investigated as the size was not measured in our cultures.

Another explanation is that, if DSi is not limiting, silicification in diatoms increase with decreasing growth rates: Si is incorporated during some phases of the cell cycle (mainly the G2+M phase) and when the growth rate decreases, more time is spent in these phases and

more Si is incorporated (Martin-Jézéquel et al. 2000; Claquin et al. 2002). Lower growth rates, and thus lower silica content can be induced by unfavourable temperature or light limitation and, although this is unlikely to have occurred in our culture medium, also by nitrogen, phosphorus or micronutrient limitation (Martin-Jézéquel et al. 2000; Ragueneau et al. 2000). As a result, Si/C ratios decrease with increasing light availability (Brzezinski 1985; Claquin et al. 2002). In contrast, the cellular Si content decreases in case of silica limitation (Ragueneau et al. 2000; Martin-Jézéquel et al. 2000). This should not have been the case in our cultures but DSi concentrations could reach potentially limiting levels in the tidal river (Chapter 3).

The fact that silica is mainly incorporated during the G2+M phase induces that cellular Si content can vary by a factor of 2 within the cell cycle (Claquin and Martin-Jézéquel 2005), but this effect should not be observed in asynchronous cultures (Martin-Jézéquel et al. 2000). However, the cellular C content varies during the light/dark cycle, which may not be synchronised with the cell cycle (Ragueneau et al. 2000), and diurnal variations by a factor of 2 of the Si/C ratio can be observed (Brzezinski 1985; Claquin and Martin-Jézéquel 2005).

The Si deposition and the cellular Si content may also be affected by other parameters such as salinity, pH, the concentration of some metals and pCO_2 (Ragueneau et al. 2000; Claquin and Martin-Jézéquel 2005), but these should not have varied from one measurement to another. In addition, one should note that *C. meneghiniana* is a diatom species that gather morphologically identical but genetically different taxa, which may exhibit different Si metabolism characteristics (Muylaert et al. in prep). However, both strains were isolated from the Scheldt and thus it is improbable that they would be different taxa. Finally, although this should only concern the natural environment, diatoms tend to build thicker frustules in response to grazing pressure (Pondaven et al. 2007).

It could thus be assumed that the variation in the Si/C ratios in our cultures may mainly be due to size-reduction and to different growth rates induced by diverse light conditions (and maybe also due to different sampling times). This variability renders the direct comparison between *in situ* and culture Si/C ratios difficult. In particular, the growth of diatoms is light limited in the Scheldt as, following the water movement, they spend a significant time in the dark below the thin photic zone (Desmit et al. 2005). Although several other factors may also come into play, this may contribute to the fact that the *in situ* Si/C ratio (0.27, Chapter 3) was in the high range of those measured in the cultures.

3B.3 Kinetic incorporation of ^{32}Si at various DSi concentrations

Kinetic incorporation at various DSi concentrations require diatom cultures 1) at non-saturated growth, 2) at reasonably high cell concentrations and 3) in a DSi-depleted medium (below 1 μmol L^{-1} since the half-saturation constant for silica for diatoms is typically of a few micromolars, Martin-Jézéquel et al 2000). So when the diatoms in the DSi-rich WC medium attained visually sufficiently high concentrations on 04 March 2005, a few millilitres of the two suspensions were poured each in two litres of sterilised WC medium containing initially about 20 μmol L^{-1} of DSi.

After 3-5 weeks, DSi concentrations dropped to 0.4 μmol L^{-1} (Fig. 3B.1) and the two litres were distributed in 250 mL incubation bottles: 130 mL were poured in each of the 12 bottles, together with 100 mL of DSi-free WC medium. The remaining of the culture solutions were also diluted with DSi-free WC medium and filtered for the determination of BSi concentrations with the same procedure as used for samples in the Scheldt. Similar to the BSi analyses for the measurement of the Si/C content in cultures, only two 1-3 hours digestion steps were performed: all the BSi was dissolved in the first leach as the DSi concentrations in the second leach deviated by less than 1 % to half of that of the first leach.

Unlabelled 2.5 mmol L^{-1} DSi was added to 9 of the 12 bottles so that the final DSi concentrations ranged approximately from 0.5 to 22 μmol L^{-1}, and 1.5 mL of 10 % azide was added to one of the 3 bottles with no unlabelled DSi addition to evaluate the abiotic adsorption of silica onto particles. All bottles were also immediately spiked with 250 μL of the ^{32}Si source (101.9 nCi mL^{-1}, 23570 Bq μg^{-1}), which resulted in a (neglected) increase of the ambient DSi concentration by 5.7 nmol L^{-1}. Three standards of 1 mL were taken from each bottle. The solution of one of the two bottles with no unlabelled DSi or azide addition was instantly filtered to check for rapid DSi adsorption, and the other bottles were incubated for about 24 hours under a continuous light of an intensity of 120-150 μE m^{-2} s^{-1}.

At the end of incubation period, the samples were filtered on a Whatman Nuclepore, 0.4 μm pore size, Ø 47 mm polycarbonate filter, which was rinsed with Milli-Q water. The filter was folded and placed at the bottom of a scintillation vial and kept frozen until the counting of the radioactivity following the procedures described in Chapter 2. The concentration of BSi formed (BSi_{new}) was estimated as described in Chapter 2.

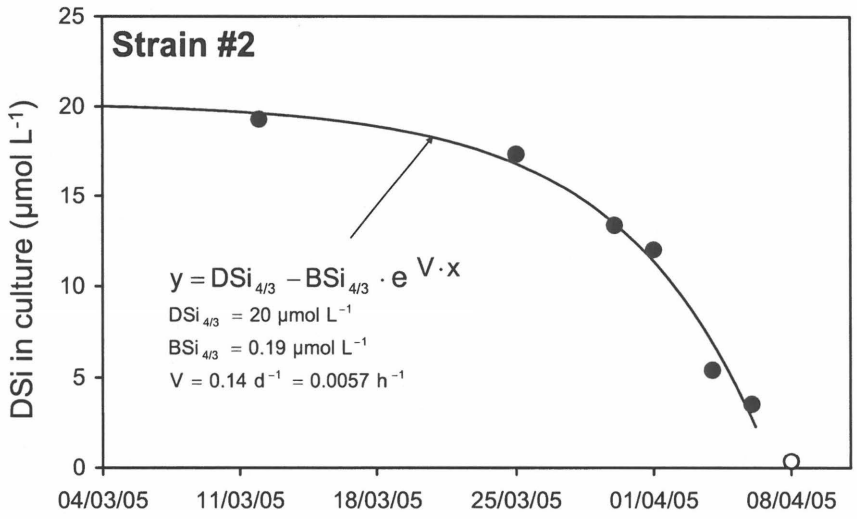

Fig. 3B.1: Evolution of the DSi concentration in the batch culture of the *C. meneghiniana* strain #2 before the ^{32}Si kinetic experiment. The data points (filled symbols) were fitted by an equation representing DSi consumption by exponentially growing diatoms. Its best-fit provided $DSi_{4/3}$ and $BSi_{4/3}$, the concentrations of respectively DSi and BSi (associated to growing diatoms) on the 04/03/2005. The open symbol indicates a measured DSi concentration which was not taken into account in the regression, as its low value may have resulted in DSi limitation of the diatom growth. Due to presumably a faster growth and/or a larger inoculum of the batch culture, DSi concentrations in strain #1 were more rapidly consumed and too few DSi measurements were performed (not shown) to allow a similar estimation of the growth rate of strain #1.

The specific uptake rate (V) was then calculated using the initial BSi concentration (BSi_0):

$$V = \frac{1}{t} \cdot \ln\left(\frac{BSi_{new} + BSi_0}{BSi_0}\right) \qquad \text{(Eq. 3B.1)}$$

with t the time duration between the ^{32}Si spike and the filtration.

When the specific uptake rates were plotted versus the ambient DSi concentrations (average of the initial and final DSi concentrations, the latter being estimated from the amount of incorporated ^{32}Si, Fig. 3B.2), they revealed, as expected, a Michaelis-Menten pattern (Martin-Jézéquel et al. 2000):

$$V = \frac{V_{max} \cdot DSi}{K_s + DSi} \qquad \text{(Eq. 3B.2)}$$

with V_{max} the theoretical specific uptake rate when the DSi concentration is infinite and K_s the half-saturation constant. Both were determined by least-square regression using PRISM 5.01, which provided also 95 % confidence intervals (Fig. 3B.2).

The K_s values differed from one strain to another but they were in the range of those generally observed (Kristiansen et al. 2000; Martin-Jézéquel et al. 2000; Ragueneau et al. 2000; Sarthou et al. 2005; Claquin et al. 2006). Higher values may have been nevertheless expected: freshwater diatoms should have higher K_s values than for marine ones, as freshwater diatoms generally benefit from higher ambient DSi concentrations (Conley and Kilham 1989; Claquin et al. 2006). Additionally, as diatoms can maintain maximum cellular division rates while DSi uptake is limited by low DSi concentrations, K_s is generally higher than the half-saturation constant for growth (K_μ) (Martin-Jézéquel et al. 2000). However, Muylaert et al. (in prep) measured higher K_μ (4 and 13 µmol L^{-1}) for two strains of *C. meneghiniana* isolated from the Scheldt.

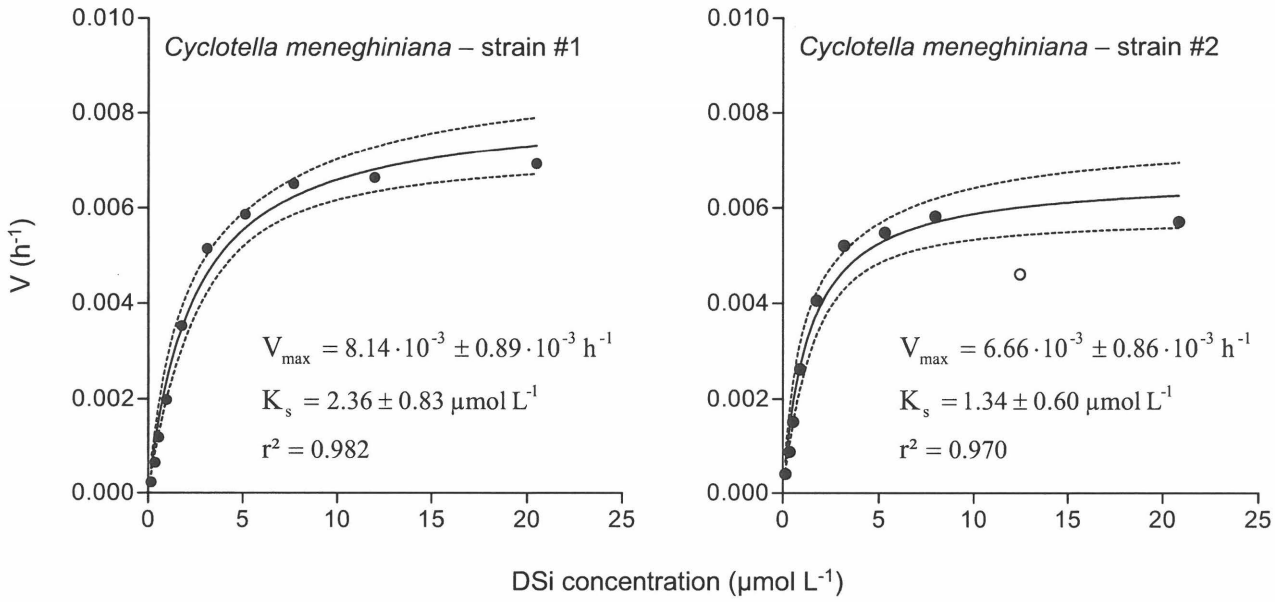

Fig. 3A.2: Specific uptake rates versus DSi concentrations (average of the initial and final DSi concentrations, the latter being estimated from the amount of incorporated ^{32}Si) for the two *C. meneghiniana* strains isolated from the Scheldt tidal river. The data points are fitted by a "Michaelis-Menten" relationship (solid curve). The dash curves represent the 95 % confidence interval of this regression. The specific uptake rate of strain #2 measured at the DSi concentration of 12 µmol L^{-1} was not taken into account in the regression (open symbol).

Our V_{max} values were almost one order of magnitude lower than those generally observed in diatom cultures (Kristiansen et al. 2000; Martin-Jézéquel et al. 2000). Muylaert et al. (in prep) also observed maximum growth rates (μ_{max}) about one order of magnitude higher (0.074 and 0.031 h^{-1}) for two strains isolated from the Scheldt. In addition, despite the fact that the same incubators were used, our V_{max} values were also significantly lower than the specific uptake rates measured at non-limiting DSi concentrations at the confluence with the Rupel (most upstream station, Chapter 5).

The low V_{max} may be explained by an overestimation of BSi_0 in Eq. 3B.1. BSi_0 was set as the BSi concentration measured at the start of the experiment, but the culture could have also contained some frustules of dead diatoms. Fig. 3B.3 displays the V_{max} and K_s that would have been obtained with different BSi_0 values in Eq. 3B.1. A small percentage of dead diatoms would not lead to a significantly different K_s but V_{max} would indeed increase. However, V_{max} higher than 0.01 or 0.02 h^{-1} are unlikely as this would have implied that most of the diatoms were dead at the onset of the experiment.

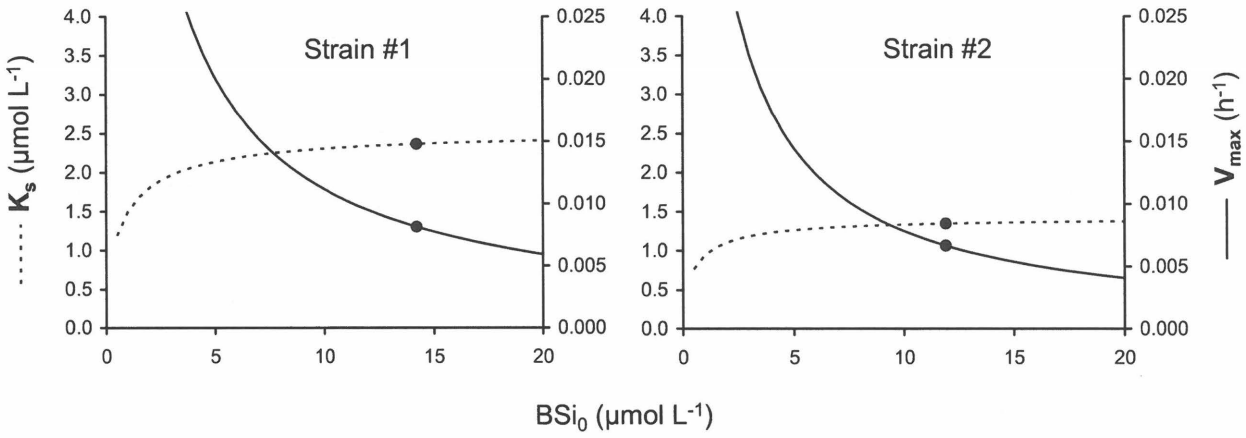

Fig. 3B.3: Half-saturation constants (K_s, grey, left axis) and specific maximum uptake rates (V_{max}, black, right axis) for the two strains calculated with varying BSi_0 values in Eq. 3B.1. The dots indicate the values for K_s and V_{max} shown in Fig. 3B.2, i.e. with BSi_0 corresponding to the BSi concentration at the start of the experiment.

For the two Scheldt strains, Muylaert et al. (in prep) obtained the lowest K_μ and μ_{max} for the culture of cells of the smallest size. Also, Leynaert et al. (2004) observed a decrease in K_s and V_{max} with decreasing cell size. So it is tempting to hypothesize that, as for the Si/C ratios, the low values for both K_s and V_{max} were due to a size-reduction effect. However, in the experiment for Leynaert et al. (2004), the decrease of the cell size was driven by limiting

iron concentrations and such a relationship between the kinetic parameters and cell size may not apply to size-reduction induced by successive divisions. Although the affinity with nutrients may generally increase (corresponding to a decrease of K_s) with decreasing cell size (Hein et al. 1995; Leynaert et al. 2004), growth rates as well as specific uptake rates generally increase with decreasing cell size (Nielsen and Sand-Jensen 1990; Hein et al. 1995; Raven and Kübler 2002).

Parallel measurements of the specific uptake rates performed on the same strains supported additionally our V_{max} values. During the monitoring of the DSi concentration in the culture before the start of the kinetic "Michaelis-Menten" experiment, strain #2 exhibited a specific uptake rate of 0.006 h^{-1} despite different culture conditions (different light exposure and temperature, light/dark cycle versus continuous light) (Fig. 3B.1). Also, using a similar method with ^{32}Si in the same incubators as for the "Michaelis-Menten" experiments (but with replete DSi concentrations), specific Si uptake rates of 0.005-0.006 h^{-1} were measured for strain #1 a few days after the "Michaelis-Menten" experiment, while rates of 0.013 and 0.022 h^{-1} were determined respectively for strain #1 and strain #2 in mid-July 2004. This suggests that, although the low V_{max} may not be related to size-reduction, they may nevertheless be due to the ageing of the cultures.

3B.4 References

Brzezinski MA (1985) The Si:C:N ratio of marine diatoms: interspecific variability and the effect of some environmental variables. J Phycol 21:347-357

Claquin P, Martin-Jézéquel V (2005) Regulation of the Si and C uptake and of the soluble free-silicon pool in a synchronised culture of Cylindrotheca fusiformis (Bacillariophyceae): effects on the Si/C ratio. Mar Biol 146:877-886

Claquin P, Martin-Jézéquel V, Kromkamp JC, Veldhuis MJW, Kraay GW (2002) Uncoupling of silicon compared with carbon and nitrogen metabolisms and the role of the cell cycle in continuous cultures of *Thalassiosira pseudonana* (Bacillariophyceae) under light, nitrogen, and phosphorus control. J Phycol 38:922-930

Claquin P, Leynaert A, Sferratore A, Garnier J, Ragueneau O (2006) Physiological ecology of diatoms along the river-sea continuum. In: Ittekot V, Unger D, Humborg C, TacAn N (eds) The silicon cycle. Human perturbations and impacts on aquatic systems. SCOPE 66. Island Press, Washington, Covelo, London. pp 121-137.

Conley DJ, Kilham SS (1989) Differences in silica content between marine and freshwater diatoms. Limnol Oceanogr 34(1):205-213

Desmit X, Vanderborght J-P, Regnier P, Wollast R (2005) Control of phytoplankton production by physical forcing in a strongly tidal, well-mixed estuary. Biogeosciences 2:205-218

Durbin EG (1977) Studies on the autoecology of the marine diatom *Thalassiosira Nordenskioeldii*. II. The influence of cell size on growth rate, and carbon, nitrogen,chlorophyll *a* and silica content. J Phycol 13(2):150-155

Guillard RRL, Lorenzen CJ (1972) Yellow-green algae with chlorophyllide c. Journal of Phycology 8(1):10-14

Hein M, Pedersen MF, Sand-Jensen K (1995) Size-dependent nitrogen uptake in micro- and macroalgae. Mar Ecol Prog Ser 118:247-253

Kristiansen S, Farbrot T, Naustvoll L-J (2000) Production of biogenic silica by spring diatoms. Limnol Oceanogr 45(2):472-478

Leynaert A, Bucciarelli E, Claquin P, Dugdale RC, Martin-Jézéquel V, Pondaven P, Ragueneau O (2004) Effect of iron deficiency on diatom cell size and silicic acid uptake kinetics. Limnol Oceanogr 49(4):1134-1143

Martin-Jézéquel V, Hildebrand M, Brzezinski MA (2000) Silicon metabolism in diatoms: implications for growth. J Phycol 36:821-840

Muylaert K, Beszteri B, Huygh W, Chepurnov V, Sabbe K, Chou L, Vyverman W (in prep) Variability in Si-limited growth among *'Cyclotella meneghiniana'* strains from different geographic origins.

Nielsen SL, Sand-Jensen K (1990) Allometric scaling of maximal photosynthetic growth rate to surface/volume ratio. Limnol Oceanogr 35(1):177-181

Pondaven P, Gallinari M, Chollet S, Bucciarelli E, Sarthou G, Schultes S, Jean F (2007) Grazing-induced changes in cell wall silicification in a marine diatom. Protist 158:21-28

Ragueneau O, Tréguer P, Leynaert A, Anderson RF, Brzezinski MA, DeMaster DJ, Dugdale RC, Dymond J, Fischer G, Francois R, Heinze C, Maier-Reimer E, Martin-Jézéquel V, Nelson DM, Quéguiner B (2000) A review of the Si cycle in the modern ocean: recent progress and missing gaps in the application of biogenic opal as a paleoproductivity proxy. Glob Planet Change 26(4):317-365

Raven JA, Kübler JE (2002) New light on the scaling of metabolic rate with the size of algae. J Phycol 38:11-16

Roubeix V, Lancelot C (2008) Effect of salinity on growth, cell size and silicification of an euryhaline freshwater diatom: *Cyclotella meneghiniana* Kütz. Transit Water Bull 1:31-38

Sarthou G, Timmermans KR, Blain S, Tréguer P (2005) Growth physiology and fate of diatoms in the ocean: a review. J Sea Res 53:25-42

Sicko-Goad LM, Schelske CL, Stoermer EF (1984) Estimation of intracellular carbon and silica content of diatoms from natural assemblages using morphometric techniques. Limnol Oceanogr 29(6):1170-1178

4 Dissolved silica concentrations and fluxes in the estuary: comparisons with the results of a conservative transport model

In this study, DSi longitudinal profiles over the entire salinity gradient in the Scheldt estuary are presented for eleven campaigns conducted at different seasons from 2003 to 2005. The applicability of the "Apparent Zero End-member" method commonly used for interpreting estuarine DSi versus salinity profiles and for estimating DSi consumption or release in the estuary is discussed. DSi profiles that would have been observed under purely conservative behaviour are simulated using a 1D transient model. The DSi dynamics in the estuary are investigated by comparing measured and modelled DSi profiles. Fluxes at the mouth of the estuary are also calculated for the eleven campaigns, and an annual DSi consumption in the estuary is estimated for a typical year.

4.1 Measured DSi concentrations along the Scheldt estuary

The DSi concentrations measured along the Scheldt estuary during the 11 campaigns are presented against salinity in Fig. 4.1, in accordance to the classical representation of concentration profiles in estuaries: salinity is a conservative tracer of the tidal oscillations and of the complex longitudinal mixing, which depends on the freshwater discharge, the shape of the estuary and the tidal prism.

Fig. 4.1 (next page): Measured DSi concentrations plotted versus salinity during the 11 sampling campaigns in the Scheldt estuary. The panels are ordered from top to bottom (seasons), then from left to right (years). The concentrations in the adjacent coastal zone are also indicated. The curves are the best fit by a 5th order polynomial. If the measurement at the mouth of the estuary was not performed at high tide, an additional data point corresponding to high tide (derived from the Waterstaat dataset, see further Fig. 4.3c and d) was included in the regression in order to obtain a complete description of the DSi versus salinity profile in the estuary by the polynomial.

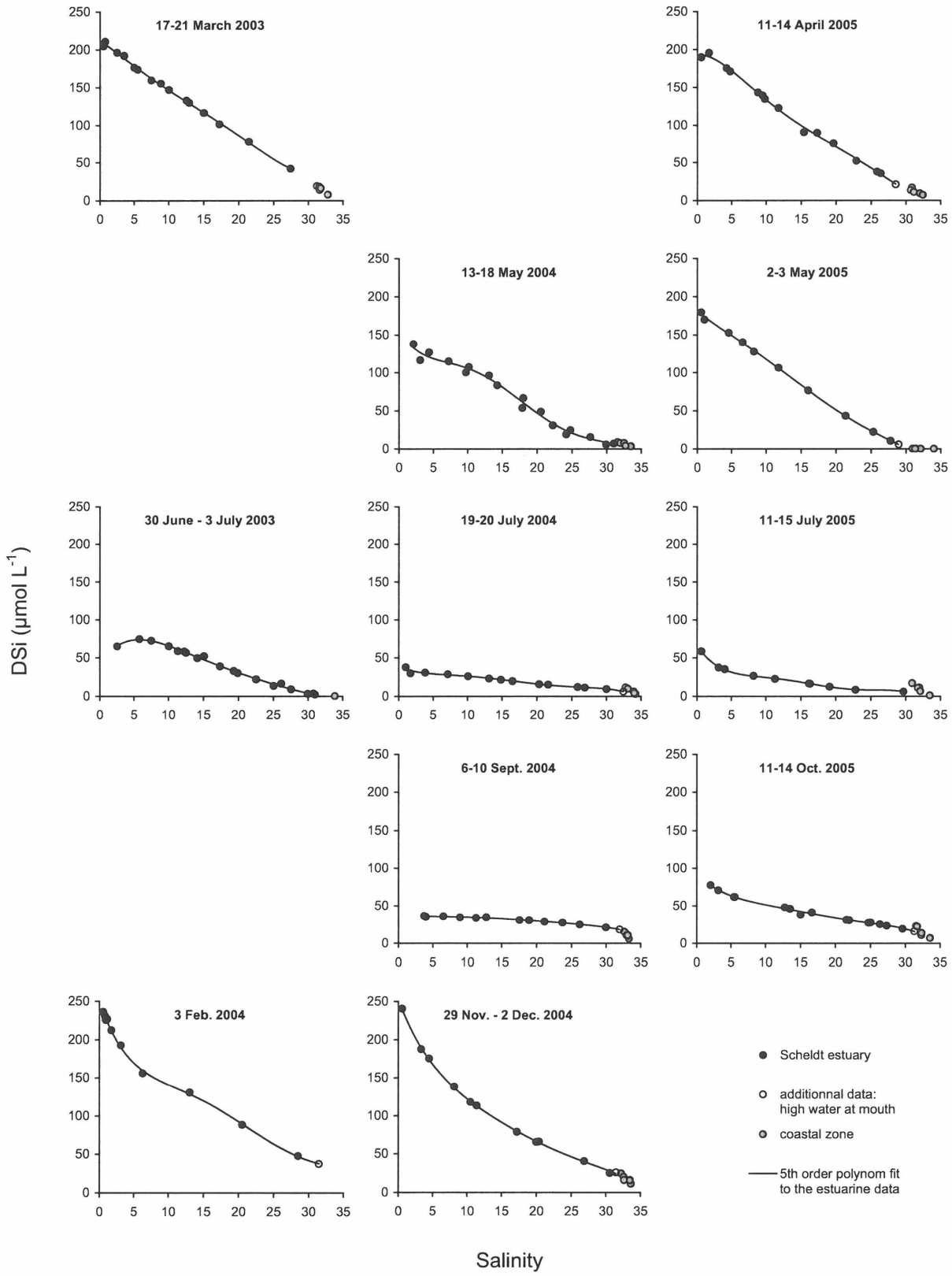
17-21 March 2003
11-14 April 2005
13-18 May 2004
2-3 May 2005
30 June - 3 July 2003
19-20 July 2004
11-15 July 2005
6-10 Sept. 2004
11-14 Oct. 2005
3 Feb. 2004
29 Nov. - 2 Dec. 2004
DSi (µmol L-1)
Salinity
Scheldt estuary
additionnal data: high water at mouth
coastal zone
5th order polynom fit to the estuarine data

Temporal variations at end-members and in the coastal zone

At the freshwater end-member, DSi concentrations were around 200-250 μmol L^{-1} from late autumn to early spring, but decreased to below 50 μmol L^{-1} from late spring to early autumn. This is in agreement with observations made in the tidal river in 2003 (Chapter 3) and also with results for dry years reported in earlier studies (e.g. Struyf et al. 2004; Van Damme et al. 2005).

At the seawater end-member, DSi concentrations also varied from a few to about 50 micromoles per litre, in accordance with the range reported by Struyf et al. (2004) at Vlissingen. Lowest concentrations were observed in late spring and summer, but DSi concentrations increased already from early autumn onwards, following the same trend as in the coastal zone (Van der Zee and Chou, 2005).

DSi concentrations in the coastal zone also decreased with salinity and were in general in continuation of those in the estuary from late autumn to early spring. In July 2004 and 2005 and in October 2005 however, DSi concentrations at the lowest salinities in the coastal zone reached values higher than those observed in the most seaward part of the estuary. This pattern suggests the existence of another source of DSi in the coastal zone in addition to the DSi supplied by the Scheldt. Lacroix et al. (2004) stipulated from a model simulation that the salinity decrease in the Belgian coastal zone, compared to offshore waters, is primarily due to the mixing with the freshwater discharged by the Rhine/Meuse system. However, when comparing freshwater nutrient concentrations of the Scheldt and the Rhine with those measured in the coastal zone, Van der Zee and Chou (2005) concluded that the freshwater fraction in the Belgian coastal water was predominantly originating from the Scheldt. The efficient BSi dissolution in the sandy coastal sediments of the deposited diatom frustules after the diatom spring bloom in the Belgian coastal zone (Ehrenhauss et al. 2004) may also be an explanation for the local increase of DSi concentrations in summer and autumn while DSi concentrations in the most marine part of the Scheldt estuary are still low. Another possible, overlooked source of DSi to the coastal zone may be the submarine groundwater discharge (Ragueneau et al. 2006): this source of water is expected to contain high DSi concentrations similar to those measured in groundwater in land (100-400 μmol L^{-1}; Delstanche et al. 2003; Chapter 3).

DSi concentrations within the estuary

In the estuary, measured DSi concentrations always decreased from the freshwater end-member to the seawater end-member, except for one sample (July 2003, Fig. 4.1). The decreasing pattern may be at least partly explained by the mixing between high-DSi freshwater and low-DSi seawater but concave and convex DSi versus salinity profiles suggest more complex dynamics, hampering their direct interpretation. Processes affecting DSi concentrations, such as diatom uptake or BSi dissolution (in the water column or in the sediments), may indeed superimpose with the mixing between freshwater and seawater, whose DSi concentrations additionally vary with time.

4.2 Methods for interpreting DSi versus salinity profiles and for estimating residual DSi fluxes at the mouth of the estuary

The DSi flux at the mouth of the estuary is also required for the estimation of the retention of DSi in the estuary. But the procedure used at the freshwater end-member (direct multiplication of the DSi concentration by the freshwater discharge) is not applicable at the seawater end-member because of the variation of the DSi concentration during a tidal cycle and of the presence of dispersive processes induced by the DSi gradient. The "Apparent Zero End-member" (AZE) method has been widely used in estuaries both to track DSi uptake or release and to estimate the residual DSi flux at the mouth of the estuary (Regnier et al. 1998 and references therein). But it has been demonstrated that this approach leads to large errors in estuaries with long water residence times, such as the Scheldt (Regnier et al. 1998) where the residence time of the water varies between one and three months (Soetaert and Herman 1995).

The "Apparent Zero End-member" method

The AZE method is only valid when the system can be assumed at steady-state (Regnier et al. 1998). The basis of the AZE method is that a straight line will be obtained when plotting DSi concentration versus salinity if DSi exhibit a conservative behaviour in the estuary. A production of DSi in the estuary (dissolution or benthic fluxes for instance) will thus be indicated by DSi versus salinity plots situated above the straight line drawn between the two end-member points and a consumption of DSi (diatom uptake or possibly sorption) will result in plots below the line (Fig. 4.2). When the system is at steady-state, the DSi fluxes

at the freshwater end-member and at the mouth of the estuary are identical if DSi behaves conservatively. In the case of a steady-state but no conservative transport of DSi, the DSi flux at the mouth and the amount of DSi consumed or released in the entire estuary can be calculated by multiplying the freshwater discharge respectively by DSi_0 and ΔDSi_0 (DSi_0 being the projection of the tangent of the most seaward part of the DSi versus salinity curve and ΔDSi_0 the difference between DSi_0 and the measured DSi concentration at the freshwater end-member, Fig. 4.2). DSi_0 corresponds to the DSi concentration at the freshwater end-member which would have led to the observed concentration gradient at the seawater end-member in the hypothesis of conservative mixing. ΔDSi_0 thus represents the DSi concentration increase at the freshwater end-member which is equivalent, when multiplied by the freshwater discharge, to all the DSi produced or consumed along the entire estuary. The same methodology could be applied at any point in the estuary.

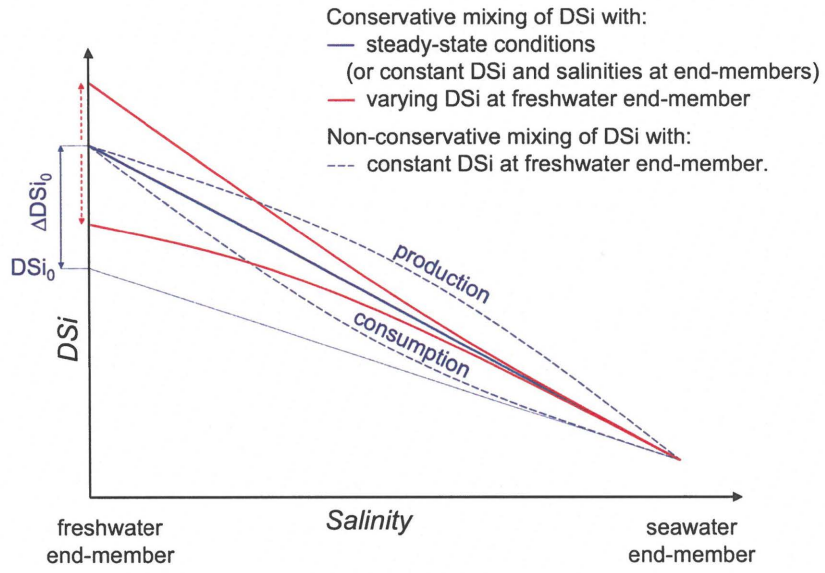

Fig. 4.2: Theoretical estuarine DSi versus salinity curves and schematic representation of the AZE method (blue curves). The red curves represent the conceptual case when DSi regularly increases (or drops) after a period of constant concentration at the freshwater end-member.

If DSi concentrations and salinities remain constant at both end-members, linear DSi versus salinity plots can also be observed, even if the system is not at steady-state because of, for instance, freshwater discharge varying with a characteristic time smaller than the residence time of the water in the estuary. In this case, departure from the straight line between end-member concentrations in the DSi versus salinity plots will still indicate DSi consumption or release (Regnier et al. 1998). However, the AZE methodology for estimating residual fluxes

at the mouth of the estuary will lead to erroneous results as, in case of varying freshwater discharge, fluxes at the freshwater end-member and at the mouth of the estuary are no longer equal due to transient hydrodynamic solute transport (Regnier et al. 1998).

Inapplicability of the AZE method in the case of the Scheldt

In the Scheldt, both DSi and discharge generally vary at the freshwater end-member at a time-scale smaller than the residence time of the water in the estuary, and the system cannot be considered at steady-state, ruling out the application of the AZE method. The DSi fluxes at the mouth of the estuary will differ from those at the freshwater end-member even if the DSi is transported conservatively. The obtained DSi versus salinity curves of the conservative mixing will also deviate from a straight line as shown on Fig. 4.2. As DSi concentrations at the freshwater end-member decreases in spring-summer but increases again in autumn-winter, a conservative mixing curve is thus expected to be convex in spring-summer and concave in autumn-winter. Such a conservative pattern would have been erroneously interpreted with the AZE method as DSi release in spring-summer and diatom uptake in autumn-winter.

Furthermore, concomitant variations in freshwater discharge induce even more complex patterns. The changes in DSi concentrations at the freshwater end-member are propagated over a longer distance in the estuary during high discharge periods than during low ones, and the longitudinal salinity profile is affected at the same time. Finally, seasonal variations at the seawater end-member come on top: DSi concentrations also vary due to DSi uptake by diatoms in the coastal zone (Van der Zee and Chou, 2005) and the salinity varies with the freshwater discharge (Prandle et al. 1997). As a result, the mixing pattern in the Scheldt estuary cannot be assumed at steady-state at any time but undergoes strong and complex transient features which can only be assessed with the help of a hydrodynamic time-resolved transport model (Regnier et al. 1998).

Use of a transport model simulating conservative transport

The DSi consumption and/or production were investigated by comparing the measured DSi versus salinity profiles with those that would have been obtained if DSi behaved conservatively between the two end-members. But, to the contrary to the AZE method in which the conservative profiles are assumed to be a straight line, they were estimated here using the 1D CONTRASTE model, which is a hydrodynamic transport model that fully describes tidal and transient phenomena (the time-step is set to 150 seconds). This model has

been extensively described in Regnier et al. (1997), Regnier et al. (1998) and Vanderborght et al. (2002). Although the hydrodynamics are resolved for the entire Scheldt tidal system, the transport of solutes is only described for the estuary (i.e. from the confluence with the Rupel to Vlissingen). It includes algorithms describing dispersive and advective mixing processes. Implementation of reactive equations is also possible, but this functionality was not used in this study as the goal was to simulate conservative transport. In addition, the model provides advective and dispersive fluxes between each adjacent cells, their sum being the instantaneous total DSi flux. The actual DSi fluxes at the mouth of the estuary (i.e. taking into account the non-conservative behaviour, hereafter designated as "calculated fluxes") could be obtained using the measured DSi versus salinity profiles, the modelled salinity distribution and the water fluxes at the mouth of the estuary. The comparison of these fluxes with the modelled conservative DSi fluxes provided an estimation of the net DSi uptake or release within the estuary (see further).

Model boundary conditions

For our purposes, the CONTRASTE model requires daily freshwater discharge, water elevation at the mouth of the estuary and daily salinity and DSi concentrations at both end-members (Regnier et al. 1998). The discharge data were provided by the Flemish Administration "Afdeling Maritieme Toegang" and the water elevation was calculated from the sum of 24 tidal harmonics (Regnier et al. 1998). The salinity and DSi concentrations at the boundaries were retrieved from several datasets (see legend of Fig. 4.3). Salinity at the freshwater end-member was set to 0.5.

The stretch of the Scheldt estuary described in the model extends from Vlissingen (km 0) up to Rupelmonde (confluence with Rupel, km 90). It is discretized by 45, 2 km long cells. One "ghost" cell is juxtaposed at each boundary to allow realistic variations of the concentrations at current reversal, but both were kept as small as possible (2 and 4 km long at the upstream and downstream boundaries, respectively). The simulation was started in 2002 with actual salinity and DSi concentrations so that model outputs during our study period (2003-2005) were independent of the initial conditions.

There was a generally good agreement between the different datasets (Fig. 4.3). Values were averaged when several DSi concentrations were available for the same day, or calculated by interpolation if no measurement was performed this day. At the mouth (Vlissingen), both the salinity and the DSi concentration strongly vary with the tidal state and

interpolation was performed only on values recorded at high tide (Fig. 4.3c and d). The temporal pattern of these concentrations will be discussed further.

Model calibration

The dispersion coefficient (K, in $m^2\ s^{-1}$, Regnier et al. 1997, 1998) was recalibrated using our own salinity data as measured at known locations and times. A very good agreement could be obtained (Fig. 4.4) when K was empirically set to increase linearly from 100 to 500 $m^2\ s^{-1}$ with increasing distance to the mouth. K is a "macro" dispersive coefficient introduced to reproduce the mixing between freshwater and seawater at the scale of the discretization. It does not have a truly physical meaning as it is not only specific to the geometry of the system, but also to the time-step and to the discretization: its value would for instance vary with the cell length. A discussion or a justification of the chosen values will thus not be attempted.

Fig. 4.3 (next page):
Boundary conditions set in the model simulations (ticks on the x-axis represent months):
a. Freshwater discharge after the confluence with the Rupel.
b. DSi concentrations measured in the lower reaches of the tidal river or at the freshwater end-member in the estuary (i.e. data measured between the confluence with the Rupel and Antwerp). Five different datasets were used.
The legend "this study (estuary)" corresponds to the measured concentrations during our 11 sampling campaigns on the Scheldt estuary, and "this study (tidal riv.)" refers to the measurements performed at Hemiksem within the study of silica in the tidal river (Chapter 3).
"OMES" measurements were performed at three different locations at the vicinity of the confluence in the framework of the OMES project ("Onderzoek naar de Milieu-Effecten van het Sigmaplan" coordinated by Prof. Patrick Meire); DSi concentrations were either measured by Departement Biologie - Onderzoeksgroep Ecosysteembeheer (Universiteit Antwerpen, "UA") or the Laboratoire d'Océanographie Chimique et Géochimie des Eaux (Université Libre de Bruxelles, "ULB").
As for "Ste Anna" values, the sampling was performed at Antwerp by L.S. Schiettecatte (Unité d'Océanographie Chimique, Université de Liège). The concentrations were measured by the LOCGE (ULB) but only samples for which the salinity was below 2 were taken into account.
The line describes the daily interpolation between measured concentrations, which were occasionally averaged if several measurements were performed during a same day.
c. DSi concentrations measured at high tide at the mouth of the estuary (DSi and salinity data from Waterstaat database, available online at www.waterbase.nl). Data measured at the mouth of the estuary measured during our sampling campaigns on the Scheldt estuary are also shown. The line represents the interpolation between measurements performed at high tide.
d. Salinity of the samples for which the DSi concentration is shown on panel c. The line represents the interpolation between measurements performed at high tide.

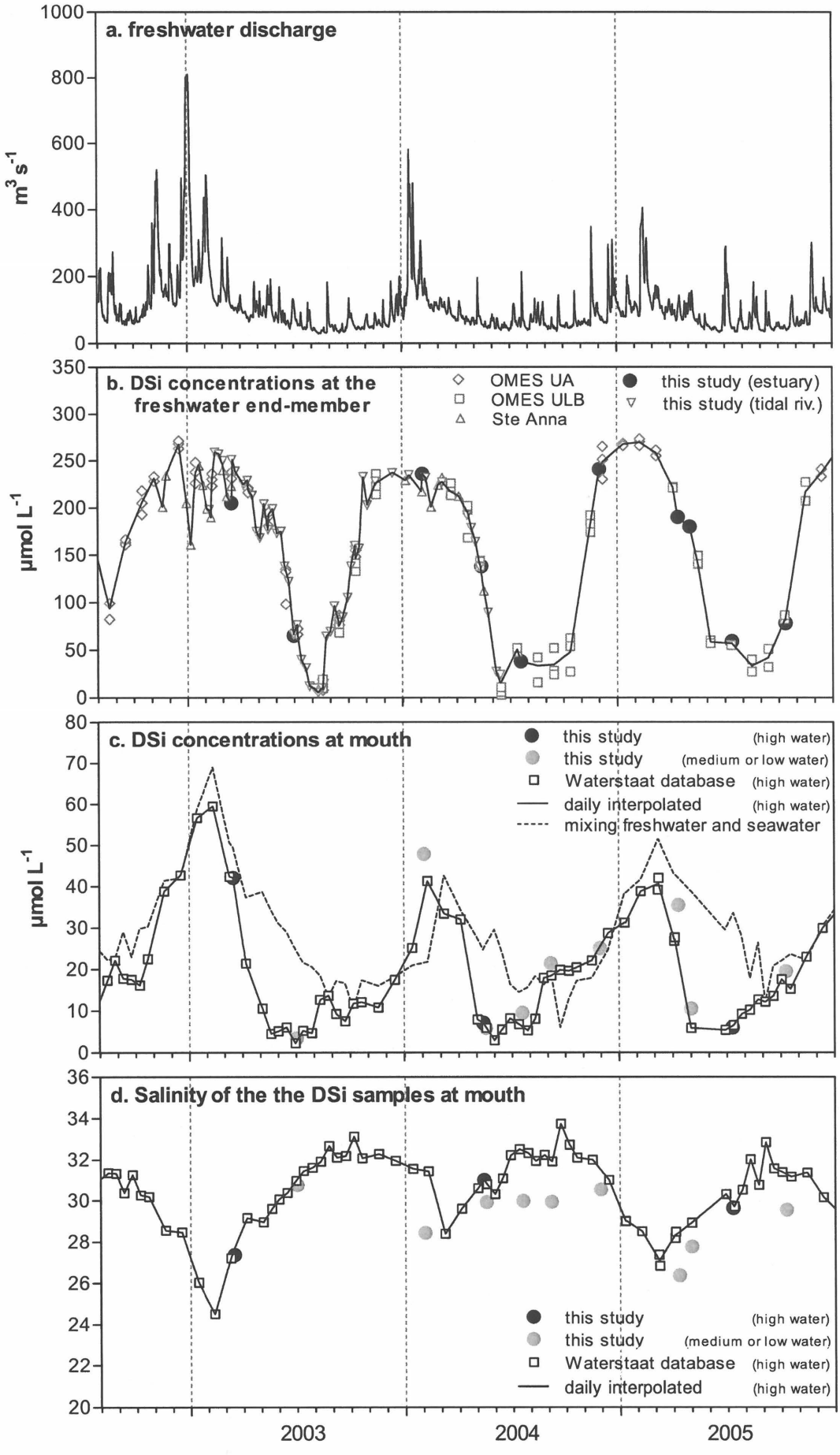
a. freshwater discharge
m3 s-1
1000
800
600
400
200
0
b. DSi concentrations at the freshwater end-member
OMES UA
OMES ULB
Ste Anna
this study (estuary)
this study (tidal riv.)
µmol L-1
350
300
250
200
150
100
50
0
c. DSi concentrations at mouth
this study (high water)
this study (medium or low water)
Waterstaat database (high water)
daily interpolated (high water)
mixing freshwater and seawater
µmol L-1
80
70
60
50
40
30
20
10
0
d. Salinity of the the DSi samples at mouth
this study (high water)
this study (medium or low water)
Waterstaat database (high water)
daily interpolated (high water)
36
34
32
30
28
26
24
22
20
2003
2004
2005

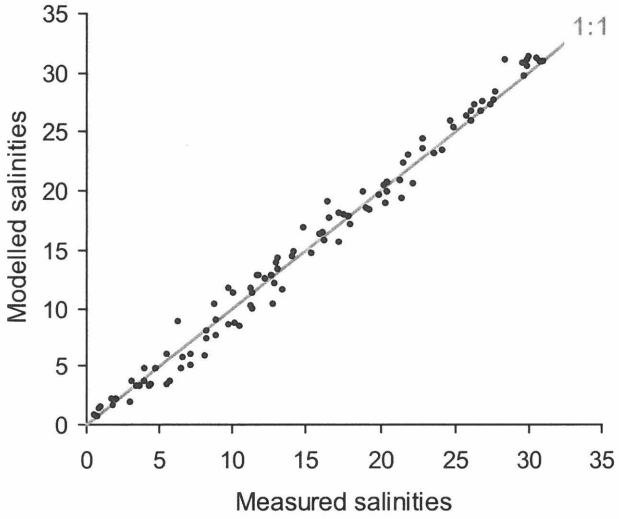

Fig. 4.4: Measured salinities during all our sampling campaigns plotted versus salinities from the model results at the same locations (linearly interpolated) and times. The grey line represents the 1:1 correlation.

Procedure for estimating the "calculated" DSi fluxes (i.e. taking into account the non-conservative behaviour)

In the model, instantaneous advective and dispersive fluxes at km 2 (boundary between cell 1 and cell 2) are respectively calculated as:

$$advflux_{1-2}^{mod} = DSi_{1-2}^{mod} \times watflux_{1-2}^{mod} \quad \text{(Eq. 4.1)}$$

$$dispflux_{1-2}^{mod} = \frac{K_{1-2} \times \left(DSi_2^{mod} - DSi_1^{mod}\right) \times section_{1-2}^{mod}}{\Delta x} \quad \text{(Eq. 4.2)}$$

with:

- DSi_1^{mod}, DSi_2^{mod} and DSi_{1-2}^{mod}, the instantaneous modelled DSi concentrations in, respectively, cell 1, cell 2 and at the boundary between cells 1 and 2,
- $watflux_{1-2}^{mod}$, the modelled water flux at the boundary between cells 1 and 2,
- K_{1-2}, the dispersion coefficient at the boundary between cells 1 and 2 (calibrated with salinity data, here 100 $m^2 s^{-1}$, see above),
- $section_{1-2}^{mod}$, the modelled instantaneous cross-section at the boundary between cells 1 and 2,
- Δx, the cell length (here 2 km).

Assuming that the shape of the measured DSi versus salinity profiles (Fig. 4.1) did not vary within the sampling period of each campaign (i.e. period comprised between the first and the last samples) at the mouth of the estuary, the instantaneous "calculated" DSi concentrations in cell 1, cell 2 and at the boundary between cells 1 and 2 (respectively DSi_1^{calc}, DSi_2^{calc} and DSi_{1-2}^{calc}) were deduced from the respective modelled salinities and using the 5th order polynomials fits (Fig. 4.1). Instantaneous "calculated" advective and dispersive fluxes were obtained replacing modelled DSi concentrations by the "calculated" ones in Eq. 4.1 and 4.2:

$$advflux_{1-2}^{calc} = DSi_{1-2}^{calc} \times watflux_{1-2}^{mod} \quad \text{(Eq. 4.3)}$$

$$dispflux_{1-2}^{calc} = \frac{K_{1-2} \times \left(DSi_2^{calc} - DSi_1^{calc}\right) \times section_{1-2}^{mod}}{\Delta x} \quad \text{(Eq. 4.4)}$$

The calculated total DSi flux was obtained as the sum of $advflux_{1-2}^{calc}$ and $dispflux_{1-2}^{calc}$. To remove the effects of tidal oscillations, modelled and calculated DSi fluxes were processed using a low-pass ideal filter with a cut-off frequency of 0.5 d^{-1}: the time-series were Fourier transformed, the frequencies higher than 0.5 d^{-1} were set to zero and the series were inverse-Fourier transformed. The cut-off frequency was chosen to remove the main tidal oscillation characterized by the M2 harmonic (0.52 d^{-1}). The spring-neap oscillations were consequently not suppressed. In order to avoid transitional oscillations at the start and at the end in the filtered time-series, instantaneous calculated DSi fluxes were calculated for the entire simulation period, but only the filtered fluxes during the sampling periods were considered. Filtered modelled and calculated fluxes were averaged over the sampling periods and the difference provided an estimate of the net DSi uptake or release in the estuary. These estimates should not be seen as instantaneous consumption or release rates; they rather provide an estimate of the integrated DSi uptake or release that underwent a parcel of water while transported and mixed with adjacent parcels along the estuary.

4.3 Seasonal evolution of the end-member DSi concentrations

At first inspection, DSi concentrations at both end-members were high when discharge was high and inversely (Fig. 4.3a-c), while the opposite was observed for the salinity at the mouth of the estuary (Fig. 4.3a and d). The summer drop in DSi concentrations at the freshwater end-member was ascribed to diatom consumption in the tidal river (Chapter 3).

This is a seasonal event which can occur only in summer when diatom growth rates are high and discharge is low (Muylaert et al. 2005). Freshwater discharge is considered as a regulating factor of diatom growth in the tidal river, as it determines the residence time of the water and thus the time allowed for diatoms to grow. Discharge and DSi consumption were indeed correlated, but other factors (such as e.g. light) may also play a significant role (Chapter 3).

Interestingly, drops in freshwater DSi concentrations could also be observed during the winter 2002-2003 and to a lesser extent, during the winter 2003-2004 (Fig. 4.3a and b). Thanks to an overall high sampling frequency, the fact that they occurred concomitantly with discharge peaks was well revealed during the winter 2002-2003 (Fig. 4.5). The Scheldt estuary being a rain-fed estuary, its discharge is directly linked to precipitation (Billen et al. 2005; Soetaert et al. 2006). The decrease in DSi concentration may be induced by dilution with runoff water which has not been in contact with DSi-rich groundwater because of soil saturation. The comparison between DSi and discharge suggests that the DSi concentration decreased regularly during the course of discharge peak but also after discharge returned to lower values (Fig. 4.5). DSi reached thus a minimum a few days after the end of the flow peak, and increased thereafter to concentrations of about 250 µmol L^{-1} within a few days. This pattern suggests a complex interaction between water and soil, involving the residence time of the water in the drainage basins. Furthermore, the last discharge peaks, although relatively small (Fig. 4.5), induced important DSi drops. This might be due to the fact that soil saturation was reached faster after a succession of rain episodes.

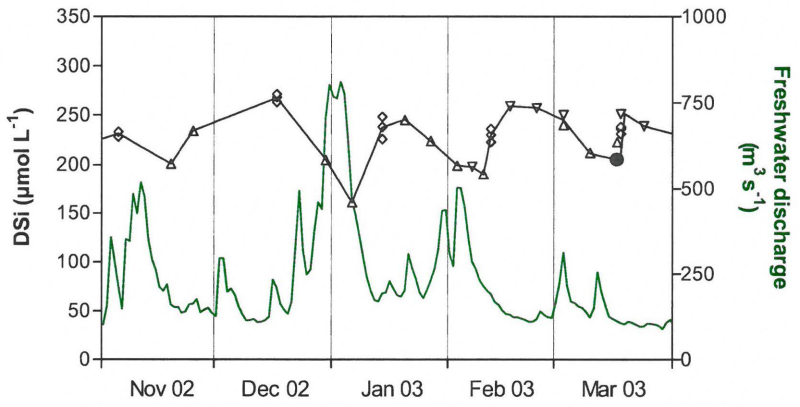

Fig. 4.5: Detail of the DSi concentrations and freshwater discharge in the freshwater end-member from November 2002 to March 2003. Data and symbols for discharge and DSi concentrations are defined in Fig. 4.3a and b.

Variations in DSi concentration at the mouth of the estuary are partially induced by the freshwater discharge as it influences the mixing ratio between DSi-rich freshwater and DSi-poor seawater. This ratio is indicated by the salinity variation at the mouth (measured at high tide, Fig. 4.3d) as the salinity in the North Sea undergoes little seasonal changes (34.26 ± 0.74, Prandle et al. 1997). Considering this mean salinity value for marine waters, the proportion of freshwater at the mouth ranged from about 5 % in summer and early autumn, to up to 30 % in February-March. However, the variations in DSi concentrations at the mouth of the estuary (Fig. 4.3c) could not be attributed solely to the mixing between freshwater and seawater. DSi consumption in the tidal river, in the estuary and in the coastal zone also plays an important role. This is highlighted by the difference between the DSi concentrations measured at the mouth of the estuary and those obtained if seawater and freshwater with DSi concentrations of respectively 2.5 μmol L^{-1} (Prandle et al. 1997) and 233 μmol L^{-1} (average DSi concentration at the tidal limits, Chapter 3) were mixed in ratios similar to the ones estimated from the salinity data (dashed line in Fig. 4.3c). The difference was minimal in winter and maximal in May-June. However, this calculation did not allow discrimating the fractions of the DSi consumed in the tidal river, in the estuary and in the coastal zone.

4.4 Comparison between the measured and the simulated profiles

Conservative DSi profiles

As the model provided DSi concentrations and salinity data every 150 seconds for each of the 45 cells, more than 28 million couples of DSi-salinity data were produced for the period 2003-2005. The sampling campaigns were generally performed over one to several days, but except for the most upstream part of the estuary in March 2003, July 2003 and May 2004, there were little variations in the instantaneous modelled DSi versus salinity profiles during the sampling periods. Individual measured DSi concentrations could be also directly compared with the modelled DSi concentrations at dates and salinities corresponding to the measurement (crosses in Fig. 4.6). For a better precision, an interpolation with respect to salinity was additionally performed between the two closest modelled DSi-salinity couples.

DSi profiles obtained by simulation of conservative transport only were generally strongly convex in spring and summer, but concave in winter (Fig. 4.6), highlighting the importance of transient phenomena and confirming the irrelevancy of the AZE method in the case of the Scheldt. Conservative DSi versus salinity profiles only approached a straight line

in end winter and early spring (campaigns of February 2004 and March 2003, Fig. 4.6). At this time, DSi consumption in the tidal river had not yet started and the DSi profile in the estuary could have re-equilibrated after 3 months of (nearly) constant DSi concentrations at the freshwater end-member (Fig. 4.3b).

The difference between the modelled and the measured DSi profiles indicated DSi uptake or release. The seasonal behaviour was found to be similar in 2003, 2004 and 2005, and four periods could be observed as illustrated by the four groups of graphs on Fig. 4.6.

Spring

DSi profiles along the salinity gradient indicated that DSi consumption in the estuary started in spring while DSi concentrations at the freshwater end-member were still high (April-May, Fig. 4.6). This implied that DSi consumption occurred earlier in the estuary than in the tidal river, and that the estuarine consumption could not be ascribed to the advection into the estuary of a diatom bloom of a freshwater origin but to a bloom of local (or marine) origin. This is in accordance with microscopic observations: the speciation of the diatom community at the freshwater end-member differs from that observed at salinities higher than 5-10 (Chapter 2). Nevertheless, whereas the largest difference between the measured and simulated profiles was observed at salinities 20-30 in May 2004 and 2005, it was around salinities 10-15 in April 2005 (Fig. 4.6). Together with the fact that phytoplankton analysis revealed the presence of a typical estuarine phytoplankton community (Chapter 2), this would suggest that the early spring diatom development was not only from marine origin. In May however, as indicated by low DSi concentrations at the marine sampling stations (Fig. 4.1), the high DSi consumption at the most seaward part of the estuary might be due to the import by tidal mixing of marine diatoms following the spring bloom in the coastal zone: these were able to further develop in the estuary due to the availability of nutrients, which were already depleted in the coastal zone (Arndt 2008).

Fig. 4.6 (next page): Comparison of the measured and modelled DSi concentrations plotted versus salinity. The measured DSi concentrations plotted versus salinity are represented by open grey circles. Instantaneous modelled DSi concentrations at salinities (occasionally linearly interpolated) and times identical to the measurements are indicated by crosses. The envelopes of all instantaneous DSi versus salinity profiles obtained within the indicated sampling period are delimitated by solid lines. The grey borders gather campaigns corresponding to the same season (see text). The indicated sampling periods correspond to the first and the last sampling performed in the estuary (i.e. not in the coastal zone). Note that scales in summer and early autumn differ from those from late autumn to spring.

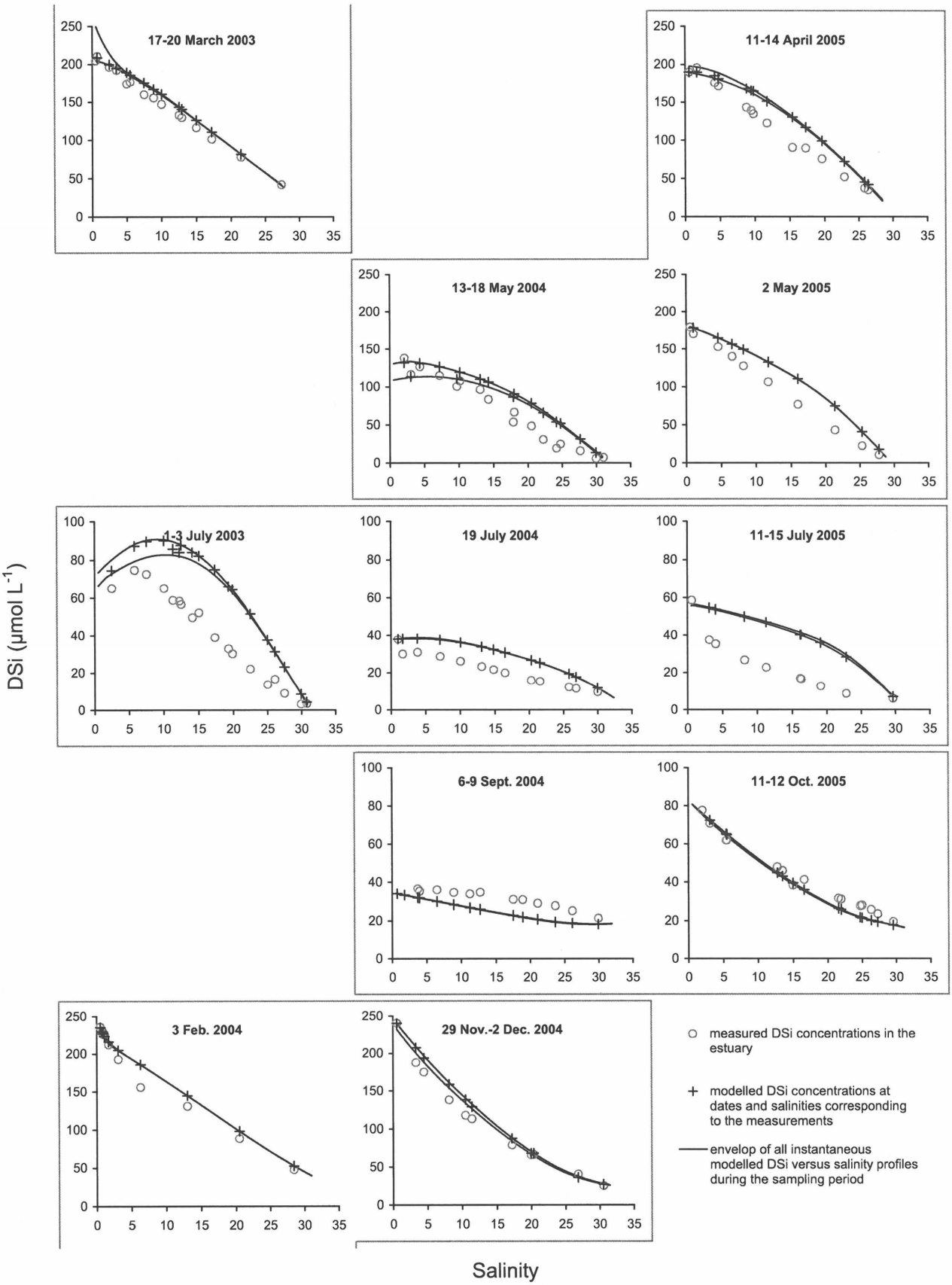
17-20 March 2003
11-14 April 2005
13-18 May 2004
2 May 2005
1-3 July 2003
19 July 2004
11-15 July 2005
6-9 Sept. 2004
11-12 Oct. 2005
3 Feb. 2004
29 Nov.-2 Dec. 2004
DSi (µmol L-1)
Salinity
measured DSi concentrations in the estuary
modelled DSi concentrations at dates and salinities corresponding to the measurements
envelop of all instantaneous modelled DSi versus salinity profiles during the sampling period

Early summer

Early summer (July) was characterised by a consumption (not reaching depletion) of the DSi before it entered the brackish reaches (Fig. 4.6). With conservative mixing only, higher concentrations would be expected around salinities 5-10 than at the freshwater end-member due to transient phenomena (July 2003). Significant DSi consumption also occurred in the saline estuary, without reducing the DSi concentrations to limiting levels except maybe in the most seaward part of the estuary. Van Damme et al. (2005) also observed concentrations episodically below 5 μmol L^{-1} during previous years, but only at the mouth of the estuary. Compared to May, more DSi was consumed in the upstream part of the estuary during the early summer (Fig. 4.6). This may be ascribed to the presence of large amounts of living diatoms originating from the diatom bloom in the tidal river (Chapters 3 and 5). However, only little DSi uptake may be expected at salinities higher than 5-10 in July 2004 and 2005 due to low concentrations of diatoms (Chapter 5). In addition to DSi uptake in the most upstream part of the estuary, the distance between measured and modelled DSi profiles may be due to the fact that DSi concentrations in mid July may have not yet re-equilibrated to conservative profiles after the spring and early summer DSi uptake, as a consequence of the enhanced residence time of the water in summer.

Late summer – early autumn

In late summer and early autumn, DSi was still consumed in the tidal river as shown by the low DSi concentrations at the freshwater end-member, but the comparison of the simulated and measured profiles indicated a net DSi release within the estuary (Fig. 4.6). Due to the dependence of the BSi dissolution rate with salinity (Yamada and d'Elia 1984; Roubeix et al. 2008; Loucaides et al. 2008), significant BSi dissolution is not expected in the tidal river (Chapter 3), but may occur in the saline estuary. Anderson (1986) also observed BSi dissolution from April to October in the Chesapeake Bay estuaries, but only in the saline estuary, immediately downstream of the diatom bloom. Dissolution is expected to occur predominantly after the diatom bloom: BSi dissolution is enhanced when temperature increases, and decreases when the material gets older (Van Cappellen et al. 2002; Gallinari et al. 2002). In particular, reverse weathering processes such as incorporation of aluminium or rapid formation of authigenic clay material on BSi surface can significantly lower or even hamper the BSi dissolution (Dixit et al. 2001; Van Cappellen et al. 2002; Michalopoulos and Aller 2004). Moreover, the apparent BSi solubility may be as low as 200 μmol L^{-1} in the

presence of large amounts of lithogenic material (Dixit et al. 2001; Gallinari et al. 2002) but lower DSi concentrations after diatom uptake may enhance the dissolution. Some dissolution may have thus also occurred already in spring and early summer but, at that time, the overall process was a net DSi consumption.

Winter

In late autumn (November) and winter (February), DSi uptake was expected to be insignificant in the estuary as no diatoms were observed in the water column during these two campaigns (Chapter 5). The measured DSi profile differed generally by less than 10 % from the simulated one. Nevertheless, the differences between measured and simulated concentrations could amount to 15 % in February and November 2004 around salinities 6-7 (Fig. 4.6). They may result in important differences in terms of fluxes due to high DSi concentrations and freshwater discharge. In addition to a hypothetical bias in the model simulations, several explanations for these differences could be put forward, such as e.g. DSi sorption, inadequate description of the boundary conditions or imprecision of the DSi measurement (Annex 4A).

The difference between the measured and modelled profiles in March was also small. But in contrast, diatoms were already present in the estuary at concentrations equivalent to that measured in April 2005 (Chapter 5). The smaller difference between modelled and measured profiles in March compared to that in April (Fig. 4.6) may suggest that the DSi consumption in March was just starting, while the effects of one month of DSi consumption may have accumulated in April due to the residence time of the water in the estuary. Rather than illustrating the winter conservative behaviour, the situation during the March campaign may thus represent the transition to spring DSi uptake.

4.5 DSi fluxes at the mouth of the estuary and DSi consumption in the estuary

Conservative DSi fluxes at the mouth of the estuary mirrored the fluxes at the freshwater end-member, yet shifted in time due to the residence time of the water (Fig. 4.7). In addition, dispersive processes along the estuary tend to level off the sharp peaks in DSi fluxes observed at the freshwater end-member. Conservative DSi fluxes at the mouth of the estuary may also occasionally be directed landwards in August-October, notably in August

2004 when DSi increased faster at the seawater end-member than in the most seaward part of the estuary.

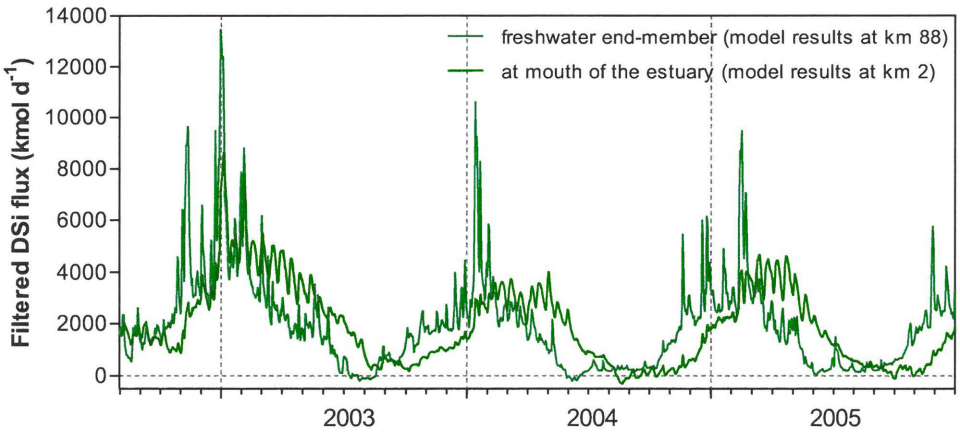

Fig. 4.7: Filtered conservative DSi fluxes at the freshwater end-member and at the mouth of the estuary for the period 2003-2005. Fluxes directed seawards are indicated here by positive values. Ticks on the x-axis represent months.

From three to four sampling campaigns were only performed per year, thus neither a reliable observation of the seasonal evolution of the DSi consumption, nor an annual budget could be performed for the years 2003, 2004 and 2005 separately. However, except for the first two months of 2003 (but no sampling campaign was performed during this period), conservative DSi fluxes at the mouth of the estuary displayed comparable patterns for 2003, 2004 and 2005 (Fig. 4.7) due to similar freshwater discharge and DSi concentrations at the end-members (Fig. 4.3). In addition, DSi versus salinity profiles suggested that the seasonal DSi behaviour was identical from one year to another (see above). The fluxes from all 11 campaigns were thus lumped into one single year, which would be typical for dry years such as 2004 and 2005 (and 2003 if the two first months are excluded, Fig. 4.8). This approach is supported by the regular annual patterns displayed by the modelled and calculated fluxes, as well as by their differences (Fig. 4.8).

Seasonal evolution of the DSi uptake in the estuary

The difference between modelled and calculated fluxes was negative from early spring to early summer indicating DSi uptake, and positive from late summer to late autumn indicating DSi release (Fig. 4.8). These findings were in accordance with the conclusions

drawn from the DSi profiles along the estuary (Fig. 4.6). As for DSi versus salinity profiles, a significant negative difference was observed in February although no DSi consumption was expected at this period of the year. Also, DSi was net released in November (which is in accordance with the very low diatom concentrations, Chapter 5), although DSi profiles exhibited a negative difference from salinity 0 to about 20.

Fluxes calculations highlighted the fact that the net DSi uptake rate was maximum in May (corresponding to most negative values: -1940 kmol d^{-1}) and that it quickly decreased in July (Fig. 4.8). This is in agreement with the low diatom concentrations observed from mid July onwards (Chapter 5). Furthermore, the net DSi release of about 400 kmol d^{-1} in September and November 2004 was attributed to BSi dissolution only, as practically no diatoms were observed in the estuary (Chapter 5).

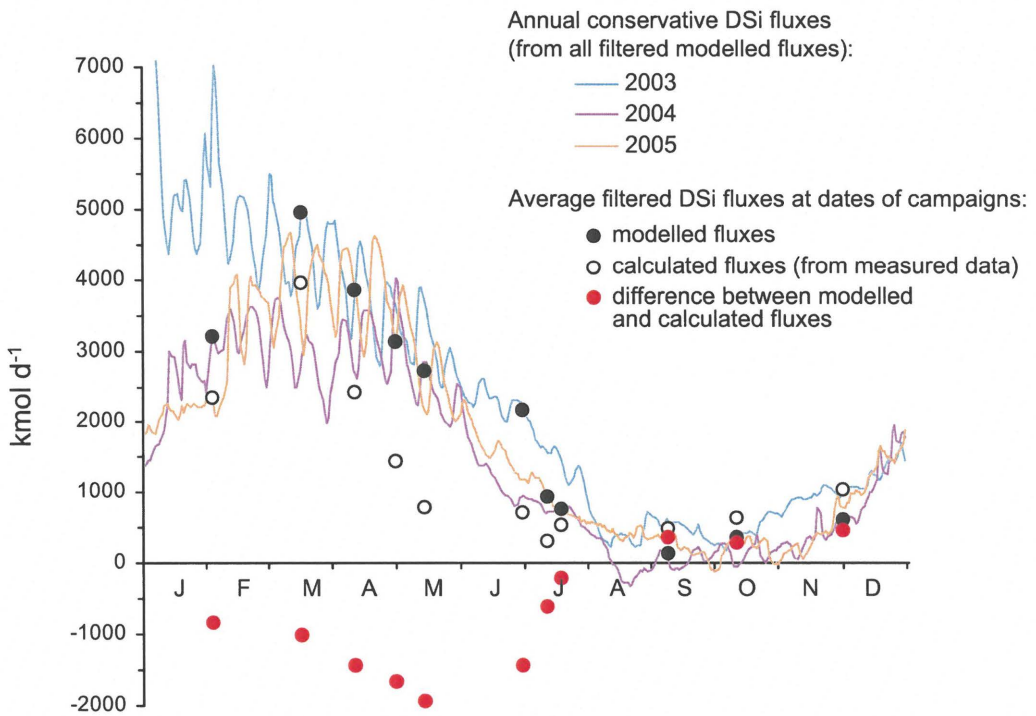

Fig. 4.8: Average modelled (solid black circles) and calculated (open circles) DSi fluxes at the mouth of the estuary during all sampling campaigns represented along a common one-year axis. The difference between the modelled and calculated DSi fluxes (solid red circles) is also indicated. Fluxes directed seawards are represented here by positive values. The (daily averaged) filtered conservative DSi fluxes at the mouth of the estuary (km 2) for 2003, 2004 and 2005 (respectively light blue, purple and orange curves) are also indicated.

Comparison with the tidal river

The timing of the DSi uptake in the estuary differed notably from that of the tidal river (Chapter 3). The DSi uptake in the estuary started and reached its maximum rate about a month before that in the tidal river, presumably because of 1) longer residence times in the estuary than in the tidal river, 2) lower SPM concentrations inducing a better light availability especially at salinities higher than 15-20 where the bloom developed and/or 3) import of diatoms from the coastal zone in spring. In the tidal river, DSi input fluxes limited the DSi consumption in summer, but in the estuary, as DSi consumption occurred earlier, when DSi input fluxes were higher, higher DSi consumption rates could be reached: the maximum DSi uptake was about twice higher in the estuary than in the tidal river. However, when expressed with respect to the surface area or the volume, the rate in the tidal river was one order of magnitude higher in the tidal river than in the estuary (Table 4.1).

Table 4.1: Water surface area and volume of the tidal river (Chapter 2) and of the estuary (given by the CONTRASTE model). The maximum DSi consumption rates for each section are indicated (as negative values) and normalised with respect to water surface area and volume.

	tidal river	**estuary**
water surface area (km^2)	14.1	265
volume (km^3)	0.060	2.5
maximum net DSi uptake:		
kmol d^{-1}	-1000	-1940
mmol m^{-2} d^{-1}	-70.9	-7.32
mmol m^{-3} d^{-1}	-16.6	-0.76

Despite the important amount of living diatoms carried from the tidal river to the estuary in summer (Chapter 5), DSi uptake in the estuary dropped from July onwards, although DSi was not entirely consumed and thus not limiting the diatom growth (Fig. 4.1). This decrease was presumably ascribed to zooplankton control of the phytoplankton biomass (Chapter 5). In contrast, no such control was observed in the tidal river, but this may be due to the different composition of the zooplankton community: it is dominated by calanoid copepods in the estuary but by rotifers in the tidal river (Soetaert and Van Rijswijk 1993; Tackx et al. 2004) and, unlike calanoid copepods, rotifers are not expected to exert a strong

grazing pressure on the phytoplankton (Muylaert et al. 2005). As a result, there was a net DSi consumption until November in the tidal river (DSi mass-balance in winter in the tidal river could not be performed due to a too low sampling frequency, Chapter 3), but in the estuary the drop in the DSi uptake by diatoms resulted in a net DSi released in late summer and autumn in the estuary.

Unlike the DSi uptake occurring in summer in the tidal river, the spring DSi consumption in the estuary is expected to have had a significant effect on the DSi availability in the coastal zone as it occurred during the coastal phytoplankton bloom. Due to the residence time of the water in the estuary, high winter riverine DSi fluxes are also of major importance as they reach the coastal zone just before and/or at the onset of the coastal diatom bloom in April. As winter riverine DSi concentrations are nearly constant, the variation of these fluxes is actually driven by the discharge pattern. However, the extent of the *Phaeocystis* bloom in the coastal zone is more influenced by the Si/N ratio than by the amount of available DSi (Lancelot 1995). Model simulations showed that the ratio between DSi and dissolved nitrogen fluxes at the mouth of the estuary in early spring is fairly constant and thus independent of the discharge (Arndt 2008).

Annual DSi fluxes and uptake

Annual conservative DSi fluxes were estimated from the filtered modelled DSi fluxes at the freshwater end-member and at the mouth of the estuary (Table 4.2). They were higher in 2003 than in 2004 and 2005 mainly due to the high discharge during winter 2002-2003 (Fig. 4.3a). The annual conservative DSi fluxes at the mouth of the estuary may also differ significantly from those at the freshwater end-member due to the accumulation of DSi in the system induced by the residence time of the water.

The "calculated" annual flux could only be determined on the basis of the 11 calculated fluxes lumped into one single typical year (Table 4.2). It was estimated as the area between the x-axis and the broken line defined by the 11 consecutive flux data points (open circles, Fig. 4.8). For the periods before February and after November, the segments were respectively drawn as if additional November and February data points were placed on preceding and following years. This provided an annual calculated flux of 505 Mmol yr^{-1}. The same procedure applied to the 11 conservative fluxes at the mouth of the estuary led to an annual flux of 705 Mmol yr^{-1} (solid black circles, Fig 4.8), which was close to the average annual flux for the period 2003-2005 when the whole dataset of filtered modelled fluxes was

taken into account (693 Mmol yr^{-1}, Table 4.2). By difference, the net annual DSi uptake amounted 200 Mmol yr^{-1}, corresponding to an annual DSi retention of 28 %.

As for the maximum net DSi uptake (Table 4.1), the net annual amount of DSi consumed (as well as DSi retention) in the estuary is two times higher than that in the tidal river, but more than one order of magnitude lower when the net DSi consumption is normalised with respect to volume or water surface area (Table 4.3). Such differences may be attributed to the shallower waters in the tidal river and to the zooplankton control on the phytoplankton in the estuary (Chapter 5).

Table 4.2: Annual DSi fluxes at the freshwater end-member and at the mouth of the estuary. Annual modelled fluxes in 2003, 2004 and 2005 at the freshwater end-member (km 88) and at mouth of the estuary (km 2) were calculated using the whole dataset of filtered instantaneous modelled fluxes. The annual modelled and calculated fluxes at the mouth of the estuary obtained by reporting the fluxes from the 11 campaigns in one single "typical" year (see text) are also indicated. The difference between the modelled and the calculated annual fluxes provides an estimation of the annual net DSi consumption.

Annual fluxes (Mmol yr^{-1}):	**freshwater end-member**	**mouth of the estuary**
from filtered modelled fluxes:		
2003	773	900
2004	578	546
2005	631	634
average	661	693
from all 11 campaigns lumped in one typical year:		
modelled annual flux		705
calculated annual flux		505
difference:		-200

Table 4.3: Net annual DSi uptake (as negative values) and DSi retention in the tidal river (Chapter 3) and in the estuary. The net annual DSi uptakes are also indicated normalised with respect to volumes and surface water areas of the tidal river and of the estuary as indicated in Table 4.1.

	tidal river	**estuary**
net annual DSi uptake:		
Mmol yr^{-1}	-102	-200
mol m^{-2} yr^{-1}	-7.20	-0.76
mmol m^{-3} yr^{-1}	-1687	-79
DSi retention (%)	14	28

Comparison with other studies in the Scheldt estuary

Only few studies about DSi dynamics in the Scheldt estuary have been yet performed. Soetaert et al. (2006) assessed DSi retentions of 22 and 20 % for the periods 1995-2000 and 2000-2002, respectively, and this is in agreement with our estimate (28 %) considering that our study period corresponded to dry years. Using model simulations, Arndt et al. (2009) found however a much smaller net amount of DSi consumed in the estuary for the year 2003, 36 Mmol yr^{-1}, corresponding to 4-5 % of the DSi inputs. However, these authors did not implement the import of diatoms from the coastal zone and the grazing pressure. As a result, they did not simulate the spring diatom bloom but estimated that DSi uptake occurred in summer, during which input DSi fluxes were low. The coastal zone was included in the model domain in other model simulations based on data from 1995 (Arndt 2008). This led to the simulation of an intense diatom spring bloom in the lower part of the estuary, resulting in a maximum DSi uptake in March at about 4500 kmol d^{-1}. Both the timing and the extent of this spring DSi uptake peak differed from our observations, but the DSi uptake in May June (1000-2000 kmol d^{-1}) and its decrease from July onwards were nevertheless in relatively good agreement with our observations. In addition, Arndt (2008) also estimated that BSi dissolution amounted 500 kmol d^{-1} from May to December, which supports our hypothesis that the net DSi release of about 400 kmol d^{-1} we observed in September and November 2004 could be ascribe to BSi dissolution only. Arndt (2008) estimated nevertheless that DSi was net consumed in summer due to significant summer and autumn diatom growth. In addition to the

fact that different years were studied, one explanation may be that zooplankton control on phytoplankton dynamics was not implemented for the estuarine domain.

Our results may also be compared with the primary production data from the Scheldt estuary, which has been extensively studied (e.g. Soetaert et al. 1994; Kromkamp and Peene 1995, 2005; Gazeau et al. 2005). Although uptake and accumulation of Si and C in diatoms cells are uncoupled and affected by different processes (Martin-Jézéquel et al. 2000; Hildebrand 2002; Claquin and Martin-Jézéquel 2005), it was assumed that, at the scale of the ecosystem, the gross DSi consumption can approach the net diatom primary production with a Si/C ratio corresponding to that in the stock of living diatoms. The gross DSi consumption would amount to 286 Mmol yr^{-1} supposing that BSi dissolution occurred from mid May (i.e. following the spring bloom, see above) until mid December (214 days) at the rate of 400 kmol d^{-1}. Considering a water surface area of 265 km^2 (Table 4.1) and a Si/C molar ratio of 0.33 for estuarine living diatoms (Chapter 5), this DSi consumption would correspond to a carbon production of 39 g m^{-2} yr^{-1}. Most studies listed above reported estimates for gross primary production presumably because of the difficulty to assess the net primary production in the Scheldt (Kromkamp and Peene 1995) but Soetaert et al. (1994) calculated a net primary production of 41 g m^{-2} yr^{-1} using model simulations. Although Soetaert et al. (1994) did not take into account the benthic phytoplankton while their contribution is implicitly included in our estimate, this estimate compares well with ours considering that diatoms account in general for 80-100 % of the phytoplankton biomass. Finally, as measurements of the annual gross primary production performed during different years provided similar results (Kromkamp and Peene 2005; Gazeau et al. 2005), the link between primary production and DSi consumption suggests that, in contrast to the tidal river, the annual DSi consumption in the estuary is not expected to vary significantly from one year to another. Nevertheless, due to higher DSi inputs during wet years, the percentage of DSi annually retained in the estuary should accordingly be lower than what is suggested by our "dry year" estimate.

4.6 References

Anderson GF (1986) Silica, diatoms and a freshwater productivity maximum in Atlantic coastal plain estuaries, Chesapeake Bay. Estuar Coast Shelf Sci 22:183-197

Arndt S (2008) Physical controls on the biogeochemical structure and functioning of a land-ocean transition system (Chapter 6). In: Arndt S. Biogeochemical transformations and fluxes in redox-

stratified environments: from the shallow coastal ocean to the deep subsurface. Ph. D. thesis. Univ. of Utrecht, The Netherlands. pp 147-179.

Arndt S, Regnier P, Vanderborght J-P (2009) Seasonally-resolved nutrient export fluxes and filtering capacities in a macrotidal estuary. J Mar Syst (in press). DOI 10.1016/j.jmarsys.2009.02.008

Billen G, Garnier J, Rousseau V (2005) Nutrient fluxes and water quality in the drainage network of the Scheldt basin over the last 50 years. Hydrobiologia 540(1-3):47-67

Claquin P, Martin-Jézéquel V (2005) Regulation of the Si and C uptake and of the soluble free-silicon pool in a synchronised culture of *Cylindrotheca fusiformis* (Bacillariophyceae): effects on the Si/C ratio. Mar Biol 146:877-886

Delstanche S (2004) Contribution à l'étude du cycle biogéochimique de la silice dans le continuum aquatique de l'Escaut. MSc. thesis. Université Catholique de Louvain, Belgium. (In French)

Dixit S, Van Cappellen P, van Bennekom AJ (2001) Processes controlling solubility of biogenic silica and pore water build-up of silicic acid in marine sediments. Marine Chemistry 73(3-4):333-352

Ehrenhauss S, Witte U, Janssen F, Huettel M (2004) Decomposition of diatoms and nutrient dynamics in permeable North Sea sediments. Cont Shelf Res 24(6):721-737

Gallinari M, Ragueneau O, Corrin L, DeMaster DJ, Treguer P (2002) The importance of water column processes on the dissolution properties of biogenic silica in deep-sea sediments I. Solubility. Geochimica et Cosmochimica Acta 66(15):2701-2717

Gazeau F, Gattuso J-P, Middelburg JJ, Brion N, Schiettecatte L-S, Frankignoulle M, Borges AV (2005) Planktonic and whole system metabolism in a nutrient-rich estuary (the Scheldt estuary). Estuaries 28(6):868-883

Hildebrand M (2002) Lack of coupling between silicon and other elemental metabolisms in diatoms. J Phycol 38:841-843

Kromkamp JC, Peene J (2005) Changes in phytoplankton biomass and primary production between 1991 and 2001 in the Westerschelde estuary (Belgium/The Netherlands). Hydrobiologia 540(1-3):117-126

Kromkamp JC, Peene J (1995) Possibility of net phytoplankton primary production in the turbid Schelde Estuary (SW Netherlands). Mar Ecol Prog Ser 121:249-259

Lacroix G, Ruddick K, Ozer J, Lancelot C (2004) Modelling the impact of the Scheldt and Rhine/Meuse plumes on the salinity distribution in Belgian waters (southern North Sea). J Sea Res 52:149-163

Lancelot C (1995) The mucilage phenomenon in the continental coastal waters of the North Sea. Sci Total Environ 165(1-3):83-102

Loucaides S, Van Cappellen P, Behrends T (2008) Dissolution of biogenic silica from land to ocean: Role of salinity and pH. Limnol Oceanogr 53(4):1614-1621

Martin-Jézéquel V, Hildebrand M, Brzezinski MA (2000) Silicon metabolism in diatoms: implications for growth. J Phycol 36:821-840

Michalopoulos P, Aller RC (2004) Early diagenesis of biogenic silica in the Amazon delta: alteration, authigenic clay formation, and storage. Geochim Cosmochim Acta 68(5):1061-1085

Muylaert K, Tackx M, Vyverman W (2005) Phytoplankton growth rates in the freshwater tidal reaches of the Schelde estuary (Belgium) estimated using a simple light-limited primary production model. Hydrobiologia 540(1-3):127-140

Prandle D, Hydes DJ, Jarvis J, McManus J (1997) The seasonal cycles of temperature, salinity, nutrients and suspended sediment in the southern North Sea in 1988 and 1989. Estuar Coast Shelf Sci 45:669-680

Ragueneau O, Conley DJ, Leynaert A, Ni Longphuirt S, Slomp CP (2006) Role of diatoms in silicon cycling and coastal marine food webs. In: Ittekot V, Unger D, Humborg C, TacAn N (eds) The silicon cycle. Human perturbations and impacts on aquatic systems. SCOPE 66. Island Press, Washington, Covelo, London. pp 163-195.

Regnier P, Mouchet A, Wollast R, Ronday R (1998) A discussion of methods for estimating residual fluxes in strong tidal estuaries. Cont Shelf Res 18:1543-1571

Regnier P, Wollast R, Steefel CI (1997) Long-term fluxes of reactive species in macrotidal estuaries: Estimates from a fully transient, multicomponent reaction-transport model. Mar Chem 58:127-145

Roubeix V, Becquevort S, Lancelot C (2008) Influence of bacteria and salinity on diatom biogenic silica dissolution in estuarine systems. Biogeochemistry 88(1):47-62

Soetaert K, Van Rijswijk P (1993) Spatial and temporal patterns of the zooplankton in the Westerschelde estuary. Mar Ecol Prog Ser 97:47-59

Soetaert K, Herman PMJ, Kromkamp JC (1994) Living in the twilight: estimating net phytoplankton growth in the Westerschelde estuary (The Netherlands) by means of an ecosystem model (MOSES). J Plankton Res 16:1277-1301

Soetaert K, Herman PMJ (1995) Estimating estuarine residence times in the Westerschelde (The Netherlands) using a box model with fixed dispersion coefficients. Hydrobiologia 311:215-224

Soetaert K, Middelburg JJ, Heip C, Meire P, Van Damme S, Maris T (2006) Long-term change in dissolved inorganic nutrients in the heterotrophic Scheldt estuary (Belgium, The Netherlands). Limnol Oceanogr 51(1, part 2):409-423

Struyf E, Van Damme S, Meire P (2004) Possible effects of climate change on estuarine nutrient fluxes: a case study in the highly nutrified Schelde estuary (Belgium, The Netherlands). Estuar Coast Shelf Sci 60(4):649-661

Tackx M, De Pauw N, Van Mieghem R, Azémar F, Hannouti A, Van Damme S, Fiers F, Daro N, Meire P (2004) Zooplankton in the Schelde estuary, Belgium and The Netherlands. Spatial and temporal patterns. J Plankton Res 26(2):133-141

Van Cappellen P, Dixit S, van Beusekom J (2002) Biogenic silica dissolution in the oceans: Reconciling experimental and field-based dissolution rates. Glob Biogeochem Cycle 16(4):1075

Van Damme S, Struyf E, Maris T, Ysebaert T, Dehairs F, Tackx M, Heip C, Meire P (2005) Spatial and temporal patterns of water quality along the estuarine salinity gradient of the Scheldt estuary (Belgium and The Netherlands): results of an integrated monitoring approach. Hydrobiologia 540(1-3):29-45

Van der Zee C, Chou L (2005) Seasonal cycling of phosphorus in the Southern Bight of the North Sea. Biogeosciences 2:27-42

Vanderborght J-P, Wollast R, Loijens M, Regnier P (2002) Application of a transport-reaction model to the estimation of biogas fluxes in the Scheldt estuary. Biogeochemistry 59:207-237

Yamada SS, D'Elia CF (1984) Silicic acid regeneration from estuarine sediment cores. Mar Ecol Prog Ser 18:113-118

4A ANNEX: Winter DSi profiles

4A.1 Possible explanations for the differences between modelled and measured DSi profiles in winter

Measured DSi versus salinity profiles were significantly lower than the conservative modelled ones in winter (February and November 2004, Fig. 4.6 in Chapter 4) although practically no diatoms were observed in the estuary (Chapter 5). Several possible explanations can be put forward.

DSi uptake by benthic diatoms

Benthic activity may be responsible for a significant fraction of the annual amount of DSi uptake as the contribution of benthic diatoms was estimated to 17 % of the annual gross primary production in the Scheldt (De Jong and de Jonge 1995; Gazeau 2005). But the benthic chlorophyll *a* was low from November to February (De Jong and de Jonge 1995). It is thus difficult to attribute the difference between measured and simulated profiles in February and November 2004 to DSi uptake by benthic diatoms.

Abiotic removal

The maximum difference between both DSi profiles was reached in the zone of maximum turbidity (Chapter 5). This suggests that the difference could be due to DSi removal by sorption. Abiotic removal in the range of 10-30 % has already been observed in low salinity areas of estuaries when ambient DSi and SPM concentrations were high (Chou and Wollast 2006).

February 2004: Overlooked DSi drops at the freshwater end-member

Another explanation could be that, similarly to what observed during winter 2002-2003 (Fig. 4.5 in Chapter 4), the discharge peak that occurred in 12-21/01/2004 may have resulted in a drop in DSi concentrations in the freshwater end-member, which would have been overlooked due to under-sampling. Three scenarios for drops in DSi concentrations were built from the DSi profile shown in Fig. 4.5, and tested with the model (Fig. 4A.1). The first alternative scenario was the most realistic in terms of the extent and the duration of the drop,

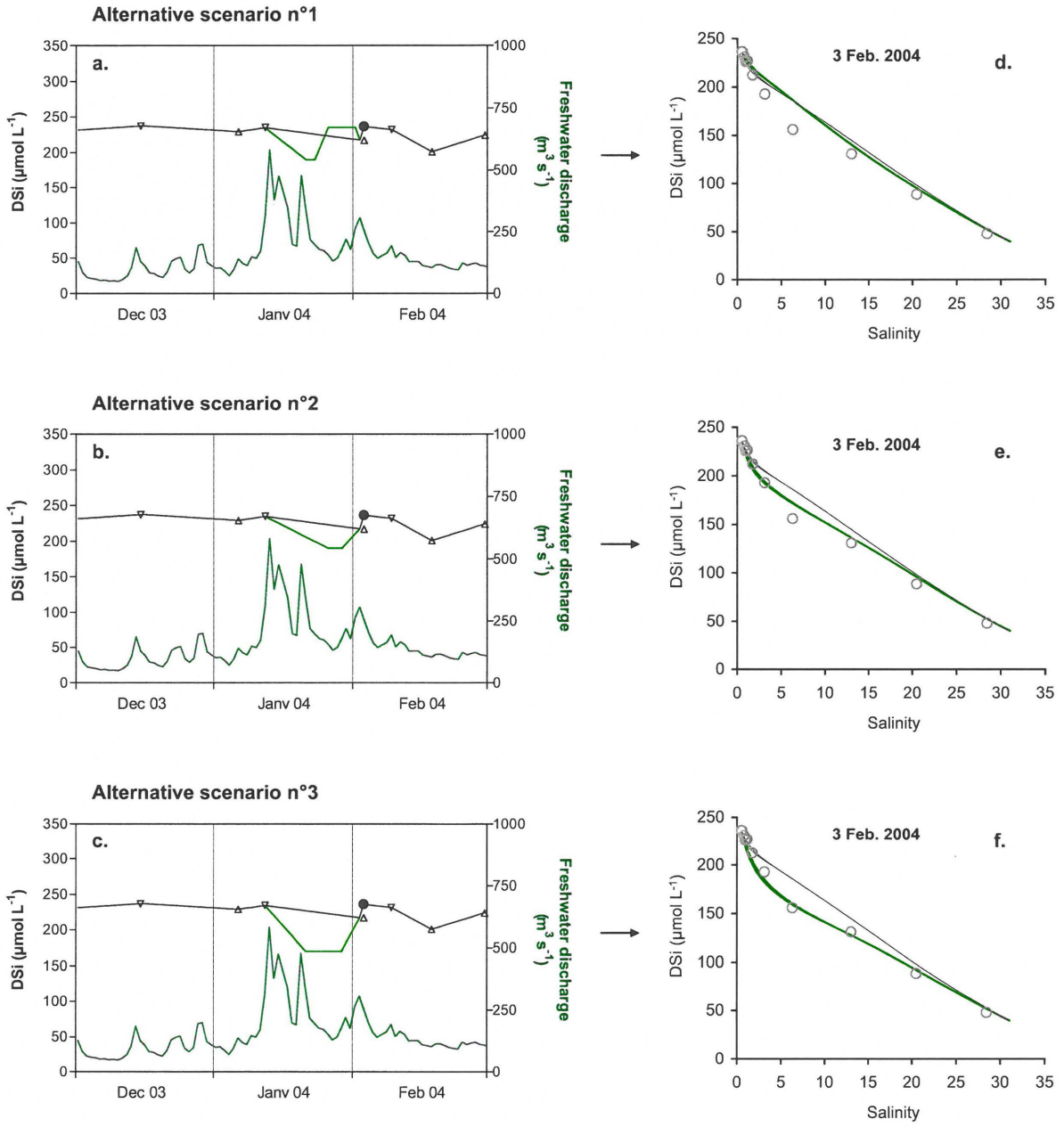

Fig. 4A.1:

a-c: Alternative scenarios of boundary conditions for the DSi concentrations at the freshwater end-member (in red, left scale). Data and symbols for the discrete and the daily interpolated DSi measurements (in black, left scale) and the freshwater discharge (in blue, right scale) are the same as in Fig. 4.3a and b in Chapter 4.

d-f: Modelled DSi concentrations obtained using alternative boundary conditions for DSi at the freshwater end-member: the plain red curves delimitate the envelopes of all the instantaneous DSi versus salinity profiles obtained within the sampling period for February 2004. The black line and the grey circles correspond to the data shown in Fig. 4.6 (Chapter 4) for February 2004 with identical symbols.

as well as of the delay between the discharge peak and the minimum DSi concentration (Fig. 4A.1a), but it could not explain the difference between the measured and the modelled DSi versus salinity profiles (Fig. 4A.1d). The modelled DSi profile better matched to the measured one when the minimum DSi concentration in the freshwater end-member was set a few days later than in scenario 1, but both profiles still significantly differed at salinity 6.3 (scenario n°2, Fig. 4A.1b and e). This low DSi measurement could only be retrieved by an extended freshwater DSi drop down to 170 µmol L^{-1} (scenario n°3, Fig. 4A.1c and f), which did not seem realistic for such a discharge peak when compared to the responses of the DSi concentrations to the discharge peaks in winter 2002-2003 (Fig. 4.5).

February 2004: mishandling of the sample

The discrepancy between the measured and the modelled DSi versus salinity profiles in February 2004 was mostly due to only one sample. An error in the DSi analysis was ruled out by replicate analyses. Nevertheless, due to the salinity effect in the DSi measurements, the expected precision is in the order of 5 %, which is significant compared to the difference between the measured and modelled DSi profiles. Also, the samples were kept at low temperature and an accidental freezing could not be ruled out. However, the effect of freezing has been tested on samples with high initial DSi concentrations (217 µmol L^{-1}): DSi concentrations measured following Koroleff (1983) decreased by a factor ranging from 3 to 10 (not shown). As no such drop was observed in the DSi profile in the estuary, this suggests that the samples had not been accidentally frozen.

February 2004: lateral input

A salinity of 8.3 was also simulated for this sample while the measured salinity was 6.3. In contrast, other modelled salinities at the locations and times of the samplings did not differ significantly from the measured ones during this campaigns (deviation of less than 0.5 at low salinities, or corresponding to less than 10 % at salinities higher than 10). But the dilution by a lateral freshwater source (with a DSi concentration of roughly 100 µmol L^{-1} so that the mix with the modelled concentration modelled at salinity 8.3 would result in that measured at salinity 6.3) was unexpected: 1) the sampling was performed in the middle of the channel so such a mixing would have required a lateral source with a significant discharge and 2) there was no such lateral freshwater source near this station (located just downstream the marsh of Saeftinge). The sampling being performed at low tide, the difference of salinity

may thus be attributed to the complex water circulation in ebb/flood channels, which could not be assessed in a 1D model. Nevertheless, this could not explain why the conservative DSi profile did not match with the measured one.

November 2004: variations in DSi concentrations at the freshwater end-member

In November 2004, the difference between modelled and measured profiles at low salinities was as well unexpected but it was observed for several data points (Fig. 4.6 in Chapter 6). Similarly, no DSi concentrations were available for the lower tidal freshwater reaches between the 12/10/2004 and the 16/11/2004 but DSi concentrations increased from 50 to 200 µmol L^{-1} between these two dates (Fig. 4.3b in Chapter 4, and Fig. 4A.2a and b). It was

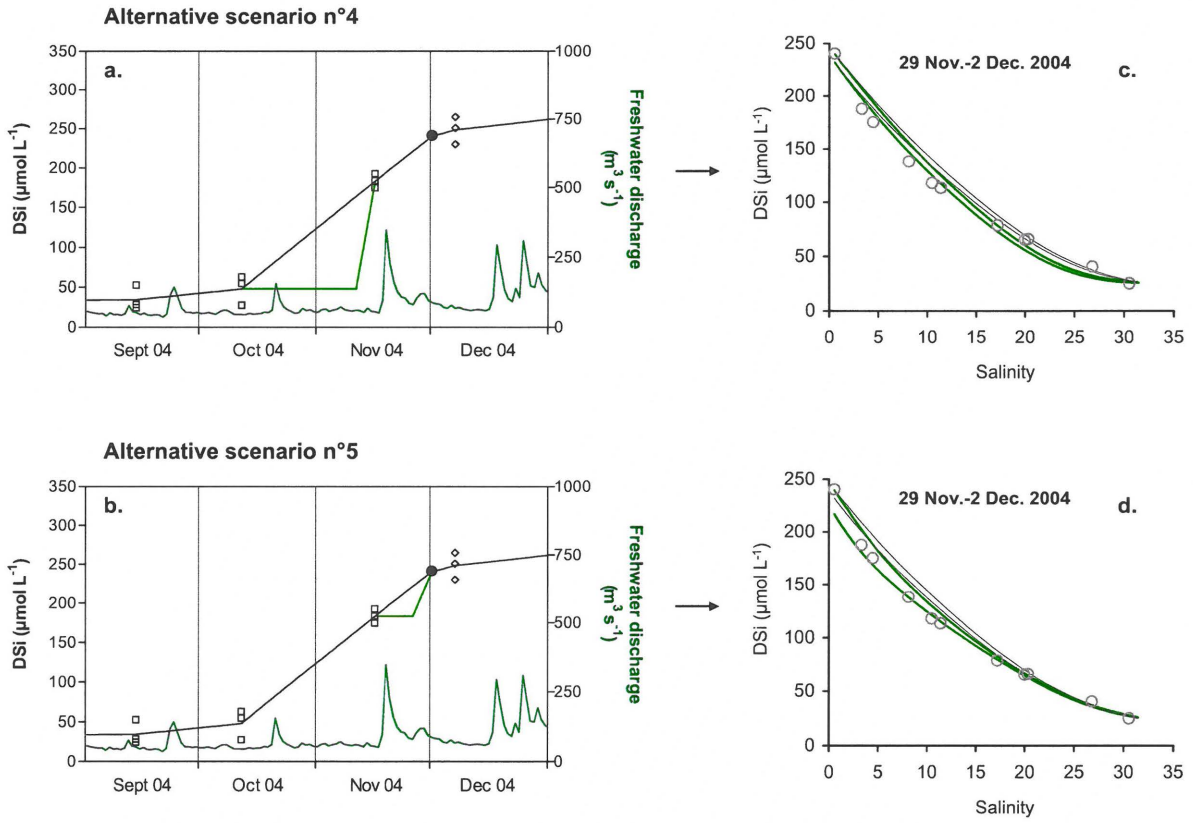

Fig. 4A.2:

a-b: Alternative scenarios of boundary conditions for the DSi concentrations at the freshwater end-member (in red, left scale). Data and symbols for the discrete and the daily interpolated DSi measurements (in black, left scale) and the freshwater discharge (in blue, right scale) are the same as in Fig. 4.3a and b in Chapter 4.

c-d: Modelled DSi concentrations obtained using alternative boundary conditions for DSi at the freshwater end-member: the plain red curves delimitate the envelopes of all the instantaneous DSi versus salinity profiles obtained within the sampling period for November 2004. The black line and the grey circles correspond to the data shown in Fig. 4.6 (Chapter 4) for November 2004 with identical symbols.

initially assumed a linear increase with time, but as the discharge remained low during the whole month of October, DSi consumption might have lasted longer. However, this could not be an explanation for higher modelled DSi concentrations than those measured in the first half of the estuary (scenario n°4, Fig. 4A.2a and c). Lower DSi concentrations in the freshwater end-member in October would in fact result in lower simulated DSi concentrations in the lower part of the estuary. Similar modelled and measured DSi versus salinity profiles would only be obtained if DSi concentration at the freshwater end-member dropped in late November (scenario n°5, Fig 4A.2b and d). However, such a drop is questionable as DSi concentrations are expected to have quickly reached the winter concentration of 230-250 $\mu mol\ L^{-1}$ with the discharge peak on the 19/11/2004. Contrasting with the large winter discharge peaks which can cause drops in DSi concentrations (Fig. 4.5), smaller discharge peaks during the productive period tend to result in an increase in DSi concentrations due to the partial or even total flushing of the diatoms in the tidal river (Chapter 3).

This highlights the need for high frequency datasets in the end-members to properly describe and interpret the DSi dynamics in the saline estuary. Arndt et al. (2007) also observed that diatoms respond quickly to short-term variations in physical conditions in the tidal freshwater reaches of the Scheldt estuary. These authors thus recommended that models of such ecosystems should be defined at adequate small time and geographical scales, and that sampling strategies should be planned accordingly.

4A.2 References

Arndt S, Vanderborght J-P, Regnier P (2007) Diatom growth response to physical forcing in a macrotidal estuary: Coupling hydrodynamics, sediment transport, and biogeochemistry. J Geophys Res 112:C05045

Chou L, Wollast R (2006) Estuarine silicon dynamics. In: Ittekot V, Unger D, Humborg C, TacAn N (eds) The silicon cycle. Human perturbations and impacts on aquatic systems. SCOPE 66. Island Press, Washington, Covelo, London. pp 93-120.

De Jong DJ, de Jonge VN (1995) Dynamics and distribution of microphytobenthic chlorophyll-*a* in the Western Scheldt estuary (SW Netherlands). Hydrobiologia 311:21-31

Gazeau F, Gattuso J-P, Middelburg JJ, Brion N, Schiettecatte L-S, Frankignoulle M, Borges AV (2005) Planktonic and whole system metabolism in a nutrient-rich estuary (the Scheldt estuary). Estuaries 28(6):868-883

Koroleff F (1983) Determination of silicon. In: Grasshoff K, Ehrhardt M, Kremling K (eds) Methods of seawater analysis. Second, revised and extended edition. Verlag Chemie, Weinheim, Deerfield Beach, Florida, Basel. pp 174-187.

5 Behaviour of the biogenic silica in the estuary: influence of phytoplankton and SPM dynamics

In this study, BSi as well as SPM and chlorophyll *a* longitudinal profiles over the entire salinity gradient in the Scheldt estuary are presented for eleven campaigns conducted at different seasons from 2003 to 2005. BSi concentrations are compared with those of chlorophyll *a* and SPM to estimate whether BSi was predominantly associated or not with living diatoms. The physiological status of the diatoms and the BSi concentration associated with growing diatoms are also investigated using ^{32}Si incorporations. In the light of these results, BSi dynamics are related and interpreted with those of the SPM and of the phytoplankton in the Scheldt estuary. A BSi mass-balance in the estuary is finally established comparing the BSi content in the SPM with an existing SPM budget in the Scheldt estuary.

5.1 Distribution of the particulate materials along the salinity gradient

SPM and BSi

The SPM concentrations in our samples exhibited high temporal and spatial variations (Fig. 5.1). The highest SPM concentrations, which exceeded 200 mg L^{-1}, were observed in the zone of salinity 0-10. The average concentrations in this zone ranged from 25 to 145 mg L-1 but no simple seasonal pattern was highlighted. Except in February 2004, lower average concentrations were encountered elsewhere in the estuary (zone of salinity 10-30) where the average SPM concentrations ranged from 10 to 60 mg L^{-1}. Additionally, SPM concentrations in the zone of salinity 10-30 were highest in winter and early spring and lowest in late summer. At the marine stations closest to the coast and/or to the mouth of the estuary, there was generally a local maximum in SPM concentrations.

The longitudinal profiles of BSi concentrations followed those of SPM concentrations and displayed identical high temporal and spatial variations (Fig. 5.1). Namely, BSi concentrations averaged over the salinity gradient in the zone of salinity 0-10 did not exhibit any seasonal pattern. They ranged from about 12 to 81 µmol L^{-1} and concentrations exceeding

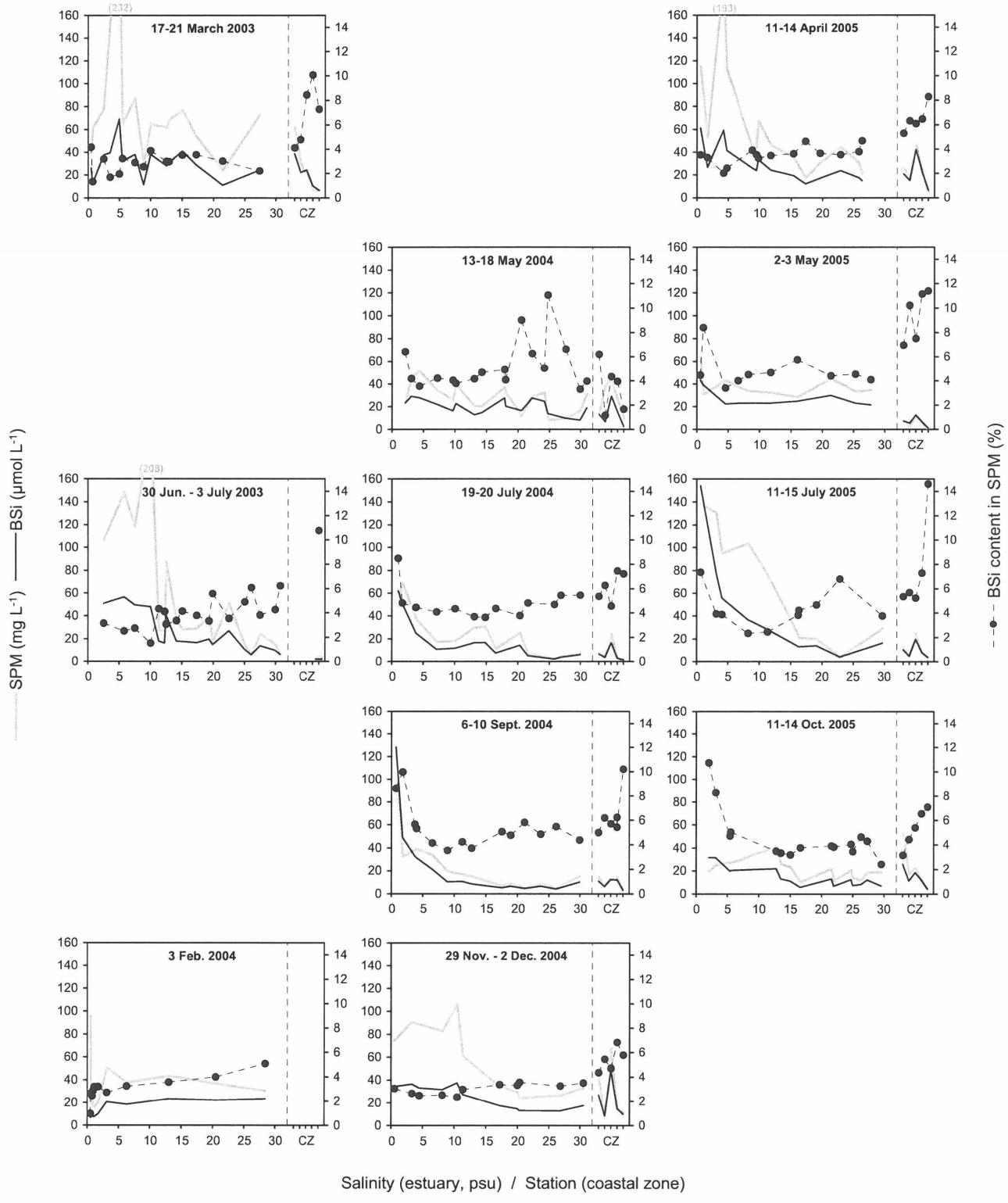

Fig. 5.1: SPM and BSi concentrations, as well as BSi contents in the SPM along the estuarine salinity gradient and in the coastal zone (CZ). In the coastal zone, the ticks represent, from left to right, the stations #710, #780, #130, #230 and #330. SPM concentrations exceeding the y-axes scales are indicated in the graphs as numbers in brackets (in grey as for the lines). Panels are ordered according to seasons (from top to bottom), then to years (from left to right).

100 µmol L^{-1} were recorded in July 2005 and September 2004 at the most freshwater sampling station (near the confluence with the Rupel). Except in February 2004, BSi concentrations were also lower in the zone of salinity 10-30 than in the zone of salinity 0-10. Average BSi concentrations in the zone of salinity 10-30 ranged from 7 to 27 µmol L^{-1} and were highest in spring and lowest in late summer. A local maximum in BSi concentrations was also regularly observed at the marine stations closest to the coast and/or to the mouth of the estuary.

Temporal and longitudinal patterns were better revealed when BSi was expressed as a fraction of the SPM (Fig. 5.1). The BSi content in the SPM (expressed as hydrated SiO_2, see Chapter 2) averaged over the salinity gradient ranged from 2.9 to 5.4 % (average 4.1 %). Highest values (8-10 %) were found in the most freshwater part (below salinity 5) in summer (except July 2003), early autumn and to a smaller extent in May. The zone of salinity 5-10 appeared to host a local minimum in all seasons, but, in winter and early spring, BSi contents in the zone of salinity 0-5 were identical to those in the zone of salinity 5-10. Elsewhere in the estuary, the BSi content rarely dropped below 2.5 %. In the zone of salinity 10-30, the BSi content progressively increased to reach contents ranging from 4 to 6 % near the mouth of the estuary. In May 2004 however, a maximum with contents reaching 10 % was observed in the zone of salinity 20-30. Except for May 2004, the BSi content was always higher at coastal stations than in the estuary.

Total chlorophyll a (Chla) and chlorophyll a associated with diatoms (DiatChla)

The highest Chl*a* and DiatChl*a* concentrations were always found in the less saline part of the estuary and those concentrations were highest in summer (Chl*a* and DiatChl*a* concentration reaching respectively 70 and 50 µg L^{-1} in mid July and September) (Fig. 5.2). With increasing salinity, both Chl*a* and DiatChl*a* dropped to below 5 µg L^{-1} around salinity 5-10 (except in July 2003). Further downstream, Chl*a* and DiatChl*a* stayed at low levels, except in May 2004, May 2005 and (beginning of) July 2003. During these three campaigns, Chl*a* and DiatChl*a* increased at salinities higher than 15, reaching maximum concentrations of 15 µg L^{-1}. The distribution of Chl*a* concentrations was in agreement with that reported since the nineties (Kromkamp and Peene 2005; Van Damme et al. 2005; Soetaert et al. 2006). Some studies also reported spring blooms at salinities higher than 15 (Boschker et al. 2005; Van Damme et al. 2005).

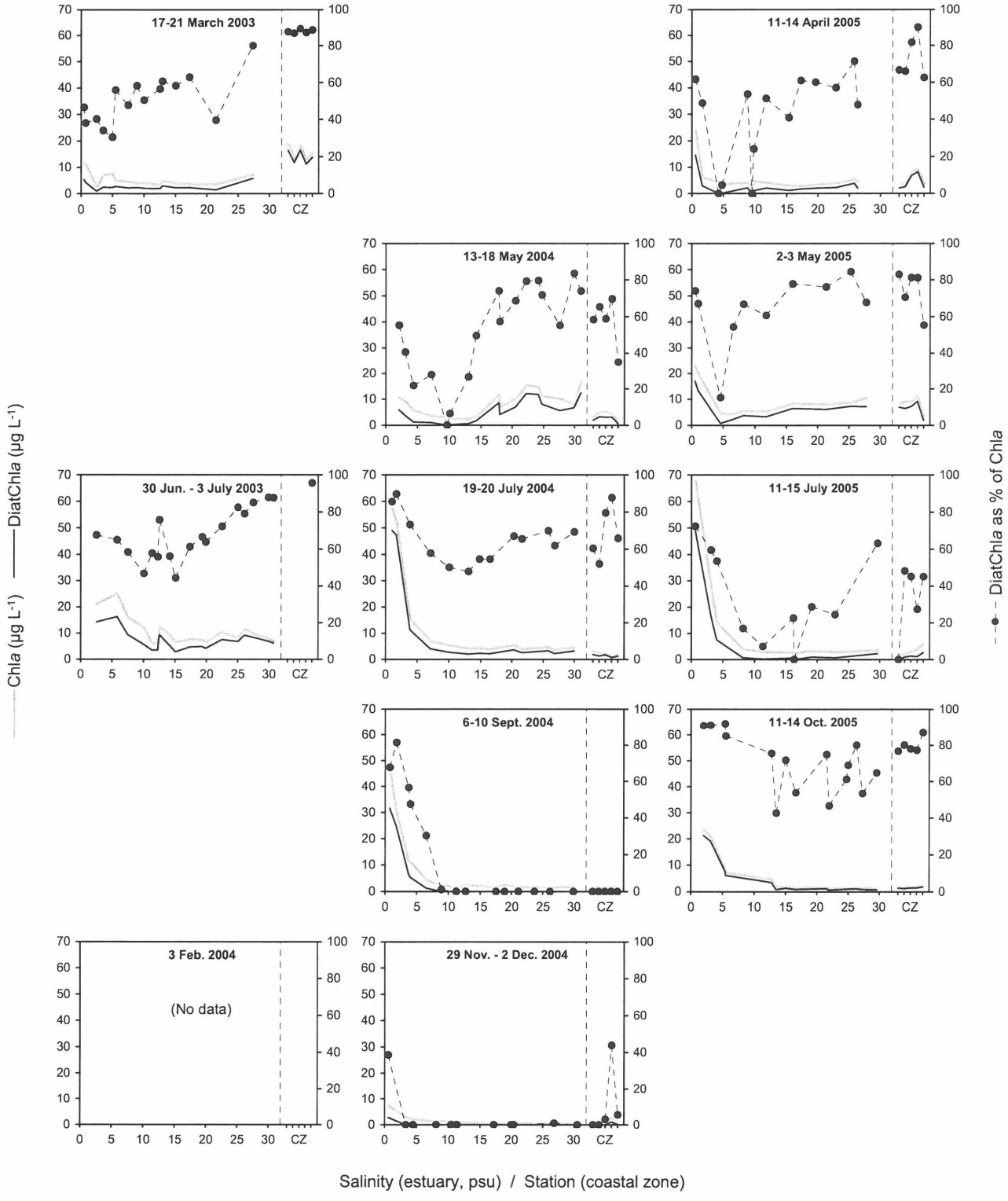

Fig. 5.2: Chl*a* and DiatChl*a* concentrations, and contributions of DiatChl*a* to Chl*a* along the estuarine salinity gradient and in the coastal zone (CZ). In the coastal zone, the ticks represent, from left to right, the stations #710, #780, #130, #230 and #330. Panels are ordered according to seasons (from top to bottom), then to years (from left to right).

Apart in September and November 2004 when the contribution of the diatoms to the total Chl*a* was negligible downstream salinity 5, diatoms were the dominant species in the estuary and represented between 50 and 90 % of the phytoplankton biomass (Fig. 5.2). The contribution of the diatoms to the Chl*a* concentration was highest at the mouth of the estuary and, to a lesser extent, at the most upstream stations, and minimum contributions were observed in the zone of salinity 5-15. Also, in all spring campaigns and in July 2005, diatoms accounted occasionally for less than half of the phytoplankton biomass in the zone of salinity 0-15, and they were not the dominant species only in May 2004 and April 2005 in the zone of salinity 5-10.

As the method could not discriminate between diatoms and *Phaeocystis*, both contributions to the total Chl*a* are lumped into DiatChl*a* (Chapter 2). *Phaeocystis* may contribute significantly to the phytoplankton biomass in April and May at salinities higher than 15 (Chapter 2). Brochard et al. (2005, 2006) observed *Phaeocystis* colonies on 3 May 2004, 2 May 2005 and 2 June 2005 at Vlissingen, but *Phaeocystis* were only found as individual cells from spring to early autumn at Hansweert (km 36, salinity 15-25). Chlorophytes were the most important species after the diatoms. They often dominated or co-dominated in the zone of salinity 5-15 (data not shown). Other phytoplankton species were also observed but they dominated the phytoplankton biomass only occasionally, principally when the diatom biomass was low: dinophytes dominated at salinities higher than 10 in September 2004, euglenophytes at salinities higher than 15-20 in November 2004 and July 2005, cryptophytes around salinity 5 in April 2005 but the cyanobacteria biomass was always minor (data not shown). The phytoplankton speciation was overall very well in accordance with previous studies (cf. Introduction).

Except for March 2003, Chl*a* and DiatChl*a* concentrations in the coastal zone were in general not significantly different from those found in the downstream part of the estuary, but always lower than those in the upstream part (Fig. 5.2). In March 2003, they were about three to five times higher than those observed in the most saline part of the estuary, but the opposite was observed in May 2004. Slightly lower marine concentrations were observed July 2004, but higher ones were measured in November 2004 and April 2005 at the two marine stations closest to the coast (#130 and #230).

Phaeocystis blooms can reach a high biomass in the coastal zone, exceeding by far that of the diatoms (Lancelot 1995; Rousseau et al. 2002; Tungaraza et al. 2003). Such event would lead to high Chl*a* concentrations (Van der Zee and Chou 2005; Muylaert et al. 2006),

which were not observed in our samples. But even if we could thus assume that we did not sample during the peak of the *Phaeocystis* bloom, *Phaeocystis* can still represent about half of the phytoplankton biomass in April and/or May before the bloom peak (Lancelot 1995; Rousseau et al. 2002; Tungaraza et al. 2003). In April and May, the phytoplankton community was thus dominated by diatoms and/or *Phaeocystis* (Fig. 5.2). The rest of the year, *Phaeocystis* are expected to be in negligible amounts (Lancelot 1995; Rousseau et al. 2002; Tungaraza et al. 2003; Muylaert et al. 2006) and DiatChl*a* represented thus only the contribution of diatoms to the total Chl*a*: diatoms dominated the phytoplankton community and represented more than 50 % of the biomass during all campaigns in the coastal zone, except in September and November 2004 (dominated by dinophytes) and in July 2005 at #710 and #230 (dominated by euglenophytes and eventually co-dominated by chlorophytes). These campaigns corresponded to those during which diatoms were not the dominant species in the downstream part of the estuary. This may be however an artefact of the CHEMTAX analysis when pigment levels are low, as microscopic investigations revealed that the diatoms and/or the *Phaeocystis* dominated the phytoplankton community all year round (Muylaert et al. 2006).

POC

Particulate organic carbon (POC) concentrations displayed high temporal variability but no clear seasonal variations were found (Fig. 5.3). Highest concentrations (up to 9 mg L^{-1}) were always observed in the zone of salinity 0-10 while POC concentrations stayed below 2 mg L^{-1} elsewhere in the estuary. As a general rule, POC concentrations decreased with increasing salinity, down to concentrations around 1 mg L^{-1} or lower at the mouth of the estuary. In the coastal zone, POC concentrations never exceeded 2 mg L^{-1} and were in general lower than 1 mg L^{-1}.

POC was poorly correlated with Chl*a* in the estuary (r^2 = 0.23, n = 137) or in the coastal zone (r^2 = 0.04, n = 46). In agreement with the observations of Abril et al. (2002), phytoplankton could represent the major fraction of the organic matter in late spring and in summer 2003 and 2004 (using a $\beta_{POC/Chla}$ of 30, as described in Chapter 2), but the contrary was observed in spring or summer 2005. The rest of the year, phytoplankton accounted in general for less than 20 % of the organic matter.

The POC dynamics were actually better correlated with those of SPM (r^2 = 0.85, n = 137 in the estuary and r^2 = 0.69, n = 47 in the coastal zone). With a conversion factor from

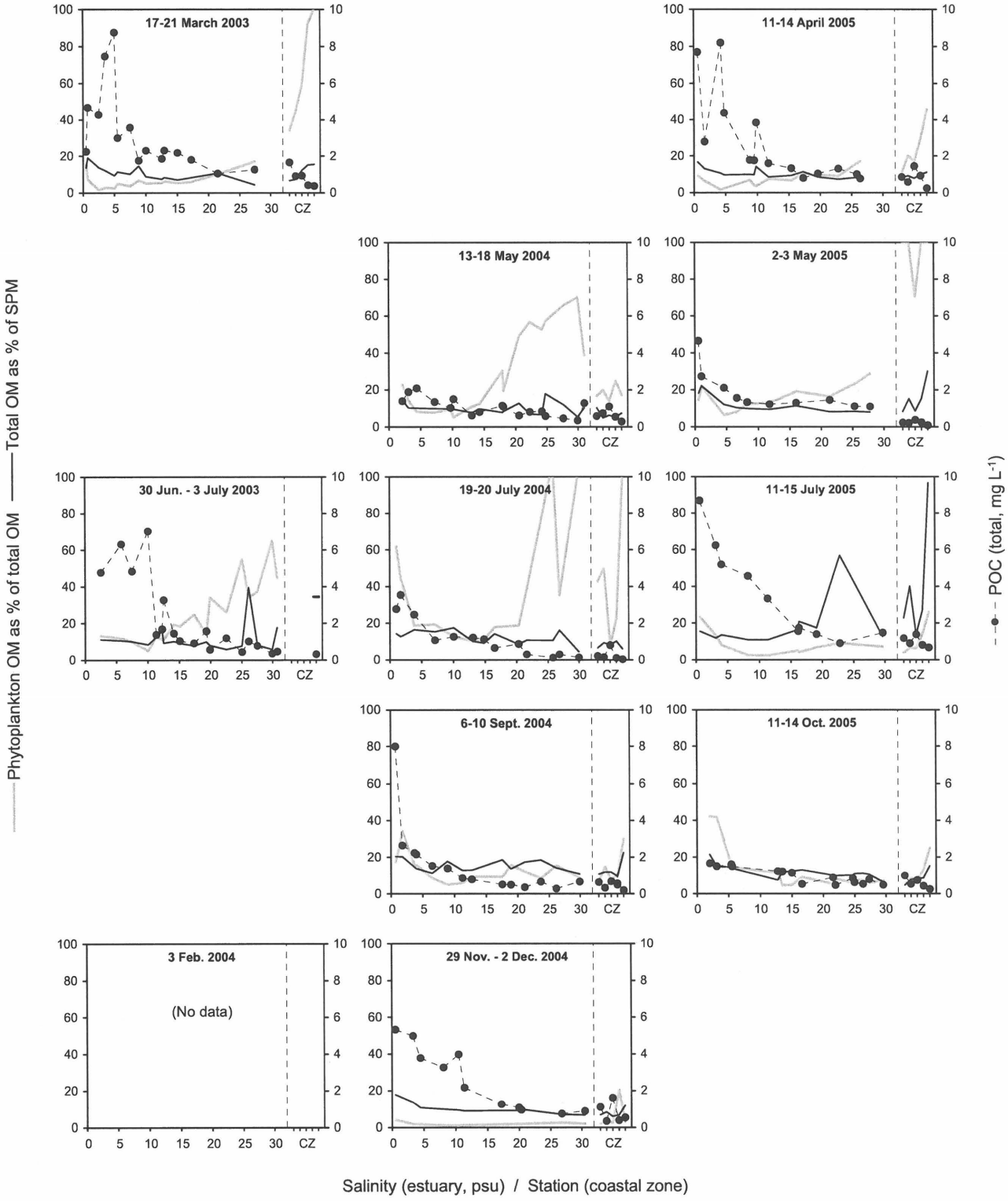

Fig. 5.3: POC concentrations and contributions of the phytoplankton to the organic matter (OM) and of the organic matter to the SPM along the estuarine salinity gradient and in the coastal zone (CZ). In the coastal zone, ticks represent, from left to right, the stations #710, #780, #130, #230 and #330. Panels are ordered according to seasons (from top to bottom), then to years (from left to right).

POC to organic matter of 2.5 g g^{-1} (ratio of the molar masses of CH_2O and C, as observed in an eutrophic estuary by Suzumura et al. 2004), the organic matter content in the SPM generally followed a regular decrease from about 10 to 20 % in the freshwater end-member to about 5 to 10 % at the mouth of the estuary. This in accordance with the findings from Abril et al. (2002) considering that the POC content in the SPM of the Scheldt estuary decreased since the nineties (Chen et al. 2005). In our data however, POC contents in the SPM did not significantly vary from one campaign to another even if episodic higher organic matter contents were found in July 2003 and 2005 at the sampling station in front of Terneuzen.

5.2 Distinction between fractions of BSi associated or not with living diatoms

Choice of a multiple regression model

As already done in the Scheldt tidal river (Chapter 3), the BSi associated with living diatoms and that constituted of detrital particles (respectively BSi_{liv} and BSi_{dct}) were discriminated performing multiple regression analysis, using DiatChl*a* and the SPM not corresponding to BSi or to the living diatom biomass (SPM_{nbld}) as explicative variables (see Chapter 2). Multicolinearity was avoided as SPM_{nbld} and DiatChl*a* were not correlated in the estuary ($r^2 = 0.04$, n = 148, DiatChl*a* were assumed to be 0 in February 2004) or in the coastal zone ($r^2 = 0.02$, n = 47). As in the tidal river, SPM_{nbld} could have been further divided in organic and inorganic fractions (using POC and DiatChl*a* data and the β ratios defined in Chapter 2), but both fractions could not be used in the same regression as they were correlated in the estuary ($r^2 = 0.83$, n = 137, no POC data available for February 2004) and in the coastal zone ($r^2 = 0.58$, n = 47). In the following, the two data points corresponding to BSi concentrations exceeding 100 µmol L^{-1} (the most upstream stations in September 2004 and July 2005, Fig. 5.1) were discarded as outliers (see further).

Regression #1:

Firstly, linear multiple regressions were performed following Eq. 2.5 (Chapter 2). As different diatom communities (with potentially different Si contents) were observed along the salinity gradient in the Scheldt estuary and in the coastal zone, data were lumped in three overlapping groups according to the salinity ranges used for the CHEMTAX analysis (see Chapter 2): salinities 0-13 (n = 73), 7-30 (n = 100) and 24-35 (n = 76). The BSi_{liv}/DiatChl*a* ratio for the three groups were respectively 1.09 ± 0.22 µmol $µg^{-1}$ (± 95 % confidence

interval), 1.19 ± 0.36 µmol µg^{-1} and 0.51 ± 0.24 µmol µg^{-1}. The first two ones were significantly different from the last one (*t*-test for equality: p = 0.005 and 0.002 respectively), but not between each other (*t*-test for equality: p = 0.667). The two first groups could therefore be lumped and, in a second step, linear multiple regressions were applied on only two distinct datasets: an estuarine one (n = 146) and a purely marine one (n = 47).

Regression #2:

For the marine stations, the regression was kept linear and the correlation coefficient between BSi measured and estimated by the regression was r^2 = 0.830 (n = 47). The partial coefficients k_1 (BSi_{liv}/DiatChl*a*) and k_2 were respectively 0.52 ± 0.29 µmol µg^{-1} and 0.66 ± 0.07 µmol mg^{-1}. Using the conversion factors, these coefficients would correspond respectively to a Si/C molar ratio in living diatoms of 0.21 ± 0.12 and to a BSi_{det} content in the residual SPM (i.e. not due to BSi_{liv} or to the living diatom biomass) of 4.17 ± 0.44 % (BSi as hydrated SiO_2, see Chapter 2).

For the estuarine dataset, the linear multiple regression (r^2 = 0.832, n = 146) led to a BSi_{liv}/DiatChl*a* of 1.08 ± 0.16 µmol µg^{-1} (corresponding to a Si/C molar ratio of 0.43 ± 0.06) and to a BSi_{det}/SPM_{nbld} of 0.366 ± 0.024 µmol mg^{-1}. The residuals did not seem to exhibit any trend when plotted against DiatChl*a* but appeared to be linked to SPM_{nbld}: the plot of BSi_{det} (BSi minus BSi_{liv}) against SPM_{nbld} exhibited a "power" relation with an exponent

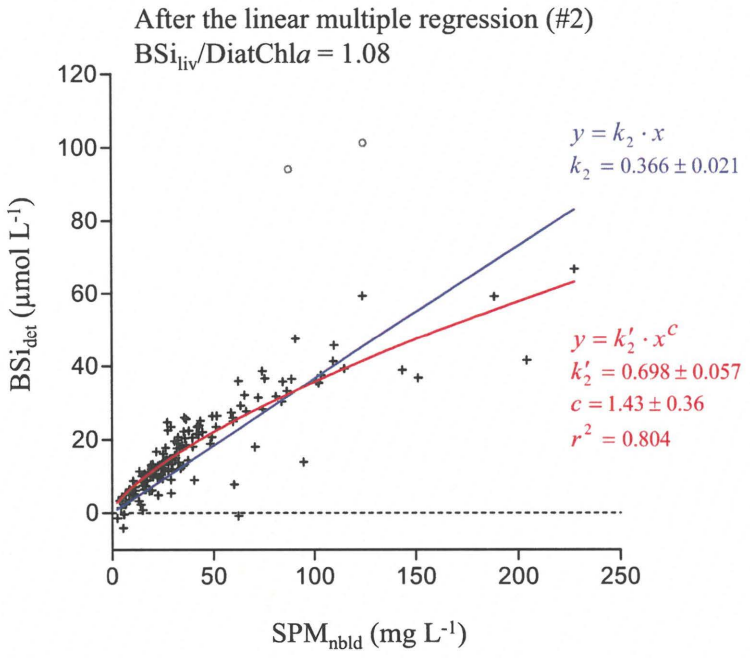

Fig. 5.4: BSi_{det} versus SPM_{nbld} after regression #2 in the estuary.

significantly lower than one (Fig. 5.4). This apparent non-linearity between BSi_{det} and SPM_{nbld} may originate from a varying BSi content in the SPM along the estuary: the upstream part of the estuary tends indeed to have higher SPM concentrations but lower BSi contents than the seaward part. This may be due to the fact that the SPM in the estuary is composed of material originating from the tidal river and from the coastal zone, which gradually mix along the salinity gradient (Verlaan et al. 1998).

Regression #3:

In order to test the previous hypothesis, the BSi_{det}/SPM_{nbld} ratio (partial coefficient k_2 in Eq. 2.5 in Chapter 2) was allowed to vary linearly along the salinity gradient according to:

$$k_2 = a_2 \cdot S + b_2 \qquad \text{(Eq. 5.1)}$$

with S the salinity, and a_2 and b_2 the partial coefficients to be fitted. The BSi_{liv}/DiatChl*a* ratio was identical to what was found in regression #2 (1.08 ± 0.16 μmol μg^{-1}, *t*-test for equality: p = 0.98) and a_2 and b_2 were respectively 0.0046 ± 0.0035 μmol mg^{-1} and 0.331 ± 0.035 μmol mg^{-1}, indicating that the variation of the BSi_{det}/SPM_{nbld} ratio along the salinity gradient was significant. However, the correlation coefficient (r^2 = 0.820, n = 146) was slightly lower than in the previous regression and, more importantly, residuals plotted against SPM_{nbld} displayed still a concave relationship, similar to that observed after regression #2.

Regression #4:

The "power" relationship presented above is derived from an empirical observation only, and no physical explanation for this relationship was attempted. Nevertheless, as the highest SPM concentrations could be associated with resuspension events, this would imply that, compared to BSi_{det}, SPM_{nbld} would be preferentially resuspended. As a fourth step, a non-linear multiple regression was finally applied on the estuarine dataset:

$$\hat{BSi} = k_1 \cdot \text{DiatChl}a + k_2' \cdot (SPM_{nbld})^c \qquad \text{(Eq. 5.2)}$$

with the coefficients k_1, k_2' and c to be fitted using a step-by-step procedure. Firstly, a linear multiple regression was performed with DiatChl*a* and $(SPM_{nbld})^c$ with the value of c given by the non-linear regression shown in Fig. 5.4. A second estimate of BSi_{liv} was thus obtained as well as a second c coefficient and the procedure was repeated. The value of c converged and varied by less than $2x10^{-5}$ % after the sixth iteration (Fig. 5.5). At that stage, the correlation between the BSi concentrations measured and estimated by the regression was improved (r^2 = 0.867, n = 146), c was equal to 0.674 ± 0.052 (± 95 % confidence interval) and was still significantly different than 1. BSi_{liv}/DiatChl*a* and k_2' were respectively 0.84 ± 0.12 μmol μg^{-1}

and 1.66 ± 0.08 µmol $mg^{-0.674}$ $L^{-0.326}$ (± 95 % confidence interval). This corresponded to a Si/C molar ratio in living diatoms of 0.334 ± 0.049 and, for the range of our SPM dataset, the BSi_{det} content in the residual SPM (see above) ranged from about 2 % to 7 % (decreasing with increasing residual SPM concentrations).

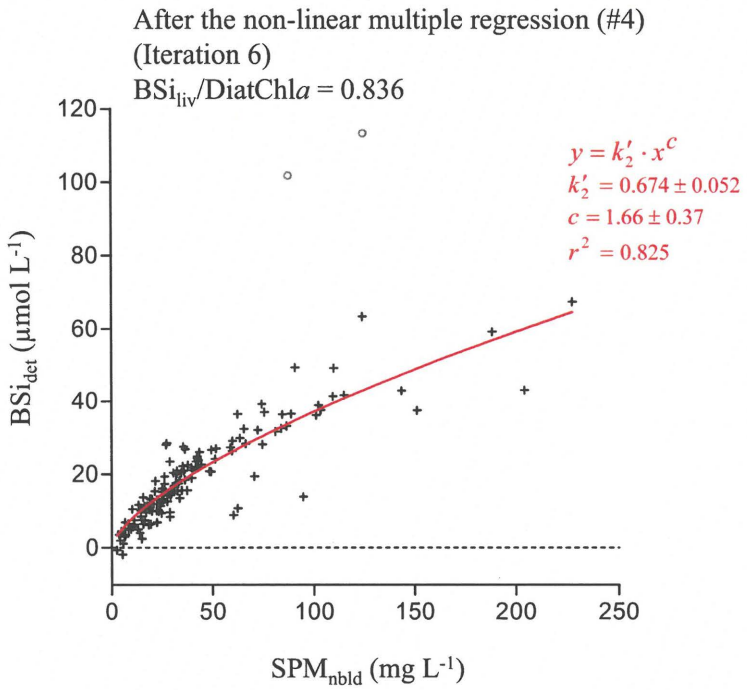

Fig. 5.5: BSi_{det} versus SPM_{nbld} after regression #4 in the estuary.

BSi estimated using the multiple regression and BSi_{liv} and BSi_{det} fractions

The variations in the measured BSi concentrations were very well captured by the multiple regression model in both the estuarine and marine areas, except for the sampling points at the freshwater end-member in September 2004 and July 2005 (Fig. 5.6). The reason why these two outliers were the only data points that did not fit to this regression scheme is unknown. The BSi concentrations recalculated using Eq. 5.2 with the coefficient as determined above or using the linear multiple regression for the tidal river with k_1 and k_2 of respectively 0.67 µmol $µg^{-1}$ and 0.48 µmol mg^{-1} (Chapter 3) provided similar concentrations, about 40-50 % lower than that measured.

In the coastal zone, only the recalculated BSi concentrations at the station #780 in May 2004 deviated significantly from that measured. Except for this sample, the differences between both profiles were not particularly higher in April and May than during the other

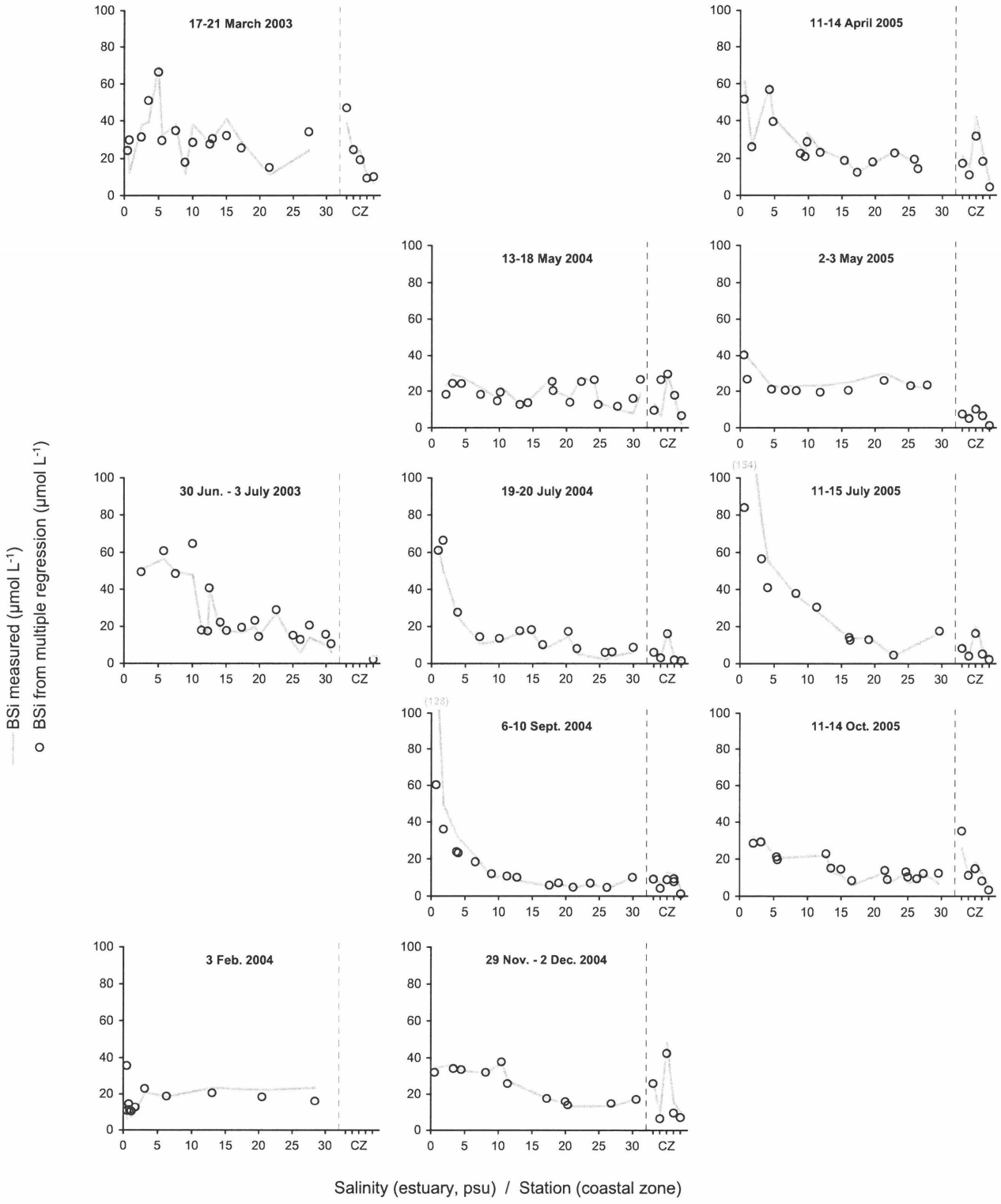

Fig. 5.6: Measured BSi concentrations (grey lines) and those estimated by the multiple regression models (open circles) along the estuarine salinity gradient and in the coastal zone (CZ). For the latter, ticks represent, from left to right, stations #710, #780, #130, #230 and #330. Panels are ordered according to seasons (from top to bottom), then to years (from left to right). The multiple regression was applied assuming that DiatChl*a* concentrations in the estuary were null in February 2004.

campaigns. This may indicate that, even if *Phaeocystis* may have contributed significantly to DiatChl*a* concentrations, their presence did not have a strong effect on the description of the BSi concentrations by the linear multiple regression model.

BSi_{liv}/DiatChl*a* in the estuary was significantly different from that in the coastal zone (*t*-test for equality: p = 0.063) but not from that in the tidal river (Chapter 3, *t*-test for equality: p = 0.511). However, in contrast to what was observed in the tidal river, BSi in the estuary and in the coastal zone was in general under the form of BSi_{det} (Fig. 5.7). Lowest BSi_{liv} contributions were generally found in the zone of salinity 5-15, due to lowest DiatChl*a* concentations (Fig. 5.2). Despite inter-annual variations, BSi_{liv} contributions in the freshwater part of the estuary were negligible in winter, increased to 20-30 % in spring and reached the highest values in July-October (from about 20 to 70 %). In the lower estuary, BSi_{liv} contributions of more than 50 % (and locally reaching 100 %) could be observed in May and July but were low from end summer to early spring. In the coastal zone, BSi_{liv} contributions always increased with distance from the coastline and contributions were only higher than 30 % in March 2003 (only at stations #230 and #330) and in May 2005.

Phytolith contribution

The Scheldt estuary is linked to 24 km² of marshes (Meire et al. 2005), in which reeds can be an important, if not major constituent of the vegetation (Soetaert et al. 2004). Reeds produce high amounts of BSi as phytoliths (Struyf et al. 2005) which may potentially end up in the water of the Scheldt after the plant decay. Indeed, all the reed aboveground biomass is entirely deposited as litter on an annual timescale (Soetaert et al. 2004). However, these

---

Fig. 5.7 (next pagae): BSi_{det} (black lines) and maximum amounts of BSi from phytoliths (grey lines) expressed as the percentage of the measured BSi concentrations along the estuarine salinity gradient and in the coastal zone (CZ). In the coastal zone, ticks represent, from left to right, stations #710, #780, #130, #230 and #330. Panels are ordered according to seasons (from top to bottom), then to years (from left to right).

To calculate the phytolith contributions in February 2004, POC concentrations were estimated using the linear decrease with salinity of the non-diatom POC content in SPM_{nbld} when the phytoplankton contribution to POC was minimal, i.e. in March 2003, November 2004, April 2005 and October 2005 ($y = -0.0835\ x + 5.26$, $r^2 = 0.439$, n = 55).

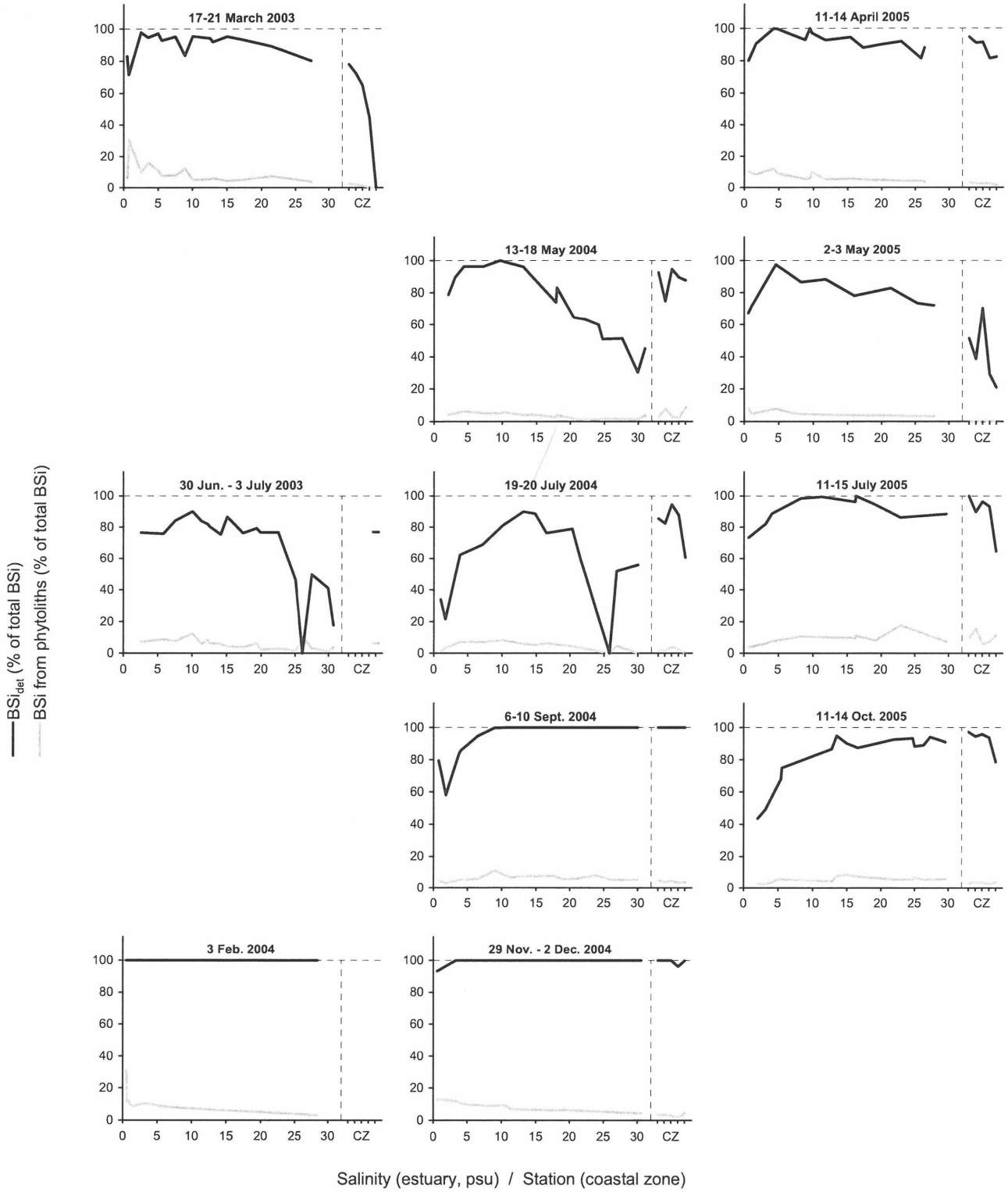
17-21 March 2003
11-14 April 2005
13-18 May 2004
2-3 May 2005
30 Jun. - 3 July 2003
19-20 July 2004
11-15 July 2005
6-10 Sept. 2004
11-14 Oct. 2005
3 Feb. 2004
29 Nov. - 2 Dec. 2004
BSi_det (% of total BSi)
BSi from phytoliths (% of total BSi)
Salinity (estuary, psu) / Station (coastal zone)

marshes do not appear to act as a source but rather as depositional sites for the SPM of the Scheldt (Van Maldegem et al. 1993; Temmerman et al. 2003). Thus, although a BSi exchange is possible between the marsh and the channel at each tidal cycle, BSi is expected to be always net imported to the marsh, as observed for marshes along the tidal river (Chapter 3).

Nevertheless, the estuarine waters carry large quantities of terrestrial material (Abril et al. 2002) and important amounts of phytoliths can be brought by soil erosion to the rivers (Cary et al. 2005). As in the tidal river (Chapter 3), the presence of phytoliths was assumed to be associated with the presence of POC from soil and vegetation, which constitute about 23 % of the non-phytoplankton POC (Abril et al. 2002). Accordingly, the phytoliths distribution in the Scheldt estuary was derived using, as a maximum estimate, the same Si/C molar ratio of 0.05 as in the tidal river (Chapter 3; Struyf et al. 2005).

Highest maximum phytolith contributions to the BSi were predicted at the most freshwater stations in March 2003 and February 2004 (31 %, Fig. 5.7) due to low BSi contents (1 %, Fig. 5.1). Apart from these samples, the phytolith contribution was never higher than 20 % and generally below 10 %. Its decrease along the salinity gradient was attributed to the decrease of the POC content in the SPM (Fig. 5.3), which may be explained by the consumption of the most labile fraction of the POC in the estuary (Abril et al. 2002). As a result, the fraction of POC from vegetation and soil, which can be considered as refractory (Abril et al. 2002; Struyf et al. 2007), may have increased. But still, the major part of the BSi_{det} in the Scheldt could not be possibly attributed to phytoliths, and it could be assumed that phytoliths actually represented only a minor fraction of the BSi in the Scheldt estuary.

5.3 ^{32}Si incorporation experiments

Kinetic experiments of ^{32}Si incorporation were performed at 8 selected stations in the estuary and at station #330 in the coastal zone in April, May and July 2005 (see Chapter 2).

Model for time-course silica uptake

Because ^{32}Si has been made available only recently, a limited number of incorporation experiments have been performed until now. In addition, uptake rates have generally been estimated from single measurements of ^{32}Si incorporation after 24 hours of incubation. Brzezinski and Phillips (1997) and Rousseau et al. (2002) nevertheless performed time-course

experiments with natural and artificial light/dark cycles and observed that the incorporation as a function of time was roughly linear. In our time-course experiments performed under constant light, the kinetics of silica incorporation displayed a significant exponential pattern (Fig. 5.8), in accordance with the model of Brzezinski and Phillips (1997):

$$BSi_{new} = BSi_0 \cdot \left(e^{V \cdot t} - 1\right) \qquad \text{(Eq. 5.3a)}$$

with BSi_{new} the amount of silica incorporated during the incubation time (μmol L^{-1}, see Chapter 2), BSi_0 the biogenic silica at the start of the incubation (μmol L^{-1}), t the duration of the incubation (h) and V the specific silica uptake rate (h^{-1}). This relation is equivalent to the relationship commonly used to estimate specific uptake rates:

$$V = \frac{1}{t} \cdot \ln\left(\frac{BSi_{new} + BSi_0}{BSi_0}\right) \qquad \text{(Eq. 5.3b)}$$

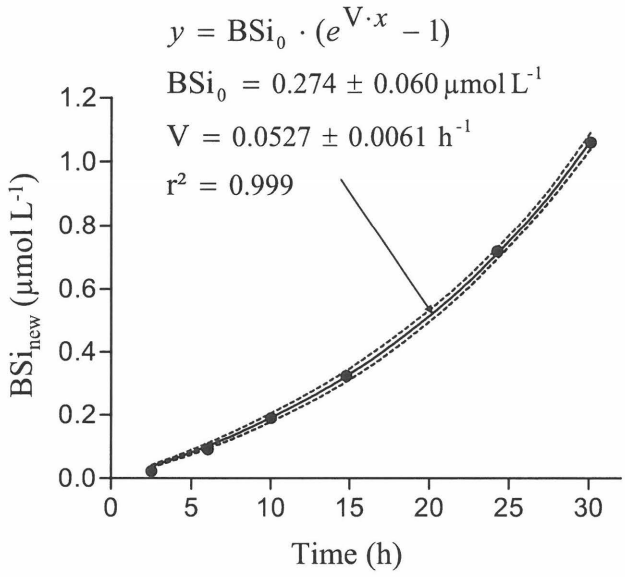

Fig. 5.8: Example of silica uptake during a time-course ^{32}Si incorporation experiment performed at the mouth of the estuary (salinity 29.6) in July 2005. BSi_{new} is calculated following Eq. 2.6 and 2.7 (Chapter 2), and the data are fitted with the exponential incorporation model (Eq. 5.3a) using PRISM 5.01. The dash lines represent the 95 % confidence interval of the regression.

BSi_0 and V (and their 95 % confidence intervals) were estimated by fitting Eq. 5.3a to our data using PRISM 5.01. The validity of the exponential uptake model was confirmed by the fact that correlation coefficients r^2 were higher than 0.98 in all experiments and higher than 0.99 in two third of the experiments, except however for the experiment at salinity 4.8 in

April 2005 which was discarded (Antwerp, km 81, r^2 exponential model of 0.88 in Fig. 5.9). Most of these correlation coefficients were higher than those that would have been obtained by linear regressions (Fig. 5.9). In addition, the linear regressions would have led to negative y-axis intercepts in all experiments (except at salinity 4.8 in April 2005, discarded). The 95 % confidence intervals for V and for BSi_0 determined using the exponential model could be however very broad (see further).

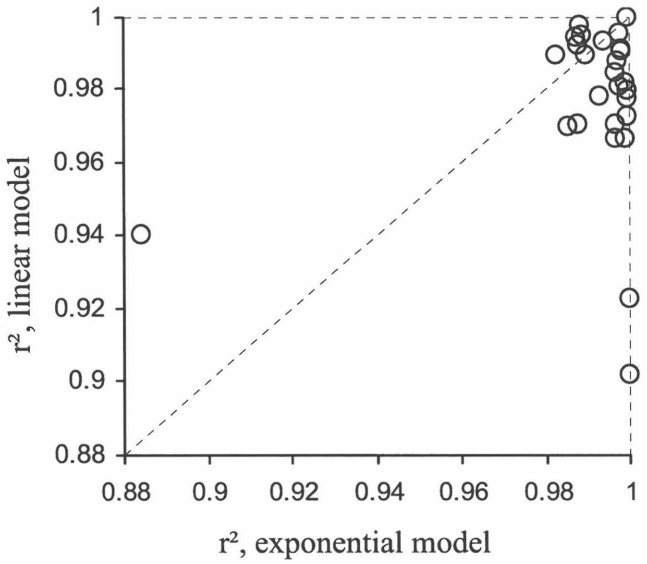

Fig. 5.9: Comparison between the correlation coefficients r^2 obtained by linear or exponential fitting of the BSi_{new} versus time profiles.

DSi addition experiment

For the DSi addition experiment performed at station #330 in July 2005, the specific uptake rates were calculated using Eq. 5.3b, with BSi_0 as calculated for this station during the time-course experiment (0.084 µmol L^{-1}). The data were well fitted by a Michaelis-Menten relationship (Martin-Jézéquel et al. 2000):

$$V = \frac{V_{max} \cdot DSi}{K_s + DSi} \qquad \text{(Eq. 5.4)}$$

with DSi the average of the initial and final DSi concentrations (the latter being estimated from the amount of incorporated ^{32}Si), V_{max} the theoretical specific uptake rate at infinite DSi concentration and K_s the half-saturation constant. V_{max} and K_s were determined by least-

square regression using PRISM 5.01, which provided also 95 % confidence intervals (Fig. 5.10). The correlation coefficient was equal to 0.889, and V_{max} and K_s were respectively equal to 0.0533 ± 0.0046 h^{-1} and 0.54 ± 0.28 µmol L^{-1}. V_{max} was in the range of the specific uptake rates measured during the other campaigns or at other stations with non-limiting DSi concentrations (see further). K_s was in the range of what has typically been measured in natural environments (from 0.5 to 5 µmol L^{-1}, e.g. Nelson and Brzezinski 1990; Nelson and Dortch 1996; Brzezinski et al. 1997; Kristiansen et al. 2000; Leynaert et al. 2001; Ragueneau et al. 2002a), although in the lower range. This might have been due to the adaptation of the diatom community may to the low DSi concentrations that prevailed since April-May (Chapter 4; Rousseau et al. 2002; Van der Zee and Chou 2005). The specific uptake rate at station #330 in July 2005 was thus only slightly, potentially limited.

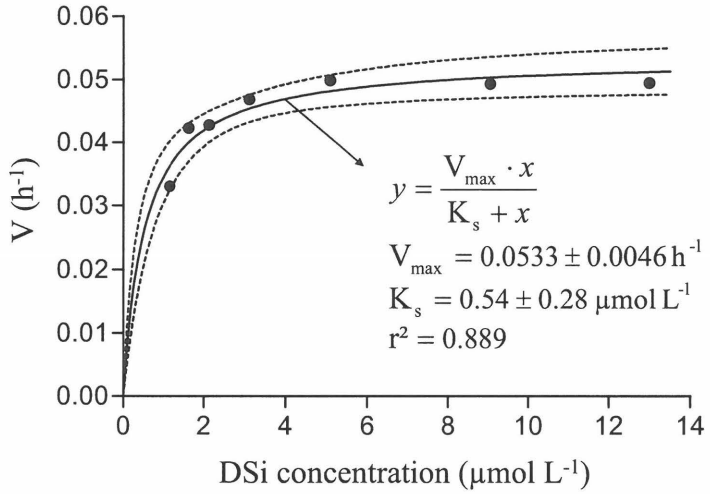

Fig. 5.10: Specific uptake rates versus the average of the initial and final DSi concentrations at the marine station #330 in July 2005. The data are fitted with a Michaelis-Menten relationship using PRISM 5.01. The dashed lines represent the 95 % confidence interval of the regression.

BSi associated with growing diatoms

BSi_0 and V were estimated in water pre-filtrated on a 400 µm mesh to prevent the presence of zooplankton in the incubation experiments. One may argue that such a pre-filtration could also retain SPM aggregates and the associated diatoms, such as the large ones frequently observed in the waters of the Scheldt (*Rhizosolenia* sp., *Odontella* sp. or *Ditylum brightwellii*) or those forming chains (*Skeletonema costatum* or *Chaetoceros* sp.). However, the pre-filtration did not induce lower DiatChl*a* concentrations, nor did it alter the DiatChl*a*/Chl*a* ratio, except at the marine station (and in the lower part of the estuary in July

2005) where the pre-filtration preferentially retained diatoms during the three campaigns (Fig. 5.11a). The differences observed in April 2005 between salinities 10 and 15 were attributed to the poor analytical precision at low Chl*a* and DiatChl*a* concentrations. Assuming that the composition of the diatom community was not significantly modified by the pre-filtration, the specific uptake rates measured in the pre-filtered water were expected to be identical to that in the non pre-filtered one. Similarly, BSi_{liv}/DiatChl*a* ratios previously estimated should also apply to the pre-filtered water and, with the measured DiatChl*a* concentrations in the pre-filtered samples, BSi_{liv} concentrations in the pre-filtered water could be determined. When comparing these concentrations with those of BSi_0, some deviations were admittedly observed. But considering the large confidence intervals in the determination of BSi_0 and above all the fact that the two methods were completely different, the similarities between BSi_0 and BSi_{liv} patterns were striking, especially when they were both compared to the total amount of BSi (Fig. 5.11b). This supported the above estimations of the BSi_{liv} concentrations in the estuary.

Specific silica uptake rates

The specific silica uptake rates varied between 0.02 and 0.1 h^{-1} (Fig. 5.11c). Highest uptake rates tended to occur around salinities 5-15, with a decreasing trend towards the sea in May 2005 while a local maximum was observed at the mouth of the estuary in April and July 2005. However, these patterns have to be taken with care considering the broad 95 % confidence intervals. The low specific uptake rate in the coastal zone in May could be due to

Fig. 5.11 (next page):

a. DiatChl*a* concentrations and DiatChl*a* contributions to Chl*a* in pre-filtered and non pre-filtered samples at selected stations in the estuary and at the marine station #330.

b. BSi_0 concentrations (in pre-filtered samples) estimated from the best-fit of Eq. 5.3a with error bars indicating the 95 % confidence intervals. BSi_{liv} concentrations in the pre-filtered water (estimated from DiatChl*a* concentrations in the pre-filtered water and the BSi_{liv}/DiatChl*a* ratios in the non pre-filtered water), as well as total BSi concentrations in the non pre-flitered water are also indicated. The stations are the same as those in panel a. Note the same data are represented in the upper and lower graphs of panel c, but with different scales.

c. Specific uptake rates and 95 % confidence intervals obtained by the best-fit of Eq. 5.3a. The stations are the same as those in panel a.

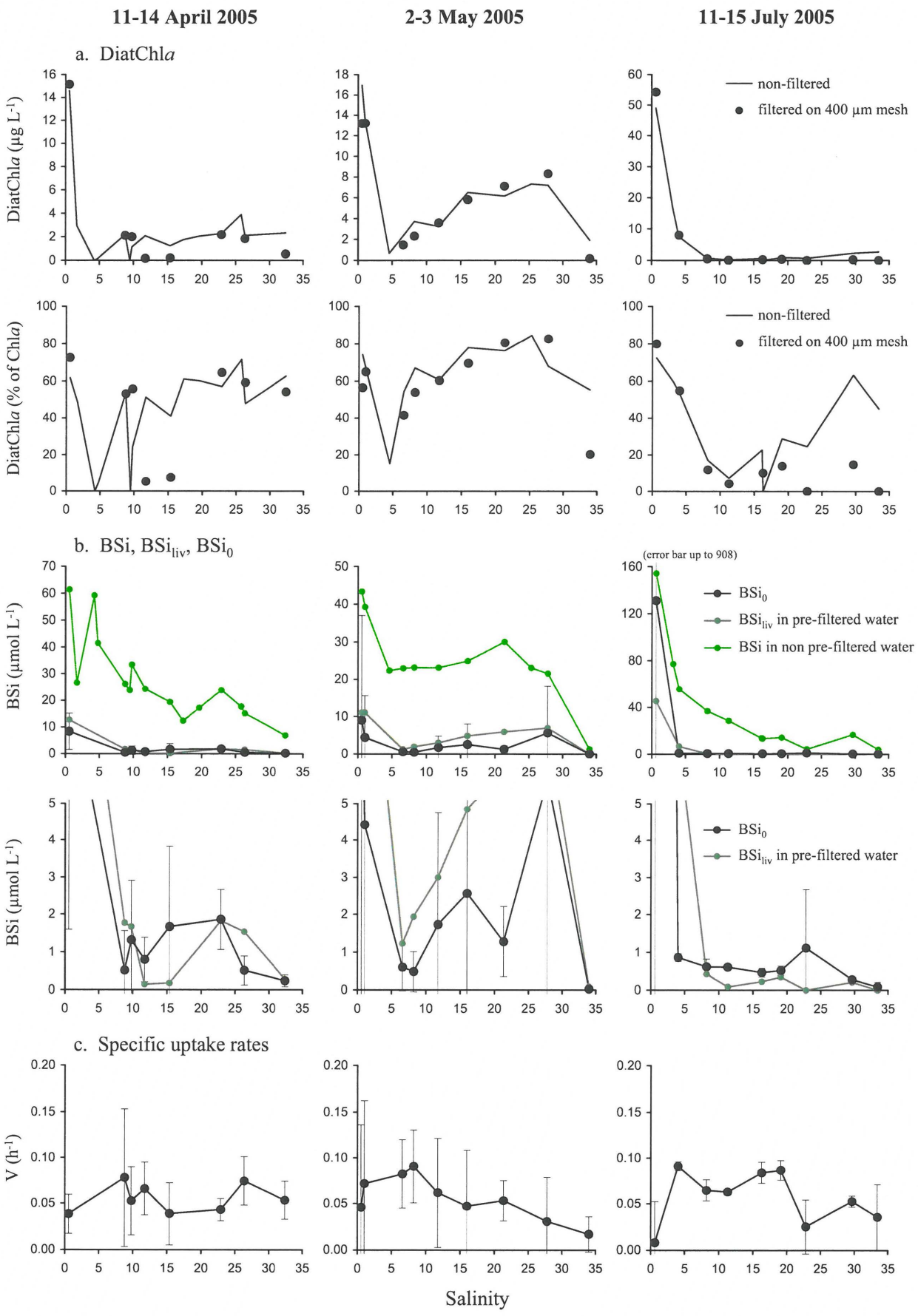
11-14 April 2005
2-3 May 2005
11-15 July 2005
a. DiatChla
DiatChla (µg L-1)
non-filtered
filtered on 400 µm mesh
DiatChla (% of Chla)
non-filtered
filtered on 400 µm mesh
b. BSi, BSiliv, BSi0
BSi (µmol L-1)
(error bar up to 908)
BSi0
BSiliv in pre-filtered water
BSi in non pre-filtered water
BSi (µmol L-1)
BSi0
BSiliv in pre-filtered water
c. Specific uptake rates
V (h-1)
Salinity

DSi limitation: the DSi concentrations were 0.2 µmol L^{-1} (Chapter 4) while the DSi addition experiment yielded a half-saturation constant of 0.54 ± 0.28 µmol L^{-1} (Fig. 5.10). Surprisingly, the lowest specific silica uptake rate (0.008 h^{-1}) was measured in July 2005 in the most upstream station (Fig. 5.11c) while the DiatChl*a* was at its highest level (Fig. 5.2), but the associated 95 % confidence interval was large: values up to 0.05 h^{-1} would also be included in this interval. When BSi_0 was forced to be equal to BSi_{liv} in Eq. 5.3a (41.0 µmol L^{-1}), a good fit was still obtained ($r^2 = 0.979$, n = 6) and V amounted to 0.022 ± 0.002 h^{-1}, which is still low but in the range of the other measurements.

Our specific uptake rates are in the range of those measured in diatom cultures (Conway and Harrison 1977; Martin-Jézéquel et al. 2000; Claquin and Martin-Jézéquel 2005). In the natural environment, although Ragueneau et al. (2002a) measured rates up to 0.15 h^{-1} (in non-limiting DSi conditions during a DSi addition experiment) in a coastal diatom bloom dominated by the fast growing *Chaeotoceros* sp., specific uptake rates generally remained lower than 0.05 h^{-1}, including in productive zones such as estuarine plumes, coastal or upwelling zones, and that even at non-limiting DSi concentrations (e.g. Nelson and Brzezinski 1990; Nelson and Dortch 1996; Brzezinski et al. 1997; Kristiansen et al. 2000; Leynaert et al. 2001; Ragueneau et al. 2002b). In those studies however, the specific uptake rates were calculated using ambient BSi concentrations and only one measurement of ^{32}Si (or ^{30}Si) incorporation per water sample (no time-course experiments). The presence of detrital BSi would thus result in an underestimation of the specific uptake rates (Nelson and Brzezinski 1990; Leynaert et al. 2001). In our experiment, such bias was avoided by the time-course methodology: BSi_0 was obtained fitting Eq. 5.3a. Further comparison between our rates and those published could not be attempted as all rates were measured under different light conditions (artificial or natural, different intensities and light/dark cycles).

In contrast, using the same light conditions (continuous exposure at 120-150 µmol quanta m^{-2} s^{-1}) for all incorporation experiments allowed us to compare uptake rates obtained at different times and/or places. The rates reflected the ability of the diatoms to grow under this fixed irradiance and thus provided a comparative estimate of the physiological status of the diatoms. However, they did not represent the *in situ* uptake rates prevailing in the Scheldt. The latter would actually be impossible to measure under a single, constant irradiance, due to the strong vertical light gradient and the vertical mixing in the Scheldt, which imply that diatoms are be exposed to strongly varying light conditions at a short time-scale. In addition, silica and carbon uptake by diatoms are uncoupled and diatoms may uptake silica in the dark:

diatoms may constitute internal pools of dissolved silica, so that silica uptake does not depend directly on the light availability but primarily on the cell cycle (Claquin and Martin-Jézéquel 2005).

In the Scheldt, despite important variations in the DiatChl*a* concentrations along the salinity gradient in April, May and July 2005, the specific uptake rate did not differ significantly from one campaign to another, suggesting that diatoms were in similar physiological status in April, May and July 2005. Dijkman and Kromkamp (2006) observed that diatoms were all in good physiological condition along the entire salinity gradient in May 2005, hypothesizing that unhealthy cells were quickly removed from the water column. In our data, a healthy state could also be assumed for salinities higher than 15 in May 2005 as diatoms were blooming, so that diatoms that grew during the incubations in April and July 2005 were also considered to be in good health even if they were in low concentrations. This was also supported by the facts that diatom growth was in the exponential phase during the incubations (Fig. 5.8). In addition, the measured specific uptake rates were among the highest ones observed in cultures or in the natural environment. The good physiological status is not surprising for April 2005, as this date could correspond to the beginning of the spring diatom growth (Chapter 4). However, the DiatChl*a* concentrations were also lower in July 2005 than in May 2005. This could have been interpreted as diatom senescence, but the fact that the uptake rates did not change from May to July 2005 supports the contrary. The grazing pressure may be a clue to this paradox (see further).

5.4 SPM and phytoplankton dynamics: implications for BSi behaviour

Phytoplankton mortality in the zone of turbidity maximum

As shown by the high BSi_{liv} fraction, the supply to the estuary of the high living diatom biomass blooming in the tidal river in summer contributed significantly to the highest BSi concentrations, which were observed in the upstream stations in summer and early autumn (Figs. 5.1, 5.2 and 5.7). However, the high diatom concentrations quickly dropped in the upper estuary (Fig. 5.2). It has been suggested that the phytoplankton mortality in the zone of salinity 0-10 was due to osmotic stress (Muylaert et al. 2000). Lionard et al. (2005) observed a decline in growth rates when the phytoplankton from the Scheldt tidal river was incubated in brackish estuarine water, but these authors also observed that osmotic stress could not be the only explanation. When isolated from the Scheldt tidal river and grown in

batch at various salinities, *Cyclotella meneghiniana* (the diatom species blooming in summer in the tidal river, Muylaert et al. 2000) even showed a good tolerance to salinity with a growth optimum at salinity about 18 (Roubeix and Lancelot 2008). Nevertheless, these species rapidly declined in the Scheldt estuary from salinity 5 onwards, to be replaced by marine or brackish species (Rijstenbil et al. 1993, Muylaert et al. 2000).

The phytoplankton decline in the zone of salinity 0-10 could also be due to light limitation (Soetaert et al. 1994, Lionard et al. 2005). Compared to the tidal river, the mean water depth is deeper in the upstream part of the brackish estuary and the turbidity increases (Lionard et al. 2005, Chen et al. 2005). Due to the hydrodynamic processes leading to the formation of a turbidity maximum, particles are retained in this zone (Chen et al. 2005) and the residence time of the phytoplankton in this light-poor area is therefore expected to be much higher than in other regions of the estuary.

Impact of grazing on phytoplankton dynamics

Ecosystem model simulations suggested that grazing by the copepod-dominated zooplankton community might control the phytoplankton biomass in the Scheldt estuary (Soetaert and Van Rijswijk 1993; Soetaert et al. 1994).

In addition to osmotic stress and light limitation, grazing may also contribute to the large drop of the phytoplankton biomass in the upper part of the estuary during summer and autumn. In the early nineties, rotifers were the dominating zooplankton species within the turbidity maximum (Soetaert and Van Rijswijk 1993; Tackx et al. 2004). Rotifers are still the dominating zooplankton community in the tidal river (Tackx et al. 2005), where they obviously cannot control the phytoplankton community, as shown by the high biomass reached by the phytoplankton (Muylaert et al. 2000; Lionard 2006). However, the oxygen content has increased since the nineties in the uppermost part of the brackish estuary due to enhancement of the water quality (Kromkamp and Peene 2005; Soetaert et al. 2006). As a consequence, the calanoid copepod *Eurytemora affinis*, which dominates the copepod community in terms of biomass in the Scheldt estuary (Soetaert and Van Rijswijk 1993), is now observed near Antwerp at salinities 0-5 (Appeltans et al. 2003). This copepod reaches its maximum abundance in early spring and it is followed by the copepod *Arcatia tonsa* in summer and early autumn (Soetaert and Van Rijswijk 1993).

Downstream of salinity 15, the copepod biomass remains low in spring but a high biomass of copepods originating from the coastal zone is observed in summer and autumn

(Soetaert and Van Rijswijk 1993). These dynamics could explain why, while phytoplankton developed in May in the lower part of the estuary, its biomass decreased in summer and early autumn despite nutrients availability and comparable light climates at least in May and July (Chl*a*: Fig. 5.2; light climate: IRMB 2003-2005; dissolved silicate: Fig. 4.1 in Chapter 4; nitrogen and phosphorus: Van der Zee and Chou 2007). This is also supported by the fact that the diatom community in July 2005 did not appear to be senescent: the physiological status of the diatoms in July 2005 was similar to that in May 2005 (see above), and Dijkman and Kromkamp (2006) observed that diatoms were in a good state in May 2005.

BSi dynamics in the zone of turbidity maximum: parallelism with those of SPM

Even when the BSi_{liv} fraction was not important, highest BSi concentrations were generally observed in the zone of salinity 0-10, associated to a turbidity maximum in the upper part of the estuary. However, this turbidity maximum was clearly seen only in half of our campaigns (March and July 2003, September and November 2004, and April and July 2005, Fig. 5.1) due to the complex spatial and temporal variations in the SPM concentrations: longitudinal as well as lateral gradients, short-term, periodic (ebb-flood or spring-neap cycles) as well as aperiodic (high discharge events) (Fettweis et al. 1998; Chen et al. 2005).

In the turbidity maximum, SPM (and thus BSi) concentrations are driven by settling and resuspension processes: SPM settles at slack water but is resuspended during ebb and/or flood (Fettweis et al. 1998, Chen et al. 2005). As a general rule, SPM increases with current velocity once a threshold (critical erosion velocity) of 0.56 m s^{-1} is exceeded, but phenomena such as scour-lag and settling-lag induce hysteresis patterns (Chen et al. 2005). The extent of the SPM resuspension during flood and ebb and of the hysteresis patterns also depends on the local morphology of the bed and on the amount of bottom material available for resuspension (Chen et al. 2005). This intense exchange of material between the water column and the sediments could explain why the BSi was mostly as BSi_{det} and the BSi content in the SPM was always below 4 % at salinities 5-10, while just upstream of this zone, in the less saline stations, BSi was mostly as BSi_{liv} and much higher contents were observed (e.g. July 2004, Figs. 5.1 and 5.7). Vertical gradients in SPM concentrations are also present (Chen et al. 2005), but the vertical variability in BSi concentrations could not be verified as only surface samples were taken.

Variability in SPM concentrations can also be observed at longer time-scales: SPM concentrations are generally higher during spring tides than during neap tides (by a factor 1.3-

1.7) and the seasonal variation of the freshwater discharge induces higher SPM concentrations in winter than in summer and a shift of the position of the turbidity maximum (comprised between km 110 during dry periods and km 50 during peak freshwater discharges) (Fettweis et al. 1998). Such variability associated with hydrodynamic forcing is also expected for BSi but advection of high amounts of BSi from the tidal river will add a supplementary contribution in the zone of salinity 0-10. In our data, no simple seasonal variation in BSi concentrations could be observed in this zone as they were presumably masked by the important short-term (tidal) variations.

SPM dynamics downstream the turbidity maximum

Downstream of the turbidity maximum, SPM concentrations did not display any significant variability within a tidal cycle (Chen et al. 2005) and seasonal variations could be observed: highest average SPM concentrations were found in winter and spring (Fig. 5.1). The same seasonal pattern was observed for BSi (Fig. 5.1). This variation was mainly due to that of BSi_{det} associated with SPM as, except for May 2004 in the most seaward part of the estuary, the contribution of BSi_{liv} was small (Fig. 5.7).

In this area, corresponding to the Dutch part of the Scheldt estuary (salinities higher than 10), tidal flats and shallow waters represent a large fraction of the total surface area of the Scheldt (respectively 19 and 10 %, Meire et al. 2005) and resuspension of SPM from tidal flats may occur due to wind-induced waves, leading to significant increases in SPM concentrations above the tidal flats and in the channel (de Jonge and van Beusekom 1995). De Jonge and van Beusekom (1995) also reported that the microphytobenthos was resuspended together with the SPM with increasing wind speed. However, the link between the SPM concentrations and the wind speed was not observed at our seasonal timescale: in particular, the weather appeared to be windier during the campaigns in July than during those in May (not shown), while SPM concentrations were lower in July than in May. Nevertheless, in addition to the grazing pressure, the settling of the phytoplankton with the SPM might have contributed to the low biomass observed in July, as the Chl*a* content of the SPM in July was not significantly lower than that in May (Figs. 5.1 and 5.2).

An important feature of the SPM dynamics in the lower part of the Scheldt is that this section of the estuary hosts a net upstream transport of particulate material (Chen et al. 2005). Van Maldegem et al. (1993) also observed a net import of mud from the coastal zone into the estuary. The SPM along the salinity gradient is thus a mix between SPM from riverine and

marine origins: at the confluence with the Rupel, the SPM is only of riverine origin, this fraction progressively decreases with increasing salinity down to the mouth of the estuary where the SPM is almost entirely of marine origin (Verlaan et al. 1998). The local turbidity maximum situated in the coastal zone (Van Alphen 1990; Fettweis and Van den Eynde 2003; Chen et al. 2005) may be the source of this SPM of marine origin. As a result, SPM from both the tidal river and the coastal zone accumulates in the Scheldt, and deposits preferentially in low currents area such as marshes, tidal flats and harbours and their access channels (Van Maldegem et al. 1993; Verlaan et al. 1997; Salden et al. 1998; Wartel et al. 2007). The link between SPM and BSi suggests that BSi also follows such behaviour. Those complex dynamics imply that the methods for estimating fluxes as applied in the tidal river or for dissolved species such as DSi in the estuary are not applicable for particulate material in the estuary, but the link between BSi and the well-studied SPM will now be used to derive a BSi mass-balance from an existing SPM budget in the Scheldt estuary.

5.5 Mud and BSi mass-balances in the Scheldt estuary

Mud is the fraction of the SPM with a granulometric size smaller than 63 μm. It contributes for about 90 % of the SPM (Verlaan et al. 1998; Chen et al. 2005), so that its dynamics were assumed to be a good estimation of those of the SPM. Mud dynamics have been extensively studied in the Scheldt estuary, as it carries the major part of adsorbed contaminants (heavy metals for instance) (Verlaan et al. 1998). Mud dynamics were also investigated because regular dredging of the accumulated mud is needed to ensure the access to the harbour of Antwerp (Verlaan et al. 1997; Wartel et al. 2007). The dredging activity also allowed the removal of old contaminated sediments from the estuary as, from 1990 onwards, no dredged material was dumped anymore in the channel, but deposited on land or in deep water areas in harbours (Verlaan et al. 1997). Several mud budgets have been established for the Scheldt estuary since the early nineties, in particular by Van Eck (1991), Van Maldegem et al. (1993), Vereeke (1994), Verlaan et al. (1997) and Salden et al. (1998). Others estimations were also performed but their results were mostly reported and/or incorporated in these studies (for instance studies by W.B.M. ten Brinke and J. Claessens were incorporated in Vereeke 1994). Wartel et al. (2007) also proposed more recently a mud balance for the Belgian part of the estuary.

These mud budgets differ from each other in terms of their methodology and the extent of the area studied, but unfortunately also in terms of results, such as for instance the amount of mud deposited or transported in the different parts of the estuary (Annex 5A). Although based on data from the early nineties, the budget from Vereeke (1994), which is an update of that of Van Maldegem et al. (1993) with newer data, was assumed to provide the best representation of the current mud balance in the estuary (Annex 5A).

Mud mass-balance proposed by Vereeke (1994)

The last two cited authors divided the entire brackish estuary into 14 compartments, of which the first 5 ones corresponded to the Belgian part of the estuary (Fig. 5.12; Van Maldegem et al. 1993; Vereeke 1994). For each compartment, mud mass-balances were performed, based on the deposition/erosion in the main channel and sandbars (estimated from comparisons of bottom maps), and the deposition in marshes and mudflats (from existing sedimentation rates). Lateral inflows and/or exports, amount of dredged and/or dumped material, measured SPM concentrations and riverine mud content in the sediments were also taken into account. The marine mud inflow at the mouth of the estuary, the least constrained parameter, was set as the closing term.

In the Belgian part of the estuary, mud was only withdrawn through lateral export (to the harbour of Antwerp) and by dredging of the mud accumulated in the access channels to the locks but, in the Dutch part of the estuary, mud dynamics were driven by the balance between natural erosion and deposition (Fig. 5.12). Mud deposition occurred principally in mudflats (compartments 7-8 and 14) and in the marsh of Saeftinge (compartments 7-8) but also in the channel (compartment 11); the important mud deposition in mudflats of compartment 14 and the erosion in the main channel and mudflats in compartment 13 induce a large local decrease of the mud transport between the compartments 13 and 14 (Fig. 5.12). Little mud was deposited or eroded in sandbars, in accordance with the fact that sediments in sandbars are mainly sandy (Van Maldegem et al. 1993).

As described in Van Alphen (1990), Van Eck et al. (1991), Van Maldegem et al. (1993) and earlier studies reported in Van Maldegem (1993), mass balance calculations indicate a significant net landwards transport of marine mud at the mouth of the estuary, with nearly as much marine as riverine mud net-imported to the estuary (Fig. 5.12). This can be explained by the residual bottom currents that are directed landwards in the marine part of the estuary (e.g. Baeyens et al. 1998). Both fractions settle within the Scheldt estuary. The

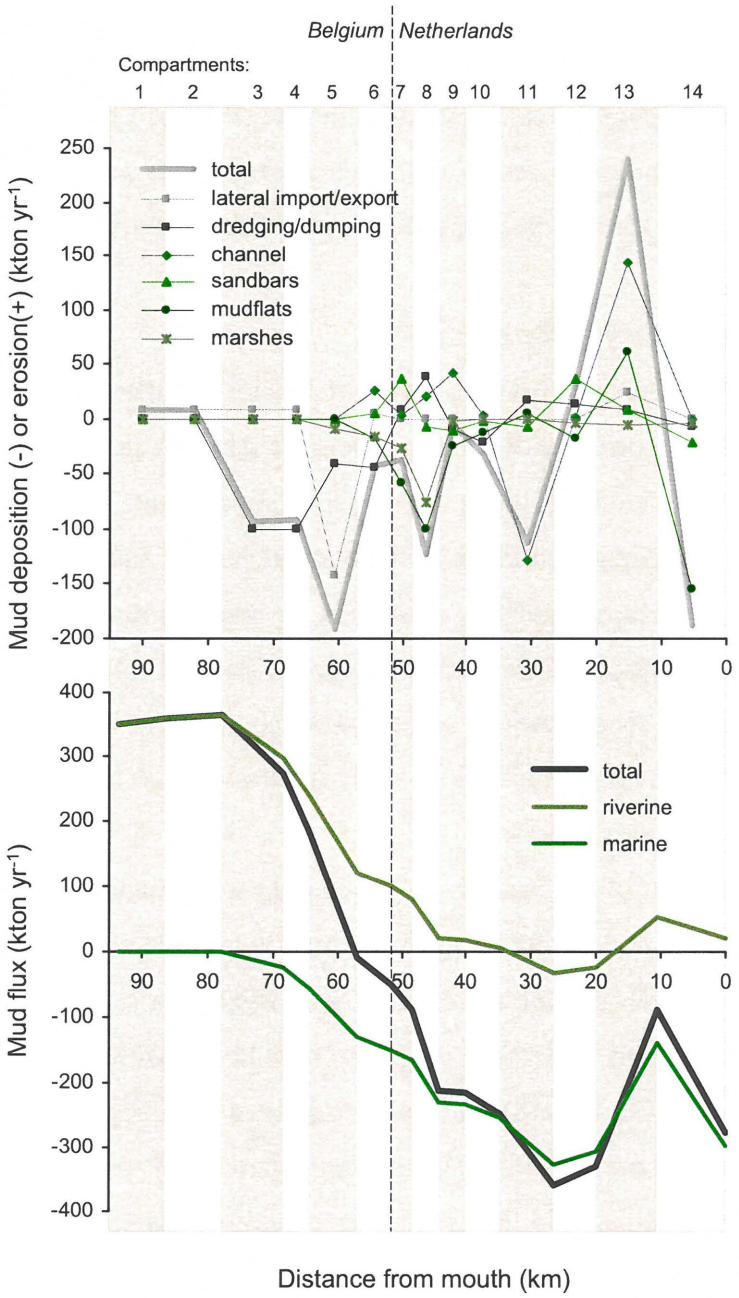

Fig. 5.12: The 14-compartment mud budget established by Vereeke (1994) for the Scheldt estuary:
upper graph: mud sources and sinks in the 14 compartments. Positive values indicate sources of mud to the water column.
lower graph: riverine, marine and total mud fluxes at the compartment boundaries. Positive values indicate fluxes directed seawards.

riverine mud entirely settles in compartments 3-8 and very little riverine mud is exported to the North Sea, which is in accordance with Verlaan (1998) who observed that the marine mud fraction accounted for more than 80 % in the water downstream km 50 in the mid nineties. All the marine mud also settles within the estuary, one third of it in the Belgian part of the estuary. Therefore, no significant amounts of marine mud go further than the limit of the salt intrusion, as observed by Verlaan et al. (1998) and Verlaan (1998). Overall, 627 kton of mud are deposited yearly in the Scheldt estuary. Assuming that the transport of BSi follows that of the mud, it appears that BSi is net imported from the coastal zone at the mouth of the estuary and that the estuary acts as a net sink for BSi of both riverine and marine origin. A quantification of these processes will be established in the following sections.

BSi as a constituent of the mud fraction

In the freshwater part of the estuary, the diatom community is dominated by small-sized diatom species (size of a few tens of micrometres), so that the BSi produced by these species is a part of the mud fraction. Downstream of the turbidity maximum area, the diatom community is also composed of small diatoms (such as *Skeletonema* sp. and *Thalassiosira* sp.) but also of larger ones (such as *Ditylum brightwellii*, *Rhisosolenia* sp., *Odontella* sp. or *Coscinodiscus* sp. whose sizes are in the order of 100 µm) (Rijstenbil et al. 1993; Muylaert and Sabbe 1999; Boschker et al. 2005; Brochard et al. 2005). Nevertheless, most of the BSi in the Scheldt estuary was described as detrital material and, although this was not verified microscopically, a large part of this BSi from large frustules was assumed to be broken pieces. Finally, although they are not expected to contribute significantly to the BSi pool, the sizes of phytoliths range from one to several tens of micrometers (Alexandre et al. 1997). BSi was thus assumed to be mostly included in the mud fraction of the SPM along the entire salinity gradient.

Annual average BSi content

In order to convert mud budget results from Vereeke (1994) into a BSi budget using the BSi contents measured during our campaigns, an annual average BSi content was needed for each compartment boundary.

Average BSi content at each compartment boundary for each campaign:

For this purpose, BSi profiles in the estuary were now plotted against the distance from the mouth of the estuary, not against salinity (Fig. 5.12). As sampling was performed

irrespective the tide phase, the average position of the sampled water parcels during the sampling periods were estimated from model simulations of the salinity using the CONTRASTE model (Chapter 4). For each campaign, all measured BSi contents were assigned to their closest compartment boundary, and averaged. If no BSi content was measured close to a boundary, the average BSi content at this boundary was calculated by linear interpolation between the next upstream and downstream boundaries. The BSi contents assigned to the upstream boundary of compartment 1 (km 94) corresponded to those measured at the most upstream stations, and if no measurement of the BSi content was performed downstream km 5, the BSi content assigned was that of the most seaward measurement.

Weighted annual average:

The BSi contents of each campaign were lumped into four distinct periods: late autumn - winter (November to February, 4 months), early spring (March April, 2 months), late spring (May June, 2 months) and summer - early autumn (July to October, 4 months). The annual average BSi content was finally calculated as the weighted average taking into account the number of months for each period, as well as a coefficient reflecting the seasonal variation of the mud influx from the freshwater and of the mud concentrations in the estuary: mud concentrations are two times higher in winter than in summer (Van Maldegem et al. 1993; Fettweis et al. 1998), and the higher winter discharge induces higher riverine mud fluxes. However, as the riverine mud fluxes decrease along the Belgian part of the estuary and become negligible downstream km 50 (Fig. 5.12), the discharge coefficient (corresponding to the mean discharge during the period) was only applied fully at the upstream boundary of the compartment 1, with a linearly decreasing pattern towards the mouth until km 50, and no discharge correction was applied downstream km 50. The same weighting procedure, applied on minimum and maximum contents measured during each of the four periods, provided respectively minimum and maximum annual average BSi contents (Fig. 5.13).

Longitudinal profile of the annual average BSi content:

The average, weighted BSi content displayed a local maxima at 3.3 % in the less saline part of the estuary and another one at 3.8 % around km 20 (Fig. 5.13). In between, there was a clear minimum at km 72 with a BSi content of 2.6 %. The BSi_{liv} content was several times lower than that of BSi_{det} and, in average, BSi_{liv} did not exceed 20 % of the total BSi content in the estuary: it was highest in the upstream part of the estuary, dropped to less than 4 % between km 50 and km 70 and reached 11-14 % in the last 40 km before the mouth. Even so, most of the variations in the total BSi content along the estuary could be attributed to the

BSi_{liv} content and the BSi_{det} content increased almost regularly from the freshwater end-member to the seawater end-member (Fig. 5.13), which is in agreement with the fact that the SPM in the Scheldt is composed of a gradual mix of material originating form the freshwater and seawater end-members (Verlaan et al. 1998).

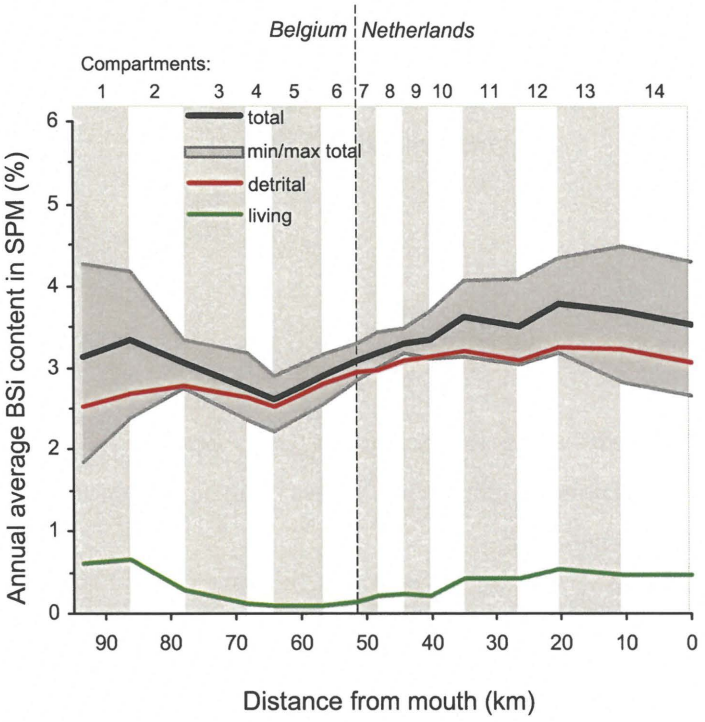

Fig. 5.13: Annual average BSi contents at the compartment boundaries. Minimum and maximum annual BSi contents (see text) are also indicated, as well as annual average BSi_{liv} and BSi_{det} contents.

BSi fluxes along the estuary

The mud fluxes from Vereeke (1994) (Fig. 5.12) were multiplied by the weighted average BSi contents (Fig. 5.13) to estimate BSi fluxes at each compartment boundary along the estuary (Fig. 5.14). Rigorously, this methodology should apply only to BSi_{det}, the fraction of BSi that, to the contrary to BSi_{liv}, followed the SPM dynamics, but the total BSi content was nevertheless used as fluxes of living diatoms were unknown and as the contribution of BSi_{liv} to the total BSi was small in terms of concentrations. As the BSi content did not strongly vary along the estuary, BSi fluxes mirrored the mud fluxes (Fig. 5.12 and 5.14). There was about as much BSi imported from the coastal zone (165 Mmol yr^{-1}) as that brought by the tidal river (184 Mmol yr^{-1}).

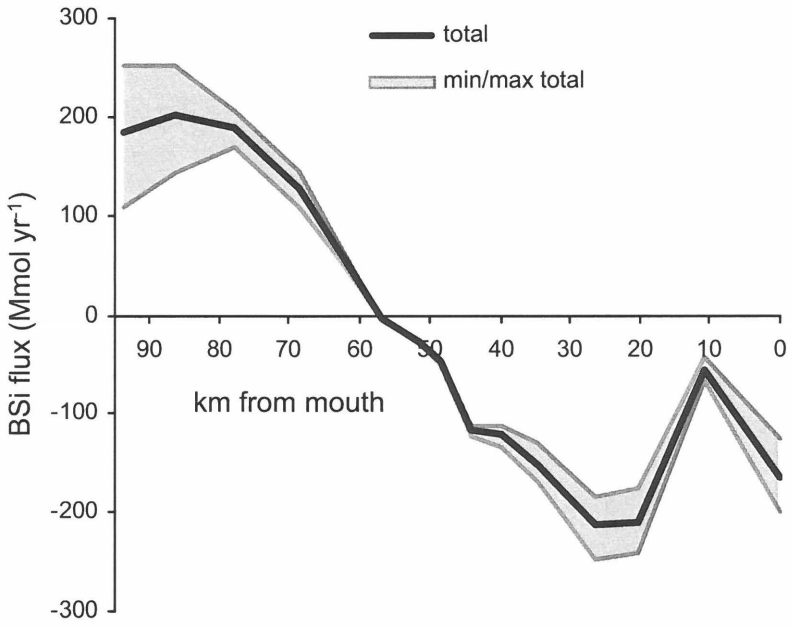

Fig. 5.14: annual BSi fluxes along the Scheldt estuary. Positive values indicate fluxes directed seawards. Minimum and maximum annual BSi fluxes estimated from minimum and maximum BSi contents (Fig. 5.13) are also indicated

The amount of marine BSi imported to the estuary at the mouth was determined as the closing term of the mud balance and there exists no other estimation to which it could be compared. Yet a net import of BSi is in accordance with the fact that BSi content is in general higher in the coastal zone than in the lower part of the estuary (Fig. 5.1): the BSi content should be higher at incoming tides than during outgoing ones, so if the tide oscillations result in net mud import to the estuary, this should also be the case for BSi. At the freshwater end-member, the BSi flux was twice higher than that directly estimated for the year 2003 (80 Mmol yr^{-1}, see Table 3.2 in Chapter 3), but this could be explained by two factors: in addition to the flux weighted average BSi content (2.65 %) being lower in 2003 than that shown in Fig. 5.13, the annual flux of riverine SPM at Hemiksem amounted to 199 kton yr^{-1} (calculated from 7 Feb. 2003 to 6 Feb. 2004 using the same procedure as for BSi in Chapter 3). This latter amount is significantly lower than in the average situation described in the mud budget from Vereeke (1994). The amount of mud discharged to the brackish estuary displays indeed large inter-annual variations: between 1992 and 2002, it varied within a factor 4.5 (Wartel et al. 2007). During this period, it averaged to 348 kton yr^{-1}, which is in accordance with the value used by Vereeke (1994) (Fig. 5.12). Also, the annual riverine mud fluxes correlated well with the annual discharge, leading to a discharge weighted average mud concentration in the

freshwater input of 81.4 ± 8.4 mg L^{-1} (± 95 % confidence interval, $r^2 = 0.75$, n = 11, negligible intercept at a 95 % confidence level, data from Wartel et al. 2007). The freshwater discharge averaged 100 m^3 s^{-1} during our study period (2003-2005) and with such an average mud concentration, the riverine mud and BSi inflows would respectively amount to 258 ± 26 kton yr^{-1} and 123 ± 13 Mmol yr^{-1}.

As for mud, most of the BSi settling is expected to occur, not in the main channel but in the accesses to locks (compartments 3-5, km 57-78) and in mudflats and marshes (notably in the marsh of Saeftinge, km 45-55, located just downstream the Belgian/Dutch border). Also, the local large decrease in the mud flux at km 11 involving settling and resuspension of mud in the main channel in compartments 13 and 14 (see above) could also be seen in the BSi flux pattern (Fig. 5.14). Settling and resuspension of BSi each compartment could not be directly estimated from the BSi fluxes as BSi is also produced within the estuary with a net yearly amount of 200 Mmol yr^{-1} (including losses due to dissolution, Chapter 4). Mud can be affected by important resuspension/deposition processes, but no sedimentary source of BSi was considered as, ultimately, this resuspended BSi must have been from either riverine, marine or autochthonous origin. As a result, considering that during our study period, an average of 165 Mmol yr^{-1} of BSi were imported from the coastal zone and 123 Mmol yr^{-1} from the tidal river and that they settled within the estuary together with BSi of autochthonous origin, 488 Mmol yr^{-1} of BSi were deposited in the estuary. With a mud deposition of 536 kton yr^{-1}, the BSi content in the deposited material would amount 5.3 %. This content being higher than what was observed along the estuary (Fig. 5.13), it would indicate preferential settling of BSi compared to the rest of the SPM, as observed between Dendermonde and Temse (Chapter 3). The amount of BSi deposited is one order of magnitude higher in the estuary than in the tidal river, but when expressed with respect to the surface area (Table 4.1 in Chapter 4), the deposition rates are close: 3.0 mol m^{-2} yr^{-1} and 1.8 mol m^{-2} yr^{-1} respectively in the tidal river and in the estuary. However, these figures do not take into account the fact that the deposition is highly spatially heterogeneous in both the tidal river and the estuary.

5.6 References

Abril G, Nogueira M, Etcheber H, Cabeçadas G, Lemaire E, Brogueira MJ (2002) Behaviour of organic carbon in nine contrasting European estuaries. Estuar Coast Shelf Sci 54:241-262

Alexandre A, Meunier J-D, Colin F, Koud J-M (1997) Plant impact on the biogeochemical cycle of silicon and related weathering processes. Geochim Cosmochim Acta 61(3):677-682

Appeltans W, Hannouti A, Van Damme S, Soetaert K, Vanthomme D, Tackx M (2003) Zooplankton in the Schelde estuary (Belgium/The Netherlands). The distribution of *Eurytemora affinis*: effect of oxygen? J Plankton Res 25(11):1441-1445

Arndt S, Vanderborght J-P, Regnier P (2007) Diatom growth response to physical forcing in a macrotidal estuary: Coupling hydrodynamics, sediment transport, and biogeochemistry. J Geophys Res 112:C05045

Baeyens W, Van Eck B, Lambert C, Wollast R, Goeyens L (1998) General description of the Scheldt estuary. Hydrobiologia 366:1-14

Boschker HTS, Kromkamp JC, Middelburg JJ (2005) Biomarker and carbon isotopic constraints on bacterial and algal community structure and functioning in a turbid, tidal estuary. Limnol Oceanogr 50(1):70-80

Brochard CJE, Koeman RPT, de Keijzer-de Haan AL, Verweij GL, Fockens K, Esselink P (2005) Biomonitoring van fytoplankton in de Nederlandse zoute wateren 2004, kite-diagrammen. Koeman en bijkerk bv, ecologisch onderzoek en advies, Haren, The Netherlands. (In Dutch)

Brochard CJE, Koeman RPT, de Keijzer-de Haan AL, Verweij GL, van Wezel R, Fockens K, Esselink P (2006) Biomonitoring van fytoplankton in de Nederlandse zoute wateren 2005, kite-diagrammen. Koeman en bijkerk bv, ecologisch onderzoek en advies, Haren, The Netherlands. (In Dutch)

Brzezinski MA, Phillips DR (1997) Evaluation of ^{32}Si as a tracer for measuring silica production rates in marine waters. Limnol Oceanogr 42(5):856-865

Brzezinski MA, Phillips DR, Chavez FP, Friederich GE, Dugdale RC (1997) Silica production in the Monterey, California, upwelling; system. Limnology and Oceanography 42(8):1694-1705

Cary L, Alexandre A, Meunier J-D, Boeglin J-L, Braun J-J (2005) Contribution of phytoliths to the suspended load of biogenic silica in the Nyong basin rivers (Cameroon). Biogeochemistry 74:101-104

Chen MS, Wartel S, Van Eck B, Van Maldegem D (2005) Suspended matter in the Scheldt estuary. Hydrobiologia 540(1-3):79-104

Claquin P, Martin-Jézéquel V (2005) Regulation of the Si and C uptake and of the soluble free-silicon pool in a synchronised culture of Cylindrotheca fusiformis (Bacillariophyceae): effects on the Si/C ratio. Mar Biol 146:877-886

Conway HL, Harrison PJ (1977) Marine diatoms grown in chemostats under silicate or ammonium limitation. IV. Transient response of *Chaetoceros debilis*, *Skeletonema costatum*, and *Thalassiosira gravida* to a single addition of the limiting nutrient. Mar Biol 43:33-43

De Jonge VN, van Beusekom JEE (1995) Wind- and tide-induced resuspension of sediment and microphytobenthos from tidal flats in the Ems estuary. Limnol Oceanogr 40(4):766-778

Dijkman NA, Kromkamp JC (2006) Photosynthetic characteristics of the phytoplankton in the Scheldt estuary: community and single-cell fluorescence measurements. Eur J Phycol 41(4):425-434

Fettweis M, Sas M, Monbaliu J (1998) Seasonal, neap-spring and tidal variation of cohesive sediment concentration in the Scheldt estuary, Belgium. Estuar Coast Shelf Sci 47:21-36

Fettweis M, Van den Eynde D (2003) The mud deposits and the high turbidity in the Belgian-Dutch coastal zone, southern bight of the North Sea. Cont Shelf Res 23:669-691

IRMB (Institut Royal Météorologique de Belgique) (2003-2005) Bulletins mensuels, Observations climatologiques, parties I et II. Institut Royal Météorologique de Belgique, Bruxelles. (In French/Dutch)

Kristiansen S, Farbrot T, Naustvoll L-J (2000) Production of biogenic silica by spring diatoms. Limnol Oceanogr 45(2):472-478

Kromkamp JC, Peene J (1995) Possibility of net phytoplankton primary production in the turbid Schelde Estuary (SW Netherlands). Mar Ecol Prog Ser 121:249-259

Kromkamp JC, Peene J (2005) Changes in phytoplankton biomass and primary production between 1991 and 2001in the Westerschelde estuary (Belgium/The Netherlands). Hydrobiologia 540(1-3):117-126

Lancelot C (1995) The mucilage phenomenon in the continental coastal waters of the North Sea. The Science of The Total Environment 165(1-3):83-102

Leynaert A, Treguer P, Lancelot C, Rodier M (2001) Silicon limitation of biogenic silica production in the Equatorial Pacific. Deep Sea Research Part I: Oceanographic Research Papers 48(3):639-660

Lionard M, Muylaert K, Van Gansbeke D, Vyverman W (2005) Influence of changes in salinity and light intensity on growth of phytoplankton communities from the Schelde river and estuary (Belgium/The Netherlands). Hydrobiologia 540(1-3):105-115

Lionard M, Muylaert K, Hanouti A, Maris T, Tackx M, Vyverman W (2008) Inter-annual variability in phytoplankton summer blooms in the freshwater tidal reaches of the Schelde estuary (Belgium). Estuar Coast Shelf Sci 79(4):694-700

Martin-Jézéquel V, Hildebrand M, Brzezinski MA (2000) Silicon metabolism in diatoms: implications for growth. J Phycol 36:821-840

Meire P, Ysebaert T, Van Damme S, Van den Bergh E, Maris T, Struyf E (2005) The Scheldt estuary: a description of a changing ecosystem. Hydrobiologia 540(1-3):1-11

Muylaert K, Sabbe K (1999) Spring phytoplankton assemblages in and around the maximum turbidity zone of the estuaries of the Elbe (Germany), the Schelde (Belgium/The Netherlands) and the Gironde (France). Journal of Marine Systems 22(2-3):133-149

Muylaert K, Sabbe K, Vyverman W (2000) Spatial and temporal dynamics of phytoplankton communities in a freshwater tidal estuary (Schelde, Belgium). Estuar Coast Shelf Sci 50(5):673-687

Muylaert K, Tackx M, Vyverman W (2005) Phytoplankton growth rates in the freshwater tidal reaches of the Schelde estuary (Belgium) estimated using a simple light-limited primary production model. Hydrobiologia 540(1-3):127-140

Muylaert K, Gonzales R, Franck M, Lionard M, van der Zee C, Cattrijsse A, Sabbe K, Chou L, Vyverman W (2006) Spatial variation in phytoplankton dynamics in the Belgian coastal zone of the North Sea studied by microscopy, HPLC-CHEMTAX and underway fluorescence recordings. J Sea Res 55:253-265

Nelson DM, Brzezinski MA (1990) Kinetics of silicic acid uptake by natural diatom assemblages in two Gulf Stream warm-core rings. Mar Ecol Prog Ser 62:283-292

Nelson DM, Dortch Q (1996) Silicic acid depletion and silicon limitation in the plume of the Mississippi River: evidence from kinetic studies in spring and summer. Mar Ecol Prog Ser 136:163-178

Ragueneau O, Chauvaud L, Leynaert A, Thouzeau G, Paulet YM, Bonnet S, Lorrain A, Grall J, Corvaisier R, Le Hir M, Jean F, Clavier J (2002a) Direct evidence of a biologically active coastal silicate pump: ecological implications. Limnol Oceanogr 47(6):1849-1854

Ragueneau O, Lancelot C, Egorov V, Vervlimmeren J, Cociasu A, Deliat G, Krastev A, Daoud N, Rousseau V, Popovitchev V (2002b) Biogeochemical transformations of inorganic nutrients in the mixing zone between the Danube River and the north-western Black Sea. Estuar Coast Shelf Sci 54(3):321-336

Rijstenbil JW, Bakker C, Jackson RH, Merks AGA, de Visscher PRM (1993) Spatial and temporal variation in community composition and photosynthetic characteristics of phytoplankton in the upper Westerschelde estuary (Belgium, SW Netherlands). Hydrobiologia 269/270:263-273

Roubeix V, Lancelot C (2008) Effect of salinity on growth, cell size and silicification of an euryhaline freshwater diatom: *Cyclotella meneghiniana* Kütz. Transit Water Bull 1:31-38

Rousseau V, Leynaert A, Daoud N, Lancelot C (2002) Diatom succesion, silification and silicic acid availability in Belgian coastal waters (Southern North Sea). Marine Ecology Progress Series 236:61-73

Salden RM, van Eck GTM, Holland ABM, Lefèvre FOB, Van Maldegem DC, de Ridder J, Spronk GC, Schouwenaar A, Verlaan PAJ (1998) Het effect van slibverwijdering in de Beneden Zeeschelde op de waterkwaliteiten slibhuishouding in de Westerschelde. Evaluatie van een bepaling uit de WVO-vergunning onderhoudsbaggerspecie. Rapport RIKZ-98.015. Ministerie van Verkeer en Waterstaat, Directoraat-Generaal Rijkswaterstaat, Rijksinstituut voor Kust en Zee/RIKZ, The Netherlands. (In Dutch)

Soetaert K, Van Rijswijk P (1993) Spatial and temporal patterns of the zooplankton in the Westerschelde estuary. Mar Ecol Prog Ser 97:47-59

Soetaert K, Herman PMJ, Kromkamp JC (1994) Living in the twilight : estimating net phytoplankton growth in the Westerschelde estuary (The Netherlands) by means of an ecosystem model (MOSES). J Plankton Res 16:1277-1301

Soetaert K, Hoffmann M, Meire P, Starink M, van Oevelen D, Van Regenmortel S, Cox T (2004) Modeling growth and carbon allocation in two reed beds (*Phragmites australis*) in the Scheldt estuary. Aquat Bot 79:211-234

Soetaert K, Middelburg JJ, Heip C, Meire P, Van Damme S, Maris T (2006) Long-term change in dissolved inorganic nutrients in the heterotrophic Scheldt estuary (Belgium, The Netherlands). Limnol Oceanogr 51(1, part 2):409-423

Struyf E, Van Damme S, Gribsholt B, Middelburg JJ, Meire P (2005) Biogenic silica in tidal freshwater marsh sediments and vegetation (Schelde estuary, Belgium). Mar Ecol Prog Ser 303:51-60

Suzumura M, Kokubun H, Arata N (2004) Distribution and characteristics of suspended particulate matter in a heavily eutrophic estuary, Tokyo Bay, Japan. Mar Pollut Bull 49:496-503

Tackx M, De Pauw N, Van Mieghem R, Azémar F, Hannouti A, Van Damme S, Fiers F, Daro N, Meire P (2004) Zooplankton in the Schelde estuary, Belgium and The Netherlands. spatial and temporal patterns. J Plankton Res 26(2):133-141

Tackx M, Azémar F, Boulêtreau S, De Pauw N, Bakker K, Sautour B, Gasparini S, Soetaert K, Van Damme S, Meire P (2005) Zooplankton in the Schelde estuary, Belgium and The Netherlands: long-term trends in spring populations. Hydrobiologia 540:275-278

Temmerman S, Govers G, Wartel S, Meire P (2003) Spatial and temporal factors controlling short-term sedimentation in a salt and freshwater tidal marsh, Scheldt estuary, Belgium, SW Netherlands. Earth Surf Process Landforms 28:739-755

Tungaraza C, Rousseau V, Brion N, Lancelot C, Gichuki J, Baeyens W, Goeyens L (2003) Contrasting nitrogen uptake by diatom and *Phaeocystis*-dominated phytoplankton assemblages in the North Sea. Journal of Experimental Marine Biology and Ecology 292(1):19-41

Van Alphen JSLJ (1990) A mud balance for Belgian-Dutch coastal waters between 1969 and 1986. Netherlands Journal of Sea Research 25(1/2):19-30

Van Damme S, Struyf E, Maris T, Ysebaert T, Dehairs F, Tackx M, Heip C, Meire P (2005) Spatial and temporal patterns of water quality along the estuarine salinity gradient of the Scheldt estuary (Belgium and The Netherlands): results of an integrated monitoring approach. Hydrobiologia 540(1-3):29-45

Van der Zee C, Chou L (2005) Seasonal cycling of phosphorus in the Southern Bight of the North Sea. Biogeosciences 2:27-42

Van der Zee C, Roevros N, Chou L (2007) Phosphorus speciation, transformation and retention in the Scheldt estuary (Belgium/The Netherlands) from the freshwater tidal limits to the North Sea. Mar Chem 106(1-2):76-91

Van Eck GTM (1991) De ontwikkeling van een waterkwaliteitsmodel voor het Schelde-estuarium (In Dutch). Water 61:215-218

Van Maldegem DC, Mulder HPJ, Langerak A (1993) A cohesive sediment balance for the Scheldt Estuary. Neth J Aquat Ecol 27(2-4):247-256

Vereeke SJP (1994) Geactualiseerde slibbalans Schelde-estuarium (2e concept). Ministerie van Verkeer en Waterstaat, Directoraat-Generaal Rijkswaterstaat, Directie Zeeland, Middelburg, The Netherlands. (In Dutch)

Verlaan PAJ, Maartense VJ, Meijerink SV, Donze M (1997) Slibtransport in de Schelde over de Belgisch-Nederlandse grens (In Dutch). H2O 30(8):255-260

Verlaan PAJ, Donze M, Kuik P (1998) Marine *vs* fluvial suspended matter in the Scheldt estuary. Estuar Coast Shelf Sci 46:873-883

Verlaan PAJ (1998) Mixing of marine and fluvial particles in the Scheldt estuary. Ph.D. thesis. Technische Universiteit Delft, The Netherlands.

Wartel S, Chen M, van Eck GTM, Van Maldegem D (2007) Influence of harbour construction on mud accumulation in the Scheldt estuary. Aquatic Ecosystem Health & Management 10(1):107-115

5A ANNEX: Mud budgets

5A.1 Literature review and selection of a mud mass-balance for the Scheldt estuary

Mud budgets for the entire estuary were built in the early nineties (Van Eck 1991; Van Maldegem et al. 1993; Vereeke 1994). They were actually based on the same box-model methodology (mud balances on 14 compartments, see text for details), but with different input and output data. Since the late nineties, mud budgets were restricted to the area upstream of the Belgian/Dutch border, as the goal of these studies was the estimation of the mud accumulation in this area and/or the amount of riverine mud supplied to the Dutch part of the estuary (Verlaan et al. 1997; Salden et al. 1998; Wartel et al. 2007). These budgets were established by a single mass-balance between different sources and sinks for mud recognized for this area, as detailed in Table 5A-1.

Impact of the access to locks on the mud dynamics

All mud budgets performed on data from the 90's and after (Verlaan et al. 1997; Salden et al. 1998; Wartel et al. 2007) agree on the fact that, due to their low water energy, the access channels to locks act as efficient mud traps, at the cost of the mud deposition in the main channel and of the mud export to the Dutch part of the estuary. Their bottom sediments are as a result almost entirely composed of mud, while those of the main channel are for the major part coarser deposits (Wartel et al. 1999). Thus, their construction in the mid-eighties (Verlaan et al. 1997) have drastically changed the mud dynamics in the upper part of the estuary. Intense dredging was required in the access channel to the locks to ensure shipping access. Most of the dredging activity was performed in the access channel to the Kallo lock, but only little export of mud is expected through this lock due its low shutting frequency (Verlaan et al. 1997; Salden et al. 1998). In contrast, most of the export to harbours is expected to be through the Zandvliet/Berendrecht lock, while the mud accumulated in the access channel was just dredged back to the estuary.

Table 5A-1: Sources and sinks of mud to the Belgian part of the Scheldt estuary (in kton yr^{-1}). The numbers in bold and italics indicate data that the authors obtained using mass-balance calculations. The grey columns correspond to mass-balances established for periods after the mid-eighties (see text).

* Average of the individual budgets for the years 1992, 1993 and 1994. In Verlaan et al. (1997), the export to harbours is missing for the year 1994 and only the budgets for the years 1992 and 1993 are closed. Here, the year 1994 is also taken into account after closing the budget following the same methodology as in Verlaan et al. (1997) with the export to the harbours taken from Salden et al. (1998).

	Van Eck 1991	Van Maldegem et al. 1993	Veereke 1994	Verlaan et al. 1997		Salden et al. 1998	Wartel et al. 2007	
date of data	1975-1985	1975-1985	1975-1985 + early nineties	1964-1986	1992-1994 *	1992-1995	1964-1986	1986-1999
riverine mud from the tidal river and lateral inputs	432	410	390	375	220	220	400	230
export to harbours	-83	-120	-150	-150	-333	-221	-	-
dredging/dumping		60	-240	-50	-447	-300	-42	-91
export to access channels		-		-				-20
accumulation/resuspension in/from bottom sediments of the channel and marshes		***-42***	***-9***	***-100***	***569***	***321***	-52	-32
export riverine mud at the Belgian/Dutch border	***-365***	***-386***	***-121***	-175	-110	-100	***-306***	***-87***
marine mud inflow at the Belgian/Dutch border	***16***	***78***	***130***	100	100	***80***		

Selected mud budget for the Dutch part of the estuary

Similarly to the budgets established for the years 1964-1986 by Verlaan et al. (1997) and Wartel et al. (2007), the mass-balances proposed by Van Eck et al. (1991) and Van Maldegem et al. (1993) were considered as not applicable to our study period (2003-2005) as they were derived from data collected before the mid-eighties, i.e. before the construction of the access to the locks. They indeed led to higher export of riverine mud to the Dutch part of the estuary than the other studies (Table 5A-1). The study from Vereeke (1994) is an update of the one of Van Maldegem et al. (1993) with more recent data and considerations. Although it is partly based on data for the period 1975-1985 (riverine mud input flux for instance), it also incorporates the amount of material dredged mostly from the access channel to the lock of Kallo (data from 1992). Other updates concern, among others, the lateral inputs and outputs and the riverine to marine mud ratios. The study from Vereeke (1994) was therefore seen as

the most reliable mud budget available for the Dutch part of the estuary, but the choice was more complicated for the Belgian part of the estuary as later budgets providing different results were also available.

Selected mud budget for the Belgian part of the estuary

Budgets from Verlaan et al. (1997) and Salden et al. (1998)

The budgets of Verlaan et al. (1997) and Salden et al. (1998) were based on the same dataset although Salden et al. (1998) included the year 1995. The methodology differed only slightly and the results presented similarities (Table 5A-1). The marine mud input flux at the Belgian/Dutch border was fixed in Verlaan et al. (1997) but deduced from the mass-balance and riverine/marine mud ratios in Salden et al. (1998). Salden et al. (1998) additionally took into account the mud contents in dredged materials and estimated their marine mud fractions. As the depth has to be maintained for shipping access to the locks, Verlaan et al. (1997) and Salden et al. (1998) estimated that the amounts of sediment dredged in the access channels to locks and behind locks provided by the Belgian authorities reflected the gross mud accumulation and export through the locks. They respectively averaged about 300 and 221 kton yr^{-1} during 1992-1995 (Salden et al. 1998). The mud flux at the border was fixed as half of the mud input flux from the tidal river and the bottom mud accumulation/resuspension was estimated by closing the budget. The unbalance between the riverine mud input flux (220 kton yr^{-1}) and the dredging and the export to ports (521 kton yr^{-1}) was thus compensated by a net bottom erosion (321 kton yr^{-1}) in the main channel and an import of marine mud from downstream (80 kton yr^{-1}). This resulted in a net annual mud flux of 20 kton yr^{-1} of mud to the downstream part of the estuary at the Belgian/Dutch border (Salden et al. 1998). Verlaan et al. (1997) also calculated a net bottom mud erosion and similar net fluxes ranging from 0 to 25 kton yr^{-1} in 1992-1994 and averaging 10 kton yr^{-1}.

Budget from Wartel et al. (2007)

The results from Wartel et al. (2007) differed significantly from those of Verlaan et al. (1997) and Salden et al. (1998) (Table 5A-1). The methodology and the data used were also different. The mud accumulation was directly determined using bottom maps of 1986 and 1999 and it is the mud transport at the Belgian/Dutch border which was determined by closing the budget. Wartel et al. (2007) observed little net mud accumulation in the access channels to the Kallo and Zandvliet/Berendrecht locks (8 and 13 kton yr^{-1} respectively), but also a small net mud accumulation in bottom sediments of the channel (20 kton yr^{-1}, to which should be

added a deposition in marshes of 12 kton yr^{-1}). This observation ruled out the use of the budgets of Verlaan et al. (1997) and Salden et al. (1998) for a general representation of the mud balance in this part of the estuary. However, the high net mud outflow through the Belgian/Dutch border (87 kton yr^{-1}) that Wartel et al. (2007) estimated may appear also doubtful as the authors did not take into account the export of mud through the locks and used a low annual withdrawal of mud by dredging in their budget (91 kton yr^{-1}): they reported that 1187 kton of mud were dredged between 1992 and 1999 from the access channel to the Kallo lock while Salden et al. (1998) reported 1206 kton yr^{-1} for the period 1992-1995 only. Between 1990 and 2003, from 2 to 5 Mm^3 were withdrawn every year (Meire et al. 2005), corresponding in average to 367 kton yr^{-1} of dry material (Meire et al. 2005), or 330 kton yr^{-1} with a mud content of 90 % (Salden et al. 1998; Wartel et al. 1999). This latter annual average amount is very close to what used Salden et al. (1998).

Budget from Vereeke (1994)

Vereeke (1994) presented a somewhat intermediate situation. This author observed a net deposition (9 kton yr^{-1}, actually in marshes) which would not go against the observations of Wartel et al. (2007). Dredging and export to harbours were also taken into account, although their amounts were lower than in Verlaan et al. (1997) and Salden et al. (1998). Vereeke (1994) set the dredging to what was actually done in 1992, a year during which less material was dredged compared to the average situation.

Concerning the export to harbours, Vereeke (1994) recognized that he chose his estimate (150 kton yr^{-1}) on the low side of the available estimation range (from 150 to 350 kton yr^{-1}), which are however not known with precision (Verlaan et al. 1997; Salden et al. 1998). Verlaan et al. (1997) and Salden et al. (1998) used amounts provided by the Belgian authorities, but dredging in harbours was not performed regularly and varied strongly from one year to another (Salden et al. 1998). Salden et al. (1998) used also an amount lower than that estimated in a study they reported (from 300 to 500 kton yr^{-1} according to Winterwerp 1997, cited in Salden et al. 1998).

Variability in the riverine mud input

The budget from Vereeke (1994) also differed from the three most recent ones by the fact that the riverine mud input flux to the estuary was identical to those in the budgets established with data collected before the nineties, i.e. higher by almost a factor 2 than in the budgets from Verlaan et al. (1997), Salden et al. (1998) and Wartel et al. (2007) (Table 5A-1). Verlaan et al. (1997) and Salden et al. (1998) attributed the decrease of the riverine mud input

flux to the mud extraction and to the reduction of domestic and industrial waste discharge in the tidal river and its drainage basin. However, the riverine mud input flux is also strongly related to the freshwater discharge and displays high inter-annual variations (Verlaan et al. 1997; Wartel et al. 2007). It generally varied between 200 and 500 kton yr^{-1} but could be as high as 800 kton yr^{-1} in 1974 or as low as 100 kton yr^{-1} in 1996 and 1997 (Verlaan et al. 1997; Wartel et al. 2007). As observed by Verlaan et al. (1997) and Salden et al. (1998), the riverine mud input flux exhibited low values during the early nineties together with low freshwater discharges, but it increased again after 1998 (Wartel et al. 2007). Overall, the riverine mud input flux for 1992-2002 averaged 348 kton yr^{-1} (Wartel et al. 2007), an amount corresponding to the estimate of Vereeke (1994).

Selected mud budget

As it was the case for the Dutch part of the estuary, the budget proposed by Vereeke (1994) also seemed to be the most reliable representation of an average situation of the mud budget in the Belgian part of the estuary, even if it was not the most recent. In addition, the mud dynamics in the entire estuary were described by a single study, thus preventing potential discrepanties due to the juxtaposition of two independent studies for the two parts of the estuary.

5A.2 References

Meire P, Ysebaert T, Van Damme S, Van den Bergh E, Maris T, Struyf E (2005) The Scheldt estuary: a description of a changing ecosystem. Hydrobiologia 540(1-3):1-11

Salden RM, van Eck GTM, Holland ABM, Lefèvre FOB, Van Maldegem DC, de Ridder J, Spronk GC, Schouwenaar A, Verlaan PAJ (1998) Het effect van slibverwijdering in de Beneden Zeeschelde op de waterkwaliteiten slibhuishouding in de Westerschelde. Evaluatie van een bepaling uit de WVO-vergunning onderhoudsbaggerspecie. Rapport RIKZ-98.015. Ministerie van Verkeer en Waterstaat, Directoraat-Generaal Rijkswaterstaat, Rijksinstituut voor Kust en Zee/RIKZ, The Netherlands. (In Dutch)

Van Eck GTM (1991) De ontwikkeling van een waterkwaliteitsmodel voor het Schelde-estuarium (In Dutch). Water 61:215-218

Van Maldegem DC, Mulder HPJ, Langerak A (1993) A cohesive sediment balance for the Scheldt Estuary. Neth J Aquat Ecol 27(2-4):247-256

Vereeke SJP (1994) Geactualiseerde slibbalans Schelde-estuarium (2e concept). Ministerie van Verkeer en Waterstaat, Directoraat-Generaal Rijkswaterstaat, Directie Zeeland, Middelburg, The Netherlands. (In Dutch)

Verlaan PAJ, Maartense VJ, Meijerink SV, Donze M (1997) Slibtransport in de Schelde over de Belgisch-Nederlandse grens (In Dutch). H2O 30(8):255-260

Wartel S, Parker R, Francken F, Shelton P (1999) Schelde lithology (1 map). KBIN, Brussels, Belgium.

Wartel S, Chen M, van Eck GTM, Van Maldegem D (2007) Influence of harbour construction on mud accumulation in the Scheldt estuary. Aquatic Ecosystem Health & Management 10(1):107-115

6 Summary and general discussion

The major results obtained in this study are summarised and the DSi and silica retention in the Scheldt are compared with those observed in other estuaries. The overall functioning of the silica dynamics in the Scheldt tidal system is further examined to highlight its main features, such as the importance of the BSi dynamics and of the influence of the coastal zone. Possible ways of refining our silica budgets are proposed and discussed. Finally, based on the results of this study and on the past long-term evolution of DSi concentrations in the Scheldt tidal system, the potential response of the silica dynamics to the improvement of the water quality and to the restoration of intertidal areas currently taking place in the tidal river is examined.

6.1 Silica dynamics in the Scheldt tidal system

Main results

DSi and BSi in the tidal river (Chapter 3)

Temporal evolution of dissolved and biogenic silica concentrations along the Scheldt tidal river and in its tributaries was investigated during one year in 2003. In the tributaries, DSi concentrations remained high and BSi concentrations were low throughout the year. In the tidal river during summer, DSi was completely consumed and BSi concentrations increased. Overall, most of the BSi was associated with living diatoms during the productive period in the tidal river. Nevertheless, the detrital BSi was a significant fraction of the total BSi pool, of which less than 10 % could be attributed to phytoliths. The tidal river was divided into two zones for budgeting purposes. The highest productivity was observed in the zone that received the highest water discharge, as higher riverine DSi input fluxes induced presumably a less restrictive DSi limitation, but the discharge pattern could not explain all by itself the variations in DSi consumption. Silica uptake and retention in the tidal river were important at the seasonal time-scale: from May to September, 48 % of the riverine DSi was consumed and 65 % of the produced BSi was deposited, leading to a silica (DSi + BSi) retention in the tidal river of 30 %. However, when annual fluxes were considered, DSi

uptake in the tidal river amounted to 14 % of the DSi inputs and only 6 % of the riverine silica (DSi + BSi) was retained in the tidal river.

DSi in the estuary (Chapter 4)

DSi concentrations have been measured along the entire salinity gradient of the Scheldt estuary during different seasons between 2003 and 2005. Concentrations always decreased from the freshwater to the seawater end-members and thus the estuarine DSi concentrations followed the same seasonal pattern as in the tidal river: high concentrations in winter and low ones in summer and early autumn. However, the DSi versus salinity profiles displayed concave or convex patterns, which were not solely induced by the mixing between freshwater and seawater, but also by the superimposed effects of diatom DSi uptake or DSi release by BSi dissolution. As the commonly used "Apparent Zero End-member" method for interpreting DSi profiles and estimating DSi fluxes at the mouth of the estuary is irrelevant in the case of the Scheldt, measured DSi profiles were compared to conservative ones which were obtained using fully-transient model simulations. DSi fluxes at the mouth of the estuary could also be calculated and the net DSi consumption or release could be quantified. The DSi consumption was maximum in May with a rate of 7.3 mmol m^{-2} d^{-1}, but it dropped quickly in July and a net release of DSi was observed from late summer onwards. The drop in the net DSi consumption was attributed to grazing control of the diatom growth. The net annual DSi consumption amounted to 0.76 mol m^{-2} yr^{-1}, leading to a retention of 28 % of the total DSi input. These maximum and annual estimates, as well as the DSi retention in the estuary were two times higher than in the tidal river, but when normalised with respect to water surface area the DSi uptake rates were one order of magnitude lower in the estuary than in the tidal river.

BSi in the estuary (Chapter 5)

BSi, DiatChl*a* and SPM concentrations have been measured over the entire salinity gradient in the estuary during different seasons between 2003 and 2005. Multiple regressions between these concentrations indicated that, in contrast to the tidal river, the major part of the BSi (85 % in average) did not follow the dynamics of the living diatoms but rather that of the SPM. However, similar to that observed in the tidal river, phytoliths could only account for a small fraction of the detrital BSi. Time-course ^{32}Si incorporation experiments were also performed in April, May and July 2005. In addition to specific DSi uptake rates, these experiments provided estimations of the concentrations of BSi corresponding to growing diatoms. Even if the methodologies were completely different, these estimates compared well

to that of the BSi associated with living diatoms obtained using multiple regressions. Additionally, similar specific uptake rates were measured during the three campaigns, suggesting that diatoms were in a similar health status even if chlorophyll a concentrations dropped from May to July. This supports the hypothesis that the decrease in the phytoplankton biomass in July can be ascribed to grazing pressure. The longitudinal and temporal variations in the BSi profiles were interpreted based on the correlation between the BSi dynamics and those of the SPM and, to a lesser extent, DiatChl*a*. Highest BSi concentrations were observed in the most freshwater part of the estuary, not only due to the advection of large amounts of diatoms from the tidal river, but also (and mainly) due to the presence of the turbidity maximum. This implies that, similar to SPM, BSi concentrations exhibited also a high temporal variability. In the zone of salinity 10-30, BSi was expected to be predominantly of marine origin. An annual BSi mass-balance was deduced from an existing SPM budget in the estuary: in addition to the autochthonous production of BSi, about the same amount of BSi was imported from the coastal zone to the estuary as that carried by the tidal river. The estuary appeared thus as a net sink for important amounts of BSi of different origins.

Comparisons with other estuarine ecosystems

DSi retention

Gross DSi consumption rates, which correspond to gross diatom (or BSi) productivity, were estimated from net DSi consumption rates assuming BSi dissolution to be insignificant in the tidal river (Chapter 3) and to amount to 400 kmol d^{-1} from mid May to mid December (214 days) in the estuary (Chapter 4) (Table 6.1). Although the annual productivity in the tidal river and in the estuary differed by almost one order of magnitude, rates assessed in both systems were in the range of those measured worldwide. The few direct measurements of annual gross productivities displayed a high variability ranging from 0.2 to 8.3 mol m^{-2} yr^{-1} (global estimate: 0.6-0.8 mol m^{-2} yr^{-1}, Ragueneau et al. 2000). Gross annual productivities in estuaries estimated by mass-balances are scarce but the values assessed for the Scheldt tidal system are also in the range of those estimated for other estuarine systems, such as for example the Great Ouse estuary (0.6-0.8 mol m^{-2} yr^{-1}, Rendell et al. 1997, assuming a water surface area of 2.2 km^2, Nedwell and Trimmer 1996) or the Chesapeake Bay estuary (2.7 mol m^{-2} yr^{-1}, D'Elia et al. 1983). Productivities of the same order of magnitude were also estimated in other semi-enclosed systems: e.g. 0.91 mol m^{-2} yr^{-1} in the Bay of Brest

(Ragueneau et al. 2005), 2.2 and 5 mol m^{-2} yr^{-1} in impoundments of the upper Mississippi River (Triplett et al. 2008), 3.8 mol m^{-2} yr^{-1} in the Jiaozhou Bay (Liu et al. 2008).

Table 6.1: Net and gross DSi annual consumption (indicated with a negative sign as for Tables 4.2 and 4.3 in Chapter 4) in the tidal river, in the estuary and in the entire Scheldt tidal system (see text for estimation of the gross DSi consumption). Surface areas correspond to those indicated in Table 4.1 (Chapter 4).

	tidal river	**estuary**	**tidal river + estuary**
annual DSi consumption (mol m^{-2} yr^{-1})			
net	-7.20	-0.76	-1.08
gross		-1.08	-1.39

One should nonetheless bear in mind that these retentions and rates reflect only a fraction of the functioning of the silica biogeochemical cycle, which can largely differ from one estuary to another. Firstly, the DSi retention estimates are largely influenced by the DSi inputs normalised with respect to water surface area. For instance, DSi displayed a conservative behaviour in one third of the estuaries listed in Roubeix (2007), such as in the Great Ouse estuary: despite a productivity around 0.6-0.8 mol m^{-2} yr^{-1} (Nedwell and Trimmer 1996; Rendell et al. 1997), the DSi inputs normalized with respect to the water surface area (72 mol m^{-2} yr^{-1}) do not leave room for a significant DSi retention (less than 1 %). Nonetheless, as DSi is completely consumed in spring before entering the Great Ouse estuary (Rendell et al. 1997), the overall retention in the entire continuum may reach a higher percentage. Also, BSi dissolution has been shown to be a major process in many estuaries (or in semi-enclosed bays). Due to the increase of its rate with salinity (Roubeix et al. 2008; Loucaides et al. 2008), BSi dissolution is predominantly observed at salinities higher than 10 and in coastal bays (Anderson 1986). It may constitute a DSi source which largely exceeds the riverine DSi inputs and thus sustains the major part of the diatom productivity (D'Elia et al. 1983; Yamada and D'Elia 1984; Ragueneau et al. 2005; Liu et al. 2008). As a result, the DSi retention depends then on the burial rate and can reach high values: e.g. 65 % in the Chesapeake Bay estuary (D'Elia et al. 1983) or 48 % in the Bay of Brest (where the BSi dissolution is in fact enhanced by benthic suspension feeders, Ragueneau et al. 2005). Even,

in the Jiaozhou Bay, a net import of DSi is from the adjacent Yellow Sea is also observed, so that the DSi retained in the bay exceeds several times that delivered by the rivers (Liu et al. 2008).

The functioning of the silica cycle in the Scheldt lies between the two extreme cases described above. In the Scheldt, the BSi dissolution of 400 kmol d^{-1} observed from mid May to mid December would lead to an annual flux of 0.32 mol m^{-2} yr^{-1}. This rate is several times smaller than the gross BSi production, which is thus mainly sustained by the riverine DSi inputs. This dissolution rate is also almost one order of magnitude lower than those in other estuaries reported by Yamada and D'Elia (1984). It may be attributed to the high amount of lithogenic material in the Scheldt estuary (Wartel 1977; Bouezmarni and Wollast 2005) which can lower the BSi dissolution efficiency (Dixit et al. 2001).

The DSi retention that we estimated for the Scheldt tidal system is nevertheless higher than the average estuarine retention of 20 % estimated by DeMaster (1981) as well as the value of 25 % for temperate rivers used by Tréguer et al. (1995) in his global silica budget. Also, our retention is among the highest range of the 19 worldwide estuarine DSi retentions reported by Roubeix (2007): 90 % exhibited a retention lower than 30 % and the average retention was 15 %. Compared to other estuaries, the Scheldt tidal system can thus be considered as an efficient filter for DSi. This may be due to the fact that the Scheldt is composed of two systems where DSi is consumed during different periods: overall, DSi is consumed from early spring until early autumn. Also, in the case of the Scheldt, the fact that only a small fraction of the BSi produced is expected to dissolve leads to an increased DSi retention.

BSi mass-balance

Even if BSi has been recognized as an important constituent of the riverine silica pool available at biological time-scales in downstream reaches (Conley 1997), there exists hardly any study reporting BSi mass-balances in estuaries. In particular, BSi mass-balances can be hampered by the lack of knowledge concerning BSi fluxes at the mouth of the estuary (e.g. Pastuszak et al. 2008). Also, as in the Scheldt tidal river in winter (Chapter 3), the large difference between DSi and BSi fluxes impedes the estimation of the *in situ* BSi production by DSi mass-balance calculations (Triplett et al. 2008). In the Scheldt, a key feature of the BSi budget is the net import of BSi at the mouth of the estuary. A net import of BSi from the coastal zone was as well observed by DeMaster (1981) in the Long Island Sound and Liu et al. (2008) in Jiaozhou Bay. The accumulation of coastal diatoms in the Kinsale estuary was

also described by Muylaert and Raine (1999). However, not all estuaries act as a sink for fluvial, marine and autochthonous BSi in the same extent as the Scheldt. This may only apply to macrotidal estuaries with long water residence times, which are able to accumulate sediments; in estuaries with short water residence times, flushing of the sediments may occur during freshets (Uncles et al. 2002). In addition, there exists an equilibrium between bed morphology, sediment supply and critical shear stress (Friedrichs 1995), so the intensive dredging activity in the Scheldt (Meire et al. 2005) may result in maintained high SPM deposition rates.

Comparison of the silica dynamics in the tidal river and that in the estuary

Silica exhibited contrasting behaviours in the tidal river and in the estuary, at the seasonal as well as at the annual timescale. The effects of the two aquatic systems on the transport of silica to the coastal zone were also different. Although the DSi was entirely consumed in summer in the tidal river, the transport of silica was not affected in a way that would have been critical for the coastal zone, both at the seasonal and annual timescales (Chapter 3). As BSi dynamics were linked to those of DSi, the DSi retention in the tidal river was counterbalanced by the net BSi production: the retention of the total amount of silica (6 %) was lower than that of DSi (14 %, Chapter 3; Table 6.2). In contrast, the DSi consumption in the estuary occurred in spring, when DSi in the coastal zone could reach limiting levels. Furthermore, not only DSi retention in the estuary was significant at an annual timescale (28 %), but the estuary acted also as a sink for the BSi of freshwater, marine and autochthonous origins. Considering DSi and BSi inputs at the freshwater end-member of respectively 705 Mmol yr^{-1} and 123 Mmol yr^{-1} (Chapters 4 and 5) and, at the seawater end-member, DSi outputs of 505 Mmol yr^{-1} but BSi inputs of 165 Mmol yr^{-1}, the annual silica retention in the estuary amounted to 59 %, which, in contrast to the tidal river, was higher than that of DSi (Table 6.2).

A direct juxtaposition of DSi and BSi mass-balances in the tidal river and the estuary was not possible. As these studies were applied to different years, the output fluxes estimated for the tidal river in Chapter 3 did not correspond to the input fluxes to the estuary in Chapters 4 and 5. Nevertheless, in order to better visualize the silica dynamics in the entire Scheldt tidal system, an annual budget normalised to the silica inputs by tributaries (with a BSi to DSi ratio as indicated in Table 3.2, Chapter 3) was constructed (Fig. 6.1), based on the relative DSi and silica retentions indicated in Table 6.2.

Table 6.2: DSi and (total, i.e. dissolved plus biogenic) silica retention (%) in the tidal river, in the estuary and in the entire Scheldt tidal system (as defined in Eq. 2.8a and b, Chapter 2).

	tidal river	estuary	tidal river + estuary
DSi retention (%)	14	28	39
silica retention (%)	6	59	61

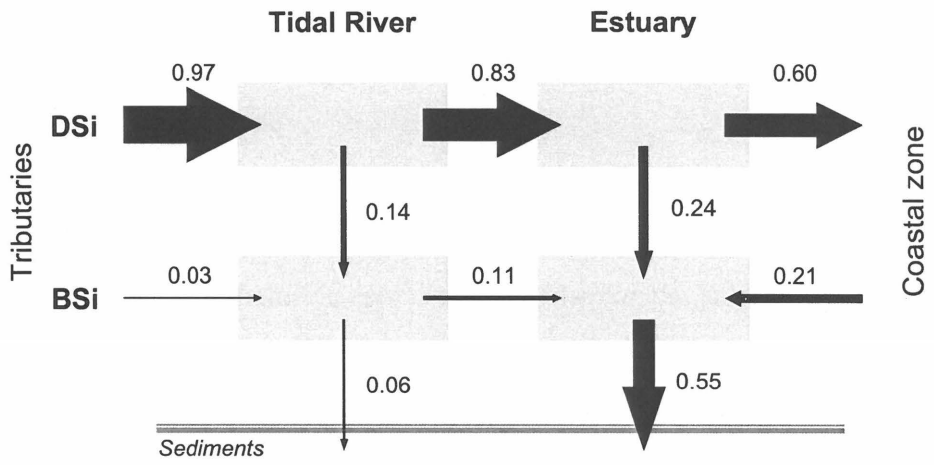

Fig. 6.1. Annual silica mass-balance (normalised to the riverine silica inputs) for the entire Scheldt tidal system. Arrow thickness is proportional to the magnitude of the flux. Horizontal arrows indicate net DSi or BSi fluxes and vertical arrows indicate net DSi consumption and net BSi deposition. The mass-balance has been constructed using DSi and silica retentions indicated in Table 6.2 and a ratio of BSi to DSi in the tributaries of 3 % (see Table 3.2, Chapter 3).

Overall, DSi and silica retentions of respectively 39 % and 61 % could be estimated for the Scheldt tidal system (Table 6.2): the Scheldt tidal system was thus an important filter for silica in the land-ocean continuum. Although the effects of the diatom uptake on DSi concentrations were more noticeable in the tidal river than in the estuary (Chapters 3 and 4), the predominant role of the estuarine silica dynamics in the overall retention of silica in the tidal system is highlighted in Fig. 6.1.

DSi retention in the tidal river was lower than that in the estuary (Table 6.2). Although there was a limitation by low summer DSi input fluxes (Chapter 3), the net areal DSi

consumption in the tidal river was one order of magnitude higher than that in the estuary when expressed with respect to the water surface area (Table 4.3). The DSi consumption in the estuary was not limited in spring, but was controlled in summer by the grazing pressure; even, a net DSi release was observed (Chapter 4).

The most remarkable feature in Fig. 6.1 was however that BSi was imported from the coastal zone, in constrast with the classical view of downstream transport of dissolved and particulate material in estuaries. It resulted in a silica retention in the estuary, which was one order of magnitude higher than that in the tidal river. Nevertheless, the estuary being about 20 times larger than the tidal river (Table 4.1), more BSi was deposited in the tidal river than in the estuary when expressed per water surface area. Overall, the rates of the filtering efficiency of tidal river appears be higher than those in the estuary, but overall impact of the tidal river on silica retention is limited due to its much smaller size.

Importance of the BSi dynamics

Conley (1997) stressed that BSi might have been an overlooked but significant source of silica to the global marine silica cycle because it was an important constituent of the silica pool carried by rivers. However, our study in the Scheldt estuary illustrates that, in some estuaries, BSi may be also imported from the coastal zone. Taking into account the BSi fluxes at the mouth of the estuary would thus lead to total silica fluxes lower than those when only DSi is considered. Nevertheless, the large differences between the DSi and the total silica retention estimates in the tidal river and in the estuary (Table 6.2) demonstrate that BSi dynamics need to be taken into account when investigating silica retention in estuaries. In particular, this may result in contrasting effects: DSi retention may not only be lower than that of total silica, but also higher if, for instance, a net import of BSi is observed.

In addition, it is important to note that the BSi dynamics in the Scheldt cannot be assessed based on those of diatoms only. BSi could be predominantly associated with living diatoms in summer in the tidal river (Fig. 3.3, Chapter 3) and in spring and early summer in the lower part of the estuary (Fig. 5.7, Chapter 5). However, the same observation could not be held true in the lower reaches of the tidal river or in the estuary at an annual timescale due to the importance of winter BSi fluxes. The (annual flux-weighted average) fraction of the BSi not associated with living diatoms, amounted to 42 % at Dendermonde but increased to 67 % at Temse and Hemiksem and even ranged from 80 to 97 % in the estuary (87 % at the

mouth). These high proportions indicate that the BSi dynamics shown in Fig. 6.1 are in fact mostly driven by SPM dynamics.

BSi and SPM may nevertheless still reflect uncoupled behaviours, such as e.g., a preferential settling of the BSi between Dendermonde and Temse (Chapter 3) and a varying detrital BSi content in the SPM of the estuary (Chapter 5). Finally, despite the phytolith-rich vegetation bordering the Scheldt, phytoliths were not, at first sight, expected to contribute significantly to the BSi pool.

Influence of the coastal zone

Our results also highlight the link between the biogeochemical and biological functioning of the downstream part of the Scheldt estuary and of the adjacent coastal zone. This is in contrast with the classical consideration that estuaries act as one-way filters for dissolved and particulate material of riverine origin only. This phenomenon affected the estuarine silica dynamics in different ways.

One impact on the BSi dynamics is evident: BSi was net imported from the coastal zone. Net import of DSi may also be observed during spring tides, low residual freshwater discharge and when DSi concentrations in the coastal zone reach higher levels than in the estuary in late summer (Fig. 4.1). But this phenomenon can possibly occur only during a short period (Fig. 4.8) and should be negligible at a longer timescale.

The estuarine DSi dynamics may however be strongly affected by the import of marine diatoms. As the estuarine DSi uptake occurs in spring, it could not be ascribed to the high summer diatom biomass observed in the most freshwater part of the estuary (Figs. 4.8 and 5.2) but should then be attributed to the diatoms growing in the downstream part the estuary in spring. Soetaert et al. (1994) estimated that most of the phytoplankton in this area was produced in situ, but phytoplankton studies (e.g. Muylaert et al. 2009) indicated an important intrusion of diatoms of marine origin (which is also supported by the net import of marine SPM at the mouth of the estuary, Chapter 5). Nevertheless, these phytoplankton studies revealed also the presence of truly estuarine species. Also, the fact that the spring diatom blooms may not be of marine origin only would also support our observation that the maximum DSi uptake along the salinity gradient appeared to be located further inland in April than in May (Fig. 4.6). Nevertheless, the highest overall estuarine DSi consumption was observed in May (Fig. 4.8), close to the mouth of the estuary (Fig. 4.6), and may thus be ascribed for a large part (if not principally) to diatoms of marine origin. This is also supported

by the fact that the high spring DSi consumption could be simulated in modelling studies only when the intrusion of marine diatoms was allowed by the extension of the estuarine model domain to the coastal zone (Arndt 2008; Arndt et al. 2009). In addition, not only the DSi consumption was enhanced in spring by the marine diatom intrusion, but also controlled in summer due to the intrusion of copepods from the coastal zone (Chapter 4; Soetaert and van Rijswijk 1993). Finally, BSi dynamics were significantly affected as well by this diatom intrusion, as the amount of BSi produced by their development in the estuary was comparable to the BSi fluxes from the tidal river and from the coastal zone.

The silica dynamics in the estuary were thus, to a large extent (if not principally), derived from the import of BSi and diatoms from the coastal zone. As a result, the importance of the estuarine DSi and BSi dynamics could be ascribed to their coupling with those in the coastal zone. In turn, the retention of DSi in the estuary may affect the biological functioning of the coastal zone. This highlights the significance of the exchange of dissolved and suspended material at the mouth of the estuary. The functioning of estuaries should be investigated not only from rivers to coastal zones, but in both directions, especially when lower reaches of estuaries are investigated. For modelling studies for instance, this may mean that a proper description of the processes occurring in this highly dynamic area (whose effects are generally of major importance due to the size of the area) can only be achieved by extending the model domain to the adjacent coastal zone.

6.2 Refinement of the silica mass-balance

Winter DSi fluxes

As DSi is in principle consumed between spring and early autumn, it is tempting to focus the sampling efforts on this period. However, the high freshwater discharge in winter results in fluxes which represent an important if not major part of the annual flux. So, careful estimation of winter fluxes is required to build accurate annual budgets: a small relative imprecision about silica fluxes in winter can lead to a an apparent DSi consumption or release, which can be of the same order, or even exceed, the magnitude of the processes affecting silica in summer (see imprecision concerning winter fluxes in Chapters 3 and 4). Also, the investigation of the biogeochemical behaviour of DSi in winter (i.e. whether DSi behaves conservatively or whether it is affected by BSi dissolution) is only possible if a good

precision is achieved. More data are thus needed on the behaviour of silica in winter in the Scheldt due to the imprecision for this period in our study.

BSi dissolution

The assumed contribution of the BSi dissolution in our mass-balance calculations was in agreement with those estimated by Arndt and Regnier (2007) and Arndt (2008) using model simulations. But, due to the importance of the BSi dissolution in other estuaries (see above), this process deserves to be better constrained. Results from the dissolution experiments and benthic flux measurements performed (Rebreanu 2009) in the Schledt estuary may for instance be implemented in our silica mass-balances.

Our BSi dissolution flux of 1.5 mmol m^{-2} d^{-1} prevailing from mid May to mid December (corresponding to the net DSi release in late summer and autumn of 400 kmol d^{-1}, Chapter 4) is in the same range of those estimated by Rebreanu (2009) from incubation experiments performed on cores sampled at three stations along the Scheldt estuary (summer and autumn 2005 and spring 2006, average ± SD: 1.1 ± 1.3 mmol m^{-2} d^{-1}, Rebreanu 2009), but about one order of magnitude higher than those estimated from interstitial DSi profiles at the same stations (spring, summer and autumn 2004 and 2005: 0.17 ± 0.14 mmol m^{-2} d^{-1}, Rebreanu 2009). However, not only did the average fluxes measured using the two methods differed by one order of magnitude, but fluxes measured using the same method displayed also an variability spanning over one order of magnitude. Additionally, no clear longitudinal or temporal pattern was highlighted (Rebreanu 2009). This important temporal and, especially, spatial variability may lead to a large imprecision in the direct estimation of BSi dissolution.

Furthermore, these fluxes were measured for sediment cores sampled in the navigation channel only, whereas higher fluxes are expected in lateral areas such as in mudflats, marshes or access channels to harbours, where mud deposits preferentially (Chapter 5): the BSi content determined along the navigation channel (generally less than 1 %, Rebreanu 2009) was indeed lower compared to that in the water column (2.5-4 %) or that deduced for deposited material (6 %) (Chapter 4). In addition, dredging activities in these depositional areas may result in an artificial temporal and spatial variability which appears difficult to assess.

Finally, despite a relatively low depth, BSi dissolution in the water column cannot be ruled out due to the amount of detrital BSi in the water column (Chapter 5) and to the

efficiency of the resuspension processes (Chen et al. 2005). As observed in the shallow Jiaozhou Bay (Liu et al. 2008), this source may even exceed the benthic fluxes. The contribution of the dissolution in the water column may be directly evaluated using silica stable isotopes; this can be performed concomitantly with the estimation of the BSi production (Beucher et al. 2004) or separately (e.g. Brzezinski et al. 2003).

Gross DSi uptake

The contribution of the BSi dissolution may also be estimated as the difference between the net balance of DSi and the gross DSi consumption. The latter may be directly obtained by 1) ecological model simulations that take into account the grazing pressure (e.g. Soetaert et al. 1994), 2) the direct measurement of the net phytoplankton growth, although the estimation of the phytoplankton respiration may be problematic in the Scheldt (Kromkamp and Peene 1995), or 3) the direct measurement of the DSi consumption using ^{32}Si. In contrast to the last method, the first two ones would require the use of a Si/C conversion factor, which may be a source of uncertainty.

Silica and carbon uptake are uncoupled in diatoms: diatoms can also incorporate silica in the dark (Claquin and Martin-Jézéquel 2005) and the relationship between Si uptake and depth (and thus light availability) is not expected to be as direct as it is for carbon. To obtain an accurate estimate of the *in situ* DSi uptake, incorporation experiments should then be performed on water sampled at different depths. Also, the *in situ* light intensity and temperature have to be reproduced during the incubations (as performed e.g. by Tréguer et al. 1991, Brzezinski et al. 1997 or Leynaert et al. 2001), which was not possible with our incubators.

Furthermore, because of diatom growth during the incubations, our incorporation experiments indicated that the consumption of DSi increased exponentially versus time (under constant light). Short time incubations (e.g. a few hours) may provide DSi consumption rates similar to those prevailing at the start of the incubation, but the diurnal variation of the light intensity would not be taken into account. In contrast, the importance of the grazing pressure in the Scheldt estuary cannot be neglected if DSi consumption rates are measured by performing 24 hours on-deck incubations at different light attenuations (as e.g. in Leynaert et al. 2001). However, assuming that the grazing pressure in the incubation bottles would be identical to that *in situ*, DSi consumption rates may be estimated by performing incubations on non pre-filtered water.

BSi accumulation

In the estuary, DSi and BSi fluxes could be directly calculated at the freshwater end-member but only the annual DSi flux could accurately be estimated at the seawater end-member. In our study, the annual BSi flux at the mouth of the estuary was deduced from a SPM mass-balance taken from the literature, but there was no evidence that this mass-balance was applicable to our study period. This BSi flux could have been also assessed as the closing term of the silica mass-balance if the net silica accumulation in sediments was known. However, as for the benthic flux, the latter may not be easily estimated due to the spatial and temporal (short-term and seasonal) variability of the SPM deposition (Van Maldegem et al. 1993; Fettweis et al. 1998; Chen et al. 2005) and of the BSi content in the sediment (Rebreanu 2009). In addition, the amount of BSi removed during dredging activities should be taken into account.

This should in addition provide the opportunity to better study the extent of the coupling (and/or decoupling) between the BSi and SPM dynamics. Also, the origin of the BSi (frustules of living or dead diatoms, phytoliths) should be investigated by microscopic observations and compared to the results obtained within this study at the scale of the ecosystem.

6.3 Inter-annual and long-term variations

Influence of freshwater discharge

Inter-annual variations in the silica dynamics in the Scheldt tidal system should be investigated. Our study was performed during rather dry years (Table 2.2 in Chapter 2), and different results may be obtained during years with a higher discharge. In the tidal river, the DSi retention is expected to decrease with increasing water discharge (Chapter 3). In contrast, no simple relation can be put forward for the total silica retention: the BSi production may be maximum at an intermediate water discharge (Chapter 3) but the fraction that would settle may decrease with increasing water discharge due to higher currents.

In the estuary, the diatom production seems to be unaffected by the residual freshwater discharge (Chapter 4) so the percentage of DSi retained in the estuary should decrease with increasing freshwater discharge due to higher DSi inputs at the freshwater end-member. Here again, no simple relationship can be assumed for BSi deposition in the estuary as the latter

depends for a large part on the amount of BSi carried by the tidal river. In addition, a higher winter freshwater discharge, which would result in a higher amount of DSi brought to the coastal zone in early spring (Chapter 4), may enhance the spring diatom bloom in the coastal zone, and possibly more BSi could be imported into the estuary.

The pattern of the DSi consumption and the complex SPM dynamics in the tidal river were well retrieved in model simulations performed by Arndt et al. (2007). Due to the link between BSi dynamics and those of the diatoms and of the SPM in both the tidal river and the estuary, modelling may thus appear as a powerful tool to tackle the problem of the inter-annual variations of the BSi (and thus total silica) retention in the Scheldt tidal system. This highlights the necessity to pursue modelling studies as they may be helpful not only to understand the functioning of the ecosystem, but also to predict its responses to changes, which may be difficult to investigate experimentally.

Long-term evolution of the silica cycle in the Scheldt tidal system

Past evolution related to the improvement of the water quality

Soetaert et al. (2006) reported the long term evolution of freshwater discharge, nutrients and oxygen in the Scheldt tidal system since the seventies. The annual discharge displayed significant inter-annual variations (between 100 and 200 m^3 s^{-1}, linked to the precipitation), but no long-term evolution was highlighted. In contrast, annual average DSi concentrations decreased regularly in the tidal river and in the estuary, suggesting that the changes in the biogeochemical behaviour of silica in the Scheldt during the last decades were due to other factors than water discharge.

Studies performed in the late 60s revealed that the summer DSi concentration at the freshwater end-member in the estuary (230 µmol L^{-1}, Wollast and De Broeu 1971) was similar to the annual average DSi concentration (Soetaert et al. 2006). In later studies performed in 1973, DSi concentrations at the freshwater end-member remained high all year-round at about 200-280 µmol L^{-1} (Beckers and Wollast 1976; Wollast 1978). All this suggests that, in contrast to what is observed nowadays, DSi was not consumed in the tidal river in summer. The diatom growth was probably hampered by persitent anoxic conditions (Soetaert et al. 2006), pollution (e.g. by trace metals, Zwolsman and Van Eck 1993; Bouezmarni and Wollast 2005) and/or probably higher SPM concentrations (Chen et al. 2005). The silica behaviour in the estuary was also very different in the 70s: DSi was entirely consumed in the zone of salinity 0-15 in summer (Wollast and De Broeu 1971; Wollast 1978), where

important chlorophyll *a* concentrations could also be reached (Soetaert et al. 2006). Low oxygen concentrations along almost the entire salinity gradient (Soetaert et al. 2006) may have resulted in a low grazing pressure due to the absence of copepods (which are more sensitive to low oxygen concentrations than phytoplankton).

Also, the fact that the DSi concentrations in the tidal river in the 60s and 70s were identical to that observed nowadays in winter (this study; Struyf et al. 2004; Van Damme et al. 2005) implies that the long-term decrease observed by Soetaert et al. (2006) was not due to a variation of the DSi concentration in the inputs, but principally to the increase of the DSi consumption by diatoms, presumably enhanced by the improvement of the water quality in the tidal river as also pointed out by Chou and Wollast (2006).

Future water quality enhancement and possible effects

Although the water quality in the Scheldt has been significantly improved during the last decades, further efforts were required (Van Damme et al. 2005; Soetaert et al. 2006). At the time of these studies, as well as during our study period, the Wastewater Treatment Plant of the North of Brussels (www.aquiris.be) was not yet completed and two third of the wastewaters from Brussels were still discharged into the Scheldt via the Zenne. The station became operational in March 2007, resulting in reduced organic matter and ammonium input loads to the Scheldt and thus in enhanced oxygen concentrations (Vanderborght et al. 2007; J.-P. Vanderborght, LOCGE-ULB, pers. comm.).

The historical evolution of the silica dynamics in the Scheldt suggests that this improvement in the water quality may result in significant changes in the silica cycle in the Scheldt tidal system. The overall effects are nevertheless difficult to predict. A higher water transparency may lead to an earlier development of the diatom bloom, reducing significantly the DSi fluxes to the coastal zone in spring and early summer. In contrast, a higher oxygen level at the confluence with the Rupel (Vanderborght et al. 2007) may lead to an upstream shift of copepods which were previously confined in the estuary due to too low oxygen conditions (such as the calanoid copepod *Erythemora affinis* which has generally its optimum in the freshwater, Appeltans et al. 2003; Tackx et al. 2004). As these species could effectively control the diatom growth in the estuary (Chapter 5), one could expect that this shift may result in a decrease of the DSi consumption in the tidal river. This should also directly affect the DSi and BSi concentrations in the upstream part of the estuary. Conversely, the phytoplankton and BSi distribution in the downstream part of the estuary, which are more

influenced by the conditions prevailing in the coastal zone, may also change due to altered silica (see above) and nitrogen fluxes to the coastal zone (Vanderborght et al. 2007).

As for the inter-annual variations, the effects of these changes may also be investigated using model simulations. They would however require the implementation of the description of the grazing pressure.

Restoration of intertidal areas

Finally, in addition to sea level rise and climate change, the Scheldt will undergo future artificial morphological changes (such as the deepening of the channel downstream of Antwerp), which will certainly alter the hydrodynamics and the ecological and biogeochemical functioning of the estuary (Meire et al. 2005). In particular, large intertidal habitats will be restored in flood control areas with controlled reduced tidal regimes (Meire et al. 2005; Maris et al. 2007). As for the intertidal marshes, their presence may affect the silica cycle in the Scheldt (Jacobs et al. 2008). Together with enhanced sedimentation rates, they could act as an important sink for BSi (Maris et al. 2007; Jacobs et al. 2008). As in natural marshes, part of this BSi may be recycled (Struyf et al. 2006; Jacobs et al. 2008). For example, in the 6 km² flood control area of "Kruibeke-Bazel-Rupelmonde", dissolution may possibly be enhanced due to the presence of brackish water (Maris et al. 2007). However, compared to the natural marshes and mudflats, the maintained low water height, dynamics and turbidity in these new intertidal areas should also favour benthos development (Maris et al. 2007). DSi may thus get consumed in such areas (Jacobs et al. 2008) even earlier than in the main channel, due to better light conditions and weaker hydrodynamic constraints. Also, because of the influence of the intertidal zones on the nitrogen cycle and oxygen concentrations, the presence of several flood control areas with controlled reduced tides along the Scheldt may result in a significant enhancement of the water quality in the main channel (Maris et al. 2007), which may in turn affect the silica cycle in the same way as described above for wastewater treatment.

6.4 Conclusions

Phytoplankton, nutrients and SPM dynamics in the Scheldt tidal system have been extensively investigated in several previous studies (see Chapter 2). Lately, studies focused on the long-term evolution of DSi (Van Damme et al. 2005; Soetaert et al. 2006) or on the silica cycle in marshes (Struyf et al. 2006, 2007), and model simulations were conducted to examine

the DSi fluxes and retention (Arndt et al. 2007, 2009; Arndt and Regnier 2007). Our study has been the first one to experimentally investigate the dynamics and the mass-balances of both DSi and BSi in the Scheldt tidal system, at least since the 70s. BSi concentrations have almost never been measured before. Results from this study indicate that BSi is an important constituent of the silica pool available at biological time-scales, but that their dynamics may be different from that of DSi or of the phytoplankton.

The Scheldt tidal system acts as an important sink for silica due to the conversion of a large fraction of the riverine DSi load into BSi, which in turn deposit entirely in the estuary together with large amounts of BSi imported from the adjacent coastal zone. Our study highlights thus the necessity to take BSi dynamics into account when the biogeochemical behaviour of silica in estuaries is investigated. Also, estuaries should not be considered only as filters of dissolve and particulate material of riverine origin; the import of material from the coastal was recognized as a key feature for the functioning of the estuarine silica dynamics and retention.

Although some features concerning the biogeochemical behaviour of silica in estuaries seem to present similarities, the functioning of the estuarine silica cycle appears to be site-specific. However, despite the recognition of the importance of the silica retention in the land to ocean continuum, studies about the silica cycle in estuaries are scarce and, in particular, BSi dynamics have rarely been investigated and further studies are thus required.

Finally, the understanding of the silica dynamics in the Scheldt may also benefit from additional complementary investigations. Besides a direct estimation of the gross BSi production, dissolution and accumulation, the inter-annual variability should be examined. The study of silica dynamics in the Scheldt should also be pursued as they are expected to be affected by the current improvement of the water quality and the recovery of intertidal areas in the Scheldt. This evolution offers as well the opportunity to acquire valuable knowledge about the effects of the restoration of the ecological status on silica dynamics.

6.5 References

Arndt S, Vanderborght J-P, Regnier P (2007) Diatom growth response to physical forcing in a macrotidal estuary: Coupling hydrodynamics, sediment transport, and biogeochemistry. J Geophys Res 112:C05045

Arndt S, Regnier P (2007) A model for the benthic-pelagic coupling of silica in estuarine ecosystems: sensitivity analysis and system scale simulation. Biogeosciences 4:331-352

Arndt S (2008) Physical controls on the biogeochemical structure and functioning of a land-ocean transition system (Chapter 6). In: Arndt S. Biogeochemical transformations and fluxes in redox-stratified environments: from the shallow coastal ocean to the deep subsurface. Ph. D. thesis. Univ. of Utrecht, The Netherlands. pp 147-179.

Arndt S, Regnier P, Vanderborght J-P (2009) Seasonally-resolved nutrient export fluxes and filtering capacities in a macrotidal estuary. J Mar Syst (in press). DOI 10.1016/j.jmarsys.2009.02.008

Beckers O, Wollast R (1976) Comportement de la silice dissoute dans l'estuaire de l'Escaut. In: Nihoul JCJ, Wollast R (eds) Projet Mer, Rapport Final. Volume 10: L'Estuaire de l'Escaut. Services du Premier Ministre, programmation de la Politique Scientifique, Bruxelles. pp 153-170 (In French).

Beucher C, Tréguer P, Corvaisier R, Hapette AM, Elskens M (2004) Production and dissolution of biosilica, and changing microphytoplankton dominance in the Bay of Brest (France). Mar Ecol Prog Ser 267:57-69

Bouezmarni M, Wollast R (2005) Geochemical composition of sediments in the Scheldt estuary with emphasis on trace metals. Hydrobiologia 540(1-3):155-168

Brzezinski MA, Phillips DR, Chavez FP, Friederich GE, Dugdale RC (1997) Silica production in the Monterey, California, upwelling; system. Limnology and Oceanography 42(8):1694-1705

Brzezinski MA, Jones JL, Bidle KD, Azam F (2003) The balance between silica production and silica dissolution in the sea: Insights from Monterey Bay, California, applied to the global data set. Limnol Oceanogr 48(5):1846-1854

Chen MS, Wartel S, Van Eck B, Van Maldegem D (2005) Suspended matter in the Scheldt estuary. Hydrobiologia 540(1-3):79-104

Chou L, Wollast R (2006) Estuarine silicon dynamics. In: Ittekot V, Unger D, Humborg C, TacAn N (eds) The silicon cycle. Human perturbations and impacts on aquatic systems. SCOPE 66. Island Press, Washington, Covelo, London. pp 93-120.

Claquin P, Martin-Jézéquel V (2005) Regulation of the Si and C uptake and of the soluble free-silicon pool in a synchronised culture of *Cylindrotheca fusiformis* (Bacillariophyceae): effects on the Si/C ratio. Mar Biol 146:877-886

Conley DJ (1997) Riverine contribution of biogenic silica to the oceanic silica budget. Limnol Oceanogr 42(4):774-777

D'Elia CF, Nelson DM, Boynton WR (1983) Chesapeake Bay nutrient and plankton dynamics: III. The annual cycle of dissolved silicon. Geochim Cosmochim Acta 47:1945-1955

Dixit S, Van Cappellen P, van Bennekom AJ (2001) Processes controlling solubility of biogenic silica and pore water build-up of silicic acid in marine sediments. Marine Chemistry 73(3-4):333-352

Fettweis M, Sas M, Monbaliu J (1998) Seasonal, neap-spring and tidal variation of cohesive sediment concentration in the Scheldt estuary, Belgium. Estuar Coast Shelf Sci 47:21-36

Friedrichs CT (1995) Stability shear stress and equilibrium cross-sectional geometry of sheltered tidal channels. Journal of Coastal Research 11(4):1062-1074

Jacobs S, Struyf E, Maris T, Meire P (2008) Spatiotemporal aspects of silica buffering in restored tidal marshes. Estuar Coast Shelf Sci 80(1):42-52

Kromkamp JC, Peene J (1995) Possibility of net phytoplankton primary production in the turbid Schelde Estuary (SW Netherlands). Mar Ecol Prog Ser 121:249-259

Leynaert A, Treguer P, Lancelot C, Rodier M (2001) Silicon limitation of biogenic silica production in the Equatorial Pacific. Deep Sea Research Part I: Oceanographic Research Papers 48(3):639-660

Liu SM, Ye XW, Zhang J, Zhang GS, Wu Y (2008) The silicon balance in Jiaozhou Bay, North China. J Mar Syst 74:639-648

Loucaides S, Van Cappellen P, Behrends T (2008) Dissolution of biogenic silica from land to ocean: Role of salinity and pH. Limnol Oceanogr 53(4):1614-1621

Maris T, Cox T, Temmerman S, De Vleeschauwer P, Van Damme S, De Mulder T, Van den Bergh E, Meire P (2007) Tuning the tide: creating ecological conditions for tidal marsh development in a flood control area. Hydrobiologia 588:31-43

Meire P, Ysebaert T, Van Damme S, Van den Bergh E, Maris T, Struyf E (2005) The Scheldt estuary: a description of a changing ecosystem. Hydrobiologia 540(1-3):1-11

Muylaert K, Raine R (1999) Import, mortality and accumulation of coastal phytoplankton in a partially mixed estuary (Kinsale harbour, Ireland). Hydrobiologia 412:53-65

Muylaert K, Sabbe K, Vyverman W (2009) Changes in phytoplankton diversity and community composition along the salinity gradient of the Schelde estuary (Belgium/The Netherlands). Estuar Coast Shelf Sci 82:335-340

Nedwell DB, Trimmer M (1996) Nitrogen fluxes through the upper estuary of the Great Ouse, England: the role of the bottom sediments. Mar Ecol Prog Ser 142:273-286

Pastuszak M, Conley DJ, Humborg C, Witek Z, Sitek S (2008) Silicon dynamics in the Oder estuary, Baltic Sea. J Mar Syst 73:250-262

Ragueneau O, Tréguer P, Leynaert A, Anderson RF, Brzezinski MA, DeMaster DJ, Dugdale RC, Dymond J, Fischer G, Francois R, Heinze C, Maier-Reimer E, Martin-Jézéquel V, Nelson DM, Quéguiner B (2000) A review of the Si cycle in the modern ocean: recent progress and missing gaps in the application of biogenic opal as a paleoproductivity proxy. Glob Planet Change 26(4):317-365

Ragueneau O, Chauvaud L, Moriceau B, Leynaert A, Thouzeau G, Donval A, Le Loc'h F, Jean F (2005) Biodeposition by an invasive suspension feeder impacts the biogeochemical cycle of Si in a coastal ecosystem (Bay of Brest, France). Biogeochemistry 75:19-41

Rebreanu L (2009) Study of the Si biogeochemical cycle in the sediments of the Scheldt Continuum (Belgium/The Netherlands). Ph. D. thesis. Université Libre de Bruxelles, Belgium.

Rendell AR, Horrobin TM, Jickells TD, Edmunds HM, Brown J, Malcom SJ (1997) Nutrient cycling in the Great Ouse estuary and its impact on nutrient fluxes to The Wash, England. Estuar Coast Shelf Sci 45(5):653-668

Roubeix V (2007) Transformations biogéochimiques et transfert du silicium dans la zone de transition fleuve-mer : le rôle des diatomées planctoniques. Ph. D. thesis. Université Libre de Bruxelles, Belgium. (In French and English)

Roubeix V, Lancelot C (2008) Effect of salinity on growth, cell size and silicification of an euryhaline freshwater diatom: *Cyclotella meneghiniana* Kütz. Transit Water Bull 1:31-38

Soetaert K, van Rijswijk P (1993) Spatial and temporal patterns of the zooplankton in the Westerschelde estuary. Mar Ecol Prog Ser 97:47-59

Soetaert K, Herman PMJ, Kromkamp JC (1994) Living in the twilight: estimating net phytoplankton growth in the Westerschelde estuary (The Netherlands) by means of an ecosystem model (MOSES). J Plankton Res 16:1277-1301

Soetaert K, Middelburg JJ, Heip C, Meire P, Van Damme S, Maris T (2006) Long-term change in dissolved inorganic nutrients in the heterotrophic Scheldt estuary (Belgium, The Netherlands). Limnol Oceanogr 51(1, part 2):409-423

Struyf E, Van Damme S, Meire P (2004) Possible effects of climate change on estuarine nutrient fluxes: a case study in the highly nutrified Schelde estuary (Belgium, The Netherlands). Estuar Coast Shelf Sci 60(4):649-661

Struyf E, Dausse A, Van Damme S, Bal K, Gribsholt B, Boschker HTS, Middelburg JJ, Meire P (2006) Tidal marshes and biogenic silica recycling at the land-sea interface. Limnol Oceanogr 51(2):836-846

Struyf E, Temmerman S, Meire P (2007) Dynamics of biogenic Si in freshwater tidal marshes: Si regeneration and retention in marsh sediments (Scheldt estuary). Biogeochemistry 82:41-53

Treguer P, Van Bennekom AJ, Leynaert A, Panouse M, Jacques G (1991) Production of biogenic silica in the Weddell-Scotia Seas measured with 32Si. Limnology and Oceanography 36(6):1217-1227

Triplett LD, Engstrom DR, Conley DJ, Schellhaass SM (2008) Silica fluxes and trapping in two contrasting natural impoundments of the upper Mississippi River. Biogeochemistry 87:217-230

Van Damme S, Struyf E, Maris T, Ysebaert T, Dehairs F, Tackx M, Heip C, Meire P (2005) Spatial and temporal patterns of water quality along the estuarine salinity gradient of the Scheldt estuary (Belgium and The Netherlands): results of an integrated monitoring approach. Hydrobiologia 540(1-3):29-45

Van Maldegem DC, Mulder HPJ, Langerak A (1993) A cohesive sediment balance for the Scheldt Estuary. Neth J Aquat Ecol 27(2-4):247-256

Vanderborght J-P, Folmer IM, Aguilera DR, Uhrenholdt T, Regnier P (2007) Reactive-transport modelling of C, N, and O_2 in a river-estuarine-coastal zone system: Application to the Scheldt estuary. Marine Chemistry 106:92-110

Wartel S (1977) Composition, transport and origin of sediments in the Scheldt estuary. Geologie en mijnbouw 56(3):219-233

Wollast R, De Broeu F (1971) Study of the behavior of dissolved silica in the estuary of the Scheldt. Geochim Cosmochim Acta 35:613-620

Wollast R (1978) Modelling of biological and chemical processes in the Scheldt estuary. In: Nihoul JCJ (eds) Hydrodynamics of Estuaries and Fjords. Elsevier Oceanography Series, 23, Amsterdam, Oxford, New-York. pp 63-77.

Yamada SS, D'Elia CF (1984) Silicic acid regeneration from estuarine sediment cores. Mar Ecol Prog Ser 18:113-118

Zwolsman JJG, Van Eck GTM (1993) Dissolved and particulate trace metal geochemistry in the Scheldt estuary, S.W. Netherlands (water column and sediments). Neth J Aquat Ecol 27(2-4):287-300

7 General bibliography

Abril G, Nogueira M, Etcheber H, Cabeçadas G, Lemaire E, Brogueira MJ (2002) Behaviour of organic carbon in nine contrasting European estuaries. Estuar Coast Shelf Sci 54:241-262

Admiraal W, Breugem P, Jacobs DMLHA, de Ruyter van Steveninck ED (1990) Fixation of dissolved silicate and sedimentation of biogenic silicate in the lower river Rhine during diatom blooms. Biogeochemistry 9:175-185

Alexandre A, Meunier J-D, Colin F, Koud J-M (1997) Plant impact on the biogeochemical cycle of silicon and related weathering processes. Geochim Cosmochim Acta 61(3):677-682

Anderson GF (1986) Silica, diatoms and a freshwater productivity maximum in Atlantic coastal plain estuaries, Chesapeake Bay. Estuar Coast Shelf Sci 22:183-197

Antajan E, Chrétiennot-Dinet M-J, Leblanc C, Daro M-H, Lancelot C (2004) 19'-hexanoyloxyfucoxanthin may not be the appropriate pigment to trace occurrence and fate of *Phaeocystis*: the case of *P. globosa* in Belgian coastal waters. J Sea Res 52:165-177

Appelo CAJ, Postma D (eds) (1996) Geochemistry, groundwater and pollution. A.A.Balkema, Rotterdam.

Appeltans W, Hannouti A, Van Damme S, Soetaert K, Vanthomme D, Tackx M (2003) Zooplankton in the Schelde estuary (Belgium/The Netherlands). The distribution of *Eurytemora affinis*: effect of oxygen? J Plankton Res 25(11):1441-1445

Arndt S, Vanderborght J-P, Regnier P (2007) Diatom growth response to physical forcing in a macrotidal estuary: Coupling hydrodynamics, sediment transport, and biogeochemistry. J Geophys Res 112:C05045

Arndt S, Regnier P (2007) A model for the benthic-pelagic coupling of silica in estuarine ecosystems: sensitivity analysis and system scale simulation. Biogeosciences 4:331-352

Arndt S (2008) Physical controls on the biogeochemical structure and functioning of a land-ocean transition system (Chapter 6). In: Arndt S. Biogeochemical transformations and fluxes in redox-stratified environments: from the shallow coastal ocean to the deep subsurface. Ph. D. thesis. Univ. of Utrecht, The Netherlands. pp 147-179.

Arndt S, Regnier P, Vanderborght J-P (2009) Seasonally-resolved nutrient export fluxes and filtering capacities in a macrotidal estuary. J Mar Syst (in press). DOI 10.1016/j.jmarsys.2009.02.008

Baeyens W, Van Eck B, Lambert C, Wollast R, Goeyens L (1998) General description of the Scheldt estuary. Hydrobiologia 366:1-14

Beckers O, Wollast R (1976) Comportement de la silice dissoute dans l'estuaire de l'Escaut. In: Nihoul JCJ, Wollast R (eds) Projet Mer, Rapport Final. Volume 10: L'Estuaire de l'Escaut. Services du Premier Ministre, programmation de la Politique Scientifique, Bruxelles. pp 153-170 (In French).

Beucher C, Tréguer P, Corvaisier R, Hapette AM, Elskens M (2004) Production and dissolution of biosilica, and changing microphytoplankton dominance in the Bay of Brest (France). Mar Ecol Prog Ser 267:57-69

Bidle KD, Azam F (1999) Accelerated dissolution of diatom silica by marine bacterial assemblages. Nature 397:508-512

Billen G, Lancelot C, Meybeck M (1991) N, P, and Si retention along the aquatic continuum from land to ocean. In: Mantoura RFC, Martin J-M, Wollast R (eds) Ocean Margin Processes in Global Change, Dahlem Workshop Report. Wiley-Interscience pp 19-44.

Billen G, Garnier J, Rousseau V (2005) Nutrient fluxes and water quality in the drainage network of the Scheldt basin over the last 50 years. Hydrobiologia 540(1-3):47-67

Blecker SW, McCulley RL, Chadwick OA, Kelly EF (2006) Biologic cycling of silica across a grassland bioclimosequence. Glob Biogeochem Cycle 20:GB3023

Boschker HTS, Kromkamp JC, Middelburg JJ (2005) Biomarker and carbon isotopic constraints on bacterial and algal community structure and functioning in a turbid, tidal estuary. Limnol Oceanogr 50(1):70-80

Bouezmarni M, Wollast R (2005) Geochemical composition of sediments in the Scheldt estuary with emphasis on trace metals. Hydrobiologia 540(1-3):155-168

Brochard CJE, Koeman RPT, de Keijzer-de Haan AL, Verweij GL, Fockens K, Esselink P (2005) Biomonitoring van fytoplankton in de Nederlandse zoute wateren 2004, kite-diagrammen. Koeman en bijkerk bv, ecologisch onderzoek en advies, Haren, The Netherlands. (In Dutch)

Brochard CJE, Koeman RPT, de Keijzer-de Haan AL, Verweij GL, van Wezel R, Fockens K, Esselink P (2006) Biomonitoring van fytoplankton in de Nederlandse zoute wateren 2005, kite-diagrammen. Koeman en bijkerk bv, ecologisch onderzoek en advies, Haren, The Netherlands. (In Dutch)

Brzezinski MA (1985) The Si:C:N ratio of marine diatoms: interspecific variability and the effect of some environmental variables. J Phycol 21:347-357

Brzezinski MA, Phillips DR (1997) Evaluation of ^{32}Si as a tracer for measuring silica production rates in marine waters. Limnol Oceanogr 42(5):856-865

Brzezinski MA, Phillips DR, Chavez FP, Friederich GE, Dugdale RC (1997) Silica production in the Monterey, California, upwelling; system. Limnology and Oceanography 42(8):1694-1705

Brzezinski MA, Jones JL, Bidle KD, Azam F (2003) The balance between silica production and silica dissolution in the sea: Insights from Monterey Bay, California, applied to the global data set. Limnol Oceanogr 48(5):1846-1854

Canfield DE, Kristensen E, Thamdrup B (2005) The Silicon Cycle. In: Canfield DE, Kristensen E, Thamdrup B (eds) Aquatic Geomicrobiology. Advances in Marine Biology 48. Academic Press, Elsevier pp 441-463.

Carbonnel V (2003) Mise au point d'une méthodologie pour la détermination de la silice biogène dans le milieu estuarien. Mémoire présenté en vue de l'obtention d'un DEA en Sciences de la Terre et Géographie. Univ. Libre de Bruxelles, Belgium. (In French)

Cary L, Alexandre A, Meunier J-D, Boeglin J-L, Braun J-J (2005) Contribution of phytoliths to the suspended load of biogenic silica in the Nyong basin rivers (Cameroon). Biogeochemistry 74:101-104

Chen MS, Wartel S, Van Eck B, Van Maldegem D (2005) Suspended matter in the Scheldt estuary. Hydrobiologia 540(1-3):79-104

Chen MS, Wartel S, Temmerman S (2005) Seasonal variation of floc characteristics on tidal flats, the Scheldt estuary. Hydrobiologia 540(1-3):181-195

Chou L, Wollast R (2006) Estuarine silicon dynamics. In: Ittekot V, Unger D, Humborg C, TacAn N (eds) The silicon cycle. Human perturbations and impacts on aquatic systems. SCOPE 66. Island Press, Washington, Covelo, London. pp 93-120.

Claquin P, Martin-Jézéquel V, Kromkamp JC, Veldhuis MJW, Kraay GW (2002) Uncoupling of silicon compared with carbon and nitrogen metabolisms and the role of the cell cycle in continuous cultures of *Thalassiosira pseudonana* (Bacillariophyceae) under light, nitrogen, and phosphorus control. J Phycol 38:922-930

Claquin P, Martin-Jézéquel V (2005) Regulation of the Si and C uptake and of the soluble free-silicon pool in a synchronised culture of *Cylindrotheca fusiformis* (Bacillariophyceae): effects on the Si/C ratio. Mar Biol 146:877-886

Claquin P, Leynaert A, Sferratore A, Garnier J, Ragueneau O (2006) Physiological ecology of diatoms along the river-sea continuum. In: Ittekot V, Unger D, Humborg C, TacAn N (eds) The silicon cycle. Human perturbations and impacts on aquatic systems. SCOPE 66. Island Press, Washington, Covelo, London. pp 121-137.

Conley DJ, Kilham SS (1989) Differences in silica content between marine and freshwater diatoms. Limnol Oceanogr 34(1):205-213

Conley DJ, Schelske CL, Stoermer EF (1993) Modification of the biogeochemical cycle of silica with eutrophication. Mar Ecol Prog Ser 101:179-192

Conley DJ (1997) Riverine contribution of biogenic silica to the oceanic silica budget. Limnol Oceanogr 42(4):774-777

Conley DJ (2002) Terrestrial ecosystems and the global biogeochemical silica cycle. Glob Biogeochem Cycle 16(4):68(1)-68(7)

Conley DJ, Likens GE, Buso DC, Saccone L, Bailey SW, Johnson CE (2008) Deforestation causes increased dissolved silicate losses in the Hubbard Brook Experimental Forest. Glob Change Biol 14(11):2548-2554

Conway HL, Harrison PJ (1977) Marine diatoms grown in chemostats under silicate or ammonium limitation. IV. Transient response of *Chaetoceros debilis*, *Skeletonema costatum*, and *Thalassiosira gravida* to a single addition of the limiting nutrient. Mar Biol 43:33-43

Correll DL, Jordan TE, Weller DE (2000) Dissolved silicate dynamics of the Rhode River watershed and estuary. Estuaries 23(2):188-198

Cushing DH (1989) A difference in structure between ecosystems in strongly stratified waters and in those that are only weakly stratified. J Plankton Res 11(1):1-13

D'Elia CF, Nelson DM, Boynton WR (1983) Chesapeake Bay nutrient and plankton dynamics: III. The annual cycle of dissolved silicon. Geochim Cosmochim Acta 47:1945-1955

Datnoff LE, Snyder GH, Korndorfer GH (eds) (2001) Silicon in agriculture. Studies in Plant Science 8. Elsevier B.V.

De Jong DJ, De Jonge VN (1995) Dynamics and distribution of microphytobenthic chlorophyll-*a* in the Western Scheldt estuary (SW Netherlands). Hydrobiologia 311:21-31

De Jonge VN, van Beusekom JEE (1995) Wind- and tide-induced resuspension of sediment and microphytobenthos from tidal flats in the Ems estuary. Limnol Oceanogr 40(4):766-778

De Sève MA (1993) Diatom bloom in the tidal freshwater zone of a turbid and shallow estuary, Rupert Bay (James Bay, Canada). Hydrobiologia 269/270:225-233

Delstanche S (2004) Contribution à l'étude du cycle biogéochimique de la silice dans le continuum aquatique de l'Escaut. MSc. thesis. Université Catholique de Louvain, Belgium. (In French)

DeMaster DJ (1981) The supply and accumulation of silica in the marine environment. Geochimica et Cosmochimica Acta 45:1715-1732

Derry LA, Kurtz AC, Ziegler K, Chadwick OA (2005) Biological control of terrestrial silica cycling and export fluxes to watersheds. Nature 433:728-731

Desmit X, Vanderborght J-P, Regnier P, Wollast R (2005) Control of phytoplankton production by physical forcing in a strongly tidal, well-mixed estuary. Biogeosciences 2:205-218

Dijkman NA, Kromkamp JC (2006) Photosynthetic characteristics of the phytoplankton in the Scheldt estuary: community and single-cell fluorescence measurements. Eur J Phycol 41(4):425-434

Dijkman NA, Kromkamp JC (2006) Phospholipid-derived fatty acids as chemotaxonomic markers for phytoplankton: application for inferring phytoplankton composition. Mar Ecol Prog Ser 324:113-125

Dixit S, Van Cappellen P, van Bennekom AJ (2001) Processes controlling solubility of biogenic silica and pore water build-up of silicic acid in marine sediments. Marine Chemistry 73(3-4):333-352

Dougan WK, Wilson AL (1974) The absorptiometric determination of aluminium in water. A comparison of some chromogenic reagents and the development of an improved method. Analyst 99:413-430

Durbin EG (1977) Studies on the autoecology of the marine diatom *Thalassiosira Nordenskioeldii*. II. The influence of cell size on growth rate, and carbon, nitrogen,chlorophyll *a* and silica content. J Phycol 13(2):150-155

Ehrenhauss S, Witte U, Janssen F, Huettel M (2004) Decomposition of diatoms and nutrient dynamics in permeable North Sea sediments. Cont Shelf Res 24(6):721-737

Elliot M, McLusky DS (2002) The need for definitions in understanding estuaries. Estuar Coast Shelf Sci 55:815-827

Fettweis M, Sas M, Monbaliu J (1998) Seasonal, neap-spring and tidal variation of cohesive sediment concentration in the Scheldt estuary, Belgium. Estuar Coast Shelf Sci 47:21-36

Fettweis M, Van den Eynde D (2003) The mud deposits and the high turbidity in the Belgian-Dutch coastal zone, southern bight of the North Sea. Cont Shelf Res 23:669-691

Friedrichs CT (1995) Stability shear stress and equilibrium cross-sectional geometry of sheltered tidal channels. Journal of Coastal Research 11(4):1062-1074

Gallinari M, Ragueneau O, Corrin L, DeMaster DJ, Treguer P (2002) The importance of water column processes on the dissolution properties of biogenic silica in deep-sea sediments I. Solubility. Geochimica et Cosmochimica Acta 66(15):2701-2717

Garnier J, d'Ayguesvives A, Billen G, Conley DJ, Sferratore A (2002) Silica dynamics in the hydrographic network of the Seine River. Océanis 28(3-4):487-508

Gazeau F, Gattuso J-P, Middelburg JJ, Brion N, Schiettecatte L-S, Frankignoulle M, Borges AV (2005) Planktonic and whole system metabolism in a nutrient-rich estuary (the Scheldt estuary). Estuaries 28(6):868-883

Geider RJ (1987) Light and temperature dependence of the carbon to chlorophyll *a* ratio in microalgae and cyanobacteria: implications for physiology and growth of phytoplankton. New Phytol 106:1-34

Guillard RRL, Lorenzen CJ (1972) Yellow-green algae with chlorophyllide c. Journal of Phycology 8(1):10-14

Hein M, Pedersen MF, Sand-Jensen K (1995) Size-dependent nitrogen uptake in micro- and macroalgae. Mar Ecol Prog Ser 118:247-253

Hellings L, Dehairs F, Tackx M, Keppens E, Baeyens W (1999) Origin and fate of organic carbon in the freshwater part of the Scheldt Estuary as traced by stable carbon isotope composition. Biogeochemistry 47:167-186

Hildebrand M (2002) Lack of coupling between silicon and other elemental metabolisms in diatoms. J Phycol 38:841-843

Holmes GT (2008) Nutrient supply, water residence time, temperature, and grazing as controls of size-fractionated phytoplankton biomass in shallow temperate estuarine ecosystems. Dissertation Abstracts International 69(1):Suppl. B, 198p

Humborg C, Pastuszak M, Aigars J, Siegmund H, Mörth C-M, Ittekot V (2006) Decreased silica land-sea fluxes through damming in the Baltic Sea catchment - significance of particle trapping and hydrological alterations. Biogeochemistry 77:265-281

IRMB (Institut Royal Météorologique de Belgique) (2003-2004) Bulletins mensuels, Observations climatologiques, parties I et II. Institut Royal Météorologique de Belgique, Bruxelles. (In French/Dutch)

Jacobs S, Struyf E, Maris T, Meire P (2008) Spatiotemporal aspects of silica buffering in restored tidal marshes. Estuar Coast Shelf Sci 80(1):42-52

Jordan TE, Correll DL, Weller DE (1997) Relating nutrient discharges from watersheds to land use and streamflow variability. Water Resources Research 33(11):2579-2590

Kamatani A, Oku O (2000) Measuring biogenic silica in marine sediments. Mar Chem 68(3):219-229

Kelly EF, Chadwick OA, Hilinski TE (1998) The effect of plants on mineral weathering. Biogeochemistry 42:21-53

Koeman RPT, Brochard CJE, Fockens K, Verweij GL, Esselink P (2004) Biomonitoring van fytoplankton in de Nederlandse zoute wateren 2003, kite-diagrammen. Koeman en bijkerk bv, ecologisch onderzoek en advies, Haren, The Netherlands. (In Dutch)

Koroleff F (1983) Determination of silicon. In: Grasshoff K, Ehrhardt M, Kremling K (eds) Methods of seawater analysis. Second, revised and extended edition. Verlag Chemie, Weinheim, Deerfield Beach, Florida, Basel. pp 174-187.

Kristiansen S, Farbrot T, Naustvoll L-J (2000) Production of biogenic silica by spring diatoms. Limnol Oceanogr 45(2):472-478

Kromkamp JC, Peene J (1995) Possibility of net phytoplankton primary production in the turbid Schelde Estuary (SW Netherlands). Mar Ecol Prog Ser 121:249-259

Kromkamp JC, Peene J (2005) Changes in phytoplankton biomass and primary production between 1991 and 2001in the Westerschelde estuary (Belgium/The Netherlands). Hydrobiologia 540(1-3):117-126

Kronvang B, Bruhn AJ (1996) Choice of sampling strategy and estimation method for calculating nitrogen and phosphorus transport in small lowland streams. Hydrol Process 10:1483-1501

Lacroix G, Ruddick K, Ozer J, Lancelot C (2004) Modelling the impact of the Scheldt and Rhine/Meuse plumes on the salinity distribution in Belgian waters (southern North Sea). J Sea Res 52:149-163

Lancelot C (1995) The mucilage phenomenon in the continental coastal waters of the North Sea. Sci Total Environ 165(1-3):83-102

Lemaire E, Abril G, de Wit R, Etcheber H (2002) Distribution of phytoplankton pigments in nine European estuaries and implications for an estuarine typology. Biogeochemistry 59:5-23

Leynaert A, Treguer P, Lancelot C, Rodier M (2001) Silicon limitation of biogenic silica production in the Equatorial Pacific. Deep Sea Research Part I: Oceanographic Research Papers 48(3):639-660

Leynaert A, Bucciarelli E, Claquin P, Dugdale RC, Martin-Jézéquel V, Pondaven P, Ragueneau O (2004) Effect of iron deficiency on diatom cell size and silicic acid uptake kinetics. Limnol Oceanogr 49(4):1134-1143

Leynaert A, Tréguer P, Nelson DM, Del Amo Y (1996) ^{32}Si as a tracer of biogenic silica production: methodological improvements. In: Baeyens J, Dehairs F, Goeyens L (eds) Integrated marine system analysis. Minute of the first workshop meeting. VUB, Brussels, Belgium. pp 29-35.

Lionard M, Muylaert K, Van Gansbeke D, Vyverman W (2005) Influence of changes in salinity and light intensity on growth of phytoplankton communities from the Schelde river and estuary (Belgium/The Netherlands). Hydrobiologia 540(1-3):105-115

Lionard M (2006) Spatio-temporal phytoplankton dynamics along the Scheldt-North Sea continuum based on HPLC/CHEMTAX pigment analysis. Ph. D. thesis. Univ. of Ghent, Belgium.

Lionard M, Muylaert K, Tackx M, Vyverman W (2008) Evaluation of the performance of HPLC-CHEMTAX analysis for determining phytoplankton biomass and composition in a turbid estuary (Schelde, Belgium). Estuar Coast Shelf Sci 76(4):809-817

Lionard M, Muylaert K, Hanouti A, Maris T, Tackx M, Vyverman W (2008) Inter-annual variability in phytoplankton summer blooms in the freshwater tidal reaches of the Schelde estuary (Belgium). Estuar Coast Shelf Sci 79(4):694-700

Liu SM, Ye XW, Zhang J, Zhang GS, Wu Y (2008) The silicon balance in Jiaozhou Bay, North China. J Mar Syst 74:639-648

Llewellyn CA, Gibb SW (2000) Intra-class variability in the carbon, pigment and biomineral content of prymnesiophytes and diatoms. Mar Ecol Prog Ser 193:33-44

Loucaides S, Van Cappellen P, Behrends T (2008) Dissolution of biogenic silica from land to ocean: Role of salinity and pH. Limnol Oceanogr 53(4):1614-1621

Lucas CH, Banham C, Holligan PM (2001) Benthic-pelagic exchange of microalgae at a tidal flat. 2. Taxonomic analysis. Mar Ecol Prog Ser 212:39-52

Mackey MD, Mackey DJ, Higgins HW, Wright SW (1996) CHEMTAX - a program for estimating class abundances from chemical markers: application to HPLC measurements of phytoplankton. Mar Ecol Prog Ser 144:265-283

Maris T, Cox T, Temmerman S, De Vleeschauwer P, Van Damme S, De Mulder T, Van den Bergh E, Meire P (2007) Tuning the tide: creating ecological conditions for tidal marsh development in a flood control area. Hydrobiologia 588:31-43

Martin-Jézéquel V, Hildebrand M, Brzezinski MA (2000) Silicon metabolism in diatoms: implications for growth. J Phycol 36:821-840

McLusky DS (1993) Marine and estuarine gradients - an overview. Neth J Aquat Ecol 27(2-4):489-493

Meire P, Ysebaert T, Van Damme S, Van den Bergh E, Maris T, Struyf E (2005) The Scheldt estuary: a description of a changing ecosystem. Hydrobiologia 540(1-3):1-11

Michalopoulos P, Aller RC (2004) Early diagenesis of biogenic silica in the Amazon delta: alteration, authigenic clay formation, and storage. Geochim Cosmochim Acta 68(5):1061-1085

Moatar F, Meybeck M (2005) Compared performances of different algorithms for estimating annual nutrient loads discharged by the eutrophic River Loire. Hydrol Process 19:429-444

Moatar F, Person G, Meybeck M, Coynel A, Etcheber H, Crouzet P (2006) The influence of contrasting suspended particulate matter transport regimes on the bias and precision of flux estimates. Sci Total Environ 370:515-531

Moatar F, Meybeck M (2007) Riverine fluxes of pollutants: Towards predictions of uncertainties by flux duration indicators. C R Geosci 339:367-382

Muylaert K, Van Kerckvoorde A, Vyverman W, Sabbe K (1997) Structural characteristics of phytoplankton assemblages in tidal and non-tidal freshwater systems: a case study from the Schelde basin, Belgium. Freshw Biol 38:263-276

Muylaert K, Sabbe K (1999) Spring phytoplankton assemblages in and around the maximum turbidity zone of the estuaries of the Elbe (Germany), the Schelde (Belgium/The Netherlands) and the Gironde (France). Journal of Marine Systems 22(2-3):133-149

Muylaert K, Raine R (1999) Import, mortality and accumulation of coastal phytoplankton in a partially mixed estuary (Kinsale harbour, Ireland). Hydrobiologia 412:53-65

Muylaert K, Sabbe K, Vyverman W (2000) Spatial and temporal dynamics of phytoplankton communities in a freshwater tidal estuary (Schelde, Belgium). Estuar Coast Shelf Sci 50(5):673-687

Muylaert K, Van Wichelen J, Sabbe K, Vyverman W (2001) Effects of freshets on phytoplankton dynamics in a freshwater tidal estuary (Schelde, Belgium). Arch Hydrobiol 150(2):269-288

Muylaert K, Tackx M, Vyverman W (2005) Phytoplankton growth rates in the freshwater tidal reaches of the Schelde estuary (Belgium) estimated using a simple light-limited primary production model. Hydrobiologia 540(1-3):127-140

Muylaert K, Gonzales R, Franck M, Lionard M, van der Zee C, Cattrijsse A, Sabbe K, Chou L, Vyverman W (2006) Spatial variation in phytoplankton dynamics in the Belgian coastal zone of the North Sea studied by microscopy, HPLC-CHEMTAX and underway fluorescence recordings. J Sea Res 55:253-265

Muylaert K, Sabbe K, Vyverman W (2009) Changes in phytoplankton diversity and community composition along the salinity gradient of the Schelde estuary (Belgium/The Netherlands). Estuar Coast Shelf Sci 82:335-340

Muylaert K, Beszteri B, Huygh W, Chepurnov V, Sabbe K, Chou L, Vyverman W (in prep) Variability in Si-limited growth among *'Cyclotella meneghiniana'* strains from different geographic origins.

Nedwell DB, Trimmer M (1996) Nitrogen fluxes through the upper estuary of the Great Ouse, England: the role of the bottom sediments. Mar Ecol Prog Ser 142:273-286

Nelson DM, Tréguer P, Brzezinski MA, Leynaert A, Quéguiner B (1995) Production and dissolution of biogenic silica in the ocean: revised global estimates, comparison with regional data and relationship to biogenic sedimentation. Glob Biogeochem Cycle 9(3):359-372

Nelson DM, Brzezinski MA (1990) Kinetics of silicic acid uptake by natural diatom assemblages in two Gulf Stream warm-core rings. Mar Ecol Prog Ser 62:283-292

Nelson DM, Dortch Q (1996) Silicic acid depletion and silicon limitation in the plume of the Mississippi River: evidence from kinetic studies in spring and summer. Mar Ecol Prog Ser 136:163-178

Nielsen SL, Sand-Jensen K (1990) Allometric scaling of maximal photosynthetic growth rate to surface/volume ratio. Limnol Oceanogr 35(1):177-181

Officer CB, Ryther JH (1980) The possible importance of silicon in marine eutrophication. Mar Ecol Prog Ser 3:83-91

Pastuszak M, Conley DJ, Humborg C, Witek Z, Sitek S (2008) Silicon dynamics in the Oder estuary, Baltic Sea. J Mar Syst 73:250-262

Peterson DH, Smith RE, Hager SW, Harmon DD, Herndon RE, Schemel LE (1985) Interannual variability in dissolved inorganic nutrients in Northern San Francisco Bay Estuary. Hydrobiologia 129:37-58

Ploug H, Iversen MH, Koski M, Buitenhuis ET (2008) Production, oxygen respiration rates, and sinking velocity of copepod fecal pellets: Direct measurements of ballasting by opal and calcite. Limnol Oceanogr 53(2):469-476

Pondaven P, Gallinari M, Chollet S, Bucciarelli E, Sarthou G, Schultes S, Jean F (2007) Grazing-induced changes in cell wall silicification in a marine diatom. Protist 158:21-28

Prandle D, Hydes DJ, Jarvis J, McManus J (1997) The seasonal cycles of temperature, salinity, nutrients and suspended sediment in the southern North Sea in 1988 and 1989. Estuar Coast Shelf Sci 45:669-680

Ragueneau O, Tréguer P, Leynaert A, Anderson RF, Brzezinski MA, DeMaster DJ, Dugdale RC, Dymond J, Fischer G, Francois R, Heinze C, Maier-Reimer E, Martin-Jézéquel V, Nelson DM, Quéguiner B (2000) A review of the Si cycle in the modern ocean: recent progress and missing gaps in the application of biogenic opal as a paleoproductivity proxy. Glob Planet Change 26(4):317-365

Ragueneau O, Lancelot C, Egorov V, Vervlimmeren J, Cociasu A, Deliat G, Krastev A, Daoud N, Rousseau V, Popovitchev V (2002) Biogeochemical transformations of inorganic nutrients in the mixing zone between the Danube River and the north-western Black Sea. Estuar Coast Shelf Sci 54(3):321-336

Ragueneau O, Chauvaud L, Leynaert A, Thouzeau G, Paulet YM, Bonnet S, Lorrain A, Grall J, Corvaisier R, Le Hir M, Jean F, Clavier J (2002) Direct evidence of a biologically active coastal silicate pump: ecological implications. Limnol Oceanogr 47(6):1849-1854

Ragueneau O, Chauvaud L, Moriceau B, Leynaert A, Thouzeau G, Donval A, Le Loc'h F, Jean F (2005) Biodeposition by an invasive suspension feeder impacts the biogeochemical cycle of Si in a coastal ecosystem (Bay of Brest, France). Biogeochemistry 75:19-41

Ragueneau O, Savoye N, Del Amo Y, Cotten J, Tardiveau B, Leynaert A (2005) A new method for the measurement of biogenic silica in suspended matter of coastal waters: using Si:Al ratios to correct for the mineral interference. Cont Shelf Res 25(5-6):697-710

Ragueneau O, Conley DJ, Leynaert A, Ni Longphuirt S, Slomp CP (2006) Responses of coastal ecosystems to anthropogenic perturbations of silicon cycling. In: Ittekot V, Unger D, Humborg C, TacAn N (eds) The silicon cycle. Human perturbations and impacts on aquatic systems. SCOPE 66. Island Press, Washington, Covelo, London. pp 197-213.

Ragueneau O, Conley DJ, Leynaert A, Ni Longphuirt S, Slomp CP (2006) Role of diatoms in silicon cycling and coastal marine food webs. In: Ittekot V, Unger D, Humborg C, TacAn N (eds) The silicon cycle. Human perturbations and impacts on aquatic systems. SCOPE 66. Island Press, Washington, Covelo, London. pp 163-195.

Rapport Scaldit (2004) Analyse transnationale de l'état des lieux du District hydrographique international de l'Escaut : projet pilote pour le test des documents guides européens. Scaldit, Vlaamse Milieumaatschappij, Erembodegem. (In French)

Raven JA, Kübler JE (2002) New light on the scaling of metabolic rate with the size of algae. J Phycol 38:11-16

Raven JA, Waite AM (2004) The evolution of silicification in diatoms: inescapable sinking and sinking as escape? New Phytol 162:45-61

Rebreanu L (2009) Study of the Si biogeochemical cycle in the sediments of the Scheldt Continuum (Belgium/The Netherlands). Ph. D. thesis. Université Libre de Bruxelles, Belgium.

Regnier P, Wollast R, Steefel CI (1997) Long-term fluxes of reactive species in macrotidal estuaries: Estimates from a fully transient, multicomponent reaction-transport model. Mar Chem 58:127-145

Regnier P, Mouchet A, Wollast R, Ronday R (1998) A discussion of methods for estimating residual fluxes in strong tidal estuaries. Cont Shelf Res 18:1543-1571

Rendell AR, Horrobin TM, Jickells TD, Edmunds HM, Brown J, Malcom SJ (1997) Nutrient cycling in the Great Ouse estuary and its impact on nutrient fluxes to The Wash, England. Estuar Coast Shelf Sci 45(5):653-668

Reynolds CS, Descy J-P, Padisák J (1994) Are phytoplankton dynamics in rivers so different from those in shallow lakes? Hydrobiologia 289:1-7

Reynolds CS (1988) Potamoplankton: paradigms, paradoxes and prognoses. In: Round FE (ed) Algae and the aquatic environment. Biopress, Bristom. pp 285-311.

Rijstenbil JW, Bakker C, Jackson RH, Merks AGA, de Visscher PRM (1993) Spatial and temporal variation in community composition and photosynthetic characteristics of phytoplankton in the upper Westerschelde estuary (Belgium, SW Netherlands). Hydrobiologia 269/270:263-273

Roubeix V (2007) Transformations biogéochimiques et transfert du silicium dans la zone de transition fleuve-mer : le rôle des diatomées planctoniques. Ph. D. thesis. Université Libre de Bruxelles, Belgium. (In French and English)

Roubeix V, Becquevort S, Lancelot C (2008) Influence of bacteria and salinity on diatom biogenic silica dissolution in estuarine systems. Biogeochemistry 88(1):47-62

Roubeix V, Lancelot C (2008) Effect of salinity on growth, cell size and silicification of an euryhaline freshwater diatom: *Cyclotella meneghiniana* Kütz. Transit Water Bull 1:31-38

Rousseau V, Leynaert A, Daoud N, Lancelot C (2002) Diatom succesion, silification and silicic acid availability in Belgian coastal waters (Southern North Sea). Marine Ecology Progress Series 236:61-73

Sabater S (2009) Diatoms. In: Likens GE (eds) Encyclopedia of Inland Waters. Volume 1. Elsevier, Oxford. pp 149-156.

Salden RM, van Eck GTM, Holland ABM, Lefèvre FOB, Van Maldegem DC, de Ridder J, Spronk GC, Schouwenaar A, Verlaan PAJ (1998) Het effect van slibverwijdering in de Beneden Zeeschelde op de waterkwaliteiten slibhuishouding in de Westerschelde. Evaluatie van een bepaling uit de WVO-vergunning onderhoudsbaggerspecie. Rapport RIKZ-98.015. Ministerie van Verkeer en Waterstaat, Directoraat-Generaal Rijkswaterstaat, Rijksinstituut voor Kust en Zee/RIKZ, The Netherlands. (In Dutch)

Sarthou G, Timmermans KR, Blain S, Tréguer P (2005) Growth physiology and fate of diatoms in the ocean: a review. J Sea Res 53:25-42

Schuchardt B, Schirmer M (1991) Phytoplankton maxima in the tidal freshwater reaches of two coastal plain estuaries. Estuar Coast Shelf Sci 32:187-206

Schuchardt B, Haesloop U, Schirmer M (1993) The tidal freshwater reach of the Weser Estuary: riverine or estuarine? Neth J Aquat Ecol 27(2-4):215-226

Sicko-Goad LM, Schelske CL, Stoermer EF (1984) Estimation of intracellular carbon and silica content of diatoms from natural assemblages using morphometric techniques. Limnol Oceanogr 29(6):1170-1178

Soetaert K, Van Rijswijk P (1993) Spatial and temporal patterns of the zooplankton in the Westerschelde estuary. Mar Ecol Prog Ser 97:47-59

Soetaert K, Herman PMJ, Kromkamp JC (1994) Living in the twilight: estimating net phytoplankton growth in the Westerschelde estuary (The Netherlands) by means of an ecosystem model (MOSES). J Plankton Res 16:1277-1301

Soetaert K, Herman PMJ (1995) Estimating estuarine residence times in the Westerschelde (The Netherlands) using a box model with fixed dispersion coefficients. Hydrobiologia 311:215-224

Soetaert K, Hoffmann M, Meire P, Starink M, van Oevelen D, Van Regenmortel S, Cox T (2004) Modeling growth and carbon allocation in two reed beds (*Phragmites australis*) in the Scheldt estuary. Aquat Bot 79:211-234

Soetaert K, Middelburg JJ, Heip C, Meire P, Van Damme S, Maris T (2006) Long-term change in dissolved inorganic nutrients in the heterotrophic Scheldt estuary (Belgium, The Netherlands). Limnol Oceanogr 51(1, part 2):409-423

Struyf E, Van Damme S, Meire P (2004) Possible effects of climate change on estuarine nutrient fluxes: a case study in the highly nutrified Schelde estuary (Belgium, The Netherlands). Estuar Coast Shelf Sci 60(4):649-661

Struyf E, Van Damme S, Gribsholt B, Middelburg JJ, Meire P (2005) Biogenic silica in tidal freshwater marsh sediments and vegetation (Schelde estuary, Belgium). Mar Ecol Prog Ser 303:51-60

Struyf E, Dausse A, Van Damme S, Bal K, Gribsholt B, Boschker HTS, Middelburg JJ, Meire P (2006) Tidal marshes and biogenic silica recycling at the land-sea interface. Limnol Oceanogr 51(2):836-846

Struyf E, Temmerman S, Meire P (2007) Dynamics of biogenic Si in freshwater tidal marshes: Si regeneration and retention in marsh sediments (Scheldt estuary). Biogeochemistry 82:41-53

Struyf E, Van Damme S, Gribsholt B, Bal K, Beauchard O, Middelburg JJ, Meire P (2007) *Phragmites australis* and silica cycling in tidal wetlands. Aquat Bot 87:134-140

Suzumura M, Kokubun H, Arata N (2004) Distribution and characteristics of suspended particulate matter in a heavily eutrophic estuary, Tokyo Bay, Japan. Mar Pollut Bull 49:496-503

Tackx M, De Pauw N, Van Mieghem R, Azémar F, Hannouti A, Van Damme S, Fiers F, Daro N, Meire P (2004) Zooplankton in the Schelde estuary, Belgium and The Netherlands. Spatial and temporal patterns. J Plankton Res 26(2):133-141

Tackx M, Azémar F, Boulêtreau S, De Pauw N, Bakker K, Sautour B, Gasparini S, Soetaert K, Van Damme S, Meire P (2005) Zooplankton in the Schelde estuary, Belgium and The Netherlands: long-term trends in spring populations. Hydrobiologia 540:275-278

Tande KS, Slagstad D (1985) Assimilation efficiency in herbivorous aquatic organisms - The potential of the ratio method using ^{14}C and biogenic silica as markers. Limnol Oceanogr 30(5):1093-1099

Temmerman S, Govers G, Wartel S, Meire P (2003) Spatial and temporal factors controlling short-term sedimentation in a salt and freshwater tidal marsh, Scheldt estuary, Belgium, SW Netherlands. Earth Surf Process Landf 28:739-755

Tréguer P, Van Bennekom AJ, Leynaert A, Panouse M, Jacques G (1991) Production of biogenic silica in the Weddell-Scotia Seas measured with 32Si. Limnology and Oceanography 36(6):1217-1227

Tréguer P, Nelson DM, Van Bennekom AJ, DeMaster DJ, Leynaert A, Quéguiner B (1995) The silica balance in the world ocean: a reestimate. Science 268:375-379

Tréguer P, Pondaven P (2000) Silica control of carbon dioxide. Nature 406:358-359

Triplett LD, Engstrom DR, Conley DJ, Schellhaass SM (2008) Silica fluxes and trapping in two contrasting natural impoundments of the upper Mississippi River. Biogeochemistry 87:217-230

Tungaraza C, Rousseau V, Brion N, Lancelot C, Gichuki J, Baeyens W, Goeyens L (2003) Contrasting nitrogen uptake by diatom and Phaeocystis-dominated phytoplankton assemblages in the North Sea. Journal of Experimental Marine Biology and Ecology 292(1):19-41

Turner RE, Qureshi N, Rabalais NN, Dortch Q, Justic' D, Shaw RF, Cope J (1998) Fluctuating silicate:nitrate ratios and coastal plankton food webs. Proc Natl Acad Sci USA 95:13048-13051

Uncles RJ, Stephens JA, Smith RE (2002) The dependence of estuarine turbidity on tidal intrusion length, tidal range and residence time. Continental Shelf Research 22(11-13):1835-1856

Van Alphen JSLJ (1990) A mud balance for Belgian-Dutch coastal waters between 1969 and 1986. Netherlands Journal of Sea Research 25(1/2):19-30

Van Cappellen P, Dixit S, van Beusekom J (2002) Biogenic silica dissolution in the oceans: Reconciling experimental and field-based dissolution rates. Glob Biogeochem Cycle 16(4):1075

Van Damme S, Struyf E, Maris T, Ysebaert T, Dehairs F, Tackx M, Heip C, Meire P (2005) Spatial and temporal patterns of water quality along the estuarine salinity gradient of the Scheldt estuary (Belgium and The Netherlands): results of an integrated monitoring approach. Hydrobiologia 540(1-3):29-45

Van der Zee C, Chou L (2005) Seasonal cycling of phosphorus in the Southern Bight of the North Sea. Biogeosciences 2:27-42

Van der Zee C, Roevros N, Chou L (2007) Phosphorus speciation, transformation and retention in the Scheldt estuary (Belgium/The Netherlands) from the freshwater tidal limits to the North Sea. Mar Chem 106(1-2):76-91

Van Eck GTM (1991) De ontwikkeling van een waterkwaliteitsmodel voor het Schelde-estuarium (In Dutch). Water 61:215-218

Van Maldegem DC, Mulder HPJ, Langerak A (1993) A cohesive sediment balance for the Scheldt Estuary. Neth J Aquat Ecol 27(2-4):247-256

Vanderborght J-P, Wollast R, Loijens M, Regnier P (2002) Application of a transport-reaction model to the estimation of biogas fluxes in the Scheldt estuary. Biogeochemistry 59:207-237

Vanderborght J-P, Folmer IM, Aguilera DR, Uhrenholdt T, Regnier P (2007) Reactive-transport modelling of C, N, and O_2 in a river-estuarine-coastal zone system: Application to the Scheldt estuary. Marine Chemistry 106:92-110

Verbanck M, Vanderborght J-P, Wollast R (1994) Major ion content of urban wastewater: assessment of per capita loading. Research Journal Water Pollution Control Federation 61(11/12):1722-1728

Vereeke SJP (1994) Geactualiseerde slibbalans Schelde-estuarium (2e concept). Ministerie van Verkeer en Waterstaat, Directoraat-Generaal Rijkswaterstaat, Directie Zeeland, Middelburg, The Netherlands. (In Dutch)

Verlaan PAJ, Maartense VJ, Meijerink SV, Donze M (1997) Slibtransport in de Schelde over de Belgisch-Nederlandse grens (In Dutch). H2O 30(8):255-260

Verlaan PAJ (1998) Mixing of marine and fluvial particles in the Scheldt estuary. Ph.D. thesis. Technische Universiteit Delft, The Netherlands.

Verlaan PAJ, Donze M, Kuik P (1998) Marine *vs* fluvial suspended matter in the Scheldt estuary. Estuar Coast Shelf Sci 46:873-883

Wartel S (1977) Composition, transport and origin of sediments in the Scheldt estuary. Geologie en mijnbouw 56(3):219-233

Wartel S, Parker R, Francken F, Shelton P (1999) Schelde lithology (1 map). KBIN, Brussels, Belgium.

Wartel S, Chen M, van Eck GTM, Van Maldegem D (2007) Influence of harbour construction on mud accumulation in the Scheldt estuary. Aquatic Ecosystem Health & Management 10(1):107-115

WLHO (Waterbouwkundig Laboratorium en Hydrologisch Onderzoek) (1966) Stormvloeden op de Schelde, parts 3 and 4. Borgerhout, Antwerp. (In Dutch)

Wollast R, De Broeu F (1971) Study of the behavior of dissolved silica in the estuary of the Scheldt. Geochim Cosmochim Acta 35:613-620

Wollast R (1974) The silica problem. In: Goldberg ED (ed) The Sea, Vol. 5. Wiley, New York. pp 359-392.

Wollast R (1978) Modelling of biological and chemical processes in the Scheldt estuary. In: Nihoul JCJ (eds) Hydrodynamics of Estuaries and Fjords. Elsevier Oceanography Series, 23, Amsterdam, Oxford, New-York. pp 63-77.

Wollast R, Mackenzie FT (1983) The global cycle of silica. In: Aston SR (ed) Silicon Geochemistry and Biogeochemistry. Academic Press, London. pp 39-76.

Wollast R (1988) The Scheldt estuary. In: Salomons W, Bayne BL, Duursma EK, Förstner U (eds) Pollution of the North Sea. An Assessment. Springer-Verlag, Berlin, Heidelberg, New-York, London, Paris, Tokyo. pp 183-193.

Wright SW, Jeffrey SW (1997) High-resolution HPLC system for chlorophylls and carotenoids of marine phytoplankton. In: Jeffrey SW, Mantoura RFC, Wright SW (eds) Phytoplankton pigments in oceanography: guidelines to modern methods. UNESCO Publishing, Paris. pp 327-341.

Yamada SS, D'Elia CF (1984) Silicic acid regeneration from estuarine sediment cores. Mar Ecol Prog Ser 18:113-118

Zwolsman JJG, Van Eck GTM (1993) Dissolved and particulate trace metal geochemistry in the Scheldt estuary, S.W. Netherlands (water column and sediments). Neth J Aquat Ecol 27(2-4):287-300